Investigating the existence of neural stem cells in the adult mouse cerebellum and third ventricle

Shelanah Salih MSc, BSc

School of Medicine/Department of Cancer and Stem Cells

The University of Nottingham

Thesis submitted to The University of Nottingham for the degree of

Doctor of Philosophy

September 2015

Acknowledgements

All praise is to ALLAH, the Almighty, the greatest of all, for giving me opportunity and strength to do my research in the UK for 4 years. Allah, without your support, compassion and mercifulness, this thesis would not have been completed.

I would like gratefully acknowledge my main supervisor, Dr Virginie Sottile for her support, advice, and guidance throughout my PhD study. She offered me invaluable assistance not only during my research and writing process, but in other aspects of my personal life which helped me to stay on the tract. Special thanks to my second supervisor, Dr. Lisa Chakrabarti for her help and advice and providing me with the mutant *pcd* mice used in this study.

I would like to thank Dr. Stephanie Strohbuecker who taught me cell culture technique and her contiguous advice and help during the rest of my work in the lab. I wish also to thank Ms Maria M. Barbadillo for her valuable microscope training, Dr.Hassan Rashidi who trained me on the microtome and the tissue processor.

I am very thankful to Ms Caroline Reffin, the division administrator for her endless help.

Finally I am deeply indebted to the ministry of higher education-Kurdistan Regional Government (KRG), IRAQ for funding this project.

This work was conducted in the Wolfson Centre for Stem Cells, Tissue Engineering and Modelling (STEM).

Abstract

In mammals, adult neurogenesis in the subventricular zone (SVZ) of the lateral ventricle and the subgranular zone (SGZ) of the dentate gyrus produces neurons contribute to learning and memory functions. However, more recent evidence suggests that neurogenesis may also happen in other regions of the brain such as striatum, spinal cord, and hypothalamus (Reviewed in (Riddle, 2007)). It is important to determine if neurogenesis also occurs in non-neurogenic regions of the adult brain such as CB and 3V. This would be of importance for potential future therapeutic applications for brain repair, and also to help understand the fundamental function of the different regions of the adult brain.

This thesis tested the hypothesis that neural stem cells (NSCs) are present in the mature cerebellum (CB) and the lining of the third ventricle (3V). Based on this hypothesis, one of the major goals of this thesis was to isolate and characterise NSCs isolated from CB and 3V of adult mouse and weather they could generate neuronal and glial cells in vitro. Immunohistochemical analysis for NSC-associated markers revealed that the mature CB in mouse, chick, and primates contains a population exhibiting NSCs characteristics. Results showed that this population was the Bergmann glial located in the Purkinje cell layer (PCL) of the cerebellar cortex, which express Sox1, Sox2, Sox9, BLBP, and GFAP in a similar pattern. Some of these markers are common for neural stem/progenitor cells or radial glial cells in other brain regions.

Abstract

Observations in the 3V revealed that tanycytes lining the ependymal layer also express NSC and astrocytic markers. Moreover, cells were isolated from the CB and 3V of adult GFP+/-Sox1 mice and tested their ability to form neurospheres, their response to EGF and FGF-2, and their differentiation into neurons, astrocytes, and oligodendrocytes. CB and 3V-isolated cells were found to grow in culture, expand, and differentiate into neuronal and glial phenotypes. It was also observed that CB-derived NSCs could survive and differentiate into neuronal and glial lineages after long term removal of either EGF or FGF-2, although cultures were optimal in the presence of both mitogens. We also observed that cells cultured in either EGF or FGF-2 for 3 weeks had different effects on both CB and LV cells in terms of cell fate specification toward neuronal and glial lineages. This finding suggests the heterogeneity of NSCs population in the adult brain. The identification and mapping of the different NSC populations present in the adult brain offers some important opportunities for regenerative medicine approaches.

In order to better characterise the cerebellar population of cells identified above, adult Bergmann glial was observed in a mouse model of cerebellar damage caused by the loss of PCs in *pcd*^{5J} mutant mice. Calbindin immunostaining at different time-points showed that PC degeneration was visible at P21, then progressed rapidly and became considerable at P26 (nearly 70-80% loss), and by P100 all PCs were lost. Immunohistochemical analysis on sections of CB from pcd and wild type counterparts revealed an increase in Bergmann glia cells at P100 as well as the upregulation of GFAP expression. GFAP+ BG exhibited thick

disorganised processes in the molecular layer (ML) at P100 in the mutant mice, with some cell bodies mispositioned in the ML, and significant shrinkage of both ML and internal granular layer (IGL). The increase in the number of Sox1+, Sox2+, and Sox9+ BG in 3 month old mutant mice was not visible at earlier time points analysed. These findings indicate that the PCs loss in pcd^{5J} mice precede and possibly trigger the increase in the Sox1+, Sox2+ and Sox9+ cell population in the CB. Our results also showed that no proliferation activity was observed in the pcd mouse CB at revealed by Ki67 staining, suggesting that the CB microenvironment might not be permissive for neurogenesis even after PCs loss. In vitro isolation of NSCs the CB of P21 *pcd* mice was carried out, and although cultures appear slower to establish than wild type controls these cells did form neurospheres and express NSC markers. Further characterisation of CB-derived NSCs from *pcd* mice and their growth and differentiation potential will help better understand the dynamics and possible therapeutic targets for neurodegenerative disorders affecting the CB. The characterisation of CB and 3V derived NSCs from adult mouse CB has provided important information regarding their differences with NSCs derived from neurogenic region in the brain, the lateral ventricle (LV).

Table of Contents

Acknowledgements ii
Abstract iii
Table of Contents vi
List of Figures xi
List of Tables....xvi
Abbreviations xvii
1. Introduction 1
1.1 Stem cells....2
1.1.1 Neural stem cells (NSCs) 3
1.1.2 Localization of NSCs in the brain 4
1.1.3 Derivation and culture of NSCs 6
1.1.4 Neural stem cell markers....7
1.1.5 Lineage Markers....8
1.2 Growth factor responsiveness of NSC....18
1.2.1 Fibroblast Growth Factors (FGFs) 18
1.2.2 Epidermal growth factors (EGFs) 20
1.2.3 Responsiveness of NSCs to EGF and FGF-2....21
1.3 The Cerebellum 21
1.3.1 Cerebellar structure 21
1.3.2 Cellular organization of the cerebellar cortex 24
1.3.3 Cerebellar deep nuclei 26
1.3.4 Functions of the cerebellum 27
1.4 Development of the cerebellum....28
1.5 Neuroglia of the cerebellum 30
1.5.1 Origin of cerebellar astrocytes 30
1.5.2 Radial glia as progenitors....31
1.5.3 Bergmann Glia: Description, Origin and Development....32

1.5.4 Differentiation of Bergmann Glia 34
1.5.5 Functions of Bergmann glia 34
1.5.6 Cerebellar neurons Birthdates 35
1.6 Damage to the Cerebellum 36
1.6.1 Hereditary cerebellar ataxias 36
1.6.2 Mouse models of cerebellar degeneration 37
1.6.3 Mechanisms of Purkinje cell death 41
1.7 The hypothalamus: anatomy and function 42
1.8 Tanycytes population in the third ventricle 42
1.8.1 Tanycytes: ontogeny, development and radial glia 42
1.8.2 Types of Tanycytes 43
1.8.3 Ependymal Cells 44
1.8.4 Tanycytes Functions 44
1.8.5 Markers expressed by tanycytes 44
1.8.6 Neurogenesis in the adult cerebellum and third ventricle 45
1.9 Aims of the project 48
2. Materials and Methods 1
2.1. Chemicals, reagents, and medium 1
2.2. Tissue slide preparation 1
2.2.1. Cryosectioning 1
2.3. Immunohistochemistry 2
2.3.1. Indirect immunohistochemistry 2
2.3.2. Immunostaining analysis: 3
2.4. Cell Culture 6
2.4.1. NSCs preparation 6
2.4.2. Passaging and freezing of NSCs 6
1.10 Differentiation of NSCs 8
2.4.3. Immunocytochemistry and cell counting 8
2.4.4. Cell Viability Assay 9
2.4.5. Image analysis and microscopy 9

3 Investigating the presence and distribution of neural stem cells in the mature cerebellum of mouse, primate, and chick 10

3.1 Introduction 10

3.2 Results 14

3.2.1 Sox1, Sox2, and Sox9 localisation in the postnatal cerebellum 14

3.2.2 The expression of markers commonly associated with neural stem cell markers 21

3.3 Discussion 28

3.3.1 Population of cells in the adult cerebellum expressing NCS markers 28

3.3.2 Stem cells in the mature cerebellum are of glial origin 31

3.4 Conclusions 34

4 Isolation and characterisation of cerebellar derived neural stem cells of adult GFP+/- Sox1 mouse 35

4.1 Introduction 35

4.2 Results 38

4.2.1 Primary culture of NSCs derived from mature cerebellum 38

4.2.2 Selection of the optimal seeding density for CB-NSCs experiments 39

4.2.3 Quantification of CB-NSCs grown on gelatin and laminin coated culture flasks 41

4.2.4 Effect of EGF and FGF-2 on CB derived NSCs 41

4.2.5 In vitro differentiation and immunohistochemical analysis of CB-NSCs 73

4.2.6 Effect of EC23 treatment on CB-NSCs differentiation 78

4.3 Discussion 88

4.4 Characterisation of NSCs derived from mature cerebellum 88

4.4.1 Effect of retinoic acid analogue (EC23) on the neuronal differentiation of CB NCS 89

4.4.2 Effect of EGF and FGF-2 on CB-NSCs in culture proliferation and differentiation 90

4.4.3 Dose dependent effect of EGF and FGF-2 on the proliferation of CB-NSCs 91

4.5 Prolonged withdrawal of EGF and FGF-2 on CB derived NSCs proliferation and differentiation 92

4.5.1 Effect of withdrawal of EGF and FGF-2 on CB derived NSCs proliferation 92

4.5.2 Effect of short term withdrawal of EGF and FGF-2 on CB derived NSCs differentiation 94

4.6 In vitro differentiation of CB derived NSCs 95

4.7 Conclusions 97

5 Quantitative, morphological and immunohistochemical study of Bergmann glia and Purkinje cells in Purkinje Cell Degeneration (*pcd*) 5J mutant mice 99

5.1 Introduction 99

5.2 Results 102

5.3 Phenotype of the *pcd*^{5J} mutant mice 102

5.4 PCs degeneration in the *pcd*^{5J} mutant mice 103

5.5 Sox gene expression in *pcd*^{5J} mice at different time points 106

5.6 Quantitative analysis of Bergmann glia and Purkinje cells in *pcd*^{5J} mice 110

5.7 Bergmann Glia radial fibers changes in the *pcd*^{5J} mice 116

5.8 NSCs derived from the *pcd*^{5J} ataxic cerebellum 121

5.8.1 Effect of growth factors withdrawal on the culture of pcd^{5J} derived CB-NSCs 124

5.9 Discussion 127

5.9.1 Reactive Bergmann gliosis in *pcd*^{5J} mice 127

5.9.2 NSCs derived from the cerebellum of *pcd*^{5J} mutant mice 131

5.10 Conclusions 134

6 Exploring the existence of neural stem cells in the third ventricle of adult GFP+/- Sox1 mouse 135

6.1 Introduction 135

6.2 Results 140

6.3 Neural stem cell marker expression in the 3V 140

6.3.1 SoxB analysis 140

Figure 6.4 145

6.3.2 Co-localization of Sox1 with Sox2 and Sox9 in the 3V 146

6.3.3 Co-localization of Sox1 with GFAP in the 3V 150

6.4 Characterisation of NSCs derived from the 3V 155

6.4.1 In vitro isolation and culture 155

6.4.2 Expression of NSC markers 155

6.4.3 Effect of EGF and FGF-2 withdrawal on the proliferation of NSCs derived from the third ventricle (3V) 156

6.4.4 Neural stem cells derived from the 3V have the ability to differentiate into neurons, astrocytes, and oligodendrocytes 160

6.5 Discussion 162

6.5.1 Tanycytes are radial glial cells 165

6.5.2 3V NSCs derivation and characterisation 166

6.6 Conclusions 170

7 Concluding Discussion 171

7.1 Major thesis findings 171

7.2 Is there NSCs population in the mature cerebellum and third ventricle 172

7.3 EGF and FGF-2 as mitogens for CB derived NSCs 176

7.4 Bergmann glia in the PCD^{5J} mutant mice 177

7.5 Conclusion and future directions 180

References 182

Appendix I-Chemicals, Medium, and Reagents 201

HISTOLENE CLEARING AGENT 202

Appendix II-Solutions, Buffers and Media Preparation 203

List of Figures

Figure 1.1 The hierarchy and differentiation potential of embryonic stem cells. ..4
Figure 1.2 Zones of neurogenesis with their cellular component in mouse adult brain..6
Figure 1.3 Simplified diagram of the cerebellum showing the fissures and lobules (I-X)..22
Figure 1.4 Sagittal view of mouse cerebellum through the vermis..23
Figure 1.5 Basic cerebellum structure..27
Figure 1.6 Mouse cerebellar development. After (Sillitoe and Joyner, 2007). 29
Figure 1.7 Parasagittal section through the cerebellum (A) showing the location of Bergmann glia..33
Figure 1.8 *pcd* ^{5J} mutation results from single amino acid insertion..40
Figure 1.9 Coronal section through the third Ventricle.45
Figure 2.1 Images showing the 3 regions in the adult brain dissected to derive NSCs.7
Figure 3.1 Sox1 detection in sagittal sections of mature cerebellum from mouse, non-human primate, and chick origin (A, B, and C respectively).16
Figure 3.2 Sox2 detection in sagittal sections of mature cerebellum tissue from mouse, non-human primate, and chick origin (A, B, and C respectively)..17
Figure 3.3 Sox9 detection in sagittal sections of mature cerebellum tissue from mouse, non-human primate, and chick origin (A, B, and C respectively).18
Figure 3.4 Negative controls for Fig (3.2, 3.3, and 3.4)..19
Figure 3.5 Sagittal sections of mature mouse cerebellum stained for Nestin (A) and Ki67 (B) with Calbindin (blue)..20
Figure 3.6 Double immunolabelling of calbindin and GFAP in the mature cerebellar cortex of mouse (A) , primate (B), and chick (C).24
Figure 3.7 Double immunolabelling of BLBP and Calbindin in the mature cerebellar cortex of mouse (A), primate (B) and chick (C).25
Figure 4.1 Brightfield image showing the morphology of CB and LV NSCs in culture..39
Figure 4.2 The Morphology of CB-NSCs grown at different seeding densities imaged 2 days after seeding.40

Figure 4.3 The effect of gelatin and laminin on the morphology and proliferation of CB NSCs. Cells seeded on gelatin (A) or laminin (B) coated plates.. 42
Figure 4.4 Brightfield image showing the morphology of CB and LV NSCs grown in different growth factor conditions.....44
Figure 4.5 Effects of different growth factor conditions on the proliferation of CB (A) and LV (B) NSCs. Cell metabolic assay of CB and LV cells grown for 3 days in EGF, FGF-2, EGF+FGF-2, and mitogen free (-GFs) medium. 45
Figure 4.6 Brightfield images showing the dose dependent effect of EGF+FGF-2 on the morphology and proliferation of CB and LV NSCs. 47
Figure 4.7 Dose dependent effect of EGF and FGF-2 on the proliferation and cell viability of CB (A) and LV (B) NSCs.....48
Figure 4.8 Brightfield images showing the dose dependent effect of EGF on the morphology of CB and LV NSCs.. 51
Figure 4.9 Dose dependent effect of EGF on the proliferation and metabolic activity of CB (A) and LV (B) NSCs. 52
Figure 4.10 Brightfield images showing the dose dependent effect of FGF-2 on the morphology of CB and LV NSCs.. 55
Figure 4.11 Dose dependent effect of FGF-2 on the proliferation and metabolic activity of CB (A) and LV (B) NSCs. 56
Figure 4.12 Brightfield images showing the dose dependent effect of EGF on the morphology of CB and LV NSCs.. 58
Figure 4.13 Dose dependent effect of EGF on the proliferation and cell viability of CB (A) and LV (B) NSCs. 59
Figure 4.14 Brightfield images showing the morphology of CB and LV cells (A, B respectively) grown for 3 weeks (5 passages) in EGF, FGF-2, EGF+FGF-2, and mitogen free medium.....64
Figure 4.15 Effect of 3-week withdrawal of EGF and FGF-2 on the proliferation of mouse CB (A) and LV (B) NSCs.....65
Figure 4.16 Brightfield images of CB (A) and LV (B) cells at D0 and D6 of in vitro differentiation following 3weeks culture in different growth factor conditions. 68
Figure 4.17 Effect of 3-week withdrawal of EGF and FGF-2 on the differentiation potential of CB and LV NSCs (A) and (B) respectively.. 70

Figure 4.18 Quantitative analysis of B-tub3^{+} neurons after 5 passages in EGF, FGF-2, and EGF+FGF-2 for CB (A) and LV (B) cells respectively. 72
Figure 4.19 Multi-lineage differentiation analysis of NSCs derived from CB and LV of adult mouse.. 75
Figure 4.20 Multi-lineage differentiation analysis of NSCs derived from CB (A) and LV (B) of adult mouse. 77
Figure 4.21 The effect of EC23 treatment on the in vitro differentiation response of CB and LV NSCs. 82
Figure 4.22 The effect of EC23 (retinoic acid analogue) withdrawal on the in vitro differentiation capacity of CB and LV NSCs (A) and (B) respectively. 85
Figure 4.23 The effect of EC23 on lineage marker expression after 16 days of in vitro differentiation of CB and LV NSCs. 87
Figure 5.1 Gross apperance of homzygous *pcd* and wild type brain at P21. 102
Figure 5.2 Purkinje cells degeneration in *pcd*^{5J} cerebellar sections.. ..... **Error! Bookmark not defined.**
Figure 5.3 Immunohistochemical images of cerebellar sagittal sections of P17, P21, P26, and P100 *pcd*^{5J} mutant and wild type mice double stained for Sox1 (brown) and Calbindin (blue).. 107
Figure 5.4 Immunohistochemical images of cerebellar sagittal sections of P17, P21, P26, and P100 *pcd*^{5J} mutant and wild type mice double stained for Sox2 (brown) and Calbindin (blue).. 108
Figure 5.5 Immunohistochemical images of cerebellar sagittal sections of P17, P21, P26, and P100 *pcd*^{5J} mutant and wild type mice double stained for Sox9 (brown) and Calbindin (blue).. 109
Figure 5.6 Quantification of Bergmann glia and Purkinje cell numbers in homozygous *pcd*^{5J} and wild type mice at different ages by immunostaining with Sox1 and Calbindin.. 112
Figure 5.7 Quantification of Bergmann glia and Purkinje cell numbers in homozygous *pcd*^{5J} and wild type mice at different postnatal ages by immunostaining with Sox2 and Calbindin.. 114
Figure 5.8 Quantification of Bergmann glia and Purkinje cell numbers in homozygous *pcd*^{5J} and wild type mice at different postnatal ages by immunostaining with Sox9 and Calbindin.. 115

Figure 5.9 double immunolabeling of Cabindin and GFAP in sagittal cerebellar sections of *pcd*^{5J} and wild type mice at P17 showing the distribution of BG fibers and PCs dendrities. 117
Figure 5.10 PC loss induce Bergmann gliosis in homozygous pcd5J mice. GFAP (brown) co-labelled with Calbindin (blue) in cerebellar sagittal sections of homozygous pcd^{5J} (hm) and wild type (WT) mice at different ages.. 119
Figure 5.11 Double immunostaining images showing the expression of nestin and B-tubulin 3 in sagittal sections of *pcd* mutant mice.. 120
Figure 5.12 Brightfield image of *pcd*^{5J} mutant derived NSCs at different passages.. 122
Figure 5.13 Generation of neurospheres in cultures isolated from homozygous *pcd* and wild type CB and LV. 123
Figure 5.14 Fluroscent immunostaining showing Nestin and Sox2 expression in cerebellum-derived NSC cultures from *pcd* and wt mice at P21, with dapi counterstain (blue).. 124
Figure 5.15 Effects of EGF and FGF-2 on NSCs derived from the cerebellum of *pcd*^{5J} mutant mice after 3 days in culture.. 126
Figure 6.1 GFP expression in coronal sections of adult Sox1-GFP+/− mouse third Ventricle (3V), hypothalamus, and hippocampal dentate gyrus.. 142
Figure 6.2 Sox1 expression in coronal sections of adult mouse third Ventricle (3V), hypothalamus, and hippocampal dentate gyrus.. 143
Figure 6.3 Sox2 expression in coronal sections of adult mouse third Ventricle (3V), hypothalamus, and hippocampal dentate gyrus.. 144
Figure 6.4 Sox9 expression in coronal sections of adult mouse third Ventricle (3V), hypothalamus, and hippocampal dentate gyrus.. 145
Figure 6.5 Compared expression of Sox2 and GFP in coronal sections of adult mouse third Ventricle (3V) and hippocampal dentate gyrus. 148
Figure 6.6 Co-detection of Sox9 and GFP in coronal sections of adult mouse third Ventricle (and hippocampal dentate gyrus (DG). 149
Figure 6.7 Coronal sections through the third ventricle (3V) showing GFAP expression.. 152
Figure 6.8 Coronal sections through the dorsal part of the third ventricle (3V) showing co-localization of GFP and GFAP.. 153

Figure 6.9 Coronal sections of the ventral part of 3V showing co-localization of GFP and GFAP.....154
Figure 6.10 Brightfield image showing the morphology of 3V derived neuroshpheres.....157
Figure 6.11 Effects of different growth factor conditions on mouse 3V and LV NSCs after 3 days in culture.....159
Figure 6.12 Differentiation analysis of NSCs derived from the third ventricle (3V) and lateral ventricle (LV)...161

List of Tables

Table 2.1 List of primary antibodies used in IHC and their dilutions. Abbreviation: DSHB, Developmental Studies Hybridoma Bank. 4
Table 2.2 List of secondary antibodies used for immunohistochemistry and their dilutions. 5
Table 4.1 The list of primary antibodies used in this chapter.....67
Table 4.2 Percentage of different neuronal markers after 16 days of differentiation in the presence of EC23. Values represent means ± SEM of cell counts obtained from 5 stained fields of view/marker 79

Abbreviations

3V third ventricle

ARC Arcuate nucleus

BDNF Brain derived neutrophic factor

BG Bergmann glia

BLBP Brain lipid binding protein

BLBP Brain Lipid-Binding Protein

BrdU 5-Bromo-2′-deoxyuridine

CB Cerebellum

CNPase Nucleotide phosphodiesterase

CNS Central nervous system

CSF Cerebrospinal fluid

Dapi 4',6-diamidino-2-phenylindole

DG Dentate gyrus

DMEM Dulbecco's Modified Eagle Medium

DMSO Dimethyl sulfoxide

DNA Deoxyribonucleic acid

DSHB Developmental Studies Hybridoma Bank

EGF Epidermal growth factor

EGFR Epidermal growth factor receptor

Epe, Ependymocytes

ESCs Embryonic stem cells

FBS Fetal bovine serum

FCS Fetal calf serum

FGF-2 Fibroblast growth factor

FGFR Fibroblast growth factor receptor

Fitc Fluorescence isothiocyanate

GFAP Glial fibrillary acetic protein

GFP Green Fluorescent Protein

GLAST Glutamate-aspartate transporter

HBSS Hanked Balanced Salt Solution

HP Hypothalamus

IGL Internal granular layer

LV Lateral ventricle

MAP2 Microtubule associated protein

MBP Myelin Basic Protein

ME, Median Eminence

ML Molecular layer

NaCl Sodium chloride

NeuN Neuronal Nuclei

NSCs Neural stem cells

NT3 Neurotrophin

OCT Optimal cutting temperature

PBS Phosphate buffer saline

PBS Phosphate buffered saline

PCD Purkinje cell degeneration

PCL Purkinje cell layer

PCs Purkinje cells

PFA Paraformaldehyde

PLP Proteolipid Protein

SCA Cerebrospinal ataxias

SGZ Subgranular zone

SVZ Subventrcular zone

TRed Texas Red

VMN Ventromedial nucleus

1. Introduction

The discovery of NSCs existence in the adult brain represented a breakthrough in the field of neuroscience that opened up a whole new era towards development of cellular therapies for neurodegenerative diseases. In rodents the generation of new neurons has been extensively studied in the classical neurogenic niches of the adult brain: subventricular zone (SVZ) of the lateral ventricle (LV) and the subgranular zone (SGZ) of the dentate gyrus (Oyarce et al., 2014). NSCs reside the SVZ and SGZ give rise to olfactory interneurons and granule neurons respectively (Reviewed in (Lin et al., 2015)). In addition to these well-known regions, researchers postulated that other potential regions in the adult brain exhibiting neurogenic activity such as the cerebellum (CB), hypothalamic third ventricle (3V), spinal cord, substantia nigra, and amygdala (Reviewed in (Oyarce et al., 2014)).

The data reviewed above suggest the presence of NSCs in various areas of adult brain (Palmer et al., 1997, Weiss et al., 1996, Morshead et al., 1994). However, it remains controversial whether the CB and 3V harbor similar NSCs population as the SVZ and SGZ. This thesis focus mainly to identify a population of NSCs in the mature CB and 3V compared to well-established NSCs in the adult brain. This was performed by investigating the expression of NSCs markers in the CB and 3V of adult mouse. Furthermore, an in vitro characterisation of NSCs derived from both regions was performed in terms of their expansion, response to growth factors, and capacity to differentiate into neuronal and glial linages. The second part of the present study was aimed at addressing the response of Bergmann glia to PCs loss in the CB of Purkinje cell degeneration (pcd^{5J}) mutant mice.

This chapter gives a detailed background to stem cells types focusing on NSCs in terms of their localisation, growth factor requirement, and markers associated with them. It also gives insights into the anatomy and physiology of both CB and 3V regions of adult mouse brain and neurogenesis process in the adult brain.

1.1 Stem cells

Stem cells are defined as cells capable of unlimited self-renewing through mitotic cell division, and by their potential to differentiate into different cell types (Ahmed et al., 2011). In terms of differentiation, there are three types of stem cells (Fig. 1.1), totipotent (can generate the whole organism), pluripotent (can differentiate into derivatives of the 3 germ layers), and multipotent (have limited capacity to differentiate and can only generate a subset of different cell types) (Shanthly et al., 2006). Examples of pluripotent stem cells are embryonic stem cells (ES) and embryonic carcinoma cells. (ES) cells can be defined as undifferentiated, with high telomerase activity (Thomson et al., 1998). ES cells arise from an inner cell mass of the blastocyst, these cells are the pluripotent cells, i.e. they have the ability to generate all 3 germ layers (ectoderm, mesoderm, and endoderm) (Evans and Kaufman, 1981). Adult or somatic stem cells are multipotent cells able to generate more than one cell type, but they are tissue-restricted (Bhartiya et al., 2013). Examples of adult stem cells are neural stem cells (NSCs) which are able to give rise to neurons, astrocytes, and oligodendrocytes and hematopoietic stem cells which are found in bone marrow and can differentiate into blood cells and platelets (Toma et al., 2001, Seita and Weissman, 2010). Adult stem cells have been isolated from various parts of the

body such as the liver, skin, gut, muscle, bone marrow, and adipose tissue (Bhartiya et al., 2013).

1.1.1 Neural stem cells (NSCs)

The isolation and characterisation of NSCs in various regions of adult brain raised the hope for future applications as a therapy in many neurodegenerative diseases. Moreover, the demonstration of neurogenesis in some brain regions such as the subventricular zone (SVZ) of the lateral ventricle, the dentate gyrus (DG) of the hippocampus, provides a window of opportunity into a wider regenerative capacity of NSCs (Altman and Das, 1965, Alvarez-Buylla et al., 1990, Kokoeva et al., 2007, Ponti et al., 2008).

NSCs are subset of multipotent cells present in the developing and adult CNS and capable of continuously self-renew and differentiate into neurons and glial cells (SCHWINDT et al., 2009, Gage, 2000). They are generated by the process of neurogenesis from embryonic ectoderm that leads to the formation of neuroepithelial cells (Weiner, 2008, Peyre and Morin, 2012). The neuroepithelial cells then undergo symmetric and asymmetric division (Peyre and Morin, 2012). Symmetric division gives rise to two daughter progenitor cells while asymmetric proliferation generates one stem cell and another more differentiated cell such as neuron (Rakic, 1995). The neuroepithelial cell layer forms the neural plate which folds to form the neural tube that will eventually form the brain and spinal cord (Clarke, 2003).

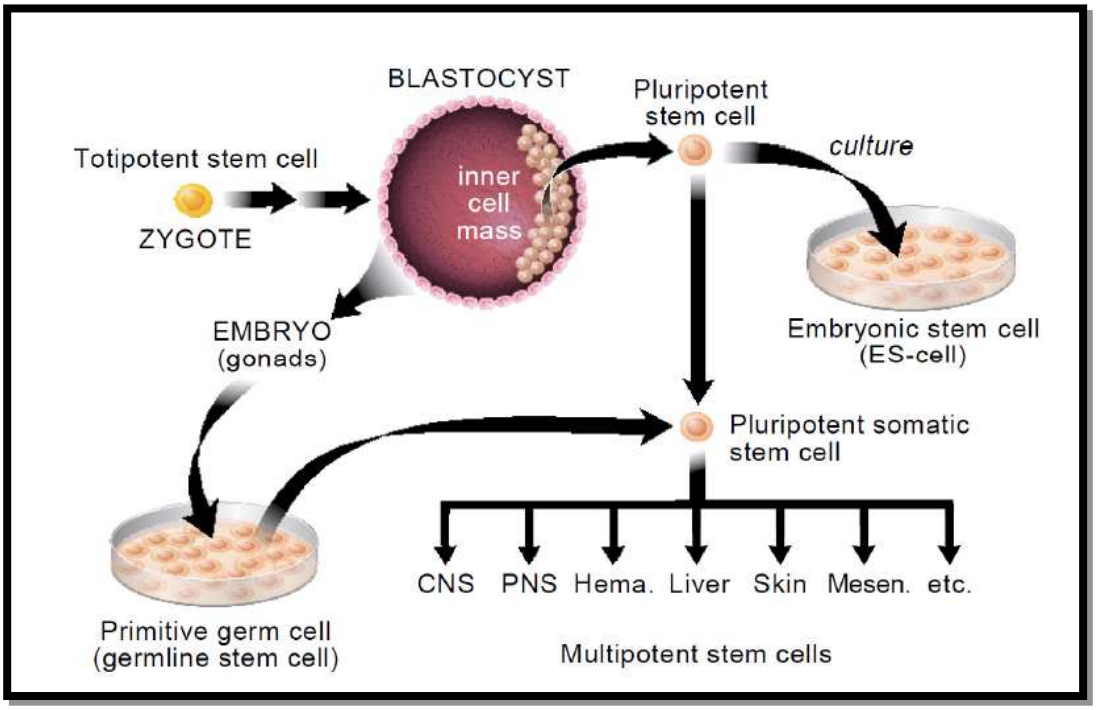

Figure 0.1 The hierarchy and differentiation potential of embryonic stem cells. The inner cell mass of the blastocyst gives rise to pluripotent stem cells which have the ability to self-renew and differentiate into all cell lineages of the body, but with more progression down the hierarchy, the differentiation potential becomes more restricted with the multipotent stem cells (after (Anderson et al., 2001)).

1.1.2 Localization of NSCs in the brain

It has been thought for decades that the regeneration of neurons in the adult brain was impossible, notably through the histological and anatomical study of Cajal, (1913). The early work of Altman in the 1960s on the rodent brain indicated that neurogenesis might take place in the hippocampus, olfactory bulb, the neocortex (Fig. 1.2) (Altman, 1969; Altman and Das, 1965; Altman and Das, 1966), and SVZ (Alvarez-Buylla and Temple, 1998), thereby contradicting the central dogma of Cajal that “In the adult centers, the nerve paths are something fixed, ended, and

immutable. Everything may die, nothing may be regenerated" (Ramón y Cajal, 1914).

In the developing brain, embryonic NSCs exist in different areas such as the VZ, SVZ, olfactory bulb, cerebral cortex, cerebellum, and the spinal cord (Bazan et al., 2004, Uchida et al., 2000). The specific regions harbouring stem cells in the brain are considered as NSC niches, where these NSCs can proliferate and differentiate in response to the available growth factors and other local molecules (Gritti et al., 2002). In the adult mouse, NSCs have been described in two specific brain regions, the subventricular zone (SVZ) of the lateral ventricle (LV) and the dentate gyrus (DG) of the hippocampus that continuously generating new neurons (Yadirgi and Marino, 2009) (Fig. 1.2). In both regions, stem cells are defined as a subset of glial cells known to support neurons in the adult brain (Doetsch, 2003). The SVZ generates neuroblasts that migrate along the rostral migratory stream (RMS) to the olfactory bulb where they differentiate into mature neurons (Doetsch and Hen, 2005). In the hippocampus, subgranular zone (SGZ) progenitors generate neurons that migrate to the granular layer and differentiate to granule cells (Doetsch, 2003, Doetsch and Hen, 2005). Progenitors in the two regions have shown the properties of stem cells in terms of self-renewing capacity and multipotentiality (Loeffler and Potten, 1997, Gage et al., 1995, Weiss et al., 1996). Other reports have further confirmed the conserved presence of NSCs that can generate neurons and glial cells throughout life in the LV and the DG regions of other species such as rat, human, and non-human primate (Reviewed in (Jin and Galvan, 2007, Gage, 2000)).

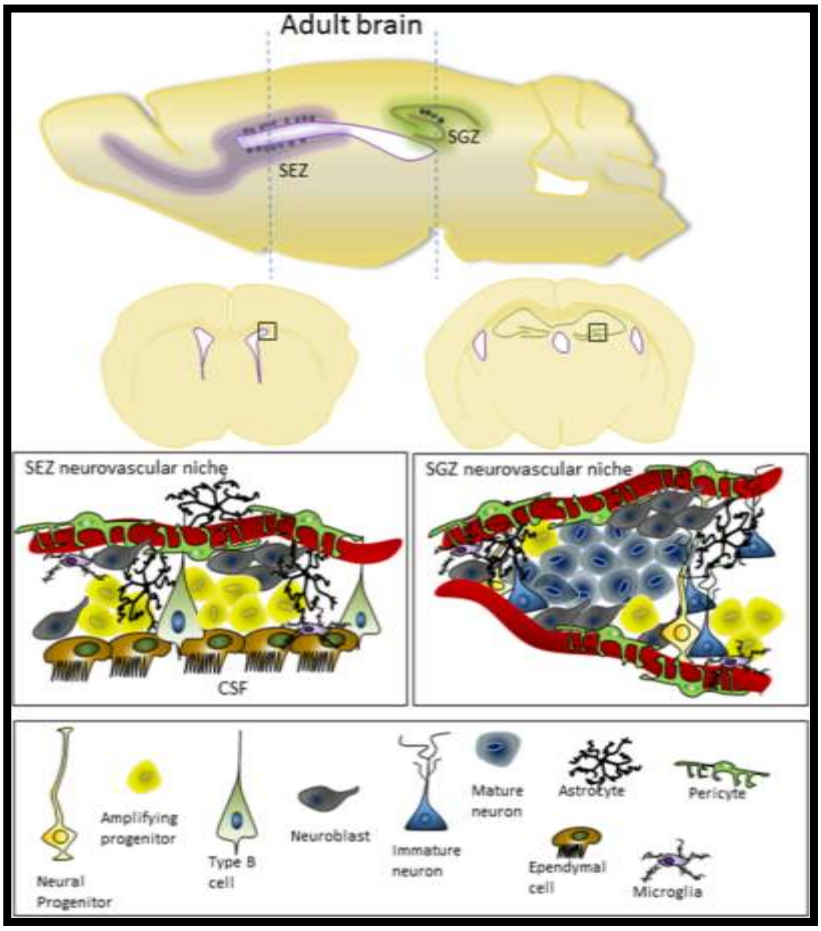

Figure 0.2 Zones of neurogenesis with their cellular component in mouse adult brain. Neurogenesis has been described in two regions of the brain, the subgranular zone (SGZ) of the hippocampus and the subventricular zone (SVZ) of the lateral ventricle (LV). (a) After (Stolp and Molnar, 2015).

1.1.3 Derivation and culture of NSCs

Over the past 23 years, different methodologies for the isolation of neural stem/progenitor cells from adult brain have been developed by different research groups. Reynolds and Weiss were the first to isolate NSCs from the striatum of both fetal and adult mouse brain (Reynolds and Weiss, 1992, Reynolds et al., 1992). The population isolated by these investigators was Nestin-positive and showed the ability to differentiate into the 3 phenotypes of the brain cells (neurons, astrocytes, and oligodendrocytes). This early study reported that the use of culture conditions based on serum free medium on a non-adhesive substrate,

supplemented with mitogens such as epidermal growth factor (EGF) or basic fibroblast growth factor (bFGF). In these conditions, these NSCs rapidly divided, forming a spherical cluster of cells known as neurospheres (Reynolds et al., 1992). Neurospheres could be dissociated into single cells and when replated into a single well, they were able to form secondary neurospheres, a subculturing method widely used for NSCs (Reynolds and Weiss, 1992). Few years later, Gage et al., (1995) were able to isolate and characterise a new population of NSCs with similar properties from the hippocampus of adult rats, which grew as monolayer in the presence of FGF-2. Subsequent in vitro studies confirmed the self-renewing and multipotent capacity of these populations (Gritti et al., 1996, Palmer et al., 1997). Following these pioneer studies, multipotent neural stem/progenitor cells have been isolated from other areas of adult brain such as the spinal cord (Weiss et al., 1996, Taupin, 2006) and the hypothalamus (Xu et al., 2005).

1.1.4 Neural stem cell markers

Given the lack of specific markers that can identify NSCs, NSCs can be characterised by their ability to self-renew and by their multipotentiality to generate neuronal and glial lineages (Loeffler and Potten, 1997). Many cells in the CNS characterised as astrocytes and radial glia may behave like stem cells (Gage et al., 1995), a suggestion further supported by Laywell et al., (2000) who demonstrated that $GFAP^+$ cells identified as astrocytes isolated from different brain regions were able to form neurospheres capable of generating neurons and glial cells in vitro.

Based on this observation, markers for astrocytes and radial glia have been used as NSC markers (Alvarez-Buylla and Garcia-Verdugo, 2002), however markers specific for NSCs are necessary for their identification at different developmental

stages since not all radial glia or astrocytes behave like stem cells (Nakano and Kornblum, 2003).

1.1.5 Lineage Markers

1.1.5.1 Markers for astrocytes and radial glia

The morphology of astrocytes differs both in vitro and in vivo. In vivo, they appear stellate, while in vitro they often appear flattened, polygonal or have long extensions (Nakano and Kornblum, 2003). A growing body of evidence suggests that radial glia are precursors of astrocytes acting like stem cells (Malatesta et al., 2000). They may show similar morphology both in vitro and in vivo and can be confused with other cells which are bipolar with long processes such as immature oligodendrocytes and neurons (Nakano and Kornblum, 2003). Studies have shown that radial glial cells might be embryonic stem cells or progenitors of astrocytes by their expression of Nestin (a marker expressed by neural progenitors) (Lendahl et al., 1990). Another study on the avian brain has showed that radial glial cells are found in regions where neurogenesis takes place (Alvarez-Buylla et al., 1990).

The most widely used marker for astrocytes is glial fibrillary acidic protein (GFAP), an intermediate filament protein (Eng et al., 2000). However, studies have reported that GFAP is expressed in other cells such as Bergmann glia, non-myelinating Schwann cells, Muller cells (McLendon and Bigner, 1994), and in the cerebellar cortex and medulla of adult mouse (Krishnan et al., 2012). GFAP may also be expressed by radial glia during embryogenesis and in the adult brain (Alvarez-Buylla et al., 1990; Hockfield and McKAY, 1985), and in radial glial cells displaying stem cells characteristics, suggesting GFAP as a marker for NSCs

(Noctor et al., 2002, Malatesta et al., 2000). Tanycytes, specialised radial glial cell lining the wall of the third ventricle (3V) have also shown to express GFAP (Rodriguez et al., 2005, Doetsch et al., 1997). Vimentin is another intermediate filament protein of the glial cells expressed mainly by immature astrocytes and the radial glia during early brain development (Von Bohlen und Halbach, 2011); whereas in the adult brain, vimentin is not expressed by the astrocytes but only in some radial glia such as Bergmann glial cells and by ependymal cells (Bramanti et al., 2010). However, Studies have described Vimentin and GFAP as classical markers for gliosis in reactive astrocytes (Zamanian et al., 2012).

Glutamate-aspartate transporter (GLAST) is another astrocytic marker that is a sodium-dependent transporter molecule localized in the cell membrane of mature astrocytes where it regulates the concentration of neurotransmitters at the excitatory synapses (Nakano and Kornblum, 2003). Studies have reported that this marker is expressed in embryonic radial glia and in the mature brain (Hartfuss et al., 2001). Other markers that belong to this category are S100B and BLBP and RC2, common markers for mature astrocytes (Landry et al., 1989, Anthony et al., 2005, Patro et al., 2015). S100B is a member of calcium and zinc binding proteins which show 97% homology among mammals implicated in the initiation and maintenance of glial mediated inflammatory state (Ralay et al., 2006). A very recent study by (Patro et al., 2015) presented a clear evidence for the suitability of S100B as a radial progenitor marker in the developing brain during the time of neurogenesis and gliogenesis. Brain Lipid-Binding Protein (BLBP) is a member of ligand-binding proteins family involved in modulating transcription by binding with nuclear receptors (Haunerland and Spener, 2004). During development, BLBP has been found to be expressed in radial glial cells in many brain regions,

and suggested to be a radial-glia-like progenitor marker because its expression is not associated with S100B (for mature astrocytes) or neuronal markers such as double cortin (DC) or Neuronal Nuclei (NeuN) (Brunne et al., 2010). However, studies have shown that BLBP might be expressed in astrocytes (Young et al., 1996). Anthony et al., (2005) reported high expression of BLBP in the mouse brain at E12 in the forebrain and in postnatal day (P6) in the cerebellum Bergmann glial cells. RC2 is another radial glial marker that is expressed in the majority of precursor cells in the embryonic brain at E12.5 and is then replaced with other radial glial markers such as GLAST and BLBP (Noctor et al., 2001, Nakano and Kornblum, 2003).

1.1.5.2 Oligodendrocytes Markers

Oligodendrocytes are neuroglial cells found within the CNS, characterized by small processes. They form myelin as they wrap around the axons (Snaidero and Simons, 2014). It is difficult to distinguish between immature (before myelin formation), mature oligodendrocytes and other brain cells with small processes such as astrocytes, thus a number of antigenic markers have been developed to identify each cell type (Baumann and Pham-Dinh, 2001). A number of antibodies are available to identify oligodendrocytes at different stages of maturation. Oligodendrocytes at early stages of development until maturation can be identified by O4 (Nakano and Kornblum, 2003), which allows to differentiate between immature neurons and immature oligodendrocytes in a mixed culture (Nakano and Kornblum, 2003). Proteolipid Protein (PLP) is a myelin protein in the CNS that plays an important role in myelination, and is expressed during the early stages of oligodendrocyte development before myelination starts (Reviewed in (Baumann and Pham-Dinh, 2001)). Myelin Basic Protein (MBP) has also been

shown to be expressed in the mature oligodendrocytes at the end of the first postnatal week (Sorg et al., 1987, Baumann and Pham-Dinh, 2001). MBP starts to mark oligodendrocytes with the beginning of myelination at P9 in mice, peaking at P18, and then remaining low in the adult, suggesting this protein as a major constituent of myelin sheath (Sternberger et al., 1978, Sorg et al., 1987). Mature oligodendrocytes can also be detected by antibodies against cyclic nucleotide phosphodiesterase (CNPase), a membrane bound enzyme found in high concentrations in myelin (Dyer et al., 1997).

1.1.5.3 Neuronal Markers

Neurons at different stages of maturity can be identified by a subset of markers that could differentiate between neurons at committed or postmitotic stages. Immature neurons can be detected by some intermediate filaments such as neurofilamnets and doublecortins. Neurofilament is an intermediate filament within the neurons composed of 3 neuron-specific proteins with molecular weights of 70, 50, and 200kDa, and is found in neuronal axon (Reviewed in (Yuan et al., 2012). Doublecortin X (DCX) is a 40kDa microtubule-associated protein highly expressed in the migrating neuroblasts, and in cell bodies and leading processes of migrating neurons, and the axons of differentiating neurons in fetal and neonatal mouse brain (Francis et al., 1999, Walker et al., 2007). In addition to embryonic brain, DCX is also found in the regions of adult brain where neurogenesis is an ongoing process such as the SVZ and the DG suggesting it as a marker for both corticogenesis and neurogenesis (Reviewed in (Walker et al., 2007)). Thus, DCX is an ideal marker for newly born neurons but not mature neurons in the developing and adult brain and its expression found to be overlapped with B-tubulin III (Nakano and Kornblum, 2003, Walker et al., 2007).

Newly and mature neurons can be detected by antibodies against some components of microtubules such as Beta tubulin III (or B-tub3) and Microtubule Associated Protein2 **(**MAP2) respectively (Luskin et al., 1997, Soltani et al., 2005). B-tub3 is the major component of the microtubule widely used as a marker of newly differentiated neurons (Luskin et al., 1997) and antibody commercially available for B-tub III is TuJ1. It is also found to be expressed in embryonic cells, and in areas where neurogenesis occur like the hippocampus (Menezes and Luskin, 1994). These microtubules have alpha and beta tubulin isoforms, each about 55kD which are found in both axons and dendrites (Nakano and Kornblum, 2003). MAP2 belongs to the family of microtubule associated proteins that promote the assembly and stabilize microtubules (Soltani et al., 2005). There are three isoforms for this marker, MAP2a is found in the late postnatal period in mouse and localized in the dendrites (Harada et al., 2002), MAP2b exist during all the developmental stages of the brain, and MAP2c are expressed during early embryonic development in the axons (Cassimeris and Spittle, 2001). The expression of this protein stops when the brain matures except in the olfactory bulb and the cerebellum (Nakano and Kornblum, 2003). The available antibodies to this protein are found to be immunoreactive in all the 3 isoforms. The expression of B-tub III is seen in immature neurons and also in neural progenitor cells while MAP2 recognizes more mature neurons (Luskin et al., 1997). Neuronal nuclear antigen (NeuN) is a member of the nuclear protein family expressed in the neurons (existing mitotic cell division to their final differentiation) in most areas of the CNS in adult mice, except in the Purkinje cells of cerebellum and olfactory bulb mitral cells (Mullen et al., 1992). This

protein is found in the nuclei and the perinuclear cytoplasm but is absent in both axons and dendrites (Mullen et al., 1992).

Another marker for postmitotic neurons is Calbindin, a D28k intracellular calcium binding protein expressed with remarkably high levels in the Purkinje cells in the cerebellum and in the granule cells of the DG (Sequier et al., 1988). It is an excellent marker for the study of both normal and degenerated PCs since the immunoreactivity for this marker did not change in both cases (Verdes et al., 2010). The expression of Calbindin first appears in the migrating PCs at E14 in mice and E17 in rats where these Calbindin^{+} PCs come in contact with the radial fibers that guide their migration (Reviewed in (Yamada and Watanabe, 2002)).

1.1.5.4 Neural stem cell markers

NSCs can be isolated using the neurosphere assay which identifies these cells based on some in vitro characteristics such as self-renewing ability and their response to growth factors such as EGF and FGF-2 (Reynolds and Weiss, 1992, Weiss et al., 1996). The use of some specific markers makes it possible to distinguish stem cells in a mixed population. However, there is no exclusive marker for NSCs; but co-expression of several of these markers has been used to identify stem cells. Some of the markers used to identify neural stem/progenitor cells are described below.

Sox gene family

A family of transcription factor genes involved in many developmental processes such as male sex determination, CNS neurogenesis, eye development, and chondrogenesis (Kiefer, 2007, Lefebvre et al., 2007). From a total of 30 Sox genes identified, 20 have been found in human and mouse genomes (Kiefer, 2007). In mammals, Sox genes are divided into 8 groups from (A-H) depending

on the phylogenetic analysis of their high motility group (HMG) box sequences (Pevny and LovellBadge, 1997). Group B is divided into 2 subgroups: SoxB1 (includes the transcriptional factors Sox1, Sox2 and Sox3) and SoxB2 (includes the transcriptional repressors Sox14 and Sox21) (Bowles et al., 2000). Sox proteins bind to DNA through their HMG domain, they either activate or repress transcription (Kiefer, 2007). SoxB1 (Sox1, Sox2, Sox3) genes are expressed during early embryogenesis in the nervous system and they are involved in cell fate determination (Uwanogho et al., 1995, Rex et al., 1997). Studies have reported that SoxB family are expressed in neural progenitor cells during development and in adult (Reviewed in (Graham et al., 2003)). Sox1 plays a critical role in neural determination and differentiation (Pevny et al., 1998). It has been shown that Sox1 expression starts with the onset of neural induction and is restricted to the neuroectoderm, before it is downregulated as the progenitor cells exit from mitosis and differentiate, suggesting Sox1 as a marker of neural progenitor cells (Pevny et al., 1998). Studies have shown that Sox1 is expressed in a population of $GFAP^+$ astrocytes in the SGZ and in CA1 region of the hippocampus, adult multipotent NSCs, and putative neural-like stem cells in the adult cerebellum (Kan et al., 2007, Venere et al., 2012, Cai et al., 2004, Sottile et al., 2006).

Expression of the transcription factor Sox2 is highly detected in embryonic stem cells (Pevny and Placzek, 2005, Masui et al., 2007) and it has been shown that the downregulation of Sox2 induces differentiation in mouse ES cells, implicating its essential role in maintaining their pluripotency (Masui et al., 2007). Moreover, Sox2 expression has been reported in proliferating NSCs and supress their differentiation, suggesting its role in maintaining neural progenitor fate (Graham

et al., 2003, Pevny and Rao, 2003). Sox2 expression was also detected in embryonic radial glia and the expression is maintained in the GFAP positive population in the SVZ of adult brain (Pevny and Rao, 2003, Graham et al., 2003).

Sox3, the third member of the subfamily SoxB1 genes, seems to be expressed in the proliferating progenitor cells during early rodent embryogenesis (Collignon et al., 1996, Rex et al., 1997). Sox3 gene expression is found to be important for normal brain development and Sox3 null mice display congenital abnormalities in some brain parts such as the hippocampus (Reviewed in (Rogers et al., 2013)). Sox9 is a member of the SoxE subgroup shown to be expressed in prechondrogenic and chondrogenic tissues (Zhao et al., 1997), in male gonads (Kent et al., 1996), and in stem/progenitor cells in the adult intestine and liver (Reviewed in (Sarkar and Hochedlinger, 2013)). It has been shown that Sox9 is critical transcription factors determining glial lineages and found to be expressed in the radial glial progenitor of embryonic and adult brain (Stolt et al., 2003, Scott et al., 2010).It is also expressed in VZ (Brazel et al., 2005; Pompolo and Harley, 2001; Ferri et al., 2004), and in the Bergmann glial cells in the PCL of postnatal cerebellum (Pompolo and Harley, 2001; Sottile et al., 2006). In all cells of the developing CNS and in the NSCs of adult subependymal zone (SEZ), Sox9 is reported to be co-expressed with Sox2 (Scott et al., 2010). Sox 9 has been shown to be co-expressed with Sox1 and Sox2 in the Bergmann glia in the adult human and mouse, suggesting Sox9 as a new candidate marker for NSCs (Sottile et al., 2006; Alcock et al., 2007).

Nestin

Nestin is recognised as an intermediate filament expressed in progenitor cells during neurogenesis (Dahlstrand et al., 1995, Lendahl et al., 1990), and found to be also expressed in the proliferating cells in the adult mouse striatum (Reynolds and Weiss, 1992). In the developing rat CNS, it is expressed in the neuroepithelium at E12, and stops being expressed by E13 and the cells become Nestin negative (Hockfield and McKAY, 1985). Following differentiation, Nestin expression ceases and is replaced by other intermediate filaments such as GFAP in astrocytes and neurofilaments in neurons ((Lendahl et al., 1990, Bazan et al., 2004). Nestin expression is not reported in the adult brain, however, it has been shown to be found in the postnatal rat cerebellum at P2, then slightly decreases at P12, and is lost by P21 when the tissue has matured (Hockfield and McKay, 1985). Rat 401 is a commercially available antibody used to detect Nestin (Hockfield and McKAY, 1985). Currently Nestin is regarded as the main marker for the identification of neural precursor cells in the CNS (Lendahl et al., 1990). Musashi is an RNA binding protein which is highly expressed in the embryonic and adult neural stem/progenitor cells (Okano et al., 2005) while, its expression is lost in the mature neurons and glial cells (Sakakibara et al., 1996).

Musashi

Musashi plays an important role in the self-renewal capacity of NSCs, repressing the translation of mRNA encoding genes of some proteins such as tramtrack69 (TTK69) thereby inhibiting neuronal differentiation, inhibiting the progression of mitotic cell division (Okano et al., 2005, Nishimoto and Okano, 2010). Musashi is expressed in Nestin-positive cells but is not expressed in mature neurons and astrocyte (Crespel et al., 2005). Thus, Musashi might represent an additional

marker for neuronal progenitor cells within the brain (Von Bohlen and Halbach, 2011).

1.1.5.5 Differentiation of NSCs

Differentiation is the process by which a neural stem cell can give rise to specialised cell type in the CNS (Jin and Galvan, 2007). In vivo, these NSCs normally migrate to the sites of differentiation in the mature brain where they have two fates, most of them fully differentiate or maintain as quiescent stem cells (Jin and Galvan, 2007). Studies have indicated that proliferation and differentiation of NSCs is affected by internal and external signalling factors (Liu et al., 2012). Defining these signalling factors is very important for promoting the desired cell fate, which is of interest for the field of regenerative medicine where the directed control of endogenous stem cells is being investigated for therapeutic purposes. In vitro, upon the removal of mitogens from the culturing media and supplementation with serum, the progenitors have been shown to differentiate into neurons, astrocytes, and oligodendrocytes (Yadirgi and Marino, 2009).

1.1.5.6 Role of NSCs in the adult brain

Endogenous NSCs normally divide and the new progenitors migrate to the sites of differentiation in the mature brain where they have two fates, most of them fully differentiate or maintain as quiescent stem cells (Jin and Galvan, 2007). Evidence from studies has shown that newly generated neurons in the hippocampus have important role in learning and memory (Gould et al., 1999, Shors et al., 2001). The latter studies have shown that the generation of cells in some areas of the brain such as SVZ, SGZ, and olfactory bulb is regulated by physiological conditions such as stress and training that finally improve the learning tasks of the

tested animals. In vitro studies suggest that NSCs isolated from the SVZ and SGZ of adult brain are able to develop into mature neurons exhibiting functional properties (Jin and Galvan, 2007). These neurons were shown to express mature neuronal markers such as NeuN and Calbindin, and neuron-specific enolase, integrate into existing functional circuitry, receive synaptic input, and play a role in memory and learning process (Reviewed in (Jin and Galvan, 2007)). In mice expressing GFP under the control of Nestin enhancer showed the ability to generate neurons with dopaminergic phenotype both in vitro and in vivo. Moreover, infusion of EGF and FGF-2 result in the activation and proliferation of endogenous NSCs in the adult mouse SVZ (Craig et al., 1996).

On the other hand, exogenous NSCs isolated from fetal and adult brain represent promising options for the repair of many neurodegenerative disorders. Cultured NSCs from different sources such as human NSCs lines, hematopoietic stem cells, embryonic stem cells, and neuronal progenitors from rodents can be transplanted into injured brain to restore neuronal networks (Reviewed in (Liu et al., 2009). Regulation of NSCs proliferation and differentiation would help to understand how to recruit endogenous or exogenous NSC for future approaches for regenerative medicine.

1.2 Growth factor responsiveness of NSC

1.2.1 Fibroblast Growth Factors (FGFs)

Fibroblast growth factors (FGFs) represent a family of growth factors consisting of 23 members of structurally related polypeptides, of which 10 are found to be expressed in the CNS of human and mouse (Ford-Perriss et al., 2001, Dono, 2003, Coutu and Galipeau, 2011). FGF-2 was first identified as a mitogen in 1974 after

been isolated from bovine pituitary gland (Coutu and Galipeau, 2011). FGFs range in size from 17 to 34 kDa with an internal core of 34 highly conserved amino acid residues (Reuss and von Bohlen und Halbach, 2003). In mammals, members of FGF ligands bind through 4 alternating splice form of tyrosine kinase receptors bound to the cell surface (Ford-Perriss et al., 2001; Dono, 2003).

FGFs bind to their receptors as monomers, resulting in the dimerization and phosphorylation of the receptor triggering initiation of an intracellular cascade of signal transduction. FGF receptor (FGFR) activation is modulated by heparin-sulfate proteoglycans, which facilitate the assembly of ligand-receptor complex (Coutu and Galipeau, 2011). FGF signaling through the FGF receptors play important role during embryonic development including patterning of germ layer, coordinating the movement of cells during gastrulation, maintenance of axial and paraxial mesoderm formation, induction of organogenesis and morphogenesis (Reviewed in (Dorey and Amaya, 2010, Goetz and Mohammadi, 2013)). Endocrine FGFs regulate various metabolic functions in the body such as lipid, phosphate, and glucose metabolism (Reviewed in (Goetz and Mohammadi, 2013). In the CNS, FGF signaling results in neural induction and anterior-posterior (AP) patterning through the blocking of bone morphogenetic protein (BMP) signaling (Reviewed in (De Robertis and Kuroda, 2004)).

FGF signaling has also been described to sustain growth in various cell types including those represented in the CNS (Dono, 2003), for which it is thought to mediate various cellular responses such as proliferation, differentiation, migration, neuronal and glial cell survival (Ciccolini and Svendsen, 1998, Ford-Perriss et al., 2001, Pollard et al., 2006).

1.2.2 Epidermal growth factors (EGFs)

Epidermal growth factors (EGFs) are a family of growth factor proteins with highly similar structural and biological activity, which play an influential role in cell growth, proliferation, and differentiation (Harris et al., 2003, Dreux et al., 2006). It is a 53-amino acid protein with a molecular weight of 6045Da with 6 cysteine residues that form 3 intramolecular disulphide bonds essential for effective receptor binding (Harris et al., 2003).

EGF receptors (EGFRs) are transmembrane glycoproteins of 4 members of ErbB family (ErbB1, ErbB2, ErbB3, and ErbB4) receptors with tyrosine kinase activity (Dreux et al., 2006). These polypeptide proteins of about 170 kDa with a single chain of 1186 amino acids consist of extracellular receptor domain, a transmembrane region, and an intracellular domain with tyrosine kinase activity (Herbst, 2004). Ligand binding to EGFR activates tyrosine kinase through phosphorylation initiating a signal transduction cascade involved in a variety of biological functions such proliferation, survival, differentiation, apoptosis, and migration (Yarden and Sliwkowski, 2001).

Reynold and Weiss, (1992), (1996) showed the first evidence concerning the proliferative effect of EGF on adult SVZ neural progenitor cells. They isolated cells from mouse LV able to generate neurons and astrocytes only when grown in EGF, forming a cluster of proliferating cells called neurospheres. Furthermore, infusion of EGF into the adult brain resulted in increased proliferation in the area surrounding the ventricles (Craig et al., 1996). They observed that cells stimulated by the EGF infusion express EGFR, suggesting the role of EGF on NSCs (Craig et al., 1996).

1.2.3 Responsiveness of NSCs to EGF and FGF-2

The responsiveness of NSCs to both EGF and FGF also differ during early and late stages of development (Tropepe et al., 1999, Zhu et al., 1999, Qian et al., 2000). FGF-2 responsive cells appear in mouse early embryonic forebrain (E8.5), and then acquire the responsiveness to EGF at later stages of development (Weiss et al., 1996). The responsiveness of neural precursor cells to EGF and FGF may also be regulated by cross-talks between the two pathways, as EGF responsiveness is influenced by FGF-2 early during development (SCHWINDT et al., 2009), and then the cells switch in growth factor responsiveness and give rise to precursors responding to both EGF and FGF-2 after a number of mitotic cell division (Ciccolini and Svendsen, 1998, Ciccolini, 2001). Moreover, many studies have revealed that culturing NSCs as neurospheres in EGF and FGF-2 before differentiation does generate more neurons and glial cells respectively (Caldwell et al., 2004, Tropepe et al., 1999, Whittemore et al., 1999).

1.3 The Cerebellum

1.3.1 Cerebellar structure

The cerebellum (Latin cerebellum; little brain) is a part of the CNS located dorsal to the brain stem (Herrup and Kuemerle, 1997). It is composed of central vermis surrounded by two lateral hemispheres (Fig. 1.3). The vermis and the hemispheres are subdivided into numerous parallel fissures defining a special pattern of 10 lobules (Fig.1.3) (Chizhikov and Millen, 2003, Sudarov and Joyner, 2007).

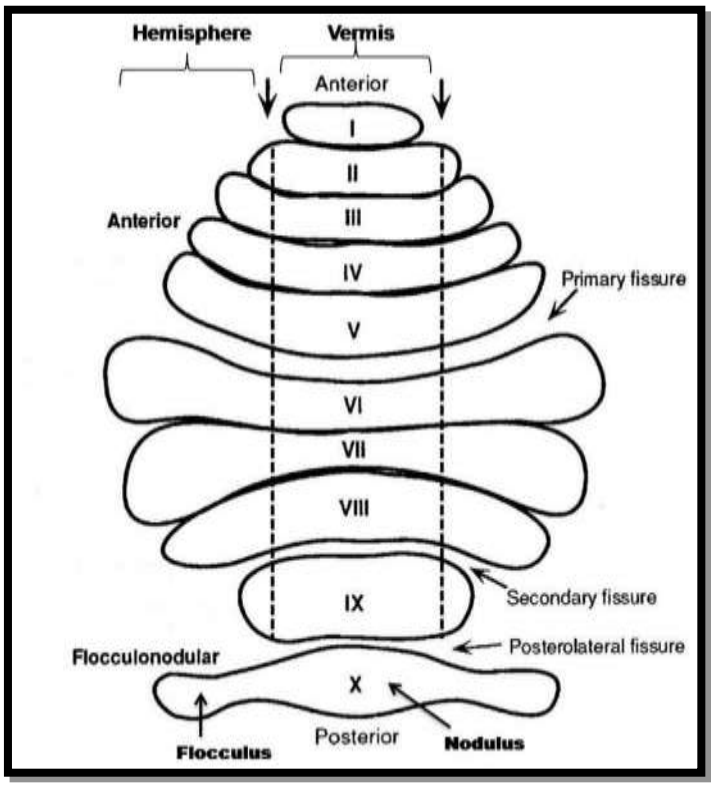

Figure 0.3 Simplified diagram of the cerebellum showing the fissures and lobules (I-X).The vermis and hemispheres are separated by the arrows and dotted line. Modified from (Herrup and Kuemerle, 1997).

A single folium consists of 3 distinct layers of well-known cell types referred to as cerebellar cortex that surround the white matter and deep cerebellar nuclei (Sudarov and Joyner, 2007). Three functional lobes can be distinguished in the gross anatomy of the cerebellar cortex, these are: (1) the anterior lobe (towards the front of the primary fissure), (2) the posterior lobe (dorsal to the primary fissure), and (3) the flocculonodular lobe (dorsal to the posterolateral fissure) (Fig. 1.3) (Hawkes, 2001, Herrup and Kuemerle, 1997).

The cerebellum is further subdivided from the rostral to the caudal axis into 10 vermal lobules mostly indicated by the roman numerals (I-X) (Fig. 1.4), the first

vermal lobules (I-V) starting from the rostral pole of the anterior lobe to the primary fissure, next are the central vermal lobules (VI-VIII) found between the primary and the secondary fissure, the 3rd lobule (IX) is located between the secondary fissure to the posterolateral fissure, and lastly the caudal most lobule (X), the flocculus and nodulus (subdivisions of the flocculonodular lobe) (Herrup and Kuemerle, 1997; Altman and Bayer, 1997). There is some species variation concerning the gross anatomy of the CB (Voogd and Glickstein, 1998). For example, the CB appears as single leaf in amphibians and reptiles, while in birds and mammals, the CB is foliated in more complex way (Voogd and Glickstein, 1998).

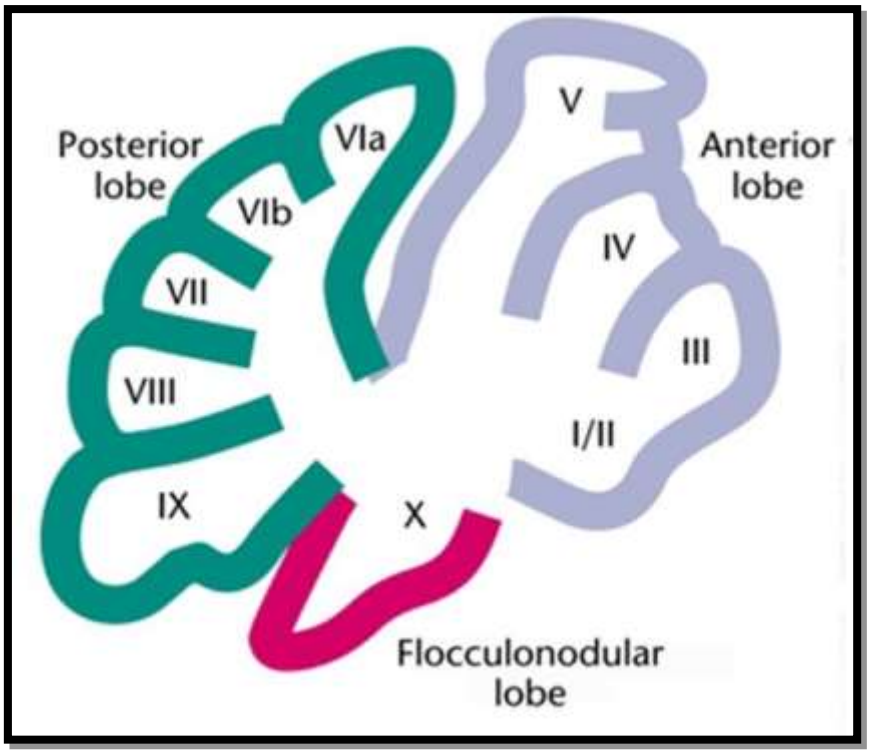

Figure 0.4 Sagittal view of mouse cerebellum through the vermis. The lobules (I-V) constitute the anterior lobe, the lobules (VI-IX) constitute the posterior lobe, and X represent the flocculonodular lobe. After (Hawkes, 2001).

1.3.2 Cellular organization of the cerebellar cortex

The cerebellum is composed of two parts:

1. Grey matter referred to as cereberal cortex with 5 different types of neurons.
2. White matter or medulla within which 4 pairs of deep cerebellar nuclei are embedded.

The cerebellar cortex is composed of three layers (Fig. 1.5) with 5 different cell types: the inner granular layer containing granule cells and Golgi cells, the outer molecular layer containing granule cell axons, Purkinje cell dendrite, Bergmann glial fibers, basket and stellate cells, and the monolayer of purkinje cells (Sudarov and Joyner, 2007).

The molecular layer contains 2 types of neurons, Basket cells which are located near the Purkinje cell bodies, and stellate cells confined to the outer molecular layer. The molecular layer also contains the dendrites of both Purkinje and Golgi cells beside the axons of granule cells (Astori et al., 2009; Carpenter, 1985). The Purkinje layer consists of numerous large cell bodies (Fig. 1.5) with their dendrites extending up to the molecular layer and their myelinated axons penetrating down to the deep cerebellar nuclei (Carpenter, 1985). While the granular layer contains numerous granule cells with chromatic nuclei; these cells have unmyelinated axons entering the molecular layer (Apps and Garwicz, 2005; Carpenter, 1985).

1.3.2.1 Purkinje cells (PCs)

One of the first neurons identified by Purkinje in 1837 (Hawkes, 2001), PCs are the largest neurons in the brain but not the most abundant (Hawkes, 2001). They are the main source of cerebellar output, forming a monolayer of cells between

the molecular and the granular layer of the cerebellar cortex (Sudarov and Joyner, 2007; Voogd and Glickstein, 1998). Their flask- shaped cell bodies (soma) sizes greatly depend on the size of the animal, with larger animals exhibiting larger cell bodies (Hawkes, 2001).

The axons of PCs are myelinated and extend down through the granular layer into the deep cerebellar nuclei (Fig. 1.5) (Voogd and Glickstein, 1998; Hawkes, 2001). They possess numerous dendrites penetrating the molecular layer, where they progressively arborize making multiple synapses (Voogd and Glickstein, 1998). These dendrities are composed of smooth shaft on which climbing fibers terminate, and a dendritic spine on which the parallel fibers terminate (Hawkes, 2001). PCs can be detected immunohistochemically with antibodies to the calcium binding protein calbindin, which can distinctively label the Purkinje cells.

1.3.2.2 Granule cell

The granule cell is the smallest and most abundant cell type in the cortex, with their dendrite synapse with the afferent mossy fibres. These densely packed cells have unmyelinated axons that extend into the upper molecular layer, bifurcate to form horizontal fibers called parallel fibers making synapses with the PCs (Fig. 1.5) (Voogd and Glickstein, 1998).

1.3.2.3 Basket Cells

The soma of the basket cells is found in the vicinity of Purkinje cell bodies. Their dendrites (Fig. 1.5) enter the molecular layer to form synaptic contact with the parallel fibers, and their unmyelinated axons surround the nearby Purkinje cell bodies in a basket-like network making inhibitory synaptic contacts with these Purkinje cells (Carpenter, 1985, Hawkes, 2001).

1.3.2.4 Stellate cells

Another type of inhibitory interneuron having their soma located in the upper molecular layer is the stellate cell (Hawkes, 2001). Their axons make synapses with the PC dendrites as well as other stellate cells (Fig. 1.5). They receive excitatory inputs from the parallel fibers to inhibit the purkinje cells by GABA neurotransmitters (Hawkes, 2001, Astori et al., 2009).

1.3.2.5 Golgi cell

The somata of this inhibitory interneuron are located in the granular layer (Fig. 1.5) (Hawkes, 2001). Their dendrites extend into the molecular layer, where they contact the synapses of the parallel fibers, while their axonal ramifications in the granular layer form inhibitory synapses with the mossy fibers within the glomeruli (Hawkes, 2001).

1.3.3 Cerebellar deep nuclei

The cerebellar deep nuclei (DCN) are clusters of neurons embedded within the white matter (Herrup and Kuemerle, 1997, Sugihara, 2011). They are the major outputs of the cerebellum (Sugihara, 2011, Baumel et al., 2009). It has been estimated that 50-100,000 neurons constitute the DCN (Baumel et al., 2009). These nuclei were first divided by Stilling (1878) into (from medial to lateral), the fastegial, the globose, the emboliform, and the dentate (Larsell and Jansen, 1972; Hawkes, 2001). They sustain their inputs, both inhibitory and excitatory, from the PCs in the cortex and climbing fibers of the inferior olive neurons (Sugihara, 2011, Baumel et al., 2009) as well as inputs from mossy fibers (Chan-Palay, 1977; Sugihara, 2011). Efferent fibers of the DCN leave the cerebellum to the

other parts of the brain through the superior and inferior cerebellar peduncles (Baumel et al., 2009).

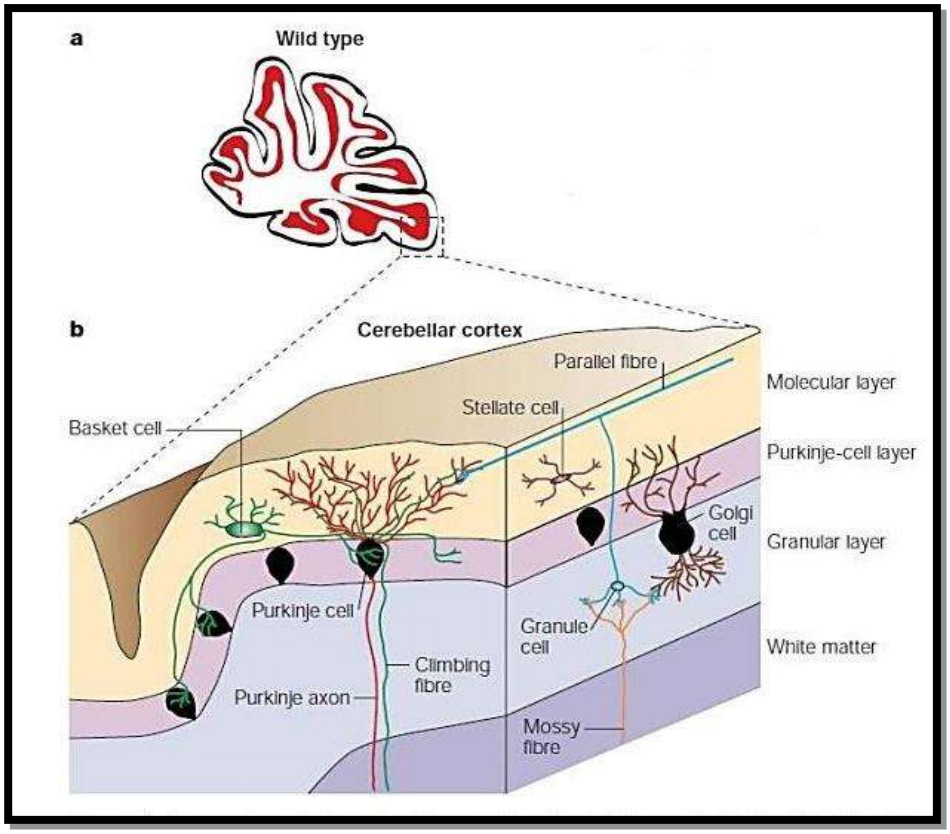

Figure 0.5 Basic cerebellum structure. The figure showing the main types of cells in the cortex, their locations and synaptic contacts. The figure also illustrates the cerebellar nuclei and their projections into the cortex. Modified from (Kobielak and Fuchs, 2004).

1.3.4 Functions of the cerebellum

The cerebellum maintains the body in an equilibrium state through the coordination of motor control, since any failure in the proper function or injury of the cerebellum leads to loss of movement control, hypotonia and ataxia (Carpenter, 1985, Herrup and Kuemerle, 1997). These functions are promoted by the distinctive organization of the cerebellar synapses and its efferent and afferent

pathways (Mauk et al., 2000). More recent evidence suggested that the cerebellum is involved in the processes of emotion, cognition, and learning (Apps and Garwicz, 2005, Sudarov and Joyner, 2007).

1.4 Development of the cerebellum

In vertebrates, the CNS arises from an epithelial sheet of cells of dorsal ectoderm, the neural plate, which closes (nearly at day E8.5 in mouse) to form the neural tube (Herrup and Kuemerle, 1997, Chizhikov and Millen, 2003). During development, the anterior end of the neural tube of the mouse embryo forms the forebrain which is composed of the telencephalon and the diencephalon, whereas the posterior parts of the neural tube give rise to the midbrain, or more often called the mesencephlaon, the hindbrain, and the spinal cord (Joyner, 2002).

The hindbrain is divided into 7 segments called rhombomeres, and the most anterior one (rhombomere 1) is called the metencephalon, from which the cerebellum arises by the embryonic day E9 in mice (Reviewed in (Sillitoe and Joyner, 2007)). The posterior rhombomeres are called the rhombencephalon (Chizhikov and Millen, 2003). Between E9-12, the dorsal rhombomere 1 rotates a 90 degree to form a wing-like cerebellar premordia which unite dorsally to form the vermis and lateral hemispheres (Sgaier et al., 2005).The cerebellum is a unique structure in the brain because its neurons arise from two germinal zones (Goldowitz and Hamre, 1998). The germinal matrix is composed of the neuroepithelial ventricular zone and a region known as trigone or rhombic lip, which later forms a secondary germinal zone, the external granular layer (EGL) (Goldowitz and Hamre, 1998). The EGL forms the internal granular layer (IGL) consisting of numerous granule cell neuroblasts that migrate through the

molecular layer guided by radial fibers of Bergmann glial cells (Goldowitz and Hamre, 1998).

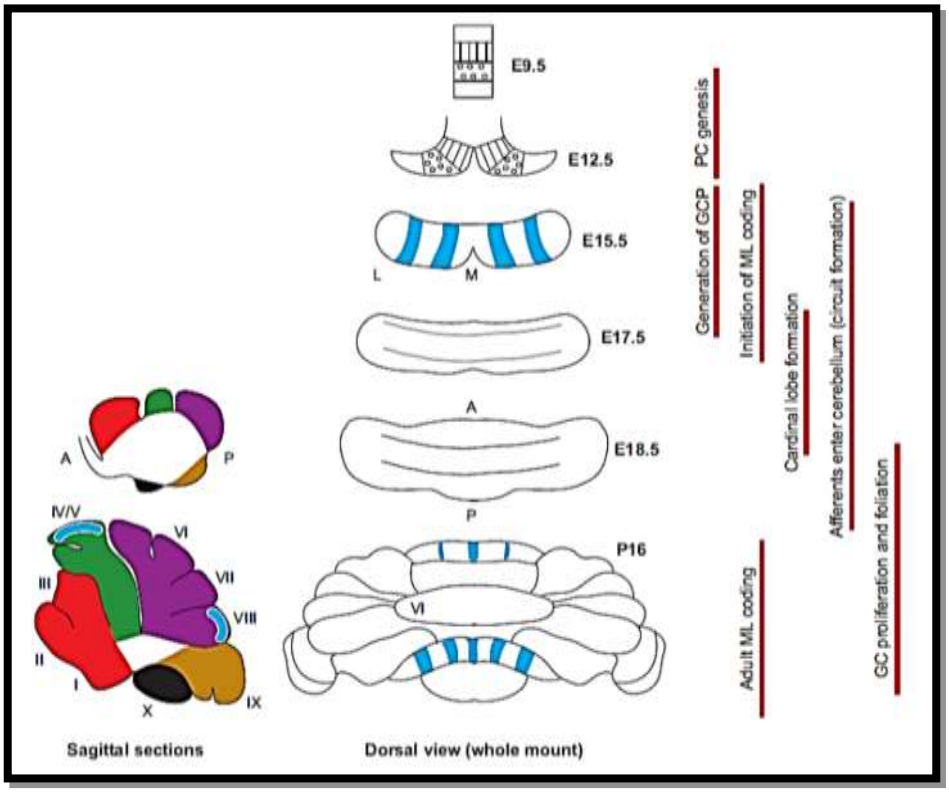

Figure 0.6 Mouse cerebellar development. After (Sillitoe and Joyner, 2007).

The cerebellum is then converted into a curved sausage-shape structure by the embryonic day E15.5. Additional structural transformation is achieved by E17, and the cerebellum becomes folded into a number of fissures (Fig. 1.6) along its anterior- posterior (AP) axis by approximately E18.5 (Sillitoe and Joyner, 2007), and the final maturation of the cerebellum is achieved by the third postnatal weeks in mice (Sillitoe and Joyner, 2007).

1.5 Neuroglia of the cerebellum

Three basic types of neuroglia have been recognized in the cerebellum, these are: (1) astrocytes, (2) microglia, and (3) oligodendrocytes. Moreover, another specific type of astrocytic neuroglia has also been identified in the cerebellum called epithelial cells of Golgi. Their process was first revealed by Bergmann (1861), but much of the knowledge about these radial glial cells was described by Ramon y Cajal (1911) and Golgi which then named Golgi epithelial cells (Larsell and Jansen, 1972).

Bergmann glial cells constitutes about 90% of cerebellar glia characterized by unipolar ovoid cell bodies located among the Purkinje cells (Fig. 1.7) (Yamada and Watanabe, 2002, Lopez-Bayghen and Ortega, 2011). BG processes (Bergmann fibers) extend and distribute radially through the molecular layer to the pial surface forming conical endfeet at their terminals (Sudarov and Joyner, 2007), where they make synapses with the PCs dendrites (Voogd and Glickstein, 1998). It is thought that the Bergmann glia radial fibers guide the granule cells migration during development, and provide structural support for Purkinje cells in the adult cerebellum (Yamada and Watanabe, 2002).

1.5.1 Origin of cerebellar astrocytes

Ramon y Cajal (1911) and later Altman and Bayer (1997) postulated that CB glia in rats originated after PC genesis at E17 by proliferating progenitor cells residing in the ventricular neuroepithelium (VN), and from NSCs in the mouse WM postnatally (Lee et al., 2005).

Two germinal zones within the VN were identified; the rhombic lip (RL) giving rise to glutamatergic neurons, granule cells, and bipolar brush cells; and the

ventricular zone from which GABAergic neurons including PCs and inhibitory neurons are originating (Reviewed in (Leto et al., 2006)).

1.5.2 Radial glia as progenitors

During CNS development, pseudostratified epithelium lining the ventricle represents the neural progenitors which become neurons and migrate out guided by the radial glial processes (Pollard et al., 2006). During the time of neurogenesis, these progenitors undergo differentiation into radial glia (Sild and Ruthazer, 2011). These radial glial cells divide asymmetrically and give rise to neurons, or intermediate progenitor cells that persist in the SVZ and serve as multipotent adult NSCs (Doetsch et al., 1999; Merkle et al., 2004). It is well known that during development besides generating astrocytes, radial glia also serve as neural progenitors in the developing and adult CNS (Alvarez-Buylla et al., 2001, Malatesta et al., 2000, Merkle et al., 2004). Radial glial cells in the adult such as Muller cells and spinal cord radial glia are capable of producing neurons and oligodendrocytes respectively in response to injury (Sild and Ruthazer, 2011). Bergmann glial is another type of radial glial cells in the adult CB that is another candidate NSCs based on previous observation demonstrated their expression of NSCs markers (Sottile et al., 2006, Alcock and Sottile, 2009) and this population will be the main focus of this thesis.

During early postnatal life, radial glia reside in the subventricular layer (SVL) and are capable of generating different cell types such as neurons, astrocytes, oligodendrocytes and ependymal cells (Merkle et al., 2004). They used cre-loxP system to specifically label radial glial cells in the striatum of neonatal mice through the injection of adenovirus expressing the cre-recombinase. This method successfully revealed that the radial glial cells in the SVZ were the source of

neurons and not only produce NSCs in the adult brain (Merkle et al., 2004). Identification of radial glial population that serve as NSCs in other parts of adult brain will be important to test whether they can give rise to neurons which may be of therapeutic value for neurodegenerative disease.

1.5.3 Bergmann Glia: Description, Origin and Development

According to Ramon y Cajal (1911), glia in the cerebellum are grouped into 3 categories based on their position and morphology (Buffo and Rossi, 2013)

1. Glial cells located in the white matter (WM) including the oligodendrocytes and characterised by their processes being aligned along the axonal tract directly.
2. Granular layer astrocytic cells with star shaped processes.
3. Bergmann glia located between Purkinje cell (PC) bodies, with long radially oriented fibers presenting the upper molecular layer ending on the pial surface.

BG is one of the earliest cells that develop in the cerebellum and persist throughout the adult life span (Sild and Ruthazer, 2011). Their cell bodies resemble other cerebellar astrocytes and are located in the PC layer (PCL) (Fig. 1.7) with their numerous processes extending up to the pial surface of the molecular layer (ML) (Xu et al., 2013). The BG fibers differ from that of the radial glia by possessing multiple fibers (from 3-6/cell) spanning the molecular layer (ML) and ending on the pial surface to form palisades parallel to the long axis of each folium (Buffo and Rossi, 2013). It is thought that BG originates from the radial glia of the ventricular zone (VZ) through the retraction of the ependymal processes and displacement of cell bodies toward the cortex (Buffo and Rossi, 2013).

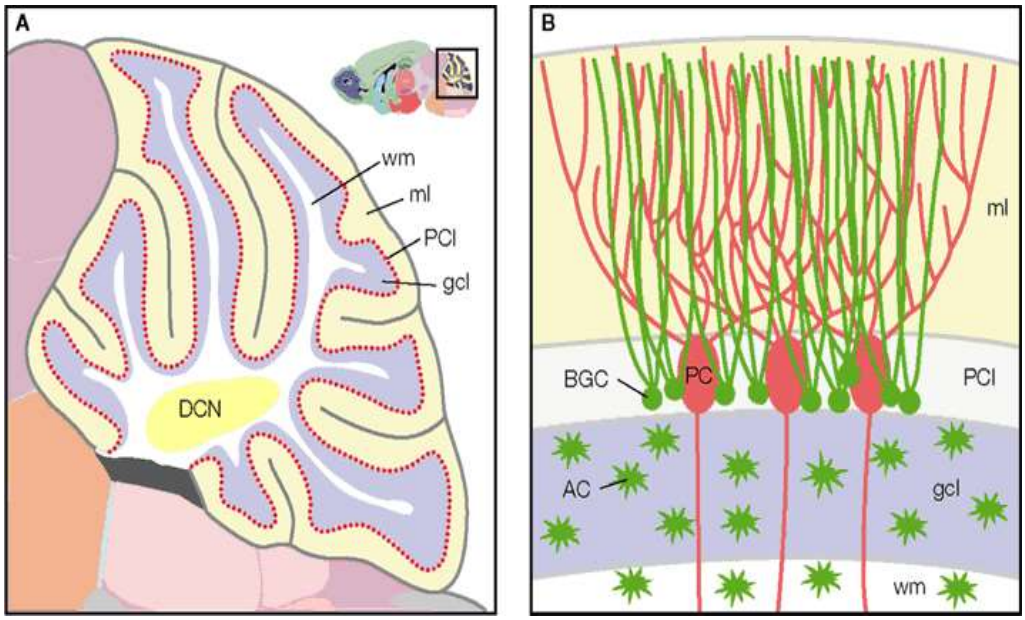

Figure 0.7 Parasagittal section through the cerebellum (A) showing the location of Bergmann glia. (B) Bergmann glial cell bodies (green) are located in the PCL between the Purkinje cell bodies (red), and their radial fibers are extended up to the pial surface of the ML. After (Tanaka et al., 2008).
PCl, Purkinje cell layer; **ml**, Molecular layer**; gcl,** granular cell layer; **wm**, white matter

Although in vivo studies showed that progenitors within the EGL only generate granule cells, in Math1/Math1 null chimeras, a specific marker for glutamatergic neurons derived from the RL, it was observed that some BG may be derived from RL precursors (Reviewed in Buffo and Rossi, 2013). However, studies have shown that BG cell bodies (from E14 to P7) migrate together with the PC bodies from the VZ crossing the mantle zone forming the PCL (Yamada et al., 2000, Yamada and Watanabe, 2002).

Morphologically, BG are largely similar between mouse, human, and monkey, but their fibers length depend on the thickness of the ML (Siegel et al., 1991). Human and monkeys have thick ML, thus having longer BG processes, while

mouse and rats have shorter distance between BG cell bodies and the pial surface (Siegel et al., 1991).

1.5.4 Differentiation of Bergmann Glia

During rat development, the radial glia somata migrate at E15 from the ventricular surface toward the pial surface, this migration coinciding with the migration of PCs and granule neurons along the radial glial fibers (Bellamy, 2006). At P15, granule cells begin to migrate from the external granular layer (EGL) to their final position in the internal granular layer (IGL) guided by BG fibers (Rakic, 1971). This migration coincides with the start of synaptogenesis by which the dendritic tree of PCs elaborates and grows actively (Yamada et al., 2000). At this time, BG undergo morphological changes in which their rod-like fibers transform into more reticular network, ensheathing the newly formed synapses on PCs (Yamada et al., 2000). By P25, neuronal migration, synaptogenesis, and BG differentiation are achieved (Bellamy et al., 2006).

1.5.5 Functions of Bergmann glia

In normal cerebellar cortex, each PC body is surrounded by 8 BG cells with their cell bodies interposed between the PC rows, ensheathing somata and dendrites of PCs, both inhibitory and excitatory synapse. This leads to the removal of glutamate from the synaptic clefts via transporters expression (Buffo and Rossi, 2013). BG is essential for the correct foliation and layering of CB cortex, and help PC dendrites elaboration, a process essential for establishing circuit connectivity (Buffo and Rossi, 2013, Reeber et al., 2014). Their radial fibers act as a scaffold during CB development guiding the granule cells that migrate inward from the EGL to the IGL (Xu et al., 2013). This indicates that BG fibers are associated

structurally and functionally with migrating granule cells during development and with mature PCs in the adult cerebellum. After development, BG is involved in many essential processes such as structural support, plasticity, synapse maintenance, and potassium homeostasis through glutamate uptake (Bellamy, 2006; Reviewed in (Koirala and Corfas, 2010). It is important for proper BG function that their fibers outgrowth and layering are based on the tight anchorage of their endfeet with subpial basement membrane (Koirala and Corfas, 2010). Alteration in BG function results in defective endfoot anchorage of their fibers to the basement membrane, which finally leads to a number of phenotypic changes including matrix disorganization, fusion of the folia at the pial surface, decreased granule cell number and migration failure (Buffo and Rossi, 2013).

1.5.6 Cerebellar neurons Birthdates

Goldwitz and Hamre, (1998) assumed that the nuclear neuron is the first neuron leaving the VZ and migrating to the cortex, and this is shown to happen during E10-12 in mice, while the Purkinje cells are born and depart from the VZ by E11-13 in mice and E13-16 in rats (Reviewed in Yamada and Watanabe, 2002). The deep cerebellar nuclei develop from both the VZ and the rhombic lip (Hoshino et al., 2005). According to study from (Altman and Bayer, 1997), the deep nuclei neurons are born by E13-15 with the highest rate of production on E14. The deep cerebellar nuclei (DCN) neurons that arise from the VZ migrate radially to their final destination (Wang et al., 2005), while neurons derived from the rhombic lip pass through the cerebellar cortex and finally migrate in a radial fashion to reach and settle in the deep cerebellum (Hoshino et al., 2005, Altman and Bayer, 1997). Final organization of the cerebellum takes place in late embryonic development (E17 in mice and E22 in rats) in which the 3 lobes are produced.

1.6 Damage to the Cerebellum

As discussed earlier in this chapter, the CB is involved in many functions such as maintaining motor coordination, emotion, cognition, and learning (Reviewed in (Rebber et al., 2013)). Any failure in the proper function or lesions of the cerebellum leads to incoordination of balance, gait ataxia, hypotonia, dystonia, vertigo, medulloblastoma, and multiple sclerosis (Carpenter, 1985; Herrup and Kuemerle, 1997, Reeber et al., 2013). Damage to the cerebellum can occur as a result of tumours, inflammation, injuries, ischemia, and hereditary neurodegerative diseases (Cendelin, 2014).

1.6.1 Hereditary cerebellar ataxias

The hereditary cerebellar ataxias comprise a group of genetic disorders characterised by progressive loss of coordination of gait, eye and hand movement, and atrophy of the cerebellum (Bird, 2015). It can be classified depending on the pattern of inheritance into autosomal recessive, autosomal dominant, mitochondrial, and X linked ataxias (Jayadev and Bird, 2013).

1.6.1.1 Autosomal Recessive Ataxia

Friedreich Ataxia is the most common ataxia occurring before 25 years of age and characterised by slow progression of the disease (Bird, 2015). This type is caused by a triplet GAA abnormal expansion in intron 1 of frataxin (FXN) (Jayadev and Bird, 2013).

In Ataxia-telangiectasia, the onset is much earlier, between 1-4 years of age (Jayadev and Bird, 2013). It is characterised by an increased risk of cancer such as leukaemia and lymphoma, frequent infections, oculomotor apraxia, and immunodeficiency (Jayadev and Bird, 2013; Bird, 2015).

1.6.1.2 Autosomal Dominant Ataxia

This type of ataxia, refers to as spinocerebellar ataxias (SCA) are a complex group of progressive degenerative diseases occurring during the third and fourth decades of age (Durr, 2010, Bird, 2015). SCA can be classified into 30 subtypes, of which 7 are caused by expansions of the CAG repeats in SCA genes (Durr, 2010, Jayadev and Bird, 2013).

1.6.2 Mouse models of cerebellar degeneration

Cerebellar development and degeneration can be studied using experimental mouse models, which can be spontaneous or induced mutant mouse models.

1.6.2.1 Spontaneous mutant mouse model

Mutation models include lurcher, staggerer, reeler, weaver, Purkinje cell degeneration (*pcd*), hot-foot, and nervous (Lalonde and Strazielle, 2007). Except for the nervous type, the mutated genes responsible for the ataxia have been identified (Lalonde and Strazielle, 2007, Cendelin, 2014). In each model, the number of PCs lost differs during the time of development until adulthood ranging between 40%-100% (Triarhou et al., 1996). As a consequence of PC loss and atrophy, granule cells also degenerate in lurcher and staggerer mutant mice (Reviewed in (Lalonde and Strazielle, 2007)).

1.6.2.2 Induced mutant mouse

These new mutant animals include induced and targeted mutations, and chemically-induced mutations (mutagen substances) (Reviewed in (Cendelin, 2014)). Many of these mouse models can be genetically engineered to include the genes responsible for some human diseases to be studied in detail.

1.6.2.2.1 Purkinje Cell Degeneration (*pcd*): Phenotypic Characteristics

Purkinje cell degeneration (*pcd*) is an autosomal recessive mutation characterised by postnatal degeneration of all PCs between P15-P45 resulting in motor impairment called ataxia (Mullen et al., 1976; Wang et al., 2007; Chakrabarti et al., 2008; Baltanas et al., 2011). Homozygous ataxic *pcd* mice are characterised by normal appearance but are smaller in size than their littermate wild-types. They can be characterized ultrastructurally by P15 and clinically after P22 (Mullen et al., 1976). Secondary to PCs loss, thalamic neurons begin to degenerate between P50-P60; retinal photoreceptors and mitral neurons in the olfactory bulbs exhibit slow degeneration during the first year of postnatal life (Reviewed in (Wang and Morgan, 2007)). Beside PC and other cell type loss, adult male *pcd* mice are infertile because of abnormal shaped immotile sperms (Mullen et al., 1976, Chakrabarti et al., 2006).

The *pcd* was first discovered in mice by Mullen et al., (1976) in the C57BR/cdJ strain. In the *pcd* mice, the cerebellum appears structurally normal at P15 with regular synaptic pattern, and the degeneration begins afterward with marked gait ataxia at P20 (time of weaning) and then progresses rapidly over a period of 2 weeks resulting in > 99% of PCs loss by P35 (Mullen et al., 1976, Wang and Morgan, 2007, Chakrabarti et al., 2008). To date, 8 phenotypic alleles of *pcd* have been reported (pcd^{1J}, pcd^{2J}….pcd^{8J}) with 3 chemically induced ($pcd^{4, 6, Btlr}$) and one arising spontaneously (Wang and Morgan, 2007, Chakrabarti et al., 2010), and the online database resource provided by the Jackson laboratory reported two more alleles, pcd^{Btlr} and pcd^{JWG} (Reviewed in (Akita and Arai, 2009)). Most of them are severe alleles such as pcd^{1J}, pcd^{3J}, and pcd^{5J} displaying a dramatic locomotive discordance (Chakrabarti et al., 2006).

1.6.2.3 Nna1 gene: Structure and Functions

Nna1 is the mutated gene for the *pcd* initially described as a protein involved in spinal motor neurons axonal regeneration, and loss of its function is considered to be the cause of PC neurodegeneration (Harris et al., 2000, Fernandez-Gonzalez et al., 2002, Chakrabarti et al., 2006, Wang et al., 2007). Nna1 is a protein of about 1218 amino acids with highly conserved zinc-dependent carboxypeptidase domain crucial for PC survival (Harris et al., 2000, Chakrabarti et al., 2010). It has been detected in different tissues such as kidney, testis, developing and adult brain (Harris et al., 2000). Nna1 is localised to both nuclear and cytoplasmic compartments, where in the nucleus of some homologues encodes a zinc-carboxypeptidase that contains nuclear localization signals and an ATP/GTP binding motif (Harris et al., 2000). In the cytoplasm, Nna1 protein localises to the mitochondria and belongs to the M14 family related to zinc-carboxypeptidase (Harris et al., 2000, Kalinina et al., 2007, Chakrabarti et al., 2010). It has been shown that the substrate and zinc-binding residues are crucial for neuronal survival in *pcd* (Wang et al., 2006, Chakrabarti et al., 2008) and for motor neuron regeneration following oxotomy (Harris et al., 2000). Nna1 carboxypeptidase activity contributes to autophagy, mitophagy, and mitochondrial abnormalities (Reviewed in (Wu et al., 2012)). Chakrabarti et al., (2006) reported that the *pcd*^{5J} mutation is the result of single amino acid insertion into the Nna1 gene (Fig. 1.8) at the position 775 resulting in destabilisation of the Nna1 protein. This mutation is an alteration of a ‘GAC’ triplet in exon 17, which encodes aspartic acid amino acid near the zinc-carboxypeptidase domain (Chakrabarti et al., 2006).

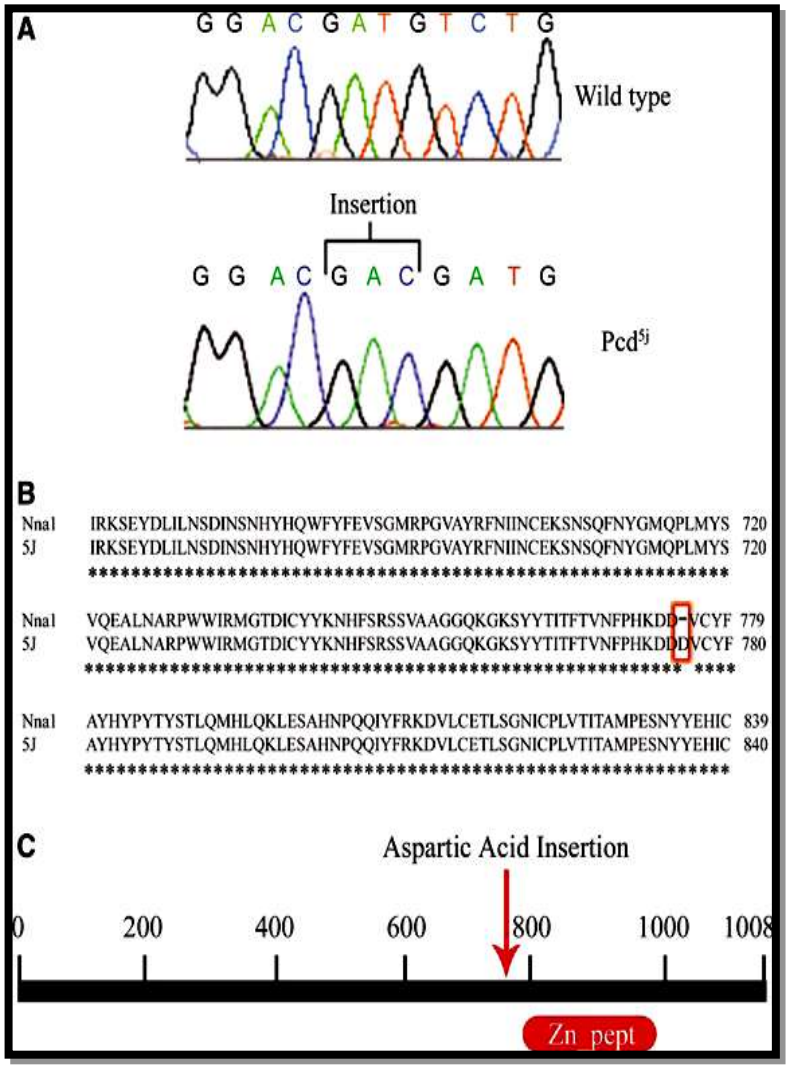

Figure 0.8 *pcd* ^{5J} mutation results from single amino acid insertion. After (Chakrabarti et al., 2006).

This alteration yields an additional aspartic acid residue beside the 2 already existing in Nna1 protein, thereby altering and destabilising its structure (Keefe et al., 1993, Chakrabarti et al., 2006). Moreover, *pcd*^{5J} mutant mice have more severe phenotypic alleles than *pcd*^{1J} and *pcd*^{3J} and these mice show marked ataxia by P25 (Wang and Morgan, 2007). Although Nna1 gene in *pcd*^{5J} mutant mice has

normal level of mRNA compared to the wild type, a dramatic decrease at the protein level has been observed (Chakrabarti et al., 2006).

1.6.3 Mechanisms of Purkinje cell death

It has been reported that PCs death occurs through the activation of apoptotic signalling pathways including DNA fragmentation and the activation of the caspase-3 (Reviewed in (Akita and Arai, 2007)). Other studies have reported alternative pathways such as endoplasmic reticulum (ER) stress-specific apoptotic pathway and caspase-12 activation (Morishima et al., 2002), and Chakrabarti et al., (2009) reported increase in the autophagy pathway activity. Systemic administration of IGF-I resulted in the restoration of behavioural function in animal models of neurodegenerative disorders through exercise activation of endogenous homeostatic mechanisms that abolish the neurodegeneration process (Reviewed in (Akita and Arai, 2007)).

1.7 The hypothalamus: anatomy and function

The hypothalamus is located at the base of the brain ventral to the thalamus and form the floor and ventral wall of the third ventricle (3V) (Daniel, 1976, Yuan and Arias-Carrion, 2011). It consists of distinct nuclei each with various functions and occupy the anterior, tuberal, and posterior regions of the hypothalamus (Halterman, 2005). The hypothalamus is involved in the regulation of body homeostasis and reproduction through the regulation of pituitary glands hormones (Kandel, 2000). Examples include eating, drinking, water balance, body temperature, and sexual activity (Yuan and Arias-Carrion, 2011).

1.8 Tanycytes population in the third ventricle

The word 'tanycyte' comes from the greek word (tanus=elongated) due to their shape and their long processes (Horstmann, 1954). They are a unique cell type located in the hypothalamic lining of the 3V (Rodriguez et al., 2010). Tanycytes are specialized unciliated cells lining the 3V wall and connecting with the hypothalamic neurons and blood vessels (Doetsch et al., 1997). Ultrastructure studies have shown that they have microvilli on their luminal surface with irregular nuclei containing dark chromatin aggregations (Rodriguez et al., 2005, Doetsch et al., 1997). The cytoplasm of the tanycytes contains numerous organelles such as mitochondria, golgi complex, lysosomes, and rough endoplasmic reticulum (RER) (Doetsch et al., 1997).

1.8.1 Tanycytes: ontogeny, development and radial glia

Early studies in rats have reported that tanycytes and radial glia start differentiation on embryonic day 18 (E18) and reach their full differentiation during the first postnatal month. Most tanycytes are produced during the 1st

postnatal week, while only few of them are generated during the 2nd postnatal week (Reviewed in (Rodriguez et al., 2005)). It has been postulated that tanycytes are transient embryonic radial glia descendants (Rodriguez et al., 2005, Rodriguez et al., 2010). Radial glia are the neuronal progenitors that serve as a scaffold for the newly formed neurons and guide them to their along their smooth processes to their final destination (Elias et al., 2007, Dale, 2011). During development, radial glial cells reside in the ventricular and subventricular zone of the brain, and then transformed into astrocytes and neurons except for small subpopulations which differentiate into tanycytes in the hypothalamus, Bergmann glia in the mature cerebellum (CB), and Muller cells in the retina (Li et al., 2004, Merkle et al., 2004, Rodriguez et al., 2005, Rodriguez et al., 2010). Although tanycytes share some features with radial glia, they possess morphological and functional characteristics (as outlined below) that distinguish them as a special radial glial cells (Rodriguez et al., 2010).

1.8.2 Types of Tanycytes

A review by Rodriguez et al., (2005) classified tanycytes into 4 subpopulations based on their location and morphological features (Fig. 1.9):

1. α1 tanycytes are located along the area of the ventromedian nucleus (VMN) and a small part of the dorsomedian nucleus (DMN), with their basal processes projecting into these nuclei.
2. α2 tanycytes are located adjacent to the arcuate nucleus (AN) spanning their processes into it.
3. β1 tanycytes are found along the lateral invaginations in the infundibular recess, with their processes ending on the perivascular space surrounding the portal capillaries located lateral to the median eminence (ME).

4. β2 tanycytes are the ventral most located tanycytes, with their cell bodies lining the floor of the infundibular recess and their long projections sent into the portal capillaries of the median zone of the ME.

1.8.3 Ependymal Cells

Another type of ciliated cells are located at the dorsal region of the 3V wall, they differ from tanycytes in that they possess functional cilia and they only have short processes directed into the hypothalamic parenchyma (Dale et al., 2011).

1.8.4 Tanycytes Functions

Tanycytes are morphologically related to radial glia in that they possess a cell body lining the ventricle and a long basal process penetrating the hypothalamic parenchyma (Rodriguez et al., 2010). Tanycytes are involved in endocrine functions such as the regulation of feeding and energy balance, appetite control (Frayling et al., 2011, Argente-Arizón et al., 2015). β2 tanycytes have an important role in the regulation of gonadotropin-releasing hormone (GnRH) secretion (Prevot et al., 2010). Tanycytes are able to detect any changes in the glucose levels thereby regulating glucose metabolism (Argente-Arizon et al., 2015). Tanycytes are one of the important components of the blood-CSF barrier at the level of the ME to prevent the leakage of blood-borne molecules into the CSF (Argente-Arizon et al., 2015).

1.8.5 Markers expressed by tanycytes

Tanycytes express a number of transporter markers such as glucose transporters GLUT-1 and GLUT-2 and Glast (Reviewed in (Rodriguez et al., 2005)), and P85, a 85 kDa protein expressed specifically by hypothalamic tanycytes (Blazquez et al., 2002). Tanycytes also express a number of molecules and markers common to

radial glia such as cytoskeletal intermediate filaments like vimentin, GFAP (Robins et al., 2013), and Nestin (Lee et al., 2012).

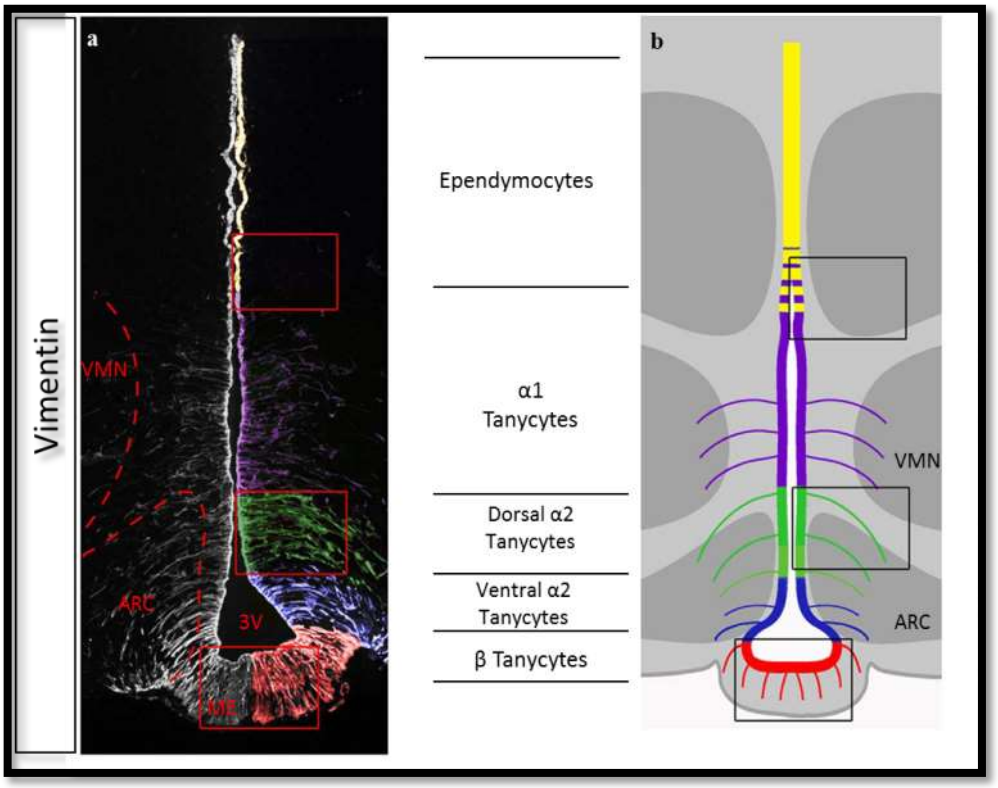

Figure 0.9 Coronal section through the third Ventricle. (a) immunostaining with vimentin antibody in the 3V showing tanycytes processes. (b) A cartoon of the types of tanycytes and their location along the ependymal layer of the 3V: purple (α1 tanycytes); green (dα1 tanycytes); blue (vα1 tanycytes); red (βtanycytes). After (Robins et al., 2013).

1.8.6 Neurogenesis in the adult cerebellum and third ventricle

In the brain, the neurogenic niches such as SVZ and SGZ should contain proliferating cells capable of self-renewing and differentiating into fully functional neurons. Under normal conditions, NSCs in these regions contribute to the generation of neurons that migrate and differentiate in the olfactory bulb and DG respectively contributing in memory and learning functions (Reviewed in (Migaud et al., 2010, Bonfanti and Peretto, 2011)).

In mammals, neurogenesis in the CB is thought to be limited to the early developmental stages of postnatal life, coinciding with the gradual disappearance of the external granule cell layer (EGL) soon after birth (Walton, 2012). However, studies in the intact CB of New Zealand white rabbits have revealed remarkable neurogenesis around puberty time and then decrease with age (Ponti et al., 2008). In the CB of non-mammal species such as adult teleost fish, neurons are generating throughout life and the brain showing striking ability for regeneration and tissue repair (Zupanc, 2006, Schmidt et al., 2013). In mammals, transplantation studies have shown that the environment within the CB may not provide specific instructive cues for the donor cells both in normal and injured CB (Suhonen et al., 1996b, Carletti and Rossi, 2005). Although the CB regarded as a static structure for many years, recent studies have indicated some neurogenic activity and the presence of NSCs in the CB of adult mouse (Alcock and Sottile, 2009). Under culture conditions, NSCs isolated from embryonic and adult mouse CB are self-renewing and capable of generating neurons and glial cells (Klein et al., 2005, Lee et al., 2005). However, in vivo studies indicated that these cells are quiescent and do not contribute to neuron generation under physiological conditions (Su et al., 2014). This may suggest that the lack of neurogenesis in normal mature CB might be due to un-permissive environment rather than absence of neural progenitor cells. Nevertheless, the discovery of endogenous stem cells in the adult brain may play regenerative roles leading to structural repair by new neurons generation in response to CB damage.

In the adult hypothalamus, neurogenesis has also been reported in mice (Kokoeva et al., 2007, Pierce and Xu, 2010), rats (Xu et al., 2005), birds and fish (Grandel et

al., 2006, Kaslin et al., 2008). Given the fact that the hypothalamus location is adjacent to the 3V, it is conceivable that cells constituting the ependymal lining of the 3V might be the source of proliferating cells. The fact that the ependymal cells lining the lateral ventricle function as NSCs further support the possibility that cells lining the ependymal layer of the 3V could also be a source of NSCs in the hypothalamus (Yuan and Corrion, 2011). Tanycyte populations lining the 3V wall have been hypothesised as neural progenitor cells generating neurons migrating into the surrounding hypothalamus in adult rats (Xu et al., 2005). Recent reports have identified the medial and ventral portion of the 3V as a neurogenic region contributes to new neurons generation (Perez-Martin et al., 2010, Lee et al., 2012). It is known that tanycytes are not homogenous population but rather they have 4 subtypes and that radial glia cell linages proved to be heterogeneous population in different parts of the brain (Kriegstein and Gotz, 2003, Rodriguez et al., 2005). Xu et al., (2005) observed that injection of GFP-recombinant adenovirus into the 3V wall labelled tanycytes population. After 2 weeks, few GFP^+ cells with neuronal morphology were detected in the hypothalamus, suggesting these came from the migration and differentiation of tanycytes (Xu et al., 2005).

1.9 Aims of the project

The evidence reviewed above queries the presence of neural stem cells in areas of the adult brain beyond the lateral ventricle and hippocampal populations. These observations suggest that despite the absence of reported neurogenesis in the adult mouse cerebellum, it may harbour a population displaying stem cell characteristics. Furthermore, evidence of some proliferative activity within the third ventricle of the hypothalamus may indicate the presence of NSCs. Cerebellar and 3V derived neural stem cells have been described to a lesser extent than stem cells in other brain regions such as the subventrcular zone and the dentate gyrus. The work outlined in this thesis will investigate populations showing stem cell characteristics in adult cerebellum and 3V, focussing on the following points:

1. Investigating the the existence of neural stem cells in the cerebellum and third ventricle of adult mouse using stem cells associated markers to determine their location and nature.
2. Isolating and characterisating neural stem cell populations derived from the cerebellum and third ventricle of adult mouse, and comparing them with those derived from a well-established NSC region, the lateral ventricle.
3. Investigating the effect of both EGF and FGF-2 for long term propagation of NSCs populations isolated from the CB and 3V parts of the adult brain.
4. Evaluating the response of NSC population identified in the CB to tissue degeneration.

2. Materials and Methods

2.1. Chemicals, reagents, and medium

Chemicals were purchased from Sigma-Aldrich unless otherwise stated. A list of chemicals, reagents, buffers, and media compositions is presented in Appendix I.

2.2. Tissue slide preparation

All mice were housed at the Biochemical Services Unit (BMSU), University of Nottingham, the adult chick samples were kindly provided by Dr C. Lopez-Margolles, and the primate samples were obtained from Twycross Zoo according to UK and EU legal requirements.

Brain cerebellar tissues of adult wild type primate (33-44 years), chick (D39), Sox1-GFP +/- (adult range from 4-12 weeks), and *pcd*^{5J} mice (2-12 weeks) were dissected, fixed in 4% PFA for 2hr for cryosectioing or for overnight when embedded in paraffin wax (appendix II). Serial 5 or 10µm thickness sagittal sections for the cerebellum and coronal sections for third ventricle were cut using Leica microtome.

2.2.1. Cryosectioning

The brain samples of adult GFP+/- Sox1 mice fixed in 4%PFA for 2h, washed with PBS to remove the PFA and then transferred to sucrose solution (15% Sucrose in PBS), and stored at 4˚C for overnight. The tissues were then moved to another sucrose solution (30% sucrose in PBS), and stored at 4˚C until tissue sank. Tissues were then embedded in OCT compound and were frozen in a bath of isopentane which had been cooled down in liquid Nitrogen. The samples were

stored at -20˚C until the time of sectioning. Sections were cut at 5µm and collected onto super frost plus slides and stored at -20 ˚C until staining.

2.3. Immunohistochemistry

2.3.1. Indirect immunohistochemistry

Sections were dewaxed, rehydrated (Carson, 1997), and then washed twice for 5 min in PBT (PBS+ 0.1% tween 20), followed by heat induced antigen retrieval step (Shi et al., 1993, Namimatsu et al., 2005) using sodium citrate buffer at pH 6.0 (appendix II). Endogenous peroxidase activity was blocked by incubating the sections in 3% H_2O_2 for 10-20min followed by 3 washes with PBS for 5 min each. Slides were then blocked in 0.1% fetal calf serum (FCS) blocking solution prepared in PBS for 1hr at room RT. Subsequently, the slides were incubated with the primary antibody diluted in blocking solution as described in (Table1) for overnight at 4°C. Sections were then washed extensively with PBS for 1 hr, incubated with secondary antibodies (see Table2) for 1hr at room temperature, and then washed 3 times with PBS for 15min each. For single immunostaining, slides were treated with DAB (3,3'-Diaminobenzidine) peroxidase substrate kit (Vector Laboratories) according to the manufacturer's instructions until brown color developed for 2-10mins (time was optimized for each primary antibody), followed by two 5min PBS washes and then mounted with (4',6-Diamidino-2-Phenylindole) Dapi-containing Vectashield (Vector Laboratories).

For double immunostaining, 2 different substrates were used for the detection of each of the antigens analysed. Slides were first incubated with DAB until brown color developed for the first antigen detection. The sections were washed 3 times with PBT and then incubated with alkaline phosphatase substrate kit (appendix II) in the dark for 20-40 min until blue color was developed for detection of the

second antigen. Finally the slides were washed with PBT 3 times, each for 5 min, and mounted with Dapi mounting medium. Primary and secondary antibodies used in this study and their respective dilutions are listed in table (2.1) and (2.2) respectively.

2.3.2. Immunostaining analysis:

For quantification of Bergmann glial cells, Sox1, Sox2, and Sox9 positive cells were counted for each *pcd* mouse with age-matched wild type littermates from 5 sagittal sections (5μm). For the assessment of Purkinje cell numbers, Calbindin-positive cells were counted for each *pcd* mouse with age-matched wild type littermates from 5 sections (5μm) (n=2). Values were shown as the number of cells per field of view ± SEM and statistical analysis was performed using Prism software (GraphPad version 6). The P-values were calculated using t-test or one way ANOVA with normally distributed data.

Table 2.1 List of primary antibodies used in IHC and their dilutions. Abbreviation: DSHB, Developmental Studies Hybridoma Bank.

Primary antibody	Host species	Localization	Dilution	Provider
Sox1	Goat	Nuclear	1:100	R&D system
Sox1	Goat	Nuclear	1:50	Santa Cruz
Sox2	Rabbit	Nuclear	1:100	Millipore
Sox9	Rabbit	Nuclear	1:100	Millipore
Calbindin	Mouse	Cytoplasmic	1:200	Sigma
S100	Rabbit	Cytoplasmic	1:200	Dako
GLAST	Rabbit	Cell membrane	1:200	abcam
GFAP	Rabbit	Cytoplasmic	1:200	Dako
BLBP	Rabbit	Nuclear& Cytoplasmic	1:200	Millipore
Nestin(Rat401)	Mouse	Cytoplasmic	1:100	DSHB
DCX	Rabbit	Cytoplasmic	1:100	Abcam
B-tubulin 3	Mouse	Cytoplasmic	1:100	Chemicon
MAP2-A488	Mouse	Cytoplasmic	1:100	Exbio
CNPase	Mouse	membrane	1:100	abcam
Ki67	Rabbit	Nucleus	1:100	Vector lab.
GFP-Fitc	Goat	Cytoplasm	1:100	Abcam
MBP	Mouse	Cytoplasm	1:200	Abcam

Table 2.2 List of secondary antibodies used for immunohistochemistry and their dilutions.

Secondary antibody	Host species	Concentration	Provider
HRP	Rabbit	1:200	sigma
HRP Anti-mouse	Mouse	1:200	sigma
HRP Anti-goat	Goat	1:200	sigma
TRed-goat	Goat	1:200	Vector lab.
TRed-mouse	Mouse	1:200	Vector lab.
TRed-Rabbit	Rabbit	1:200	Vector lab.
Fitc-Rabbit	Rabbit	1:200	Vector lab.
Alkaline phosphatase	Mouse	1:200	Vector lab.
Alkaline phosphatase	Rabbit	1:200	Vector lab.

2.4. Cell Culture

2.4.1. NSCs preparation

mNSCs were isolated from adult GFP+/- Sox1 and P21 *pcd*^{5J} mice (Fig. 2.1). The animals were sacrificed using CO_2 gas and the brains were extracted and transferred to petri dishes containing PBS. Cerebellum, lateral ventricle, and third ventricle tissues were isolated and the tissues were minced, washed in PBS and digested with accumax for 30 min at 37 °C. Tissues were then transfered to a tube and centrifuged for 5 min. to remove the accumax. After centrifugation, the supernatant was discarded and the cells were dissociated and washed with PBS, and transferred into 6 well plates containing 2 ml of NSC medium. The culture plate was maintained in an incubator at 37 °C under 5% CO_2 and fresh medium was added every 3 days. Uncoated 25cm^2 flasks were used to continuously grow NSCs. For NSCs culture medium composition see appendix II.

2.4.2. Passaging and freezing of NSCs

To passage NSCs, confluent cultured cells were treated with accutase for 3-5 min. at RT, washed with PBS and centrifuged at 200g for 5min. The supernatant was discarded and the pellet was re-suspended in 1ml NSC medium, and re-plated in 25cm^2 flasks at 1:4 to 1:5 ratio every 3-4 days. For freezing NSCs, cells were treated with accutase, centrifuged and re-suspended in 1ml NSCs medium. Cells were counted and 500 ml of the cell suspension at a concentration of 1x10^6 were added to freezing vials containing 500 ml of freezing medium (appendix II) to get a final volume of 1ml. Cells stored in -80˚C freezer for overnight and then transferred to liquid nitrogen. The cells were maintained as a monolayer culture in the presence of EGF and FGF-2 up to 40 passages without any changes in the

morphology compared to the control LV culture. After re-seeding the cells into the culture flasks they began to form neurospheres after one day in vitro and then forming a single monolayer culture the next day (Fig. 4.1).

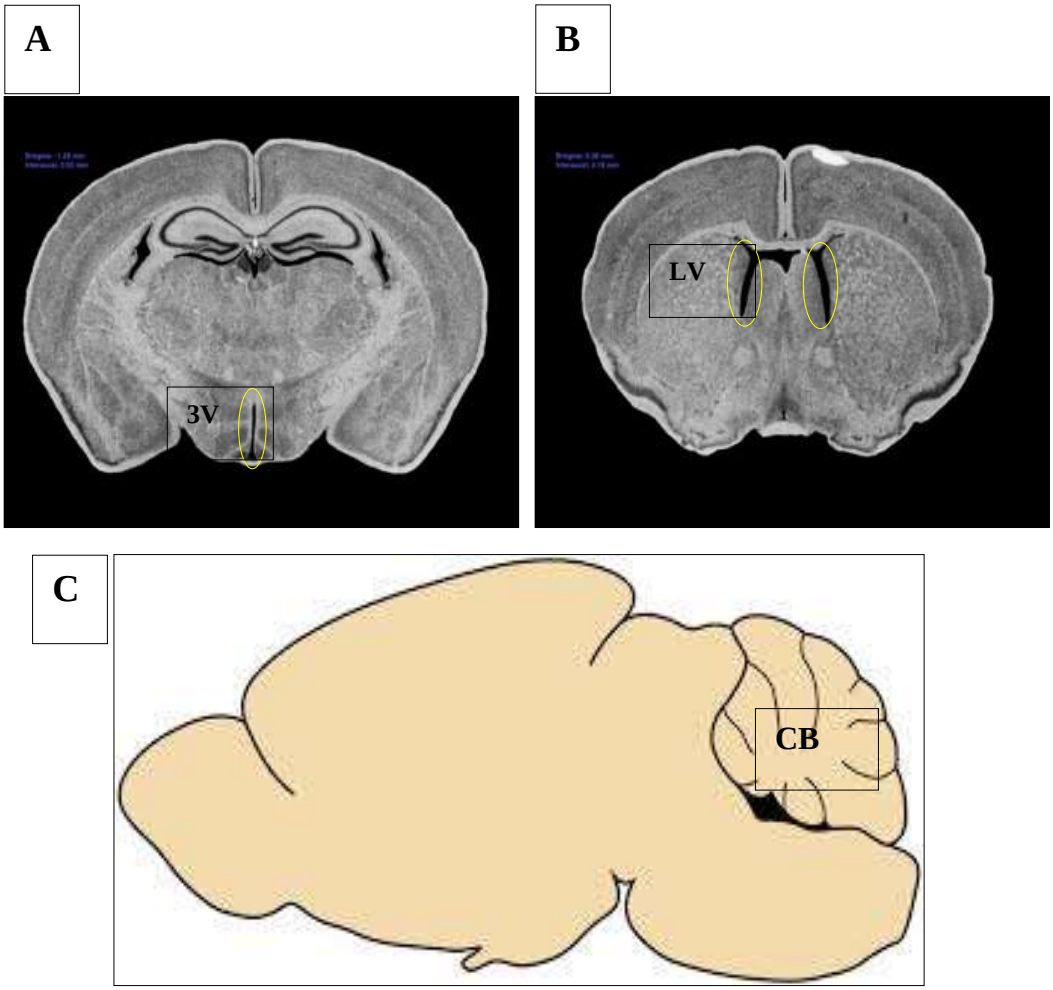

Figure 2.1 Images showing the 3 regions in the adult brain dissected to derive NSCs**.** NSCs were isolated from third ventricle (3V) (A), lateral ventricle (LV) (B), and cerebellum (CB) (C).

From http://www.mbl.org/atlas170/atlas170_frame.html

1.10 Differentiation of NSCs

To induce differentiation, confluent cultures (80-90%) were dissociated with accutase and centrifuged for 5 min. The resultant cell suspension was counted using a haemocytometer and reseeded at 75×10^3 cells/ml onto gelatin coated glass coverslips in 24 well plates. The cells were allowed to grow for 2 days in NSCs medium. After cells became nearly confluent, EGF and FGF-2 were removed and medium replaced with differentiation medium (appendix II). Cells were allowed to differentiate for either 4, 5, 6 or 11 days. Coverslips were then fixed with 4% cold PFA for 20 min at RT, washed twice with PBS and then stored at 4ºC until immunostaining.

2.4.3. Immunocytochemistry and cell counting

For staining, coverslips were washed once with (PBS+ 0.1% tween 20) for 10 minutes at room temperature (RT). Cells were then blocked in 0.1% fetal calf serum (FCS) blocking solution for 30 min at room RT. The cells were then incubated with the primary antibody prepared from the blocking solution for overnight at 4 ˚C. After 3 washes with PBS, each for 10 min, the cells then incubated with the secondary antibody prepared in PBT solution and incubated in the dark for 1 hr at RT. Coverslips were then rinsed 3 times in PBS for 15 each. The coverslips then mounted with (4',6-Diamidino-2-Phenylindole) Dapi-containing Vectashield (Vector Laboratories). Primary and secondary antibodies used in this study are listed in table (2.1) and (2.2) respectively.

For counting, immunoreactive cells for Nestin, b-tubulin, Calbindin, DCX, and MAP-2 were counted as percentages of the total dapi stained nuclei. In each experiment, at least 6 fields of view per coverslip were selected randomly for

counting, and the data expressed as the percentage of cells ± SEM, with P value calculated using one way anova.

2.4.4. Cell Viability Assay

Cell viability assay was performed using Prestoblue to evaluate the growth of NSCs in different culture conditions by measuring the metabolic cell activity in each well (Boncler et al., 2014). For this purpose, cells were seeded in gelatin-coated 24 well plates (three replicate well were seeded for each condition) at a density of 75×10^3 cells/ml in normal NSCs medium and allowed to grow for 2-3 days. Medium was then aspirated from the 24 well plates, 400µl of Prestoblue reagent was added in each well and incubated from 20-40 min. The 10X stock reagent was diluted 1 in 10 in HBSS to get a final concentration of 1X. The reaction was stopped after 40 min, and the solution was transferred into 96 well plates, each well received 100µl to get a final number of 9 wells/ each condition. The fluorescent intensity was measured at excitation 560 nm, emission 590 nm using microplate reader.

2.4.5. Image analysis and microscopy

Brightfield and fluorescent images in this study were taken with Nikon Eclipse 90i fluorescent microscope using Velocity imaging software version 5.2.1 (2007) and 6.1.1 (2012) (PerkinElmer).

3 Investigating the presence and distribution of neural stem cells in the mature cerebellum of mouse, primate, and chick

3.1 Introduction

It has been known for many years that neurogenesis is not taking place in the mammalian brain and that neuron generation after birth is impossible (Ramón y Cajal, 1914).This has proven incorrect when the generation of neurons and glia was described in two known niches of adult brain: the subventricular zone (SVZ) of the lateral ventricle (LV) and the dentate gyrus (DG) of the hippocampus (Reviewed in (Migaud et al., 2010, Bonfanti and Peretto, 2011)). Studies have reported that cells in both niches are able to generate various types of neurons such as excitatory glutamatergic neurons in the DG and inhibitory GABAergic neurons in the olfactory bulb (Reviewed in (Grandel and Brand, 2013). Evidence suggests that a population of cells migrating from the SVZ into the cortex contribute to brain repair and regeneration (Parent, 2002). Following these discoveries, new brain regions were explored regarding neurogenesis or the existence of neural stem/progenitor cells such as the spinal cord, 3rd and 4th ventricle (Weiss et al., 1996), cerebellum, and the hypothalamus (Reviewed in (Migaud et al., 2010, Bonfanti and Peretto, 2011, Yuan and Arias-Carrion, 2011)).

Until recently, there has been little evidence concerning the existence of stem cells in the postnatal cerebellum (CB); however, NSCs have been isolated from the white matter of embryonic (P7) and adult (P>42) mouse CB (Klein et al., 2005, Lee et al., 2005) displaying NSCs characteristics such as self-renewing

ability and multipotentiality. However, these neural stem-like cells are quiescent and failed to show any in vivo generation of neurons and astrocytes under physiological conditions (Su et al., 2014). Alcock et al., (2007) and Sottile et al., (2006) were able to locate these cells identified by Lee et al., (2005) at P7 in the white matter by their coexpression of Sox1 and Sox2 in the mature tissue as overlapping with the Bergmann glia (BG) in the PCL based on their expression of NSC markers Sox1, Sox2, and Sox9. It is important to understand in vivo adult NSCs in non-neurogenic niches which may provide useful information regarding their in vitro proliferation, expansion and signalling factors that may provide suitable environment for stem cell transplantation. Thus, investigating the existence of stem cells in the adult CB may provide an important source of neurons, astrocytes, and oligodendrocytes for possible therapeutic applications for neurodegenerative disorders. Based on the observations regarding the existence of NSCs in the adult mouse CB, it is important to analyse in more details the molecular profile of this population regarding the expression of NSCs associated markers which will be the main focus of this chapter.

There are common markers which have been used to assess the presence of stem cells in brain regions such as lateral ventricle (LV) and dentate gyrus (DG). Based on the analysis of NSC-associated marker expression in the LV and DG, we investigated the presence of NSC-like cells in the adult cerebellum from mouse, primate, and chick origin, and compared their relative distribution across the 3 species. Among these markers are GFAP, an intermediate filament specific for astrocytes but can be also expressed by radial glia displaying stem cells characteristics (Noctor et al., 2002, Malatesta et al., 2000); Nestin, an intermediate filament expressed by neuroepithelial cells and proliferating cells in

the adult rodent brain (Reynolds and Weiss, 1992); SoxB genes, a subfamily of SOX transcription factors including Sox1, Sox2, and Sox3 genes (Pevny et al., 1998). These genes are expressed during early embryogenesis in the nervous system, and are involved in cell fate determination and differentiation (Uwanogho et al., 1995, Rex et al., 1997, Pevny and Placzek, 2005, Koirala and Corfas, 2010). Sox1 is one of the earliest identified markers for neural precursors in the mouse embryo as well as in the adult (Pevny and Rao, 2003). Sox2 is required for maintaining NSCs and its expression is conserved in the mature CNS (Collignon et al., 1996). Co-expression of Sox1 and Sox2 in the adult brain seems to persist only in the neurogenic areas, the lateral ventricle and the hippocampus (Barraud et al., 2005, Brazel et al., 2005). However, recent studies have shown that BG in the adult mouse and human CB also express Sox1 and Sox2 (Sottile et al., 2006, Alcock et al., 2009). Sox9 is a member of the SoxE subgroup shown to be expressed in prechondrogenic and chondrogenic tissues (Zhao et al., 1997), and in male gonads (Kent et al., 1996). In the cerebellum, Sox9 has been shown to be co-expressed with Sox1 and Sox2 in the BG in the adult human and mouse, suggesting Sox9 as complementary candidate marker for NSCs (Sottile et al., 2006; Alcock et al., 2007).

In order to further investigate the characteristics of NSC-like cells in the mature CB, which could help better evaluate the repair capacity in the CB, a comparative study was carried out to:

1. Investigate the expression of the NSC markers in the adult mouse cerebellum
2. Determine the precise location and nature of this cerebellar population using double immunohistochemical analysis with a list of well-known markers for NSCs and glial cell lineage determination.
3. Assess whether the same population of cells might exist in other species chick and primate and weather Sox gene expression is preserved across different species.

3.2 Results

In this chapter, we investigated the expression of commonly used NSC markers, such as Sox1, Sox2, Sox9, Nestin, and Ki67, in adult mouse, primate, and chick cerebellum tissue. Sagittal tissue sections were generated and used to detect NSC markers as well as other markers associated with cerebellar populations such as GFAP, S100, GLAST, BLBP, RC2, Vimentin and Calbindin single and double immunohistochemical techniques.

3.2.1 Sox1, Sox2, and Sox9 localisation in the postnatal cerebellum

Immunohistochemical analysis for Sox1 and Sox2 showed that both genes were expressed in the mouse cerebellar cortex, in a pattern restricted to the Bergmann glial (BG) cells, between the Calbindin-positive PC bodies (Fig. 3.1A, 3.2A respectively). Similarly, the expression of Sox1 and Sox2 was detected in the cerebellar cortex of the adult primate (Fig. 3.1B, 3.2B respectively) and chick (Fig 3.1C, 3.2C respectively) cerebellum tissue. In both cases, the Sox1and Sox2positive populations were found in the same location to that observed in mouse cerebellum corresponding to BG present between the Calbindin-positive PC bodies.

Next, we attempted to analyse Sox9, another transcription factor previously shown to be expressed in the cerebellum of adult mouse (Sottile et al., 2006). In the adult mouse cerebellum, expression of Sox9 followed the same pattern to that observed for Sox1 and Sox2 (Fig. 3.3A), which were detected in the BG in the PCL, matching previous observations in the adult mice cerebellum (Sottile et al., 2006, Alcock et al., 2009). Sox9 positive cells were also observed in the LV of the SVZ (Pompolo and Harley, 2001), a region known to harbour precursors and

radial glia (Kordes et al., 2005), as previously reported (Stolt et al., 2003, Pompolo and Harley, 2001). Sox9 expression was also observed in a similar pattern in primate and chick cerebellum (Fig. 3.3B and C, respectively).

In mouse, the expression of Nestin, another marker for stem/progenitor cells could also be expressed by Bergmann glial cells, was then investigated to determine whether BG population was positive for this NSC marker, and whether this may correspond to Ki67 expression, a marker of proliferating cells. For this purpose, double immunostaining for Calbindin with Nestin and then Ki67 was performed on sagittal sections of adult mouse cerebellum. No detectable signal was observed for Nestin or Ki67 (Fig. 3.5A and B respectively) in Bergmann glia from the adult mouse cerebellum, and the only staining observed for Nestin was some unspecific binding in the ML (Fig. 3.5A). This negative result was in contrast with the Ki67 signal observed on positive control sections analysed alongside.

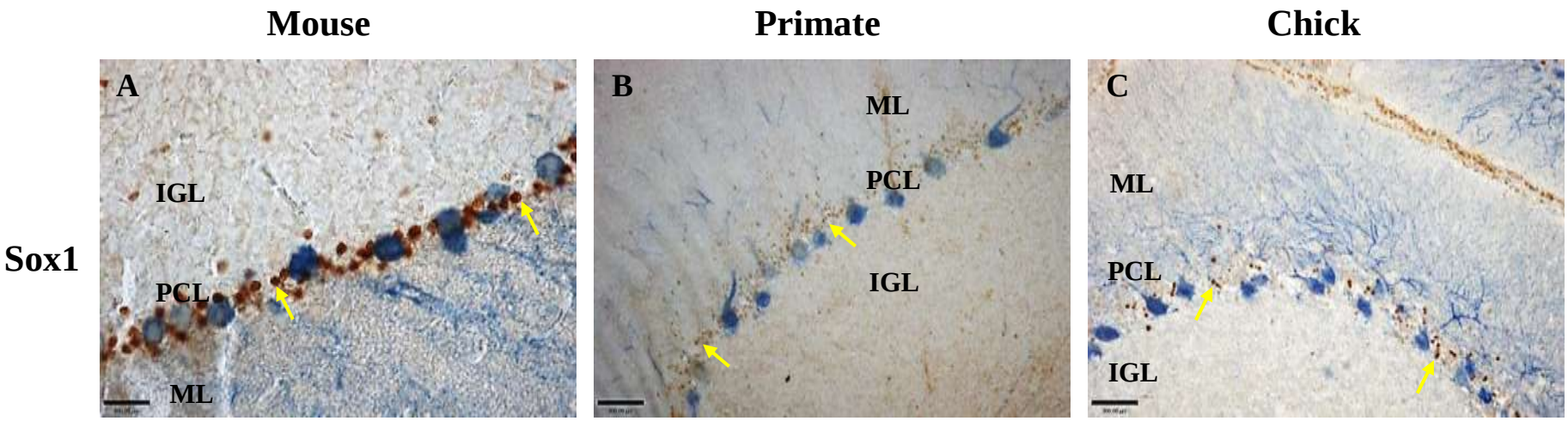

Figure 3.1 Sox1 detection in sagittal sections of mature cerebellum from mouse, non-human primate, and chick origin (A, B, and C respectively). Double immunostaining with Sox1 (brown) and calbindin (blue) confirmed that the expression Sox1 was limited to the Bergmann glia (yellow arrows) located between the cell bodies of the Purkinje cells). The pattern of Sox1expression was similar in mouse, primate and chick tissue.

Scale bar = 200 μm

IGL, internal granular layer; ML, molecular layer; PCL, Purkinje cell layer; WM, white matter.

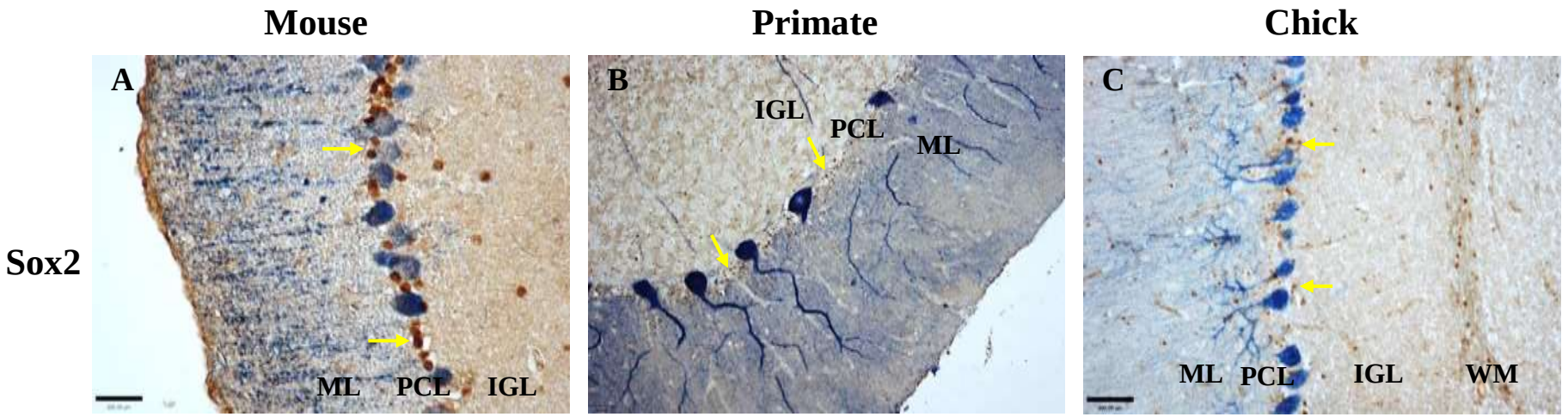

Figure 3.2 Sox2 detection in sagittal sections of mature cerebellum tissue from mouse, non-human primate, and chick origin (A, B, and C respectively). Double immunostaining with Sox2 (brown) and calbindin (blue) confirmed that the expression in the Bergmann glia (yellow arrows) in the PCL between PC bodies. In the 3 species, Sox2 expression followed the same pattern in the cerebellar cortex.

Scale bar = 200 μm in A and C; 34 μm in B

IGL, internal granular layer; ML, molecular layer; PCL, Purkinje cell layer; WM, white matter.

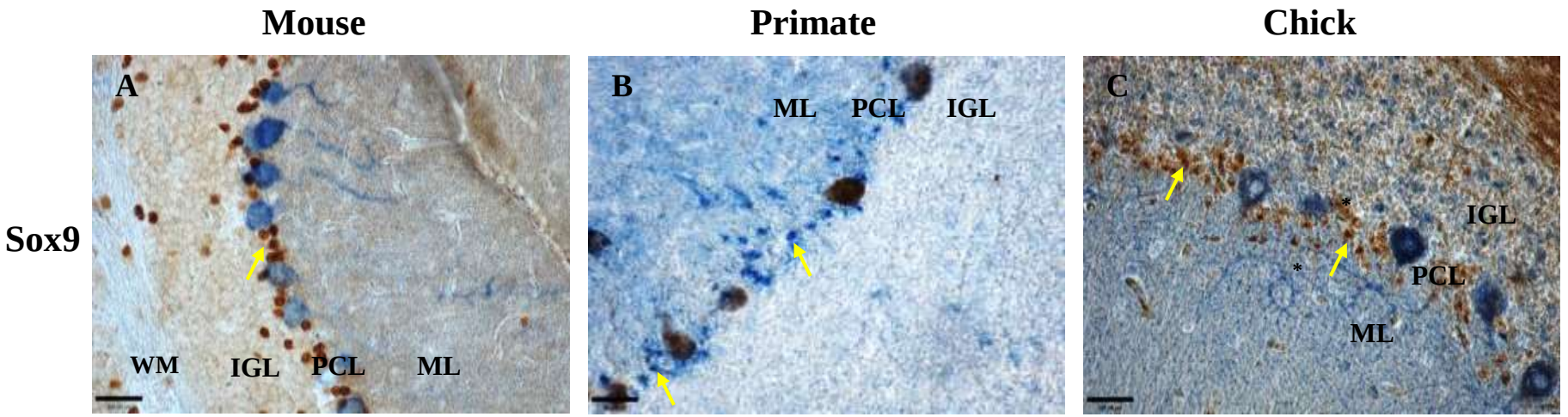

Figure 3.3 Sox9 detection in sagittal sections of mature cerebellum tissue from mouse, non-human primate, and chick origin (A, B, and C respectively). Similar to Sox1 and Sox2 in (Fig.3.2 and 3.3 respectively), double immunostaining with Sox9 and calbindin confirmed that the expression in the Bergmann glia (yellow arrows) found in the PCL between PC bodies (blue with anti-calbindin antibody in A and C; brown in B). In the 3 species, Sox9 expression followed the same pattern of staining as Sox1 and Sox2 in the cerebellar cortex.

Scale bar = 200 μm

IGL, internal granular layer; ML, molecular layer; PCL, Purkinje cell layer; WM, white matter.

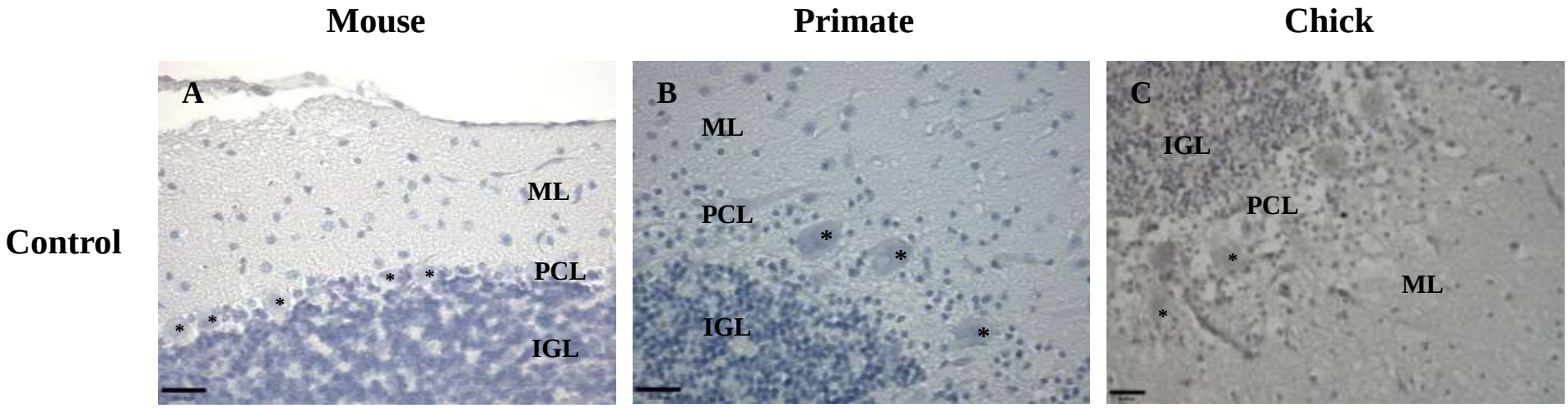

Figure 3.4 Negative controls for Fig (3.2, 3.3, and 3.4). Only secondary antibodies were applied and sections were counterstained with nuclear hematoxylin staining.

Scale bar = 200 μm in A and B; 34 μm in C

IGL, internal granular layer; ML, molecular layer; PCL, Purkinje cell layer; WM, white matter.

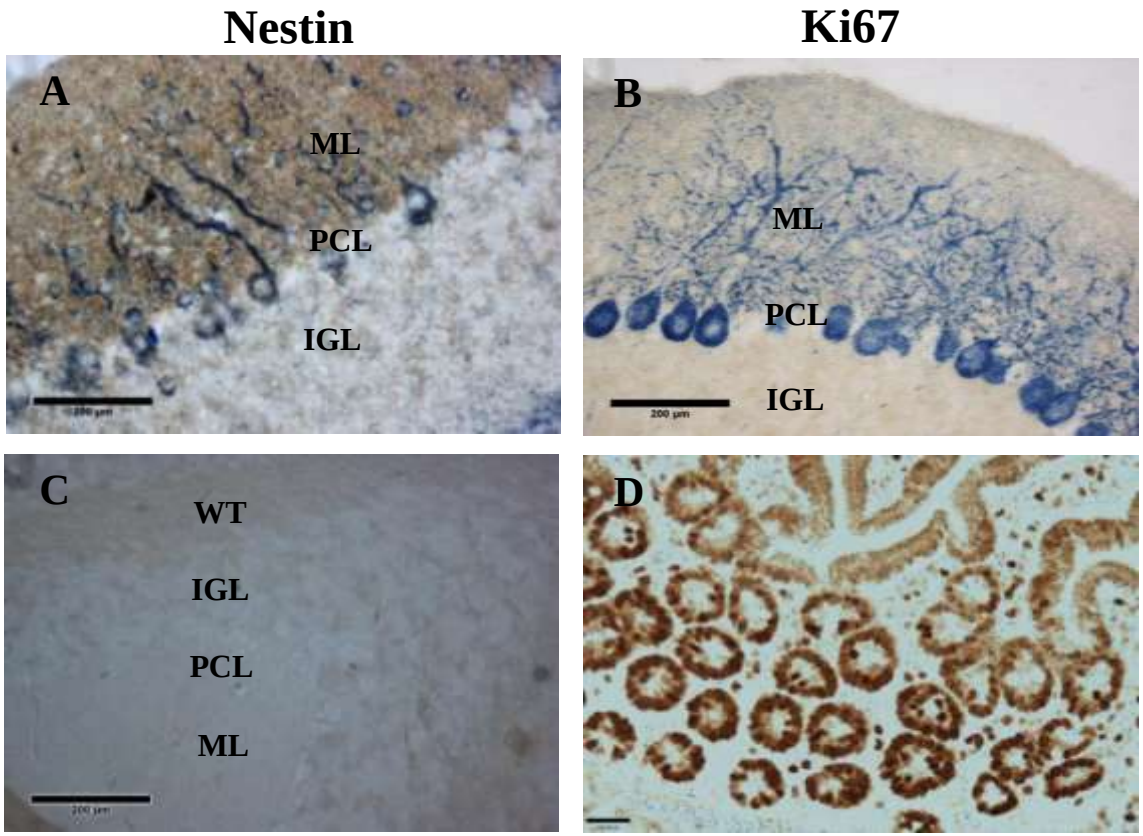

Figure 3.5 Sagittal sections of mature mouse cerebellum stained for Nestin (A) and Ki67 (B) with Calbindin (blue). Signals for Nestin and Ki67 were not detected in the Bergmann glial cells located in the PCL between the PC bodies. (C) Represent negative control incubated without primary antibody, (D) Represents positive control for Ki67 in the small intestine of adult mouse.

Scale bar = 200 μm

IGL, internal granular layer; ML, molecular layer; PCL, Purkinje cell layer; WM, white matter.

3.2.2 The expression of markers commonly associated with neural stem cell markers

To further identify the nature of these Sox1, 2, 9 positive cells in the cerebellar cortex, we analysed the expression of radial glia/astrocyte linage markers previously shown to stain NSCs and radial glia in the mature cerebellum such as BLBP and GFAP (Yamada et al., 2000, Imura et al., 2003, Hachem et al., 2007). Antibodies against GFAP strongly labelled cells located in the PCL in the mouse cerebellar cortex (Fig. 3.6A), with prominent brown-colored radial processes in the ML corresponding to the BG fibers. The location of $GFAP^+$ cells in the PCL was confirmed by the PC-specific Calbindin marker which intensely labelled the PC bodies in the PCL and their dendrites in the upper ML (Fig. 3.6 A). $GFAP^+$ astrocytes were also detected in the IGL of the cerebellar cortex. Sections from adult primate and chick cerebellum revealed strong evidence of GFAP expression in a manner closely resembling that seen in the adult mouse PCL (Fig. 3.6 B and C respectively), with long brown stained BG processes extending into the ML of cerebellar cortex as previously reported (Kotai et al., 1989). Some astrocytes with their processes were also detected in the IGL in a manner indistinguishable to that observed in the adult mouse cerebellum (Fig. 3.6 B and C respectively). These results show that GFAP detection revealed a similar pattern of staining in the mature cerebellum of the three species investigated.

BLBP is a member of a family of hydrophobic ligand-binding proteins known to be expressed by radial glial cells in different regions of the brain (Anthony et al., 2005), and it was shown to be a marker associated with the BG (Yamada and Watanabe, 2002, Hachem et al., 2007). To further confirm the nature and the location of Sox1, 2, 9 cells in the cerebellar cortex of adult mouse, primate and chick, expression of this radial glial marker was analysed in these species. In the adult mouse cerebellum, BLBP highlighted a population of cells in the

cerebellar cortex (Fig. 3.7A). The expression was restricted to BG in the PCL in a pattern consistent with published report (Hachem et al., 2007). The ML showed signal for BLBP-stained processes and no signal was detected in the IGL and the WM. Similar results was observed in the primate and chick cerebellum, where BLBP signal was found in the cell bodies of BG between the calbindin stained PCs (Fig. 3.7 B and C respectively), and visible brown staining was also observed in the ML corresponded to the radial glial fibers intermingled between the PC dendrites.

Other radial glial markers were also examined in the mouse cerebellum in this study such as S100, GLAST, RC2, and Vimentin. GLAST is an astrocyte-specific glutamate transporter marker shown to be expressed in radial glia and highly concentrated in the cerebellum (Shibata et al., 1997). In the adult mouse cerebellar cortex, GLAST-labeled cells in the PCL were identified as BG located between the negative PC bodies (Fig. 3.8A). The staining was only detected in the cell body but no staining was observed in the BG processes. Both IGL and the WM showed some immunoreactivity for GLAST (Fig. 3.8A) but no signal was detected in the ML. RC2 and Vimentin did not produce any signal in the BG in adult mouse (Fig. 3.8 B and C respectively).

Similarly to BLBP and GLAST, expression of S100 was detected in the cerebellar cortex of mouse and primate tissue (Fig. 3.9A and B). As previously shown for the other genes, S100 followed similar pattern of staining and marked the BG cell bodies in the PCL. However, I have repeated the protocol for more than 4 times and it seemed that signals observed in the chick tissue for S100 marked PC cells unspecifically and no staining was detected for BG (Fig. 3.9C), and suggested artefactual staining.

In summary, my data demonstrated the presence of a number of NSCs markers in the BG population of mature cerebellum. These markers have been reported for mouse and human (Sottile et al., 2006, Alcock et al., 2009), and here in other species such as adult chick and

primate. The results presented here also suggest that the BG population is not proliferating in normal mice and its proliferative activity needs to be examined after brain injury.

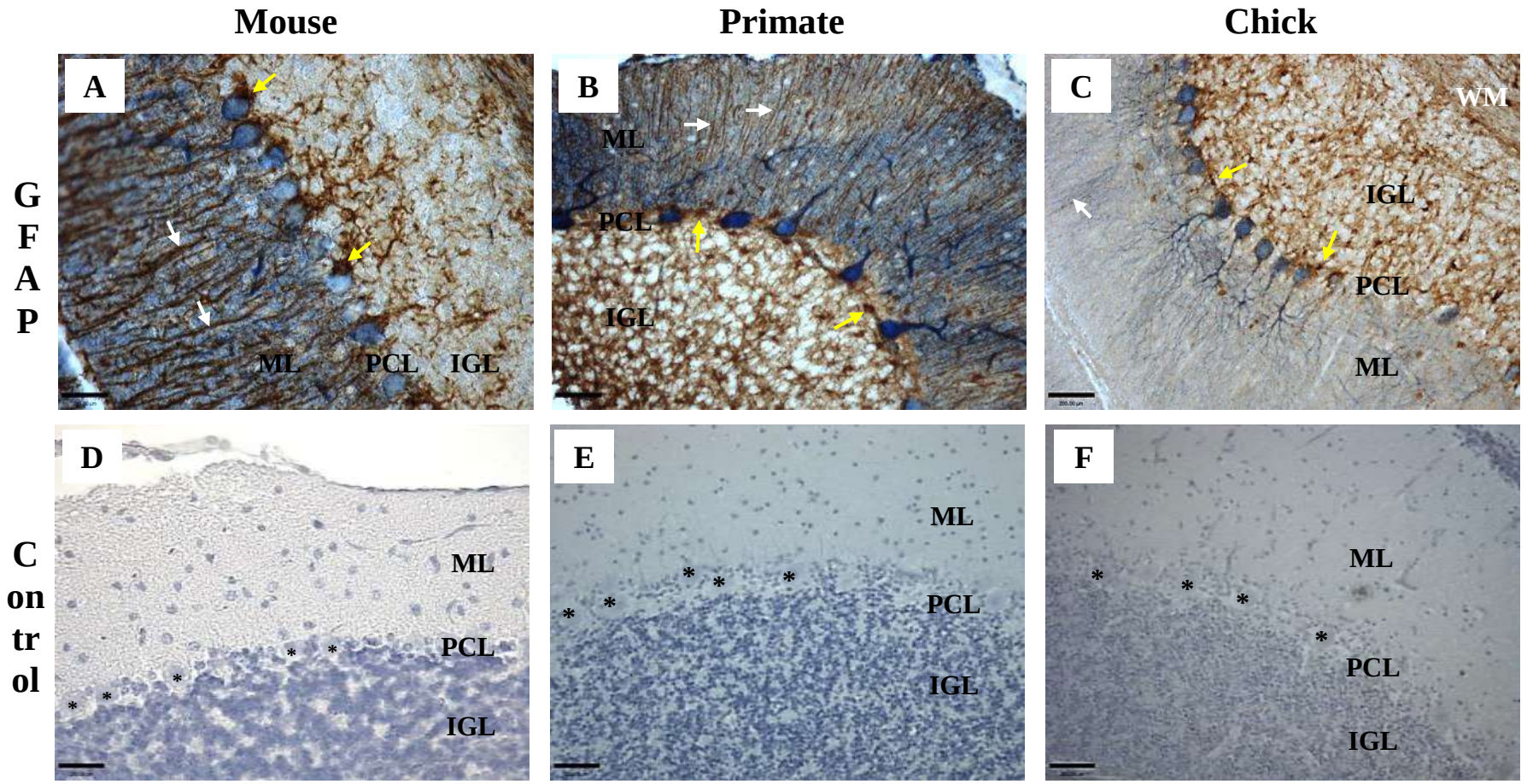

Figure 3.6 Double immunolabelling of calbindin and GFAP in the mature cerebellar cortex of mouse (A) , primate (B), and chick (C). In all species, GFAP expression (brown) is detected in the Bergmann glia (yellow arrows) between the cell bodies of Purkinje cells (stained blue with anti-calbindin antibody and highlighted with asterisks in the controls) in the Purkinje cell layer (PCL) of the cerebellar cortex. GFAP also showed intense signals in the Bergmann glia radial processes (brown, white arrows) extending up into the molecular layer (ML). In addition, GFAP expression in the astrocytes of the internal granular layer (IGL) was also detected. Negative controls (with secondary antibody only, counterstained with hematoxylin) for each species are shown in D, E, and F. scale bar = 200 μm.

IGL, internal granular layer; ML, molecular layer; PCL, Purkinje cell layer; WM, white matter.

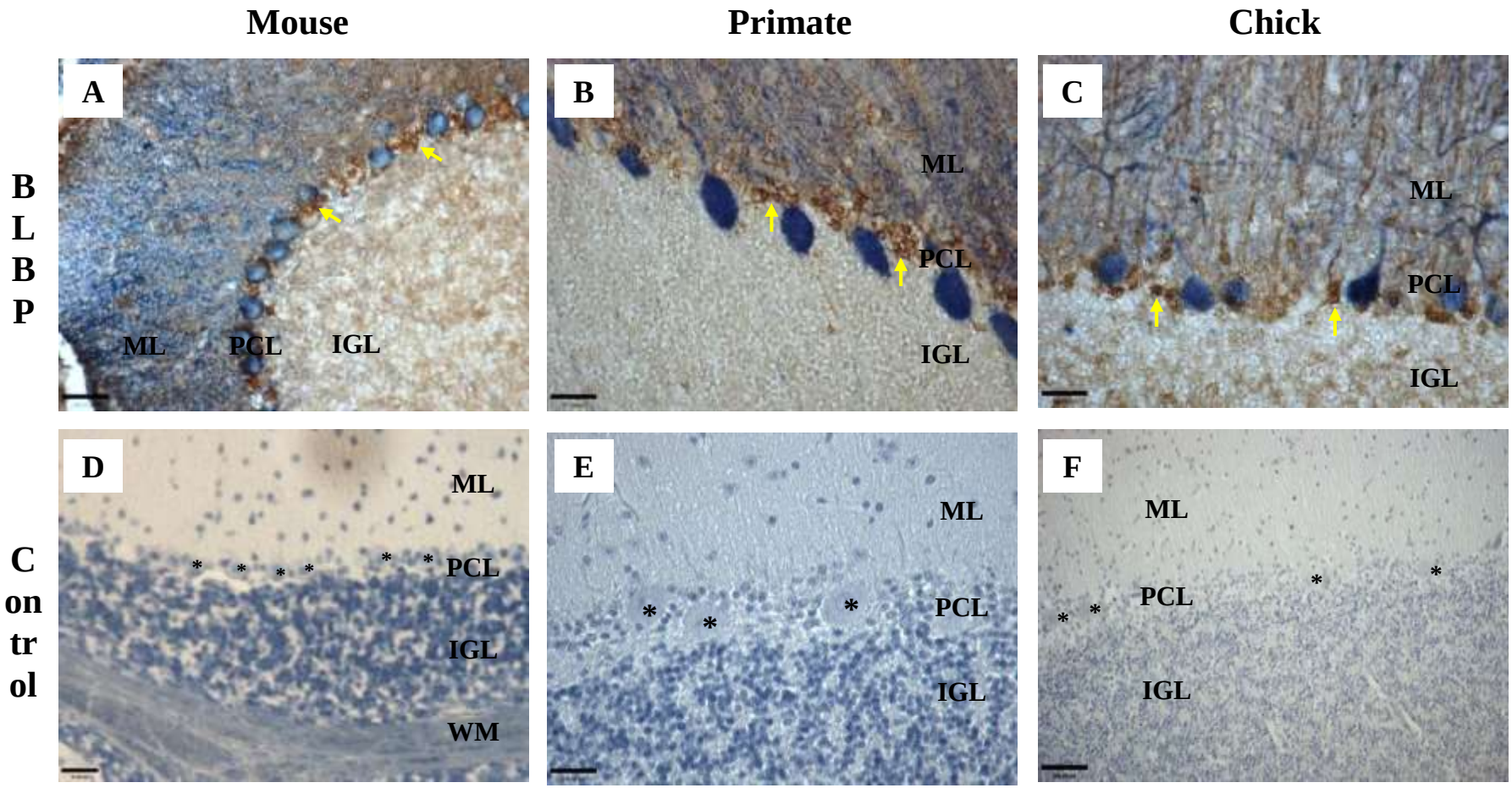

Figure 3.7 Double immunolabelling of BLBP and Calbindin in the mature cerebellar cortex of mouse (A), primate (B) and chick (C). Double immunostaining for BLBP with calbindin showed numerous brown stained Bergmann glial cells (yellow arrows) between the Purkinje cell bodies (highlighted in blue with anti-calbindin antibody and asterisks in the controls) in the Purkinje cell layer (PCL). Bergmann glia also showed brown signal in their processes which traverse the molecular layer (ML). As it can be observed, the expression pattern for this marker was similar in the cerebellar cortex for both adult primate (B) and chick (C). Negative controls (with secondary antibody only, counterstained with hematoxylin) for each species is shown in D, E, and F. scale bar = 34 μm in D; 200 μm in the rest.

IGL, internal granular layer; ML, molecular layer; PCL, Purkinje cell layer; WM, white matter.

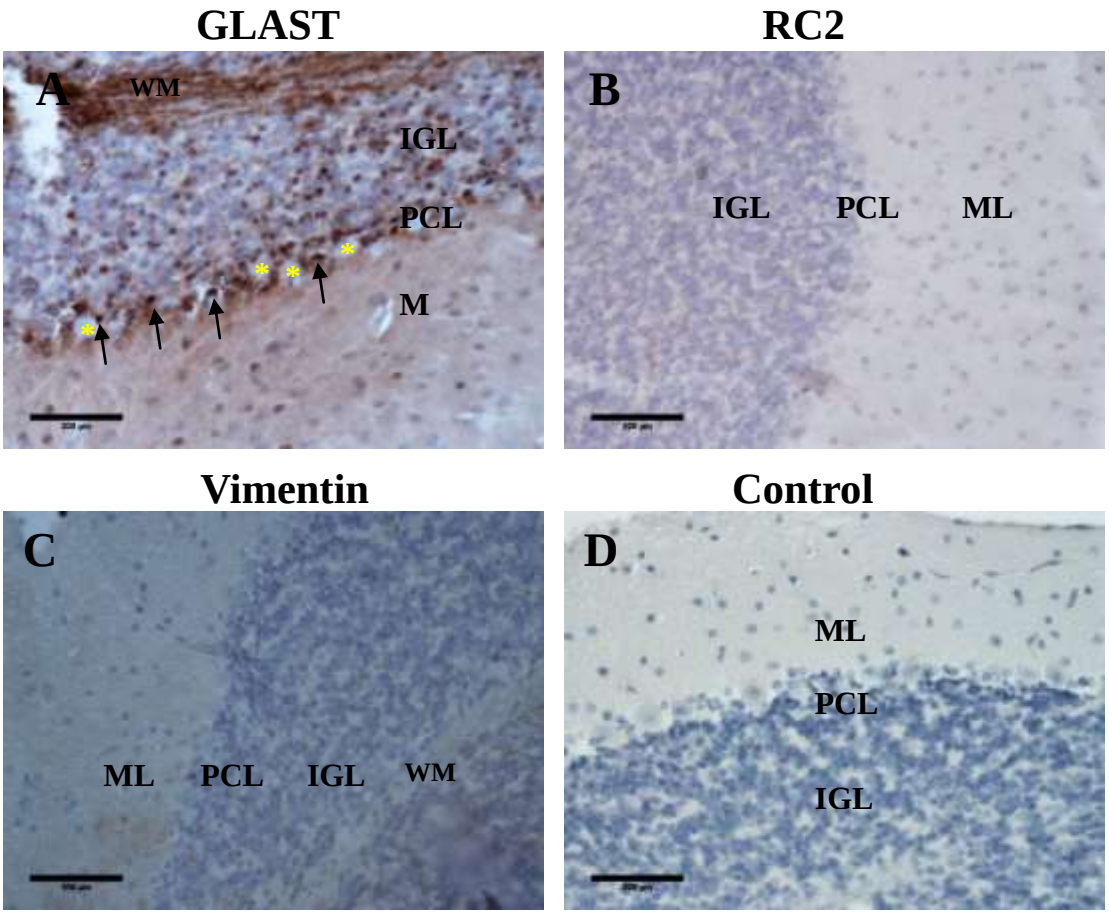

Figure 3.8 Immunostaining on sagittal sections of adult mouse cerebellum showing the expression of GLAST (A), RC2 (B), and Vimentin (C). GLAST-positive Bergmann glia located (arrows) in the PCL between Purkinje cell bodies (stars) in a pattern similar to S100 and BLBP. No signal for RC2 or Vimentin was detected in the cerebellar cortex. (D) Negative control incubated without the primary antibody.

Scale Bar= 200 μm. IGL, internal granular layer; ML, molecular layer; PCL, Purkinje cell layer; WM, white matter.

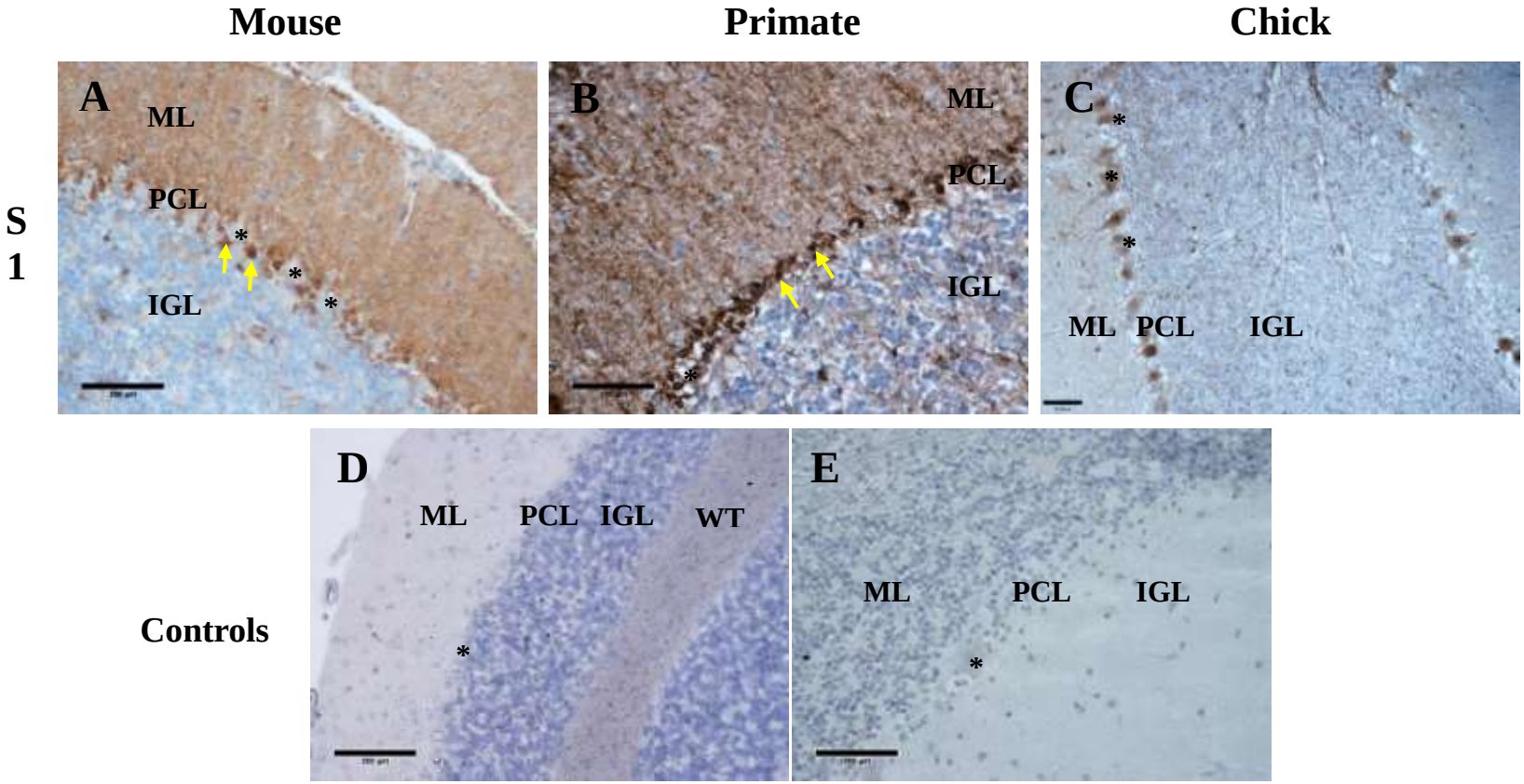

Figure 3.9 S100 immunodetection on cerebellar sagittal sections of adult mouse (A), primate (B), and chick (C). In the cerebellar sections of mouse and primate tissue, S100 (brown) showed similar pattern of expression in the Bergmann glial cells (arrows) between the PC bodies (stars). Signal for S100 in the adult chick was identified as unspecific binding. (D) and (E) Negative controls for mouse and primate respectively incubated without the primary antibody. Scale Bar= 140 µm in (B); 70 µm. IGL, internal granular layer; ML, molecular layer; PCL, Purkinje cell layer; WM, white matter.

3.3 Discussion

In this chapter, immunohistochemical analysis was used to study the presence of a population of cells in the adult cerebellum expressing NSC markers, and to compare tissue from mouse, non-human primates, and chick.

3.3.1 Population of cells in the adult cerebellum expressing NCS markers

In all of the 3 species, Sox1, Sox2, and Sox9 were expressed in the Bergmann glia cells in the cerebellar cortex as previously reported in mice (Sottile et al., 2006; Alcock et al., 2007). Analysis in adult human cerebellum revealed the same cell population were positive for Sox1/Sox2/Sox9 (Alcock et al., 2009). Interestingly, similar observations were reported for Sox2 expression in the Bergmann glia in rabbits (Ponti et al., 2008), and for Sox9 in rats (Pompolo and Harley, 2001). In order to further examine the properties of the Sox1, Sox2, and Sox9 positive population, we extended the comparative marker expression analysis to other markers associated with NSCs such as BLBP and GFAP in the cerebellar cortex of adult mice, non-human primates namely gorilla and chimps, and chick (D39). There is to date no report in the literature describing the expression of NSC markers in the adult primate and chick cerebellum, except for a study in human mature cerebellum previously mentioned (Alcock et al., 2009), and another study which demonstrated the expression of Sox1 and Sox2 in the SVZ of adult monkey, but not in the cerebellum (Tonchev et al., 2006).

The staining pattern of the NSC and radial glial markers in all species studied indicated that the immunoreactive cells were the radial glial cells in the postnatal cerebellum, the Bergmann glial cells in the PCL. However, in the adult mouse

cerebellum, cells positive of Sox1, 2, and 9 were negative for Nestin and Ki67, two markers associated with proliferating progenitor cells (Reynolds and Weiss, 1992, Morshead et al., 1994, Skardelly et al., 2014), suggesting that the Sox-positive population in the cerebellum might be quiescent in the normal tissue. This may be compatible with reports that the BG population could undergo reactive gliosis after neurodegeneration (Lafarga et al., 1998, Baltanas et al., 2013).

Sox1 and Sox2 are members of SoxB family shown to be involved in the early stages of CNS development and have an important role in maintaining NSCs identity (Pevny and Placzek, 2005; Koirala and Corfas, 2010). Sox1 expression starts with the neural plate induction and is downregulated as the neural stem cells begin to differentiate, suggesting this gene as a marker for neural progenitor cells (Pevny et al., 1998). Sox2 is required for maintaining NSCs and the expression is conserved in the developing CNS (Collignon et al., 1996). Studies have reported that downregulation of Sox2 induces neural progenitors to quit from cell cycle by losing neural progenitor markers and to start expressing neuronal differentiated markers, whereas continuous expression of Sox2 prevent progenitor differentiation (Graham et al., 2003). Thus, the mechanism by which SoxB1 family maintains the neural progenitor pool seems to be related to their role in cell cycle by regulating the timing of their exit from mitosis (Pevny and Placzek, 2005). Sox1 is widely used as NSC marker to identify neural progenitor cells both in vitro and in vivo (Li et al., 2001; Barraud et al., 2005). Furthermore, both Sox1 and Sox2 are detected in the neurogenic areas of postnatal brain such as the SVZ and the DG of the hippocampus in mice (Ferri et al., 2004; Ellis et al., 2004; Brazel et al., 2005), and Sox2 positive populations in these regions have NSCs

characteristics and behaviour in vivo (Suh et al., 2007). Reports have shown that Sox2 expression is lost upon neurospheres differentiation suggesting Sox2 as a NSC marker in the neurogenic areas in the brain (Brazel et al., 2005).

Our data has confirmed the expression of Sox1/Sox2 in the Bergmann glia of adult mouse cerebellum consistent with previous studies in the adult mice (Sottile et al., 2006; Alcock et al., 2007; Alcock and Sottile, 2007), human (Alcock et al., 2009), rabbit (Ponti et al., 2008), suggesting Sox1 and Sox2 as a general marker for Bergmann glia in the mature cerebellum. Our data also showed that the Sox1/Sox2/Sox9 positive cells in the mature cerebellum expressed other markers associated with Bergmann glia such as BLBP and GFAP as previously observed (Feng et al., 1994, Gimenez et al., 2000). This phenotype is shared with other radial glia, suggesting that Bergmann cells glia are radial glial cells that might be a source of NSCs in the mature cerebellum. Furthermore, reports in the literature have shown that in immature cerebellum, Sox1 and Sox2 positive cells were found in the white matter and become absent when cerebellum matures (Lee et al., 2005; Brazel et al., 2005), suggesting that they might be progenitors of Bergmann glia which then migrate toward their final destination in the PCL (Yamada and Watanabe, 2002).

Stem cells isolated from postnatal cerebellum were reported to be able to generate astrocytes, oligodendrocytes, and neurons upon their transplantation into the cerebellum in vitro (Lee et al., 2005, Klein et al., 2005); these findings suggest that stem-like cells in the cerebellum share functional characteristics with known adult NSCs. Neural stem progenitor cells have been isolated from different regions (but not the cerebellum) of the adult rhesus macaque brain characterized by their expression of some transcription factors such as Oct-4, Rex-1, and Sox-2

(Davis et al., 2006). Our observations in these species suggest that Sox gene expression in the cerebellum might be conserved among vertebrate species.

3.3.2 Stem cells in the mature cerebellum are of glial origin

The preliminary results of this chapter strongly implicate Bergmann glia as the stem cell population of the adult cerebellum. These unipolar cells present in the cerebellar cortex located in the Purkinje cell layer between the Purkinje cell bodies and their radial fibers extend through the molecular layer terminating at the pial surface (Yamada and Watanabe, 2002). Bergmann glial cells have been shown to arise from glial lineages as they express BLBP, GLAST, Nestin, Vimentin, and RC2 (Hockfield and McKay, 1985, Pixley and de Vellis, 1984, Hartfuss et al., 2001). In our study, GFAP, BLBP, and GLAST were detected in the adult primate and mouse cerebellum, but no Vimentin and RC2 expression. Lack of expression of these markers while retaining only GFAP expression happens after the transformation of nearly all radial glia in the brain into mature astrocytes (Parnavelas and Nadarajah, 2001). Moreover, with further development, the progeny of $GFAP^{+}$ radial glial precursors changes alongside a decrease in RC2 and increase in BLBP and GLAST, which would seem to fit with our observations (Malatesta et al., 2000). In the developing chick midbrain, (Gray and Sanes, 1992) have reported that radial glial cells are the earliest component of multipotential stem cells that contain neurons and glia suggesting that stem cells are either radial glia or become radial glia. Furthermore, a study in the avian CNS has shown the presence of radial glial precursors in the regions generating new neurons, suggesting a strong link between radial precursors and neurogenesis (Alvarez-Buylla et al., 1990).

Evidence has recently indicated that the radial glia function as neuronal precursors in the cerebral cortex and throughout CNS development (Malatesta et al., 2000; Anthony et al., 2004), and that stem cells in the adult brain might be of glial origin (Doetsch et al., 1999). A study by Malatesta et al., (2000) has shown that cells isolated from transgenic mouse expressing GFP under the control of the GFAP promoter were able to generate neurons and astrocytes in vitro, suggesting that radial glia are a heterogenous population of precursor cells (Malatesta et al., 2000). Moreover, these transgenic precursors under GFAP promoter control also contained cells positive for other glial markers that are later restricted to astrocytes such as GLAST and BLBP. The long fibers of radial glia guide neuronal migration during the development of the central nervous system (Hatten, 1999). This fact is also true for Bergmann glia radial fibers, which guide the migration of the granule cells and act as scaffold supporting the structure of the Purkinje cells (Yamada and Watanabe, 2002). After the process of migration is finished, radial glia are transformed into astrocytes except for retinal Muller cells, cerebellar Bergmann glia, and tanycytes of the third ventricle, suggesting that these radial glial cells may have another postnatal function and their role may not be restricted to neuronal guidance (Li et al., 2004; Merkle et al., 2004; Rodriguez et al., 2005; Rodriguez et al., 2010). In the cerebellum, it is possible that after the process of granule cell migration is completed around the second postnatal week (Hatten, 1999), Bergmann glia stop proliferation and they finally transform into a radial scaffold for the surrounding Purkinje cells. Studies have also reported that the transformation of the radial glial cells into astrocytes can be reverted, and that Bergmann glia may re-expresses RC2 after neurodegeneration, and Nestin after grafting embryonic Purkinje cells into the cerebellum of 3-4 months old *pcd*

mutant mouse (Sotelo et al., 1994), suggesting the quiescent state of Bergmann glial cells in the mature tissue. These studies appear to support our results that BG showed no reactivity for RC2 and Nestin in the steady state environment of the normal adult cerebellum, and opens the question of whether these cells might be activated after cerebellum injury. Altogether, results gathered here for the markers expression confirmed Bergmann glia as a Sox-positive radial glia population that is conserved across mouse, primate and chick species, and may represent quiescent stem cells in the mature cerebellum.

3.4 Conclusions

Our results confirmed the presence of a population of cells in the mature cerebellum of adult mouse, non-human primates, and chick expressing several markers known to be expressed by neural progenitor cells. Moreover, our data reveal no differences in the staining pattern of Sox1, Sox2, and Sox9 between mouse, primate and chick, and the staining location was confined to the BG cells in the mature cerebellum. These were $Sox1^{+}$ cells were detected as to be Bergmann glial cells located around the cell bodies of PCs. Furthermore, the expression pattern for the radial glial markers in Bergmann glia is consistent with radial glial phenotype in other brain regions suggesting that Bergmann glia are the radial glial cells of the mature cerebellum. Our results suggest that the Bergmann glia may represent a NSC-like population in the adult cerebellum in several species, and that Sox gene expression is highly conserved across these species. These observations highlight the importance of carrying out a thorough analysis to determine whether these Sox1 positive cells can be activated in response to the degeneration of Purkinje cells and investigate their specification, migration and differentiation capacity toward the damaged areas which provide the rationale for the next two chapters in this thesis.

4 Isolation and characterisation of cerebellar derived neural stem cells of adult GFP+/- Sox1 mouse

4.1 Introduction

Neural stem cells (NSCs) have been isolated from different regions of the developing (Reynolds et al., 1992; Uchida et al., 2000) and adult (Reynolds and Weiss, 1992; Gritti et al., 1999) mouse brain. They can be expanded and maintained in vitro in serum free medium in the presence of mitogens such as EGF and FGF-2 in vitro (Reynolds and Weiss, 1992; Weiss et al., 1996; Gritti et al., 1999). True NSCs are clonogenic with self-renewing and proliferative capacity, and they can be induced to differentiate into neuronal and glial lineages (Reynolds et al., 1992, Gage, 2000, Gritti et al., 2002). More recently, cells with NSC characteristics have also been isolated from embryonic and postnatal mouse cerebellum (Klein et al., 2005, Lee et al., 2005).

The cerebellum is one of the brain parts in which embryonic progenitors remain as radial glial cells throughout postnatal life (Malatesta et al., 2000, Anthony et al., 2004). NSCs differ in their requirements for growth factors in different parts of the brain; for example, multipotent precursors from either embryonic or adult mouse striatum can be expanded in EGF (Reynolds and Weiss, 1992). However, FGF-2 has shown to support the expansion of multipotent precursors from adult striatum and spinal cord, or both embryonic and adult hippocampus progenitors (Reviewed in (Ciccolini and Svendsen, 1998)). Other studies have shown that the combination of both mitogens are required for expansion and proliferation of NSCs isolated from forebrain or spinal cord of embryonic and adult rodents (Reviewed in (Tropepe et al., 1999)) .

Although NSCs are found in numerous regions of the adult brain such as the LV and the hippocampus, they appear to have a restricted potential regarding their differentiation into different neuronal subtypes (Doetsch, 2003a, Alvarez-Buylla and Garcia-Verdugo, 2002). Purkinje cells (PCs) are the largest neuron in the brain and main output of motor coordination of cerebellar cortex (Altman and Bayer 1997; Sudarov and Joyner, 2007). Various cerebellar disorders are linked to PC degeneration such as injuries, ischemia, intoxication, and hereditary cerebellar ataxia including Purkinje cell degeneration (pcd) (Cendelin, 2014). Stem cell transplantation in the cerebellum or other brain region depends on the ability of the grafted cells to integrate and differentiate into specific cell types. Embryonic cerebellar cell suspension grafted into the cerebellum of *pcd* mice resulted in the generation of new PCs with improved motor function (Reviewed in (Tao et al., 2010)). Generation of PC precursors from ESCs has been reported in vitro using a method of serum free culture of embryoid body-like aggregates (SFEB) treated with factors such as BMP4, Fgf8b, and Wnt3a (Su et al., 2006; Salero and Hatten, 2007; Tao et al., 2010). To date, there has been no report that describe the in vitro generation of PCs from NSCs isolated from mature CB. Thus, it would be of interest to test the ability of CB derived NSCs to generate PCs and to identify the in vitro culture conditions which may provide a suitable environment for their differentiation into mature PCs. In vitro differentiation of PCs would be important for the development of new therapeutic strategies for Purkinje cell degeneration disorders.

Aims of this chapter

1. To compare NSCs from adult mouse cerebellum with those derived from other regions in the brain, analysing their in vitro characterisation in terms of proliferation, morphology, potential differentiation, and growth factor requirements.
2. To compare the in vitro characteristics of NSC population analyses in this study with those of the population identified in Chapter 3.
3. To evaluate the in vitro differentiation potential of CB-derived NSCs into specific types of neurons in the cerebellum such as PCs.

4.2 Results

Although NSCs derived from adult cerebellum have been described (Alcock and Sottile, 2009), the growth factor responsiveness of CB-NSCs has not been examined. This chapter aimed to further characterise these NSC-like cells focusing on the responsiveness of mouse CB-NSCs to EGF and FGF-2. Furthermore, their potential ability to generate different types of neurons such as PCs in vitro has been examined as it could be of therapeutic value for some neurodegeneration diseases such as Purkinje cell degeneration (*pcd*).

4.2.1 Primary culture of NSCs derived from mature cerebellum

Cells from mature mouse cerebellum were isolated alongside NSCs isolated from the lateral ventricles (LV) and used as control in our experiments. Both CB and LV NSCs were cultured as monolayer and maintained in NSCs medium with EGF and FGF-2. The morphology of CB-NSCs in culture was similar to LV-NSCs, and both showed similar tendency to attach to the culture flasks within 24 hours of culturing (Fig. 4.1).

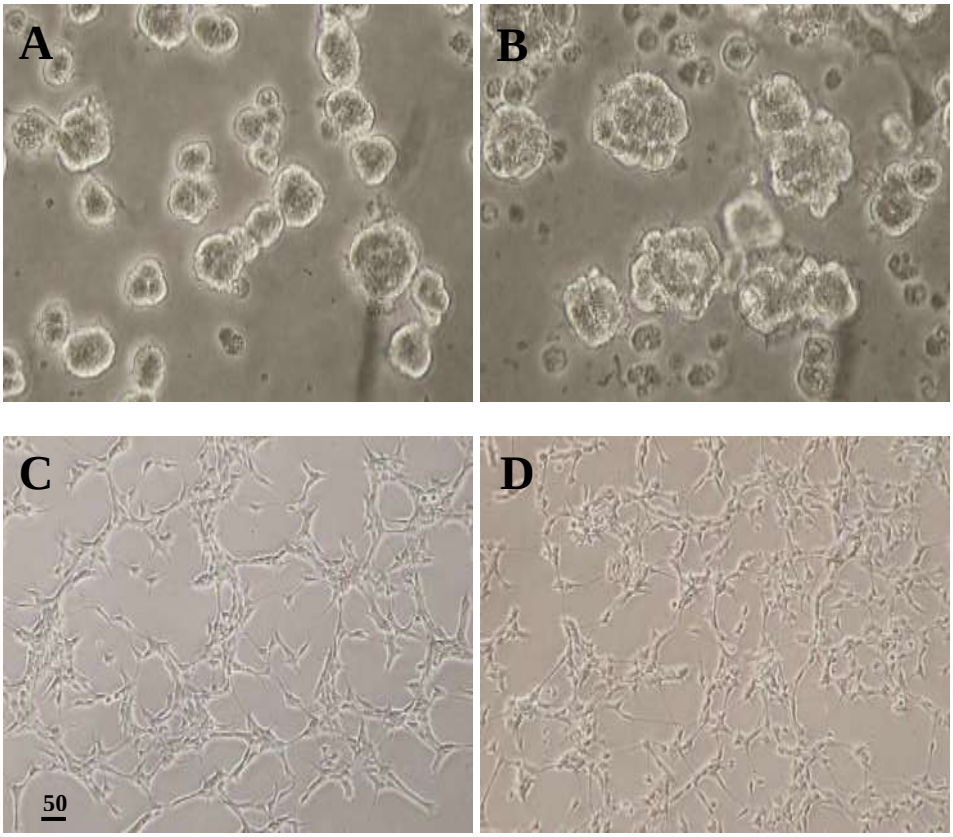

Figure 4.1 Brightfield image showing the morphology of CB and LV NSCs in culture. Both CB and LV cells formed neurospheres after 24 hr of passaging (A) and (B) respectively and they showed similar tendency to attach to culture flasks after 2 days in culture (C) and (D) respectively. Scale bar=50 µm.

4.2.2 Selection of the optimal seeding density for CB-NSCs experiments

In order to determine the optimal seeding density for CB-NSCs, various seeding densities were tested in this study. Dissociated cells were seeded onto 0.1% gelatin coated 24 well plates (with 0.5 ml of media) at seeding densities of 0.5 $x10^4$, 0.25 $x10^5$, 7.5 $x10^4$, and 1 $x10^5$ cells/ml and then the cells were allowed to grow for 2 days in culture. The optimum seeding density observed was $7.5x10^4$ cells/ml (Fig. 4.2). Cells grown at 0.5 $x10^4$ were found to be compromised in the 24 well plates and were died after 2 days (Fig. 4.2A). When seeded at $0.25x10^5$ cell/ml, the cells appeared healthy but large spaces were seen between the cells and they couldn't reach the number required for our experiments after 2 days in

culture (Fig. 4.2B). Cells seeded at 1 x10^5 cells/ml became 90% confluent the next day because of high cell number seeded (Fig. 4.2D). Only at 7.5x10^4 cells/ml did the cells display the same morphology and characteristics (Fig. 4.2C). Based on this finding, we used 7.5x 10^4 as the best density for all the experiments performed in this study.

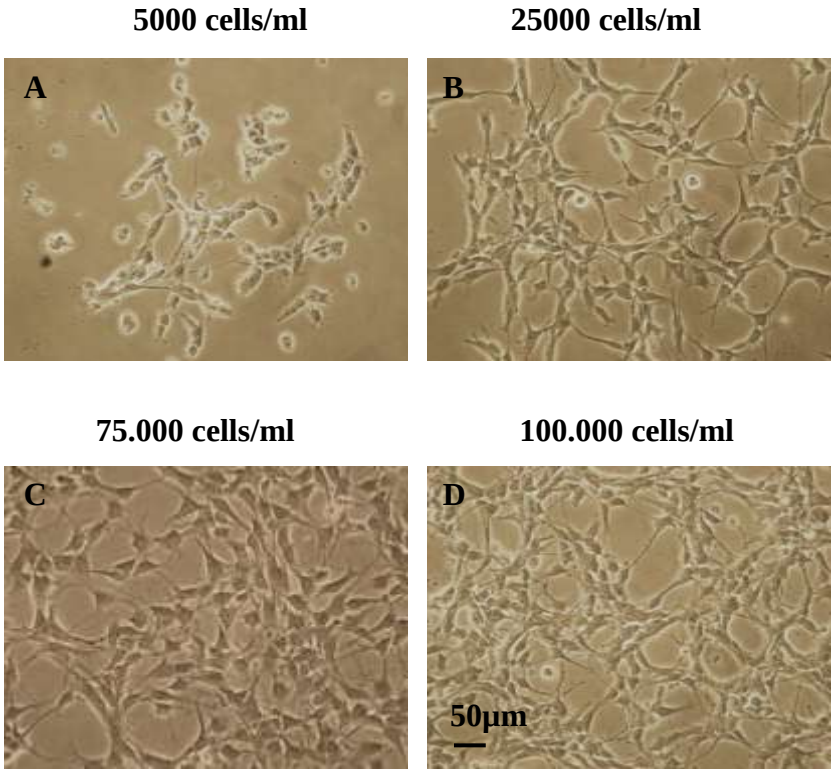

Figure 4.2 The Morphology of CB-NSCs grown at different seeding densities imaged 2 days after seeding. Cells seeded in 0.1% gelatin coated 24 well plates at 5x103, 25x103, 75x103, and 100x103 cells/ml. At very low density, the cells were compromised and couldn't survive beyond day2 in culture (A), while at high density (D), the culture reached confluency the next day. The density selected for subsequent experiments was 75x10^4 cells/ml. Scale bar =50µm

4.2.3 Quantification of CB-NSCs grown on gelatin and laminin coated culture flasks

To evaluate the effect of gelatine and laminin coating on the growth of CB-NSCS, CB-NSCs were seeded in 0.1% gelatine or laminin coated 24 well plates at a density of 75000cell/ml. After 2 days in culture, the cells were counted as well as analysed by a metabolic assay. There was no morphological difference between the cells grown on gelatin or laminin (Fig. 4.3A and B). Quantification of cell number showed no significant increase in cell number between the cells seeded on gelatin or laminin coated plates (Fig. 4.3C) indicating that CB-NSCs could attach on both laminin and gelatin coated plates without affecting there viability. Cell metabolic assay also showed that there was no significant difference between the cells grown on both coating agents (Fig.4.3D).

4.2.4 Effect of EGF and FGF-2 on CB derived NSCs

It is well known that EGF and FGF-2 are effective mitogens for the proliferation and maintaining NSCs in an undifferentiated state (McKay, 1997, Gage, 2000). Removal of these mitogens from the culture medium induces the differentiation of the cells into neurons and glia (Gritti et al., 1995, Schwindt et al., 2009). In vitro studies have shown that NSCs from the mature brain might be EGF (Reynolds and Weiss, 1992; Weiss et al., 1996a), FGF-2 (Gritti et al., 1996), or EGF+FGF-2 responsive (Lillien and Raphael, 2000). Thus, the aim of this experiment was to determine whether CB derived NSCs are EGF or FGF-2 responsive, or whether both growth factors are required for their expansion and proliferation. Moreover,

we also tested whether EGF and FGF-2 act in an additive manner on the proliferation of CB NSCs.

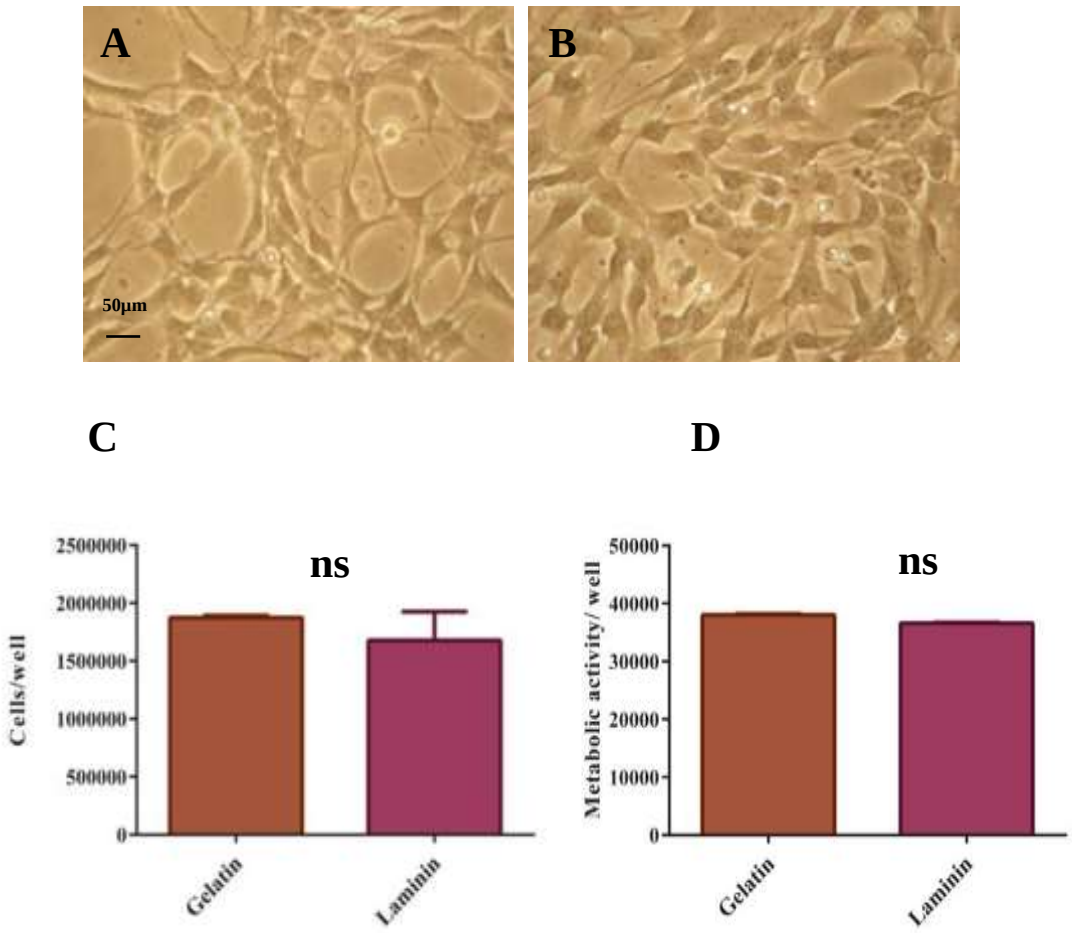

Figure 4.3 The effect of gelatin and laminin on the morphology and proliferation of CB NSCs. Cells seeded on gelatin (A) or laminin (B) coated plates. Cell number (C) and metabolioc activity (D) was not significantly different when CB cells grown for 2 days on gelatin or laminin. Data represent means ± SEM analysed by unpaired, 2 tailed student t test.

4.2.4.1 Effect of EGF and FGF-2 withdrawal on the metabolic cell activity of CB-NSCs

The effect of EGF and FGF-2 removal from the culture media was investigated for CB-NSCs and the control LV cells. To examine whether the removal of EGF or FGF-2 had an effect on the morphology and proliferation rate of CB-NSCs in monolayer culture, cells were cultured in medium with 20ng/ml of EGF, FGF-2, EGF+FGF-2 (control), or no growth factors (GFs) for 2 or 3 days followed by a cell metabolic assay. Both CB and LV NSCs cultured in EGF started to form neurospheres from day 1 in vitro (DIV1) and attached next day (DIV2) (Fig. 4.4). Morphologically, LV cells cultured in EGF resembled their control culture but they grew at lower rate (Fig. 4.4A), while EGF treatment induced hypertrophy to the CB cells which appeared as single cells extended from small neurospheres compared to their control culture (Fig. 4.4A). Interestingly, CB and LV cells grown in FGF-2 lost the spindle shaped morphology and appeared shrunken with long extensions with signs of spontaneous differentiation (Fig. 4. 4B). These cells showed similar morphology in both cultures although the CB cells were less confluent than the LV cells seeded at the same density. Cells didn't survive in medium without GFs and they died after 24 hr (Fig. 4.4D). Only the control culture containing both EGF and FGF showed typical morphology of NSCs (Fig. 4.4C). Cell metabolic assay performed after 3 days showed that GFs withdrawal had the same effect on the proliferation of CB and LV NSCs after 3 days in culture (Fig. 4. 5A and B respectively). The maximum proliferation rate was seen in the control culture when both GFs were added to the medium. However, CB and LV cells grown in EGF showed significantly higher metabolic activity than those cultured in FGF-2 and -GFs (Fig. 4.5A and B respectively).

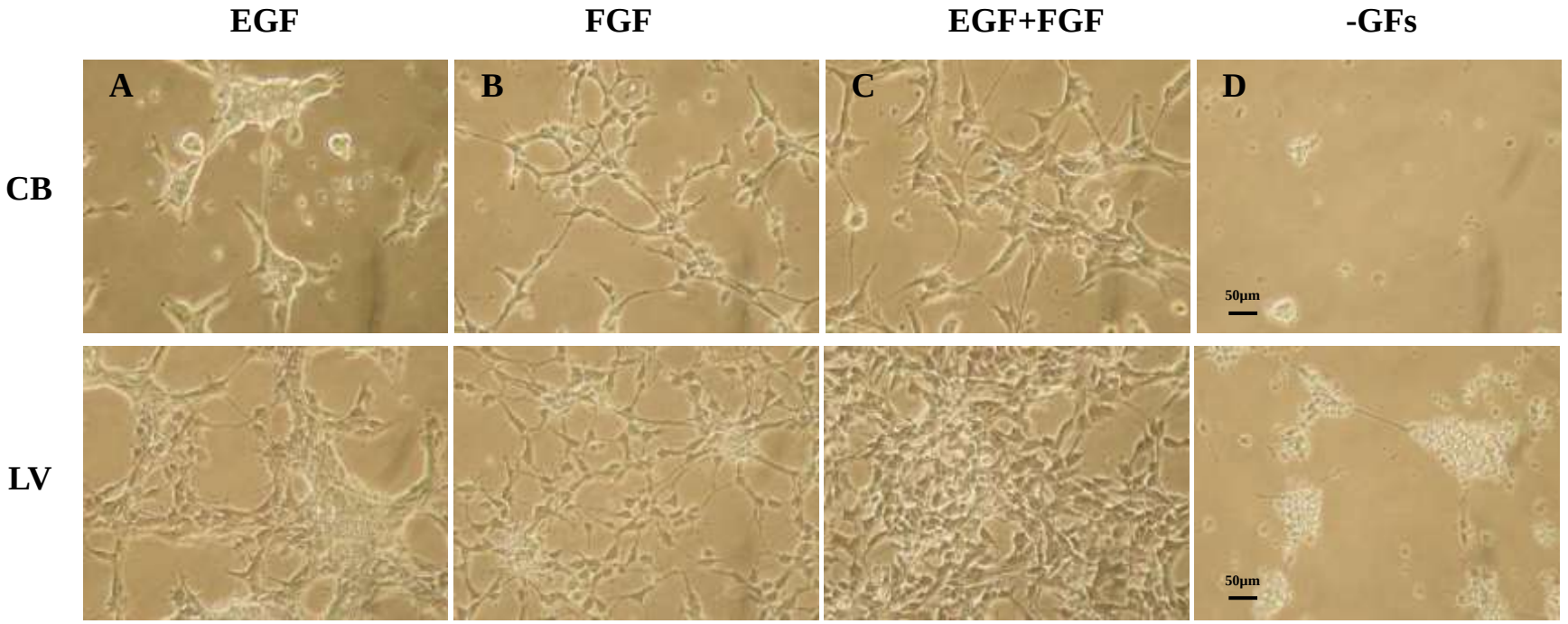

Figure 4.4 Brightfield image showing the morphology of CB and LV NSCs grown in different growth factor conditions. CB and LV cells were expanded for 2 days in EGF (20ng/ml) (A), FGF-2 (20ng/ml) (B), EGF+FGF-2 (C), and in mitogen free (-GFs) medium (D). Compared to the control culture (C), marked changes in the morphology were observed for CB and LV cells cultured in either EGF or FGF-2. (B) Cells grown in FGF-2 showed reduction in size and extended longer processes than other culture condition. When both mitogens were withdrawn from the medium, both cultures died and couldn't survive after 24 hours. EGF= epidermal growth factor; FGF-2= fibroblast growth factor. Scale bar =50µm

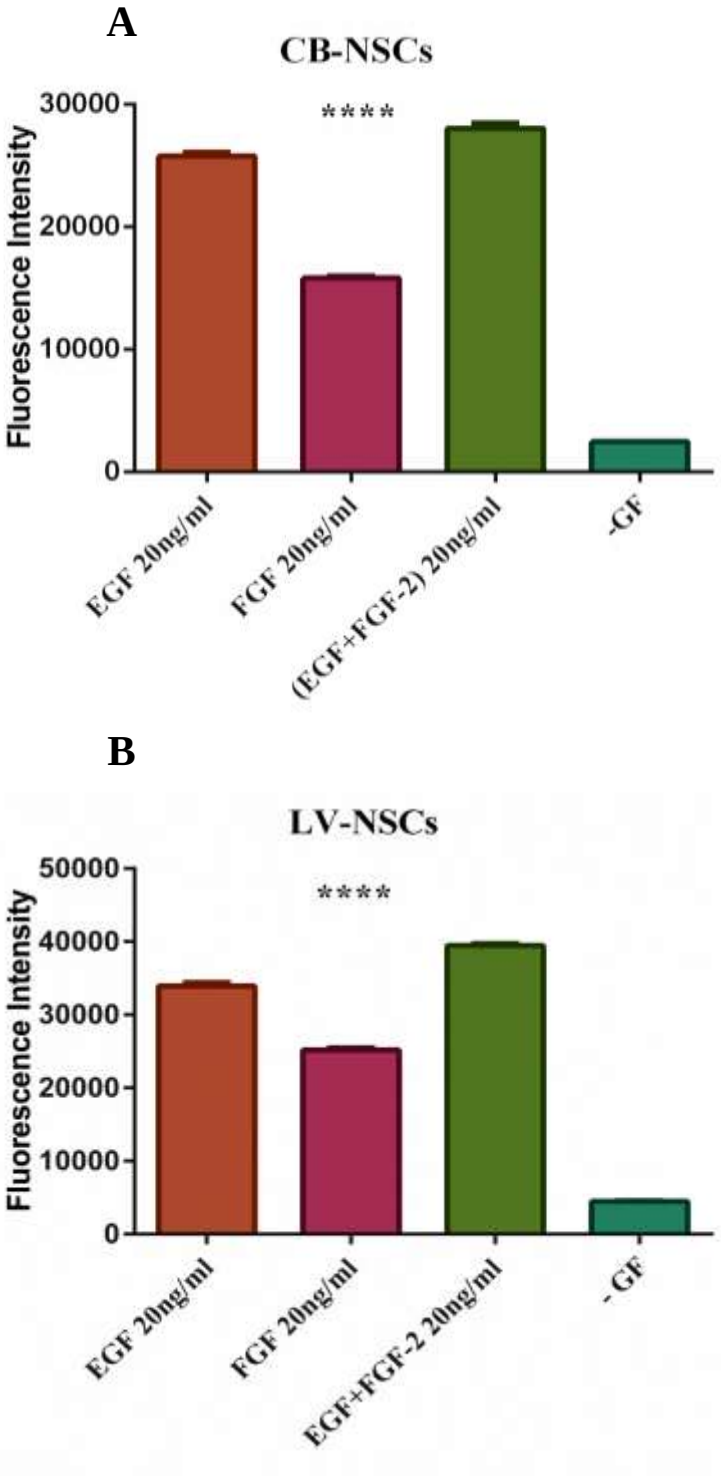

Figure 4.5 Effects of different growth factor conditions on the proliferation of CB (A) and LV (B) NSCs. Cell metabolic assay of CB and LV cells grown for 3 days in EGF, FGF-2, EGF+FGF-2, and mitogen free (-GFs) medium. The graphs show that both cells grew better in EGF than FGF-2 but the highest rate of proliferation was observed when both mitogens were added to the medium. Data are presented as means ± SEM using one-way ANOVA with Tukey's method to compare the mean of each group (**** $P < 0.0001$). EGF= epidermal growth factor; FGF-2= fibroblast growth factor. (n=9) EGF= epidermal growth factor; FGF-2= fibroblast growth factor.

4.2.4.2 Dose-dependent effect of combined EGF and FGF-2 in the culture on the morphology and proliferation of CB-NSCs

The previous dataset clearly revealed that both EGF and FGF-2 were required for CB-NSCs proliferation (see Fig. 4. 4 and 4.5 for detail). The concentration of the GFs used for normal growth and expansion of NSCs was 20ng/ml. Since the literature does not describe the effect of different doses of EGF and FGF-2 on the morphology and proliferation of CB-NSCs in adult mouse, we tested the response of CB derived NSCs to EGF and FGF-2 in a dose dependent manner by increasing the concentration of both GFs in the media. For this purpose, CB and LV NSCs were seeded onto gelatin coated coverslips for 2 days in medium containing EGF and FGF-2 at different concentrations (2, 5, 10, and 20 ng/ml of EGF+FGF-2). Brightfield images were taken at day2 in vitro to evaluate the morphology of these cells in each medium condition (Fig.4.6). At each concentration used, CB cells showed growth and the same morphology but with clear differences in cell number, which appeared to increase gradually with increasing the GFs doses (Fig. 4.6). Cell metabolic assay showed that the difference in the proliferation was only significant at 2ng/ml, whereas the slight differences between 5, 10, and 20ng/ml was not significant (Fig. 4.7). This finding suggests that the exposure to EGF and FGF-2 stimulated the proliferation at 2ng/ml and the saturation achieved at 5ng/ml for both CB and LV cells. However, a lower proliferation rate was observed when no mitogen was added in the medium, confirming them as pivotal factors for NSCs growth (Fig. 4. 6 and 4.7).

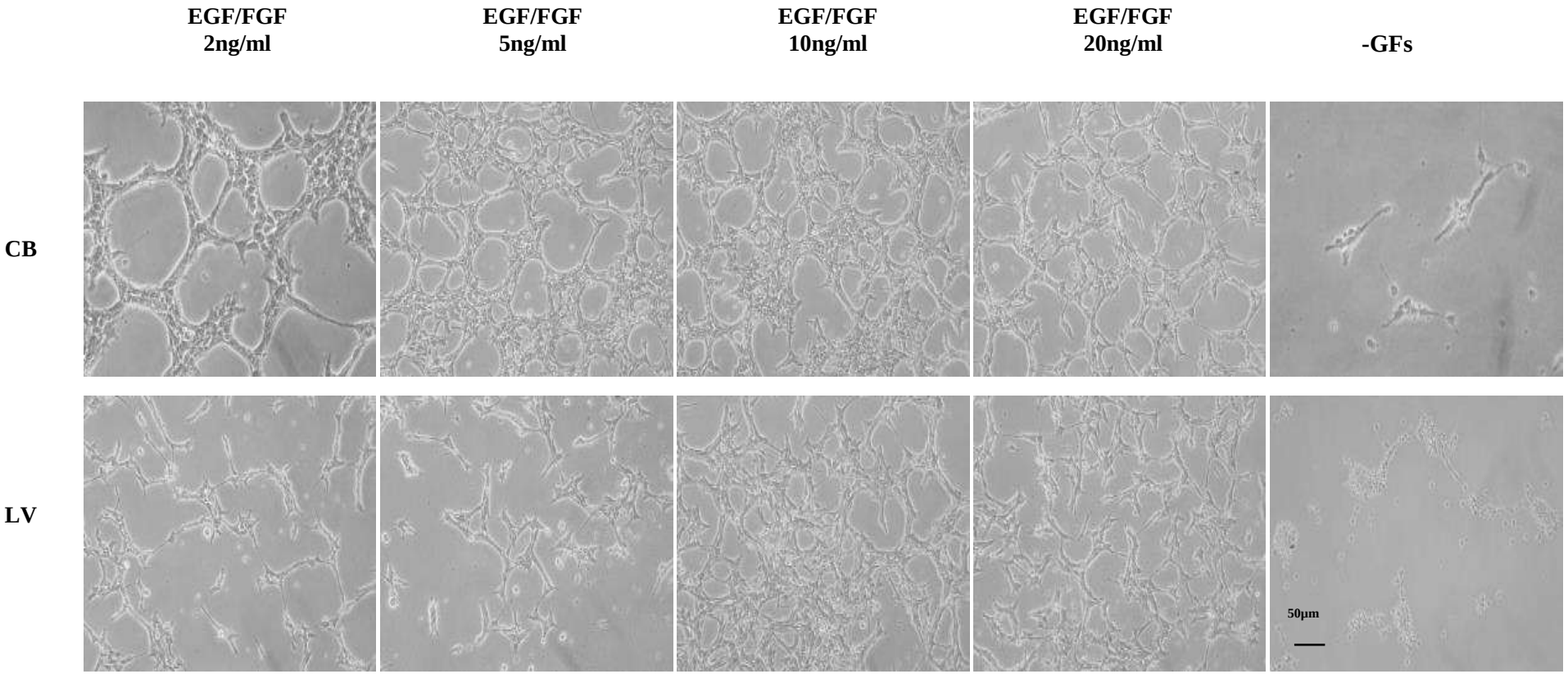

Figure 4.6 Brightfield images showing the dose dependent effect of EGF+FGF-2 on the morphology and proliferation of CB and LV NSCs. The morphology of CB cells differed in in different doses of growth factors. LV cells revealed lower rate of proliferation at 2 and 5ng/ml, and the proliferation rate was increased at higher doses of EGF and FGF-2. No growth was observed in the mitogen free media (-GFs).

EGF= epidermal growth factor; FGF-2= fibroblast growth factor. Scale bar =50µm

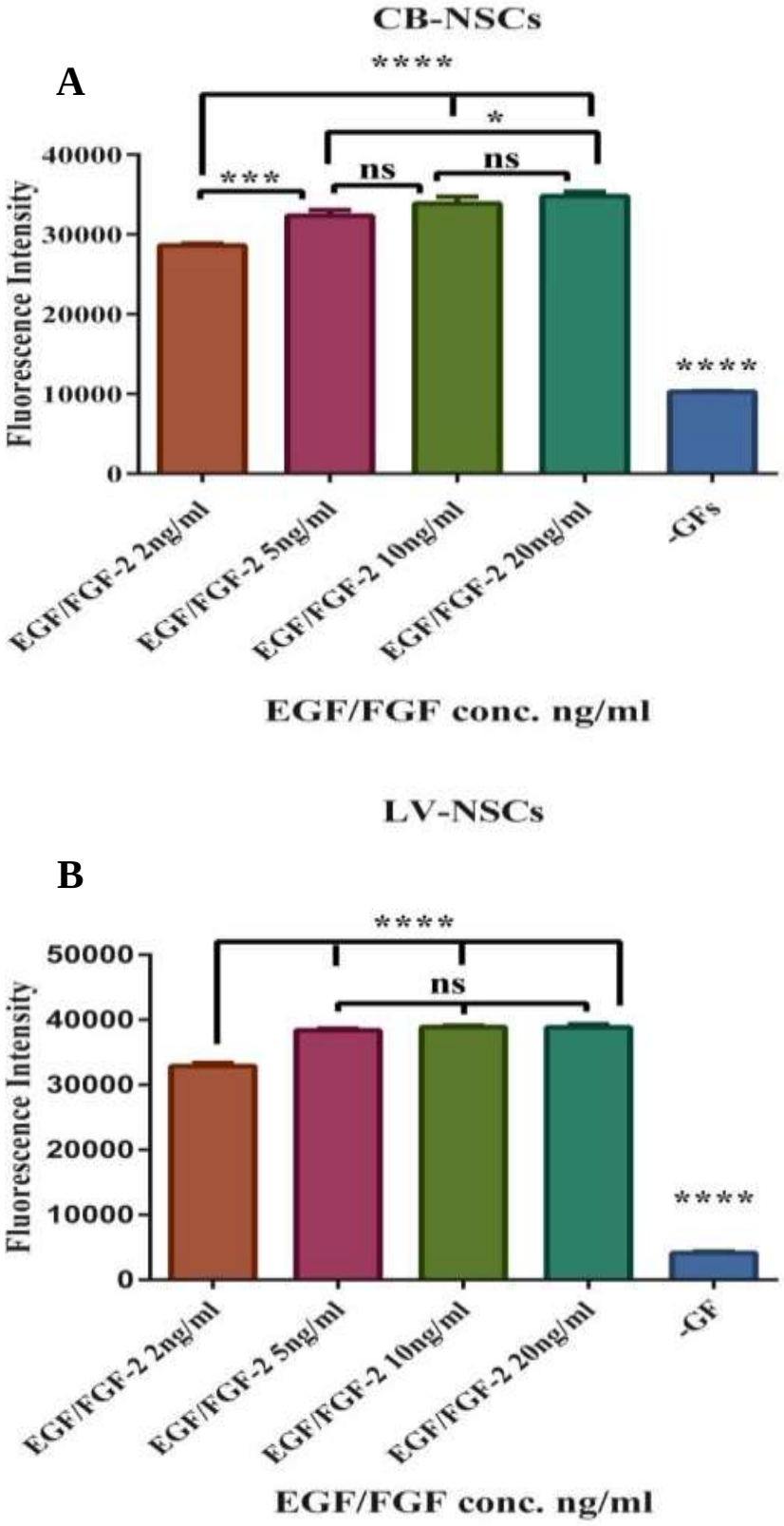

Figure 4.7 Dose dependent effect of EGF and FGF-2 on the proliferation and cell viability of CB (A) and LV (B) NSCs. EGF and FGF-2 supported proliferation at 2ng/ml and the saturation was observed at 5ng/ml for both LV and CB cells. Data are the mean ± SEM, with at least nine replicates within each condition**.** Data are presented as means ± SEM using one-way ANOVA with Tukey's method to compare the mean of each group (**** P < 0.0001, ***P<0.0002, P< 0.0253). EGF= epidermal growth factor; FGF-2= fibroblast growth factor.

4.2.4.3 Dose-dependent effect of either EGF or FGF-2 in the culture on the morphology and proliferation of CB-NSCs

4.2.4.3.1 CB and LV NSCs culture in the presence of EGF

In order to further investigate the requirement of CB-NSCs for EGF and FGF-2 for their expansion, the effects of each of the mitogens were measured in a dose dependent manner. For this purpose, both cell types were seeded at a density of $75x10^4$ on gelatin coated coverslips in 24 well plates and cultured for 2 days in different growth factors concentrations as shown in (Fig. 4.8). After 2 days in vitro the proliferation rate was measured by prestoblue cell metabolic assay (see methods 2.4.5 for detail). When cells were exposed to increasing doses of EGF, brightfield images taken at Day1 in vitro showed no obvious changes in the morphology or cell number of CB and LV cells in all medium conditions, except for LV cells grown as neurospheres at 20ng/ml EGF. Images at day 2 in vitro showed no morphological difference between different doses of EGF for CB and LV cells compared to the control (EGF+FGF-2) (Fig. 4.8) and all cells exhibited spindle shaped morphology except for LV at 20ng/ml which grew as neurospheres as Day1 (Fig. 4.8). However, we noticed slight increase in cell number between CB cells cultured in 5, 10, and 20ng/ml and LV control culture, but surprisingly LV cultures at 2ng/ml appeared to show higher cell numbers compared with their EGF+FGF control (Fig. 4.8). Most importantly, the metabolic assay showed that the response to EGF was similar between CB and LV cells, with the effect of 2ng/ml nearly as strong as (EGF+FGF-2) at 20ng/ml and the response to EGF being maximal at 5ng/ml (Fig. 4.9).

CB-NSCs

-FGF

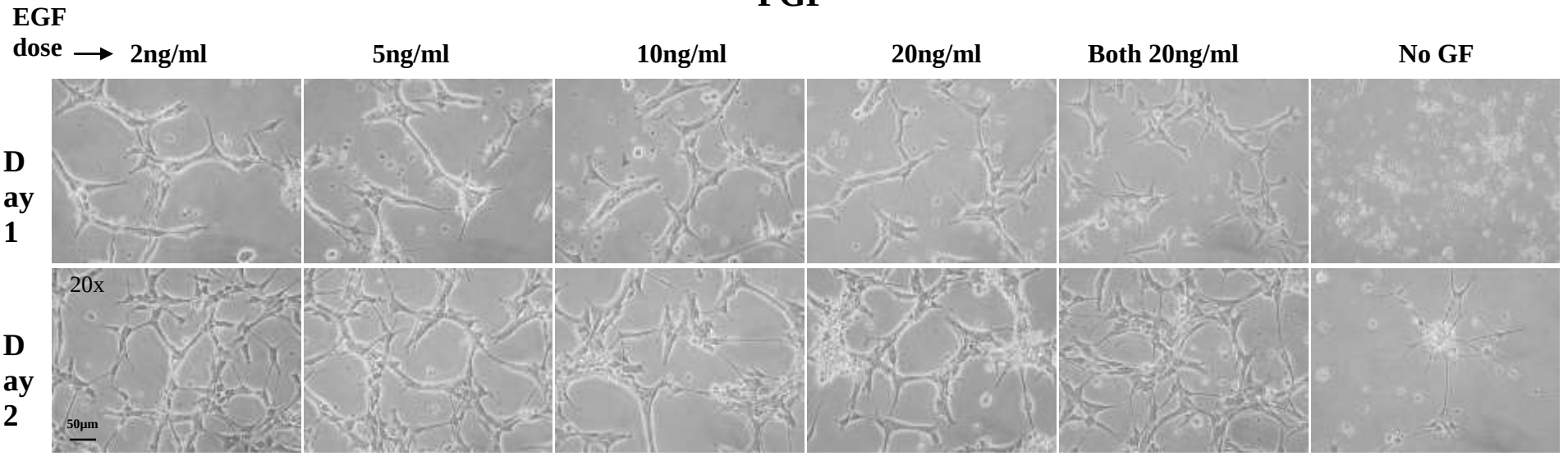

LV-NSCs

-FGF

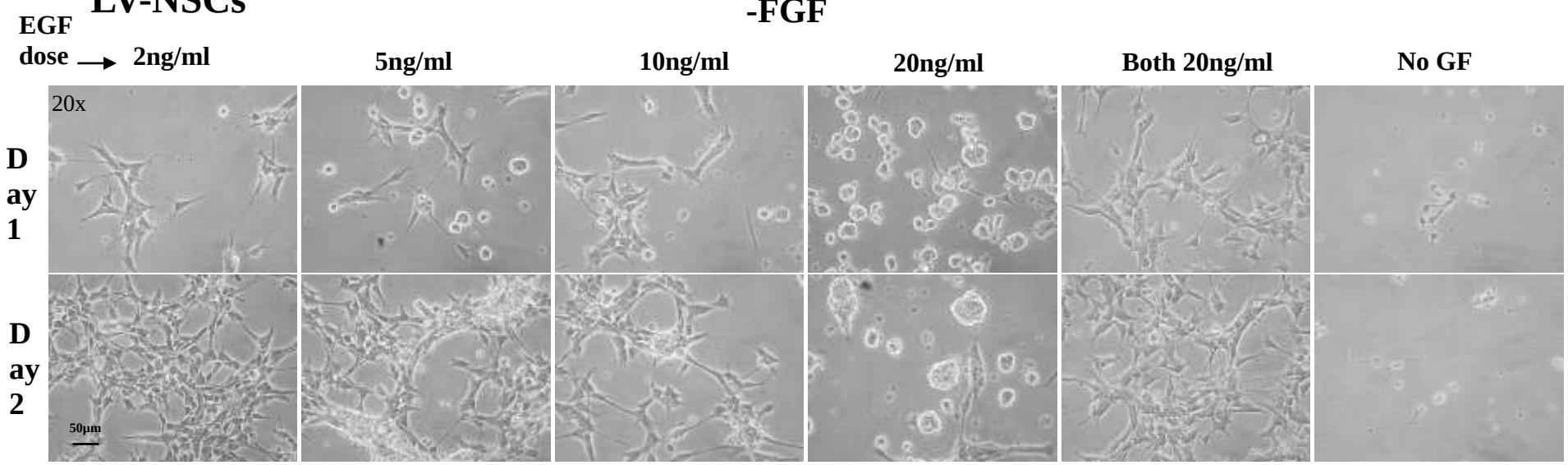

Figure 4.8 Brightfield images showing the dose dependent effect of EGF on the morphology of CB and LV NSCs. When CB and LV cells were cultured for 2 days in different concentrations of EGF (omitting FGF-2 from the media), they didn't show any morphological alteration compared to their controls (EGF+FGF-2). Interestingly, 2ng/ml of EGF was sufficient to stimulate the growth of CB and LV cells although LV cells showed lower cell number compared to CB cells seeded at the same density and they grew as neurospheres at 20ng/ml.

EGF= epidermal growth factor; FGF-2= fibroblast growth factor. Scale bar =50µm.

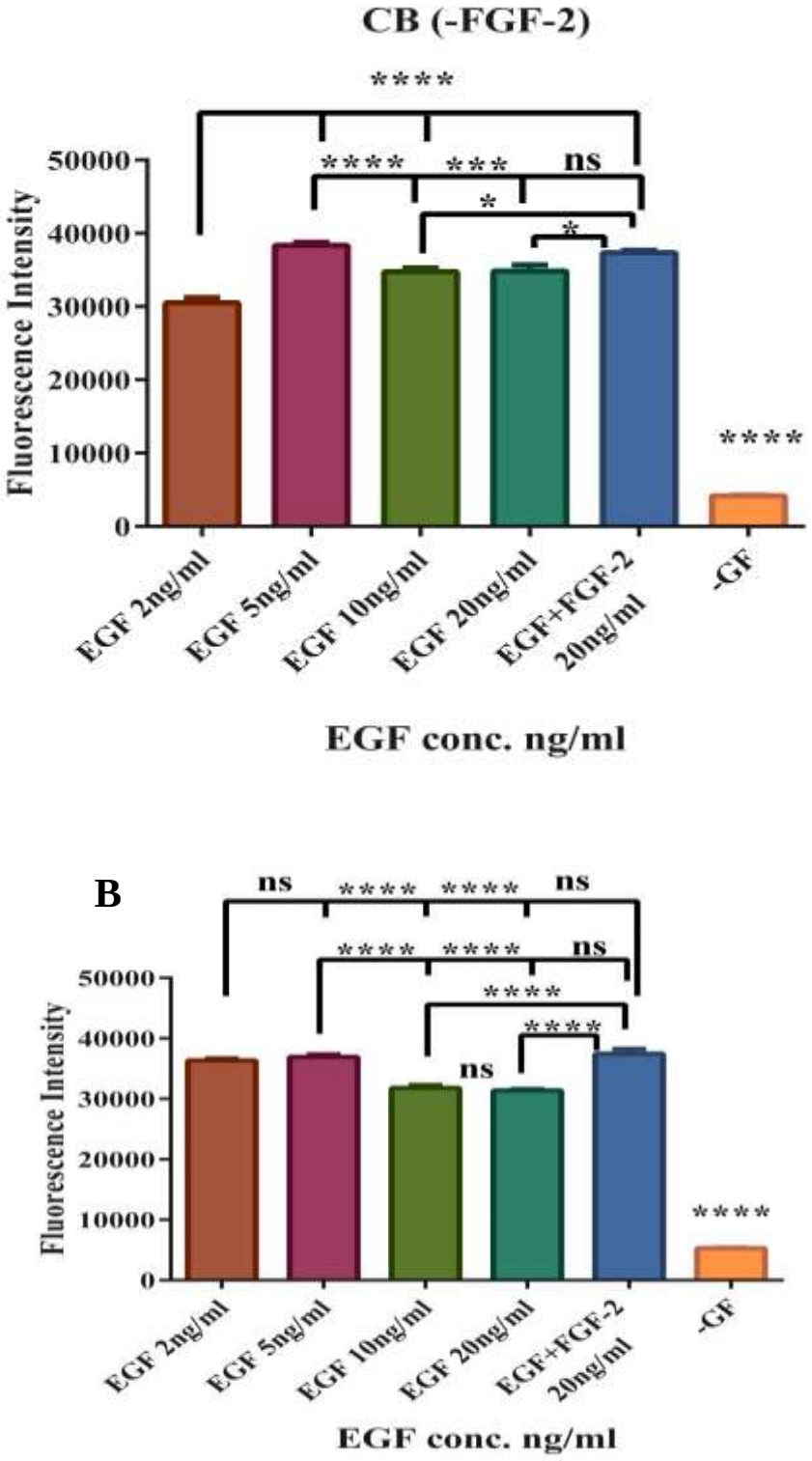

Figure 4.9 Dose dependent effect of EGF on the proliferation and metabolic activity of CB (A) and LV (B) NSCs. CB and LV cells were grown for 2 days in different doses of EGF but no FGF-2 was added to the media except for the control culture (EGF+FGF-2 20ng/ml). The mitogenic effect of EGF was readily detectable at 2ng/ml and maximal at 5ng/ml for both cells. Data are the mean ± SEM, with at least nine replicates within each condition, one-way ANOVA with Tukey's method to compare the mean of each group. (**** P< 0.0001, *** P<0.0003, P< 0.0158).

4.2.4.3.2 CB and LV NSCs culture in the presence of FGF-2

In order to test whether adding FGF-2 in a dose dependent manner had the same effect as EGF in the previous section (4.1.5.3.1), a similar experiment was carried out but here EGF was omitted from the medium and increased FGF-2 concentration used as shown in brightfield images (Fig. 4.10). The data indicated that cells cultured in FGF-2 alone displayed dramatic changes in morphology compared to those cultured in EGF alone (Fig. 4. 8). At low FGF-2 doses (2 and 5ng/ml), the cells appeared smaller in size and extended long neurites compared with their control, with high rate of cell death and spontaneous differentiation (Fig. 4.10). However, the majority of the cells were able to grow and survive in all doses used, and cells at 20ng/ml FGF were found to adopt the spindle shaped NSC morphology similar to the control culture. Metabolic cell activity showed that FGF-2 stimulated the proliferation at the lowest dose used and increased gradually with the maximum achieved at 20ng/ml. These findings strongly suggested that FGF-2 was a strong mitogen for both CB and LV cells (Fig. 4.11).

CB-NSCs

-EGF

FGF dose → 2ng/ml | 5ng/ml | 10ng/ml | 20ng/ml | E+F 20ng/ml | -GF

Day 1

Day 2

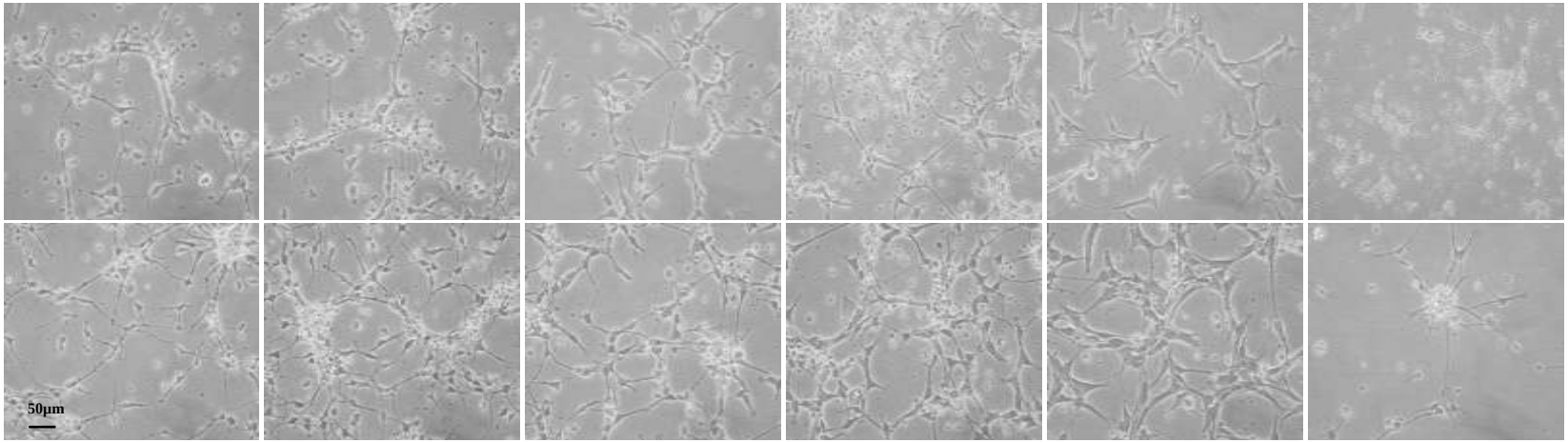

LV-NSCs

-EGF

FGF dose → 2ng/ml | 5ng/ml | 10ng/ml | 20ng/ml | E+F 20ng/ml | -GF

Day 1

Day 2

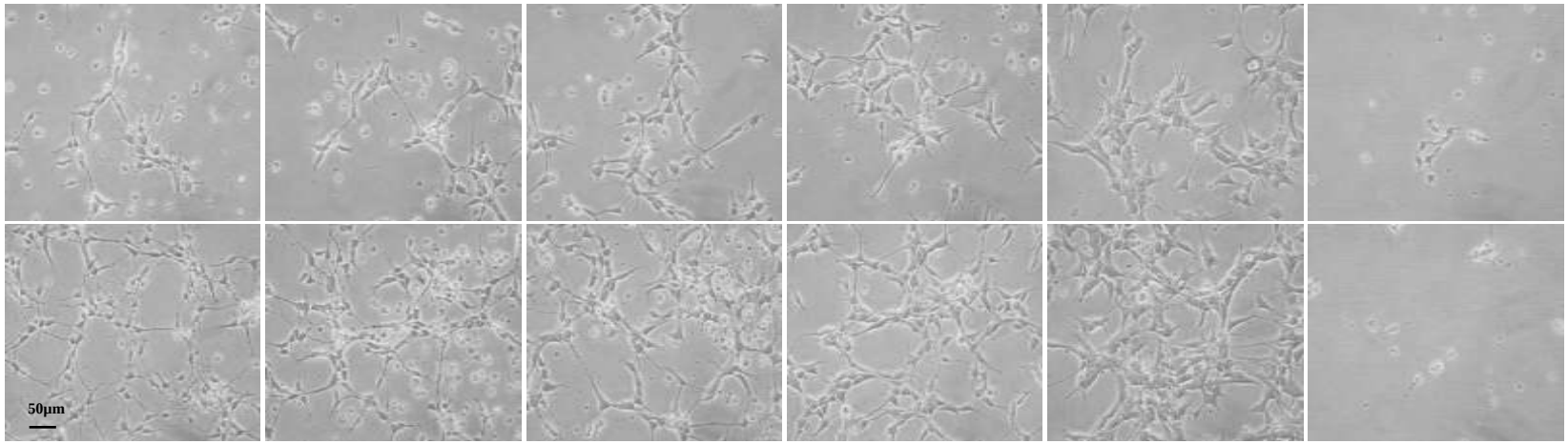

Figure 4.10 Brightfield images showing the dose dependent effect of FGF-2 on the morphology of CB and LV NSCs. CB and LV cells cultured for 2 days in different concentrations of FGF-2 (omitting EGF from the media), showed clear morphological alteration compared to their controls (EGF+FGF-2). 2ng/ml of FGF-2 was sufficient to stimulate the growth of CB and LV cells but the cells were atrophied and extended very long cell processes. As the dose of FGF-2 was increased gradually, the cells adopted the normal morphology as they appeared in the control culture (EGF+FGF-2 20ng/ml) although the cell number was not greatly affected when the dose of FGF-2 was increased.

EGF= epidermal growth factor; FGF-2= fibroblast growth factor. Scale bar =50µm

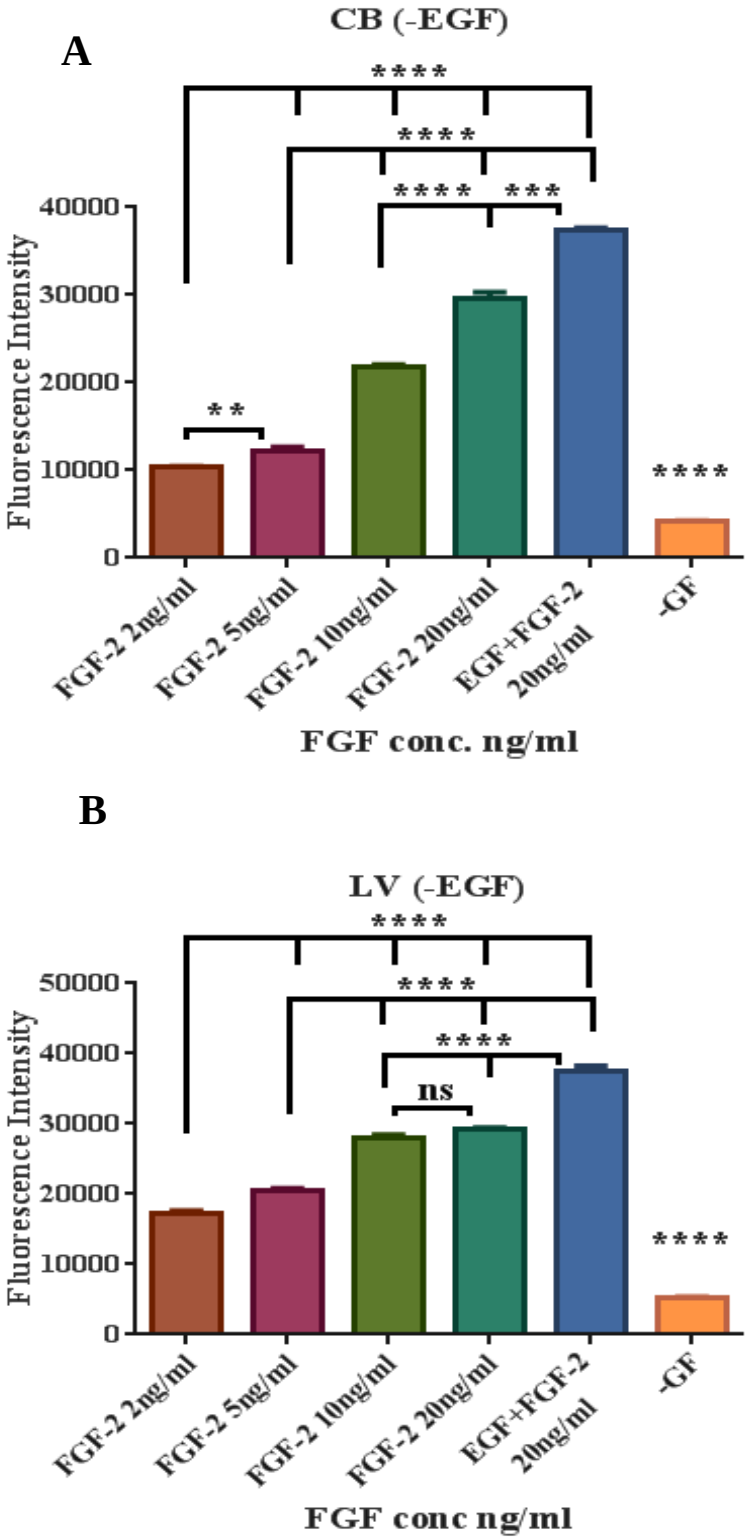

Figure 4.11 Dose dependent effect of FGF-2 on the proliferation and metabolic activity of CB (A) and LV (B) NSCs. Increasing concentrations of FGF-2 were added to the culture medium for CB and LV cells. The mitogenic effect of FGF-2 was readily detectable at 2ng/ml and the maximal response was observed in the control culture when both mitogens were used at 20ng/ml. Data are the mean ± SEM, with at least nine replicates within each condition, one-way ANOVA with Tukey's method to compare the mean of each group (**** P< 0.0001, *** P<0.0001, P< 0.0017).

4.2.4.3.3 CB and LV NSCs in EGF culture at smaller doses

The previous experiments indicated that EGF effect as a mitogen was not dose dependent on CB and LV cells although the saturation was detected as to be 5ng/ml. To see if lower concentrations could stimulate cell proliferation, the experiment in section (4.1.5.3.1) was repeated using lower doses of EGF for culturing CB and LV cells for 2 days and removing FGF-2 from the medium to avoid interfering with EGF. The EGF doses used are shown in (Fig. 4.12). Both CB and LV cells showed similar morphology at very low doses (0.1, 0.2, and 0.5ng/ml) and both appeared hypertrophied except for LV cells which grew as neurospheres at 20ng/ml as previously described in this study (see Fig. 4. 8 for detail). Cell metabolic assay showed that the stimulation of CB and LV cells was observed readily at 0.1ng/ml and increased with dose increase up to 2ng/ml for CB cells and 5ng/ml for LV cells (Fig.4.13). However, the maximum proliferation rate was detected when both mitogens were added to the media.

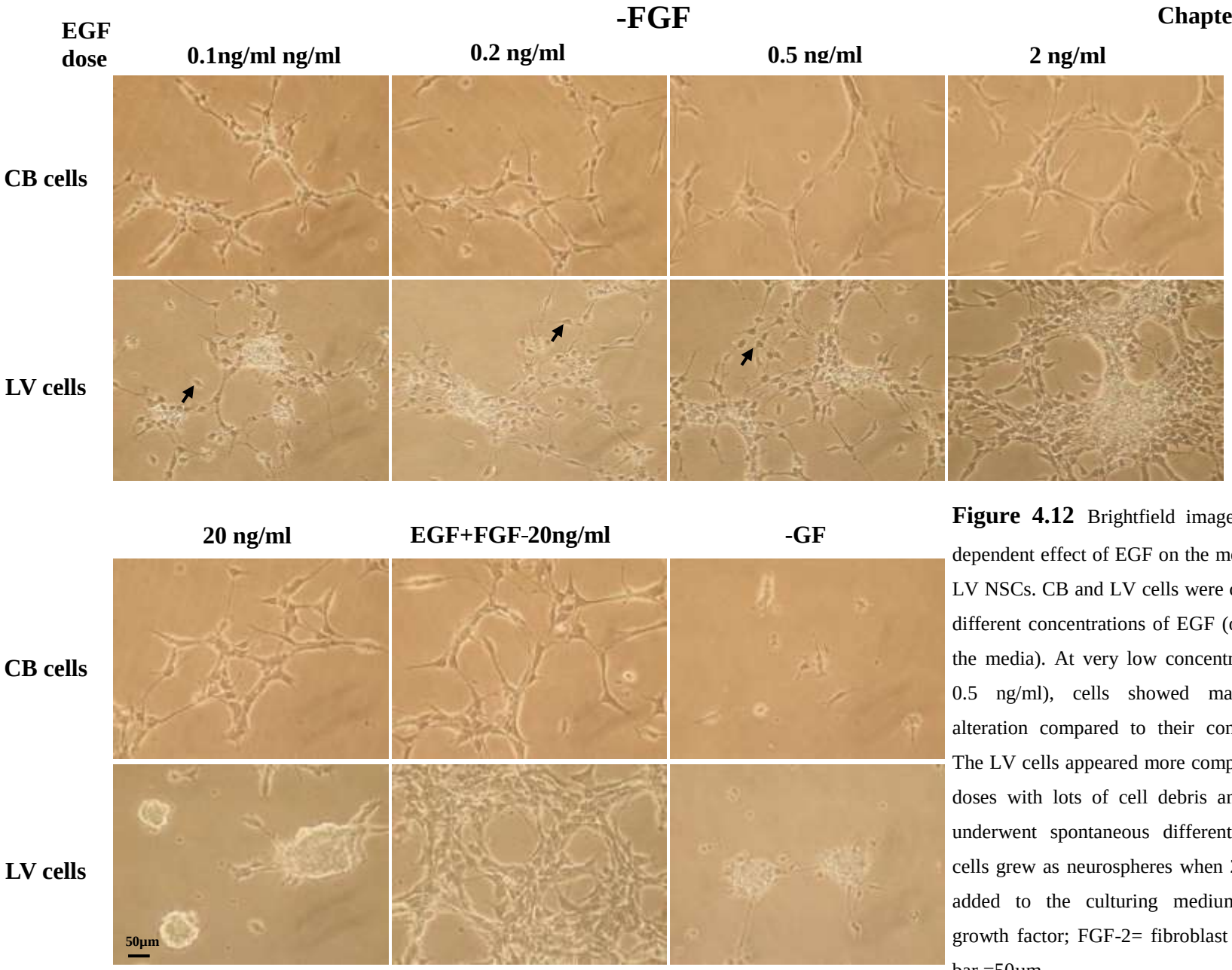

Figure 4.12 Brightfield images showing the dose dependent effect of EGF on the morphology of CB and LV NSCs. CB and LV cells were cultured for 2 days in different concentrations of EGF (omitting FGF-2 from the media). At very low concentrations (0.1, 0.2, and 0.5 ng/ml), cells showed marked morphological alteration compared to their controls (EGF+FGF-2). The LV cells appeared more compromised at the lower doses with lots of cell debris and most of the cells underwent spontaneous differentiation (arrows). LV cells grew as neurospheres when 20ng/ml of EGF was added to the culturing medium. EGF= epidermal growth factor; FGF-2= fibroblast growth factor. Scale bar =50µm.

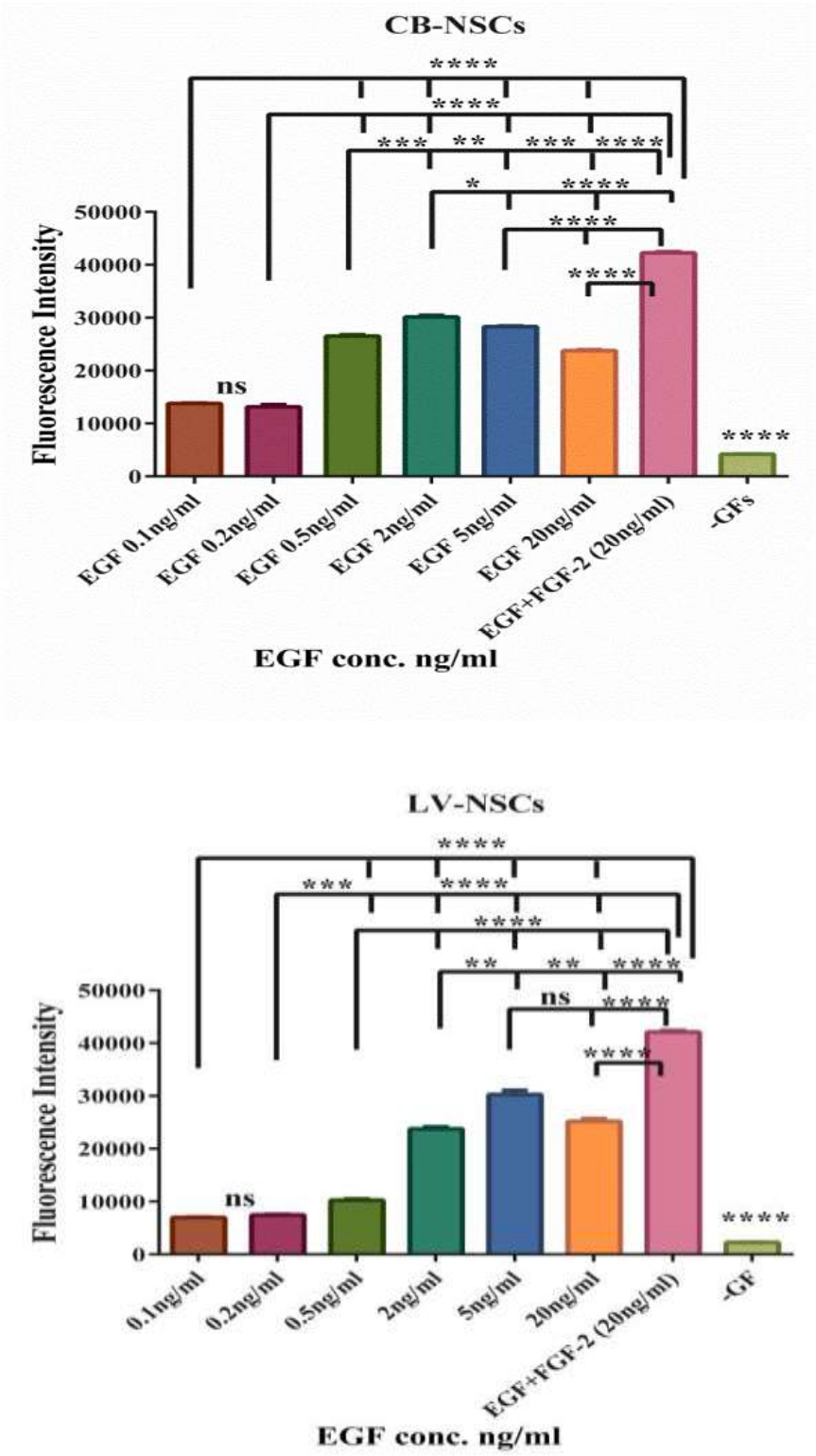

Figure 4.13 Dose dependent effect of EGF on the proliferation and cell viability of CB (A) and LV (B) NSCs. CB and LV cells were grown for 2 days in different doses of EGF but no FGF-2 was added to the media except for the control culture (EGF+FGF-2 20ng/ml). The mitogenic effect of EGF was readily detectable at 0.1ng/ml for both cells and the saturation was observed at 2ng/ml for CB cells and 5ng/ml for the LV cells. Data are presented as means ± SEM using one-way ANOVA with Tukey's method to compare the mean of each group (**** P < 0.0001, *** P <0.0003, **P<0.0026, *P< 0.0156). EGF= epidermal growth factor; FGF-2= fibroblast growth factor.

4.2.4.4 Longer term effect of EGF and FGF-2 withdrawal on the proliferation of CB-mNSCs

We have previously shown that EGF and FGF-2 stimulate the growth and proliferation of CB and LV NSCs after 2-3 days culturing in vitro, and that CB and LV cells displayed different morphology when cultured in the presence of either EGF (20ng/ml) or FGF-2 (20ng/ml) compared with the control culture (EGF+FGF-2, 20ng/ml each). To determine whether the cells could be expanded for extended periods in EGF, FGF-2, EGF+FGF-2, or in mitogen free media conditions, a 3-week withdrawal of EGF and FGF-2 was tested on CB and their control LV NSCs followed by metabolic activity measurement and in vitro differentiation for 6 days, in order to identify the phenotype of the differentiated cells. For this purpose, CB and LV NSCs were plated into T25 flasks and let to grow for 5 passages in medium with EGF, FGF-2, EGF+FGF-2, and no GFs. After 5 passages, the cells were seeded onto gelatin coated glass coverslips at a density of 7.5×10^4 and in the same conditions (EGF, FGF-2, EGF+FGF-2, and no GFs) and let to grow for 2 days until the cells became confluent (Fig. 4.14 A and B). After that the medium was changed to differentiation medium and the cells were allowed to differentiate for 6 days. After fixation with 4% PFA, immunocytochemistry was performed with specific markers to identify the differentiated cell types. The brightfield images (Fig.4.14) showing the morphology of CB and LV NSCs grown in different medium conditions for 5 passages. CB and LV NSCs grown in EGF medium showed decreasing numbers over the period of the 5 passages, but the morphology of the cells was similar to the control condition (EGF+FGF-2) (Fig. 4.14). However, cells grown in FGF-2

only showed very different morphology with smaller cell bodies extending long cellular extensions compared to those grown in the normal media (Fig. 4.14). I also noticed the formation of large neurospheres in the LV NSCs cultured in EGF at P3, which was not observed in the CB culture. CB and LV NSCs cultured in normal medium with EGF and FGF-2 showed constant degree of proliferation and morphology suggesting it as the optimum media condition for their growth and expansion. Cell viability analysis was assessed at each passaging and the data of all the metabolic cell activity measurements were averaged. Results showed significant increase in the proliferation of CB cells in EGF alone compared with FGF-2 culture, and whereas LV cells showed the same level of proliferation in EGF or FGF-2 culture (Fig. 4.15 A and B respectively). Both CB and LV cells showed significant increase and achieved highest rate of growth and proliferation in the control culture media when both mitogens were added (Fig. 4.15 A and B respectively). Moreover, cells couldn't grow in the absence of both mitogens suggesting EGF and FGF-2 are important survival factors for the growth and expansion of CB and LV NSCs.

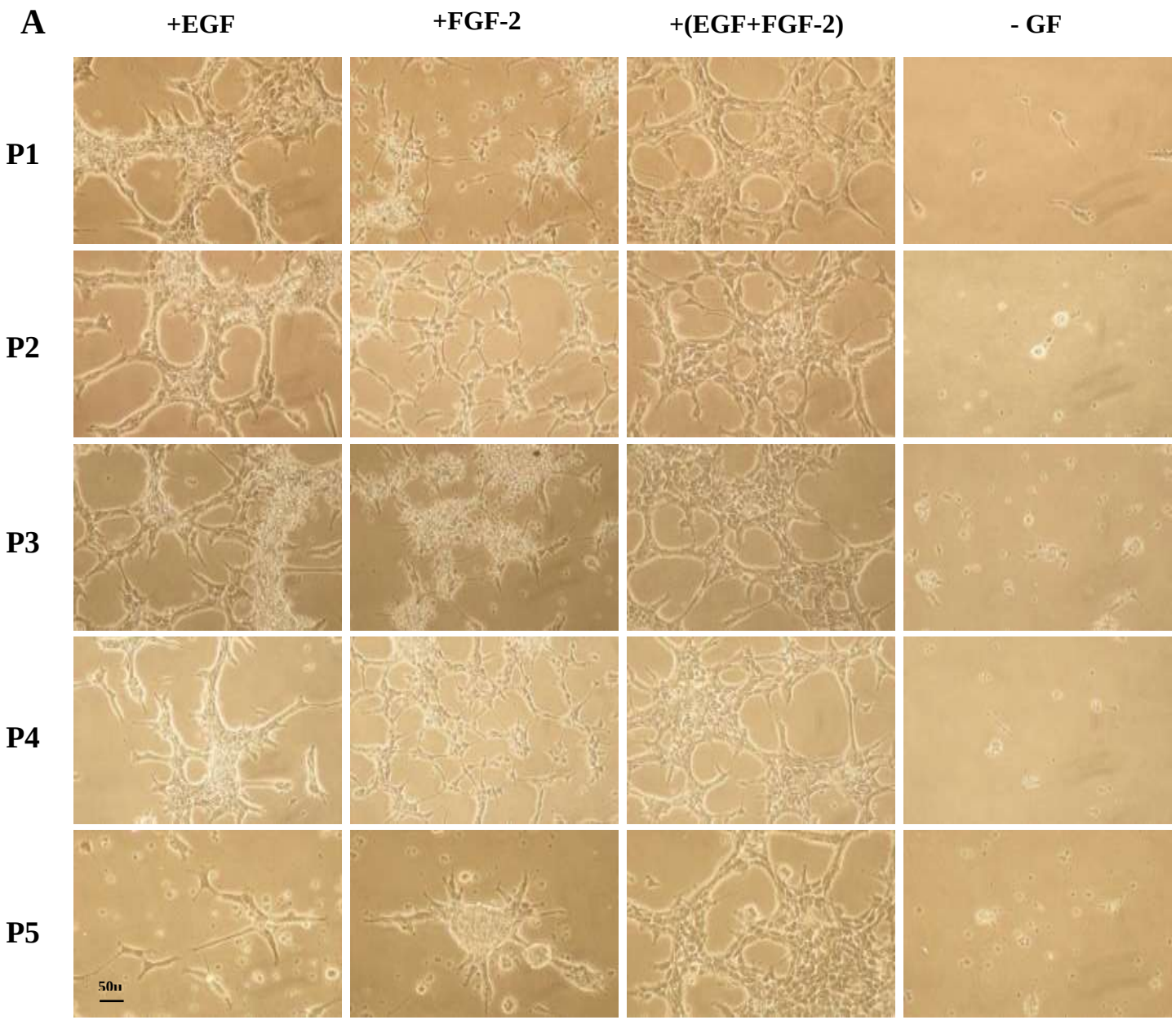
A
+EGF
+FGF-2
+(EGF+FGF-2)
- GF
P1
P2
P3
P4
P5
50u

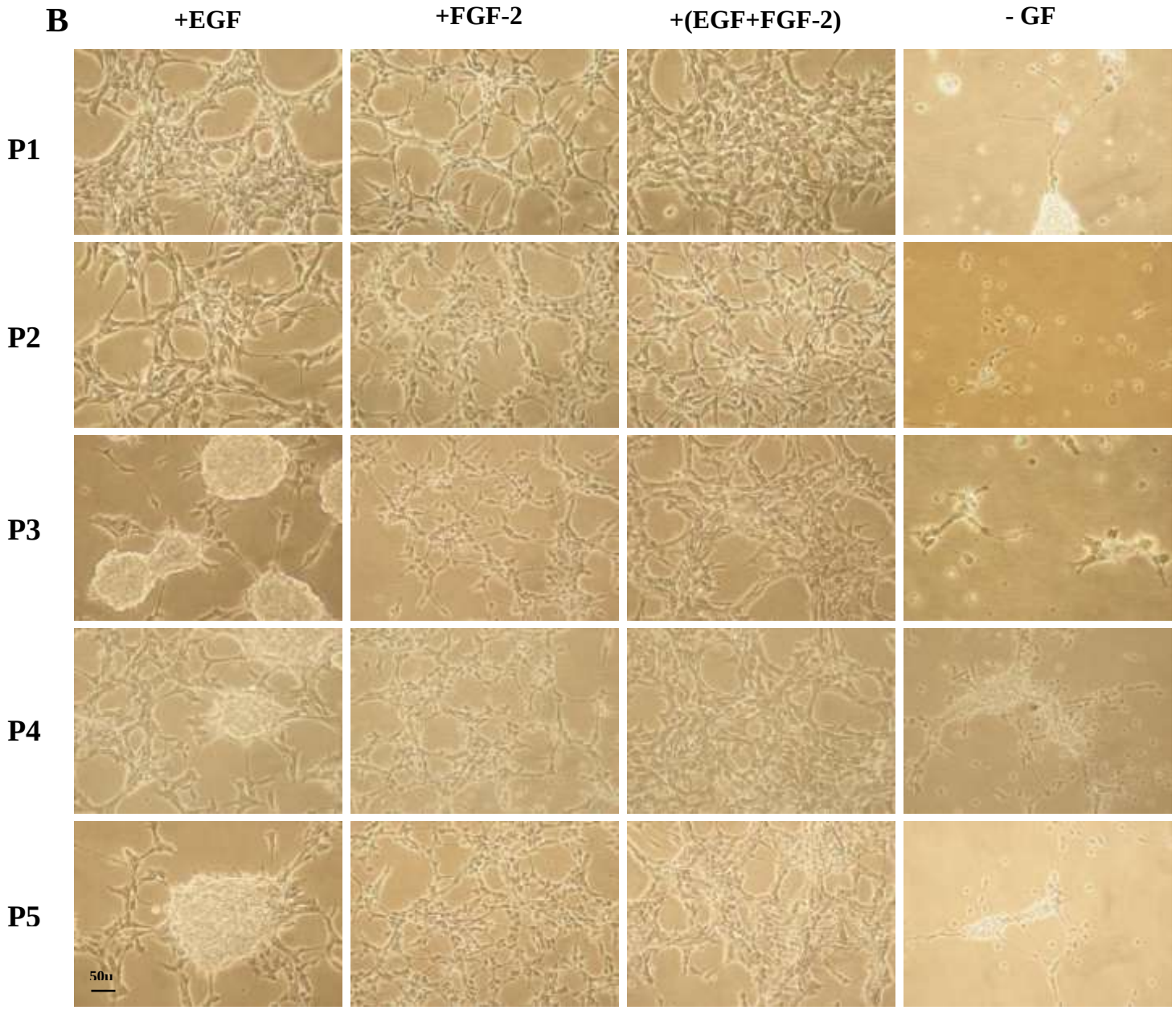
B
+EGF
+FGF-2
+(EGF+FGF-2)
- GF
P1
P2
P3
P4
P5
50u

Figure 4.14 Brightfield images showing the morphology of CB and LV cells (A, B respectively) grown for 3 weeks (5 passages) in EGF, FGF-2, EGF+FGF-2, and mitogen free medium. Both CB and LV NSCs can be expanded in EGF (20ng/ml) or FGF-2 (20ng/ml) alone for 5 passages but displayed different morphologies in each medium condition compared to the control culture containing both mitogens with large amounts of cell debris were found in each culture. LV cells tended to grow as neurospheres in EGF culture after passage 3. Both cells failed to grow in the absence of growth factors. Moreover, in FGF-2 culture, both cells reduced in size and appeared atrophied. Scale bar= 50μm.

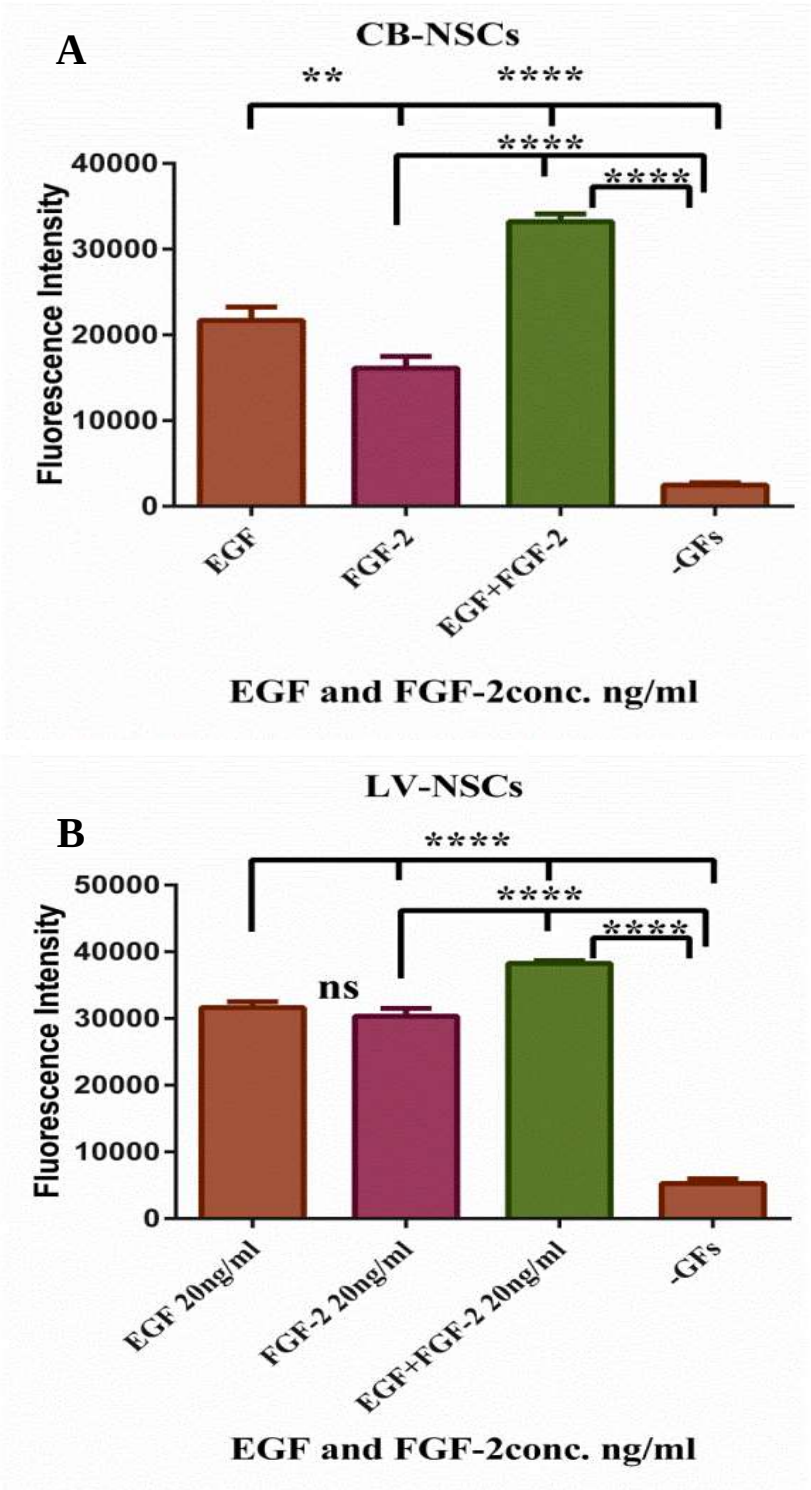

Figure 4.15 Effect of 3-week withdrawal of EGF and FGF-2 on the proliferation of mouse CB (A) and LV (B) NSCs. Averaged data of cell metabolic assay revealed that maximum proliferative rate was achieved when both growth factors were combined. There was significant increase in the proliferation between CB cells cultured in EGF and FGF-2 after 3 weeks in these cultures, whereas no significant difference was observed between LV cells grown in either in EGF or FGF-2. Data are presented as means ± SEM using one-way ANOVA with Tukey's method to compare the mean of each group (**** $P < 0.0001$, ** $P < 0.0037$). EGF= epidermal growth factor; FGF-2= fibroblast growth factor.

4.2.4.5 Longer term effect EGF and FGF-2 withdrawal on the differentiation of CB-mNSCs

In this study, we tested the hypothesis that growth factor starvation could have an effect on the differentiation capacity of NSCs. 3 weeks of EGF or FGF-2 treatments were applied before analysing the differentiation potential and the type of cells generated for both CB and LV cells. To achieve this, CB and LV NSCs were cultured in the presence of EGF (20ng/ml), FGF-2 (20/ml), or EGF+FGF-2 (20ng/ml for each) for 3 weeks, before applying a 6 days of in vitro differentiation treatment of CB and LV cells (Fig. 4.16). Images at D6 of differentiation, showed heterogeneous populations of neuronal and glial cells. To determine the phenotype of these cells, immunostaining was performed with different markers listed in table (4.1).

Analysis of immunostaining results revealed that CB and LV cells cultured for 5 passages in EGF, FGF-2, or EGF+FGF-2 did not impair their differentiation capacity toward neuronal and glial generation (Fig. 4.16A and B respectively). After 6 days of differentiation in each treatment, Nestin expression was not detected but both cultures showed expression of B-tub3, DCX (neuronal markers), and GFAP (astrocytic marker) (Fig.4.16A and B). Interestingly, FGF-2 culture greatly enhanced neurite extension which was more obvious in the LV cells as revealed by B-tub3 and DCX staining (Fig. 4.16A and B). The immunostaining analysis for GFAP also showed that slightly more astrocytes were generated in FGF-2 culture for CB cells while LV cells generated higher number of astrocytes in EGF culture.

However, there appeared to be a difference in the neuronal proportion between the type of mitogen used for both CB and LV cells (Fig. 4.18). To assess if this variation was statistically significant, the percentage of B-tub3^{+} cells was quantified for each treatment for both cell types. Interestingly, we noticed clear variation in the percentage of CB and LV cells adopted neuronal phenotype between the EGF, FGF-2, and EGF + FGF-2 culture conditions (Fig. 4.18 A and B respectively). CB cells cultured in EGF generated more neurons than FGF-2 and EGF+FGF-2 culture (Fig. 4.18A), whereas more B-tub3^{+} cells were detected in LV cells cultured in FGF-2 alone (Fig. 4.18B). Moreover, when the percentage of B-tub3^{+} cells were compared between CB and LV cells, CB cells produced significantly higher percentage of neurons in the EGF and EGF+FGF-2 culture than LV cells, while both cells generated nearly the same percentage of B-tub3 neurons in the FGF-2 culture (Fig. 4.18C).

Table 4.1 The list of primary antibodies used in this chapter

Primary Antibody	Host species	Dilution	Provider
GFAP	Rabbit	1:200	Dako
Nestin (Rat401)	Mouse	1:50	DSHB
DCX	Rabbit	1:100	Abcam
Calbindin	Mouse	1:100	Sigma
MAP2ab-A488	Mouse	1:100	Exbio/Axxora
B-tub3	Rabbit	1:100	Cell signalling
MBP	Mouse	1:200	Abcam
Sox2	Rabbit	1:200	Active Motif

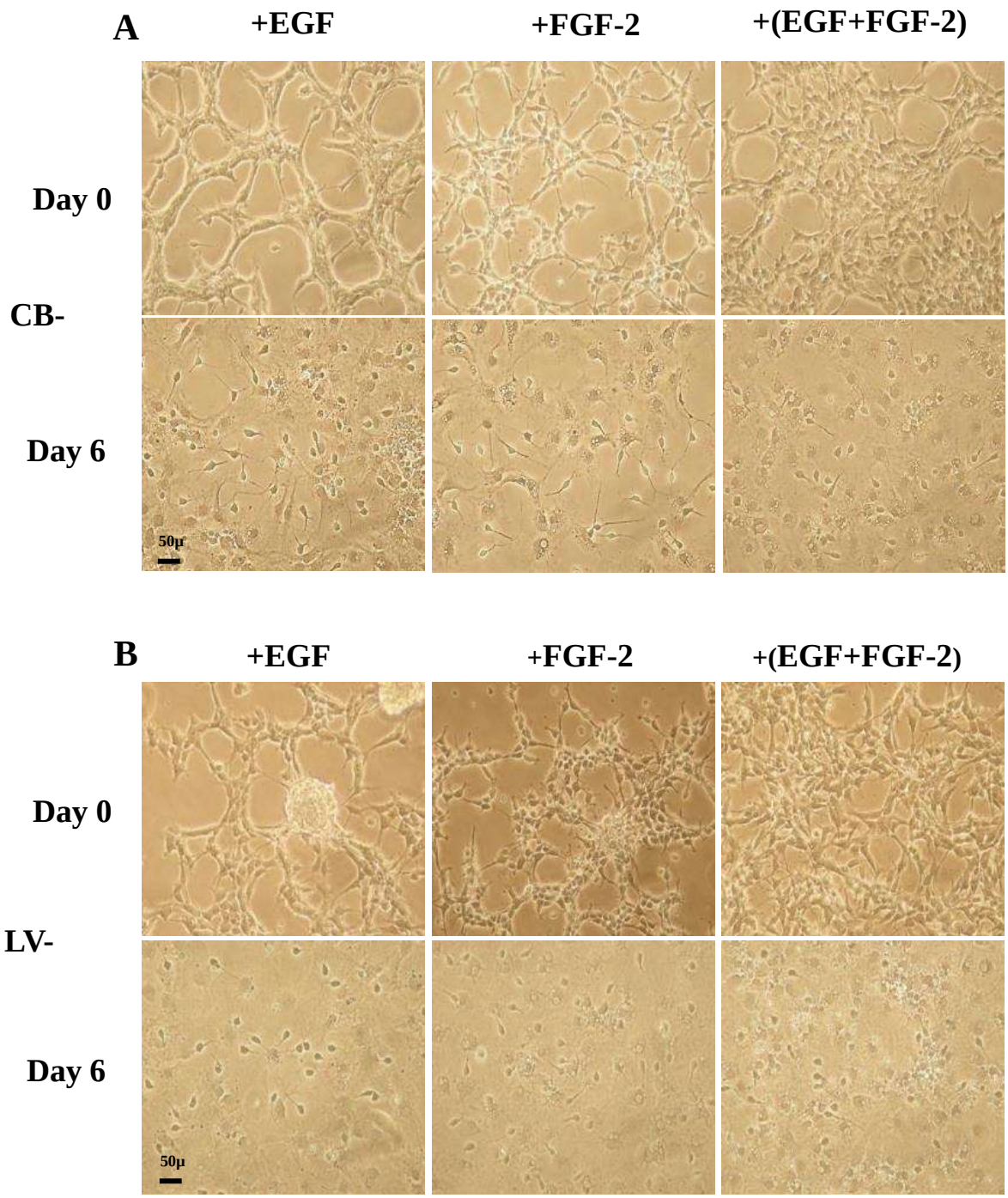

Figure 4.16 Brightfield images of CB (A) and LV (B) cells at D0 and D6 of in vitro differentiation following 3weeks culture in different growth factor conditions. CB and LV cells adopted the morphology of differentiated cells at D6. Culturing in EGF or FGF-2 alone didn't affect the differentiation capacity of both cell types. Scale bar= 50µm

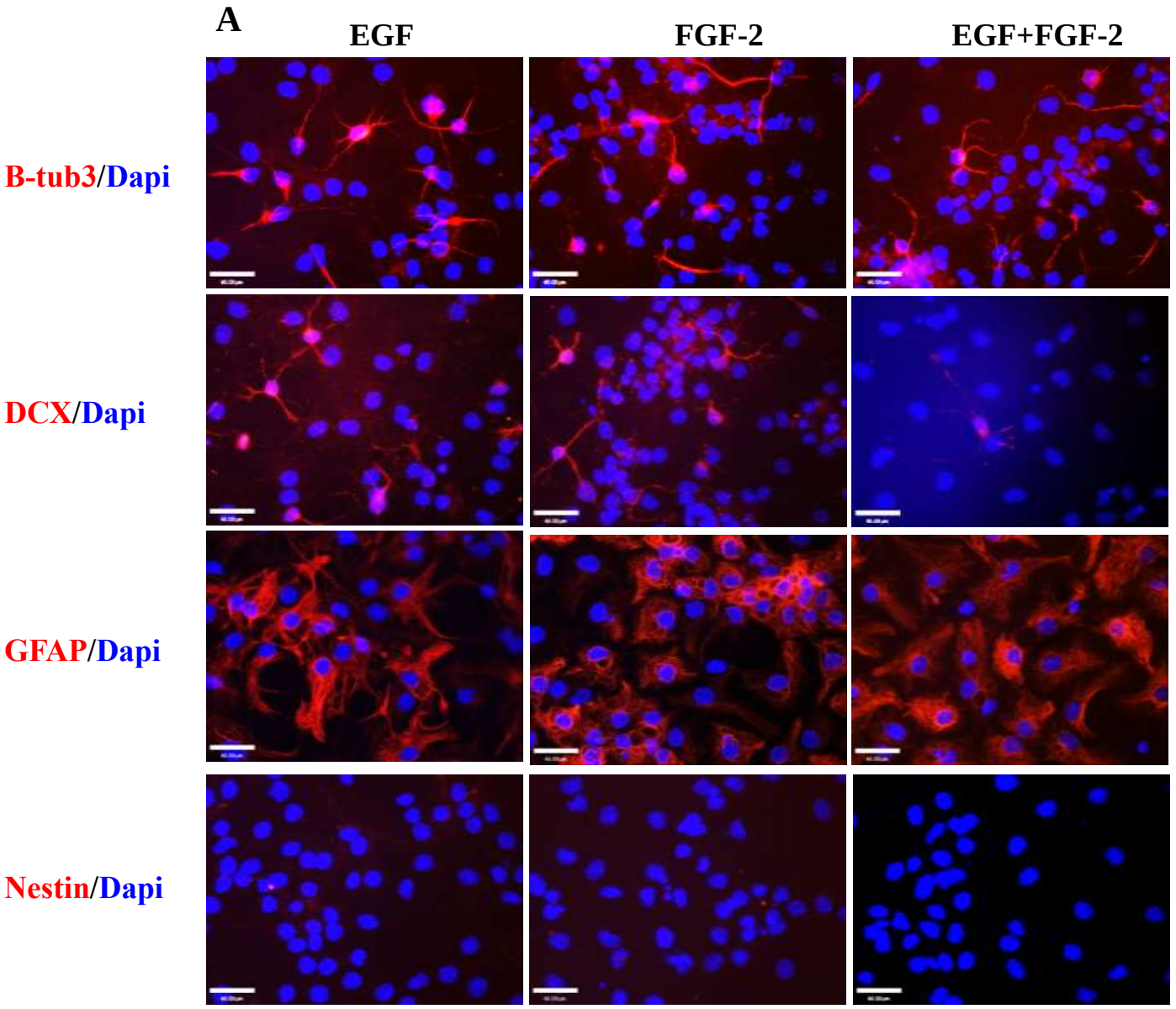
A
EGF
FGF-2
EGF+FGF-2
B-tub3/Dapi
DCX/Dapi
GFAP/Dapi
Nestin/Dapi

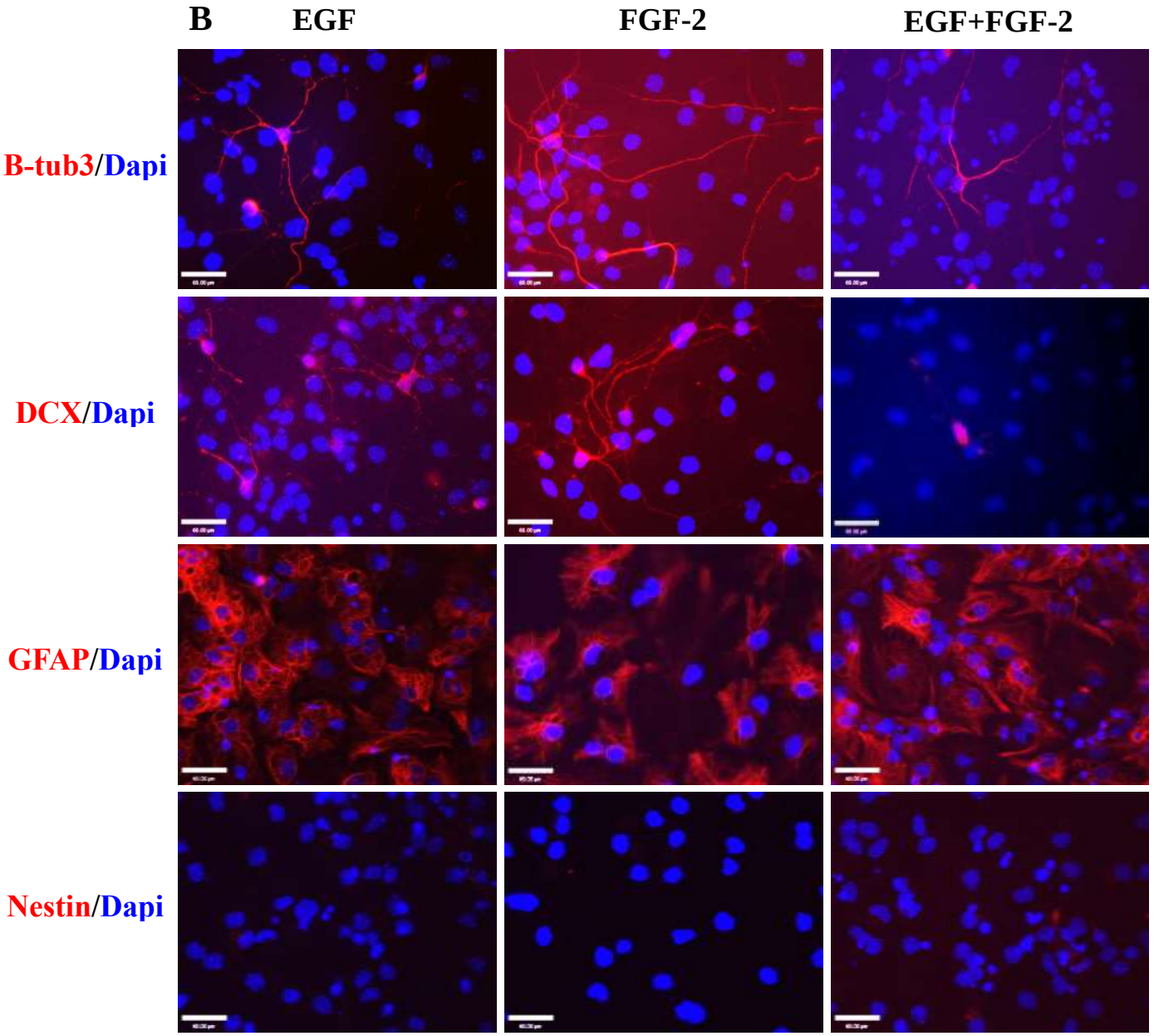

Figure 4.17 Effect of 3-week withdrawal of EGF and FGF-2 on the differentiation potential of CB and LV NSCs (A) and (B) respectively. CB and LV cells were cultured for 5 passages in EGF, FGF-2, and EGF+FGF-2 (20ng/ml) followed by 6 days of in vitro differentiation in the presence of BDNF, EC23 and serum. After fixation, cells were immunostained for Nestin (neural stem cell marker), and GFAP (astrocyte marker), B-tub3 and DCX (neuronal markers) counterstained with dapi (blue). Immunocytochemical analysis showed that culturing CB and LV cells in EGF or FGF-2 for 3 weeks did not affect the differentiation capacity toward the generation of glia and neurons. In both cell types, Nestin expression was absent at D6.

EGF= epidermal growth factor; FGF-2= fibroblast growth factor. Scale bar =60µm

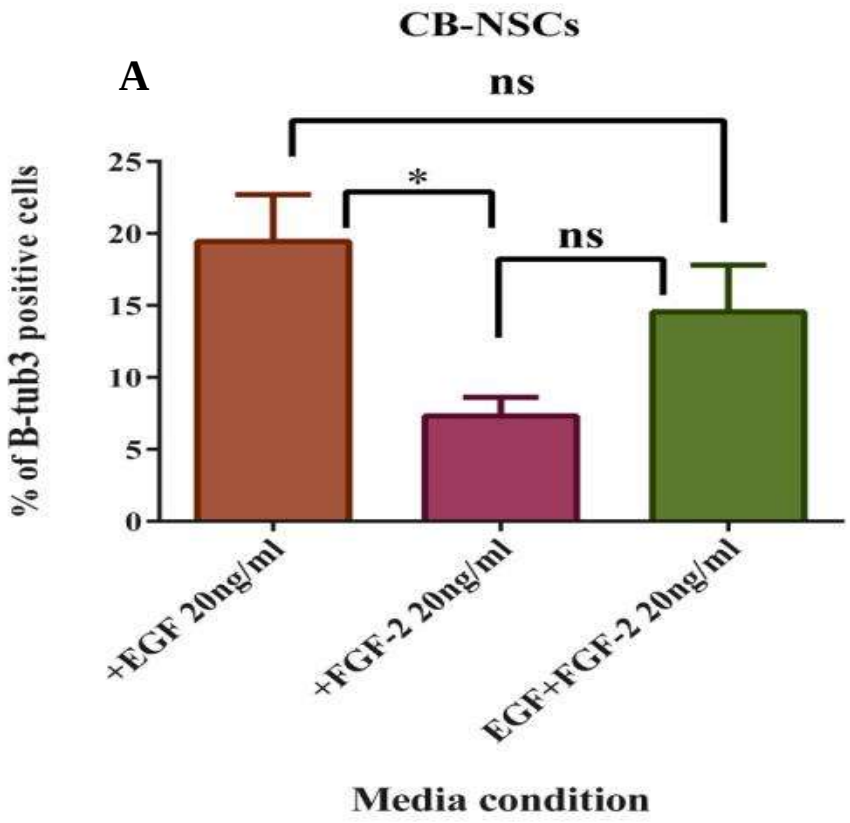
A
CB-NSCs
ns
*
ns
% of B-tub3 positive cells
25
20
15
10
5
0
+EGF 20ng/ml
+FGF-2 20ng/ml
EGF+FGF-2 20ng/ml
Media condition

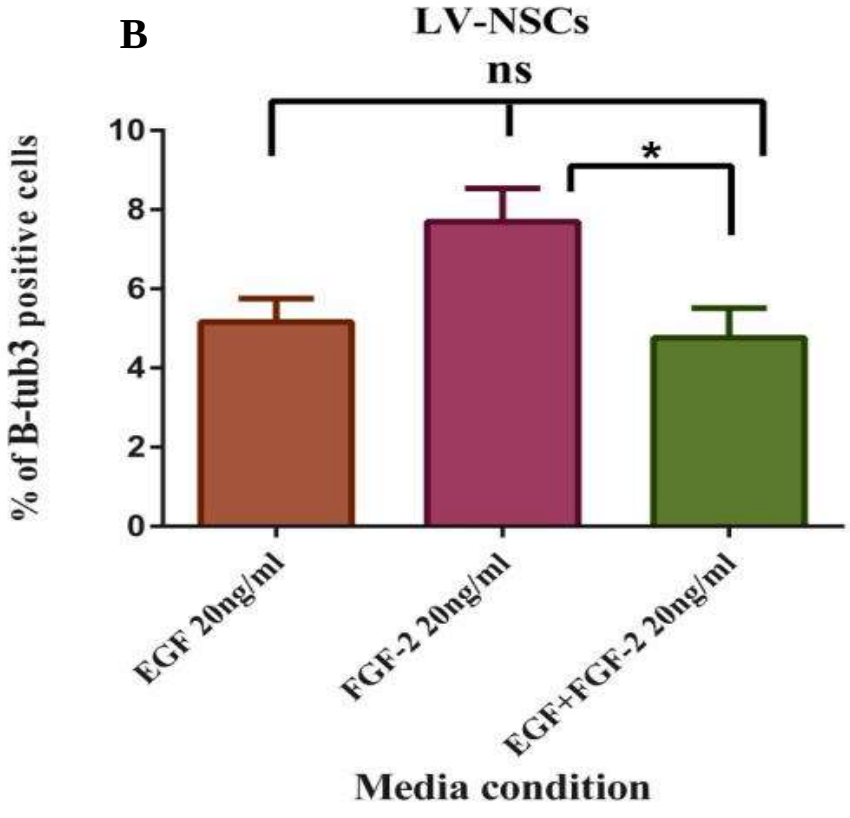
B
LV-NSCs
ns
*
% of B-tub3 positive cells
10
8
6
4
2
0
EGF 20ng/ml
FGF-2 20ng/ml
EGF+FGF-2 20ng/ml
Media condition

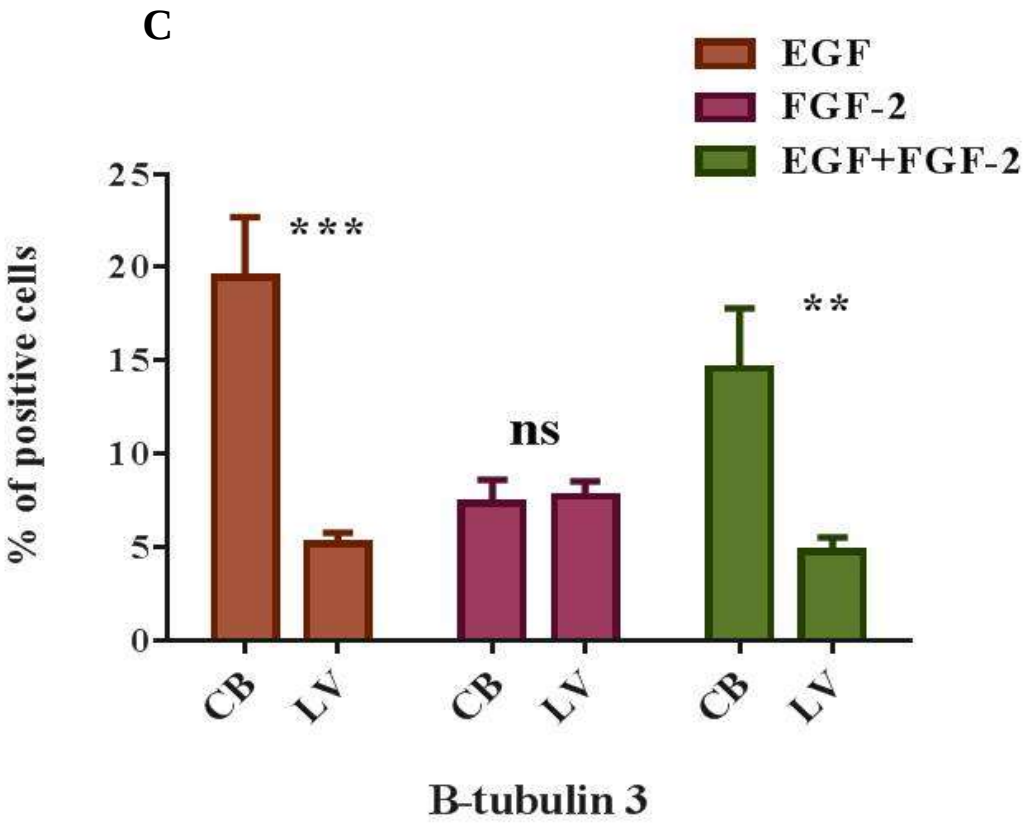

Figure 4.18 Quantitative analysis of B-tub3^{+} neurons after 5 passages in EGF, FGF-2, and EGF+FGF-2 for CB (A) and LV (B) cells respectively. CB and LV cells cultured in these medium conditions for 3 weeks followed by 6 days of differentiation. Immunostaining was performed for B-tub3 (neuronal marker) and cells were counted in 6 random fields for both cells. CB cells differentiated for 6 days generated more neurons in EGF culture while LV cells generated more neurons in FGF-2 culture**. (C)** Data from A and B were used to compare the effect of different growth factor conditions on the proportion of neurons generated after 6 days of in vitro differentiation of CB and LV NSCs. The percentage of B-tub3 positive cells was significantly higher in the EGF and EGF+FGF-2 cultures for CB cells compared to LV cells. Data are the mean ± SEM, with at least nine replicates within each condition, one-way ANOVA with Tukey's method to compare the mean of each group (***P < 0.0005, ** P< 0.0033, *P<0.0232), n=9.

4.2.5 In vitro differentiation and immunohistochemical analysis of CB-NSCs

A key feature of NSCs is their multipotent ability to give the 3 major cell types in the brain (Gage, 2000). In this experiment, undifferentiated CB and LV NSCs were seeded on gelatine coated coverslips in 24 well plates and allowed to grow for 2 days in culture in the presence of EGF and FGF-2 (20ng/ml). The cells were then induced to differentiate by removal of growth factors from the media and exposure to differentiation medium containing brain derived neurotrophic factors (BDNF), fetal calf serum (FCS), and retinoic acid analogue (EC23). The cells were maintained in the neurogenic medium for 4, 5 or 6 days before fixing and staining. To identify cell types after differentiation, we performed fluorescent immunostaining using a number of markers for neuronal and glial lineages (table 4.1). At D0, the undifferentiated cells showed immunoreactivity for Nestin but no reactivity for differentiated markers such as GFAP, B-tub3 (Fig. 4.19). After 4 and 5 days of differentiation (4.19A and B, 4.20A and B respectively), no Nestin expression was detected but the cells were immunopositive for GFAP and B-tub3 suggesting that cultures contained differentiated cells.

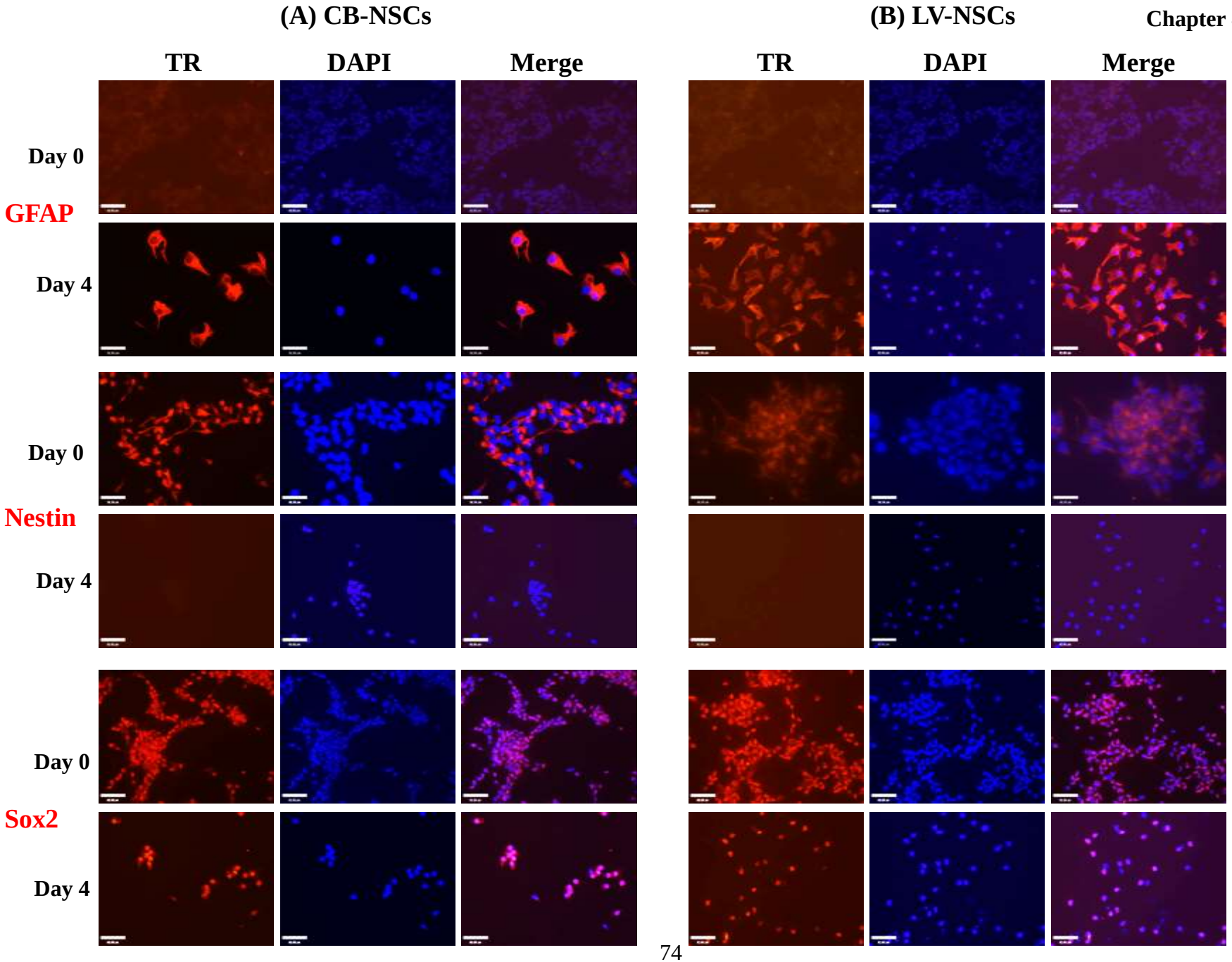
(A) CB-NSCs
(B) LV-NSCs
TR
DAPI
Merge
TR
DAPI
Merge
Day 0
GFAP
Day 4
Day 0
Nestin
Day 4
Day 0
Sox2
Day 4

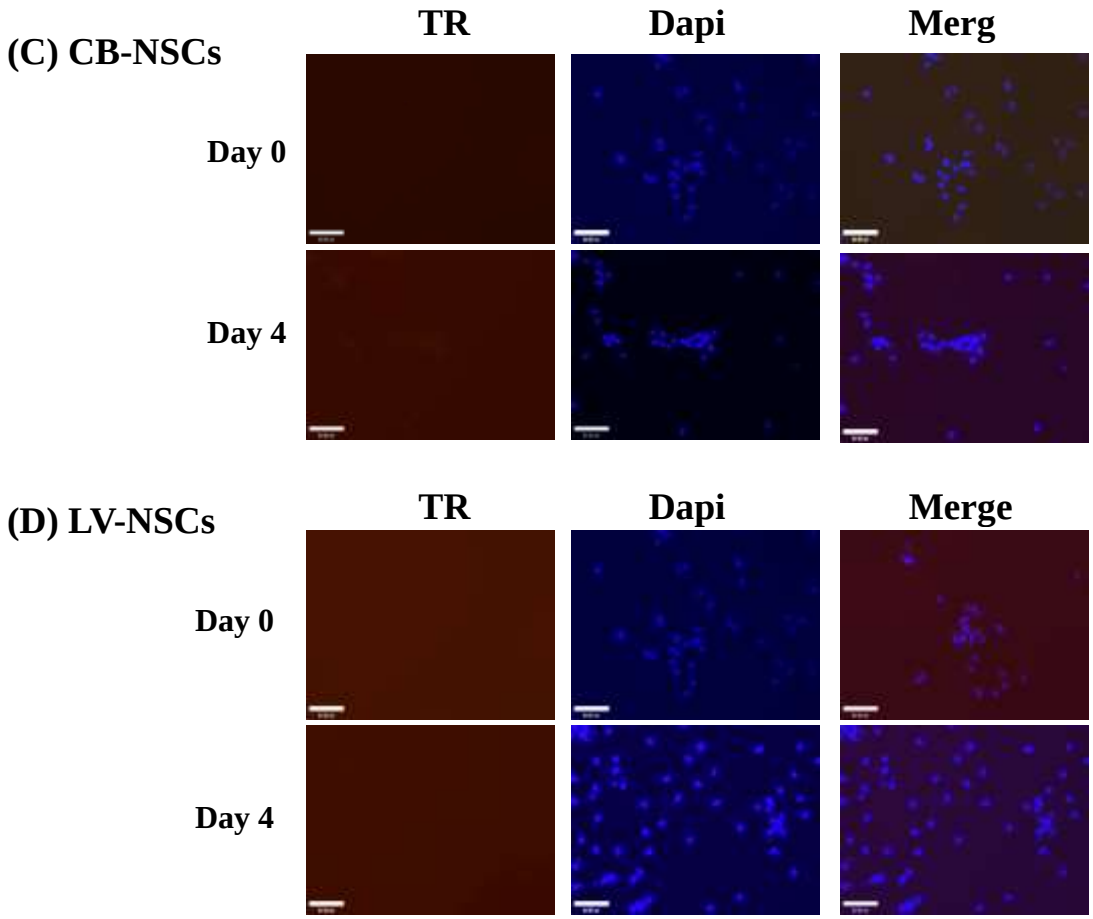

Figure 4.19 Multi-lineage differentiation analysis of NSCs derived from CB and LV of adult mouse. Immunofluorescence images of CB (A) and LV (B) NSCs after 4 days of exposure to differentiation medium. CB and LV cells were cultured for 2 days in the presence of EGF and FGF-2 followed by 4 days in the presence of BDNF, EC23 and serum. After fixation, cells at D0 (control) and D4 were immunostained for Nestin and Sox2 (neural stem cell marker), and GFAP (astrocyte marker) counterstained with dapi (blue). In both cell types, Nestin expression was detected only at D0 but Sox2 expression was

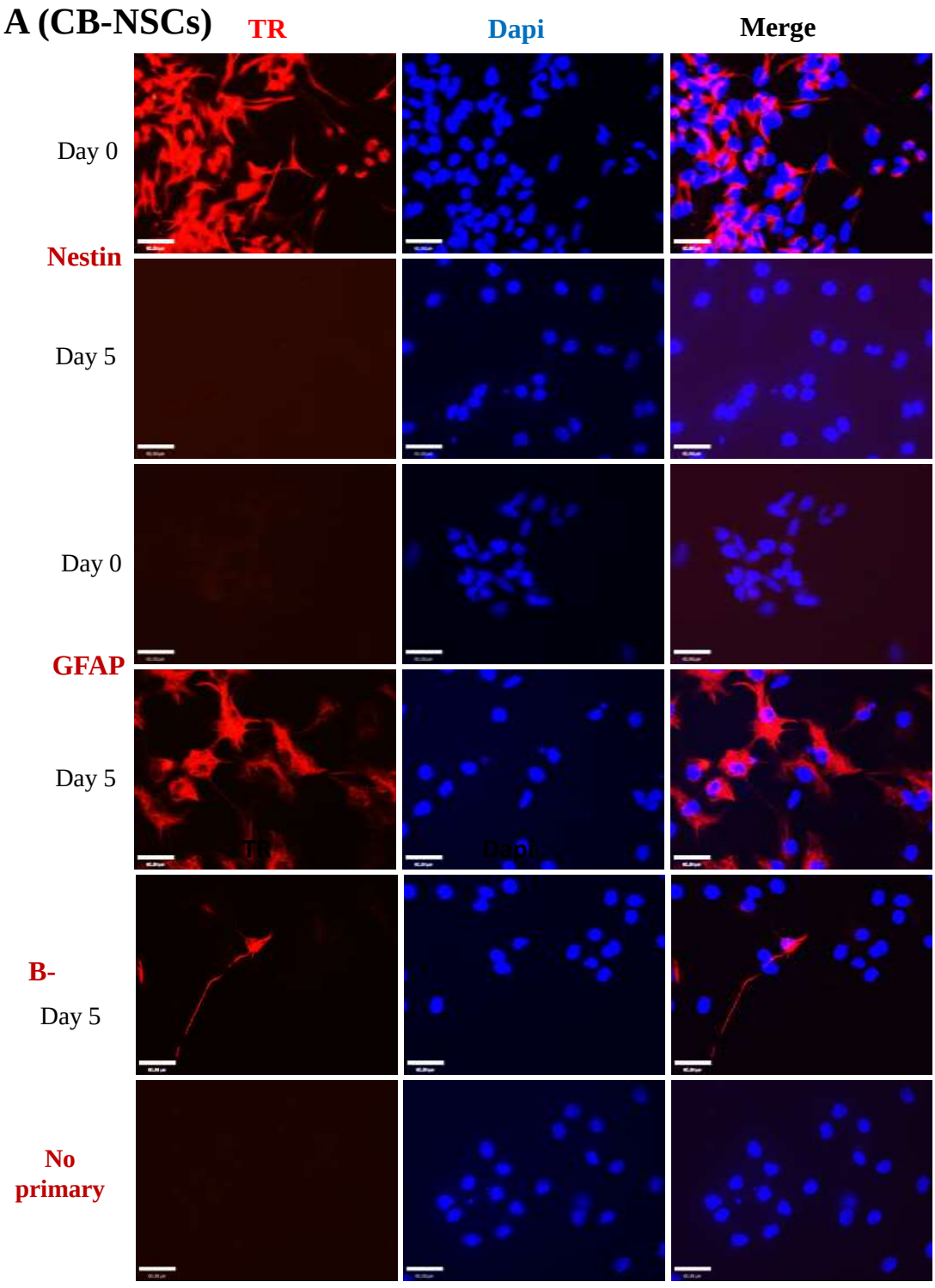
A (CB-NSCs)
TR
Dapi
Merge
Day 0
Nestin
Day 5
Day 0
GFAP
Day 5
TR
Dapi
B-
Day 5
No primary

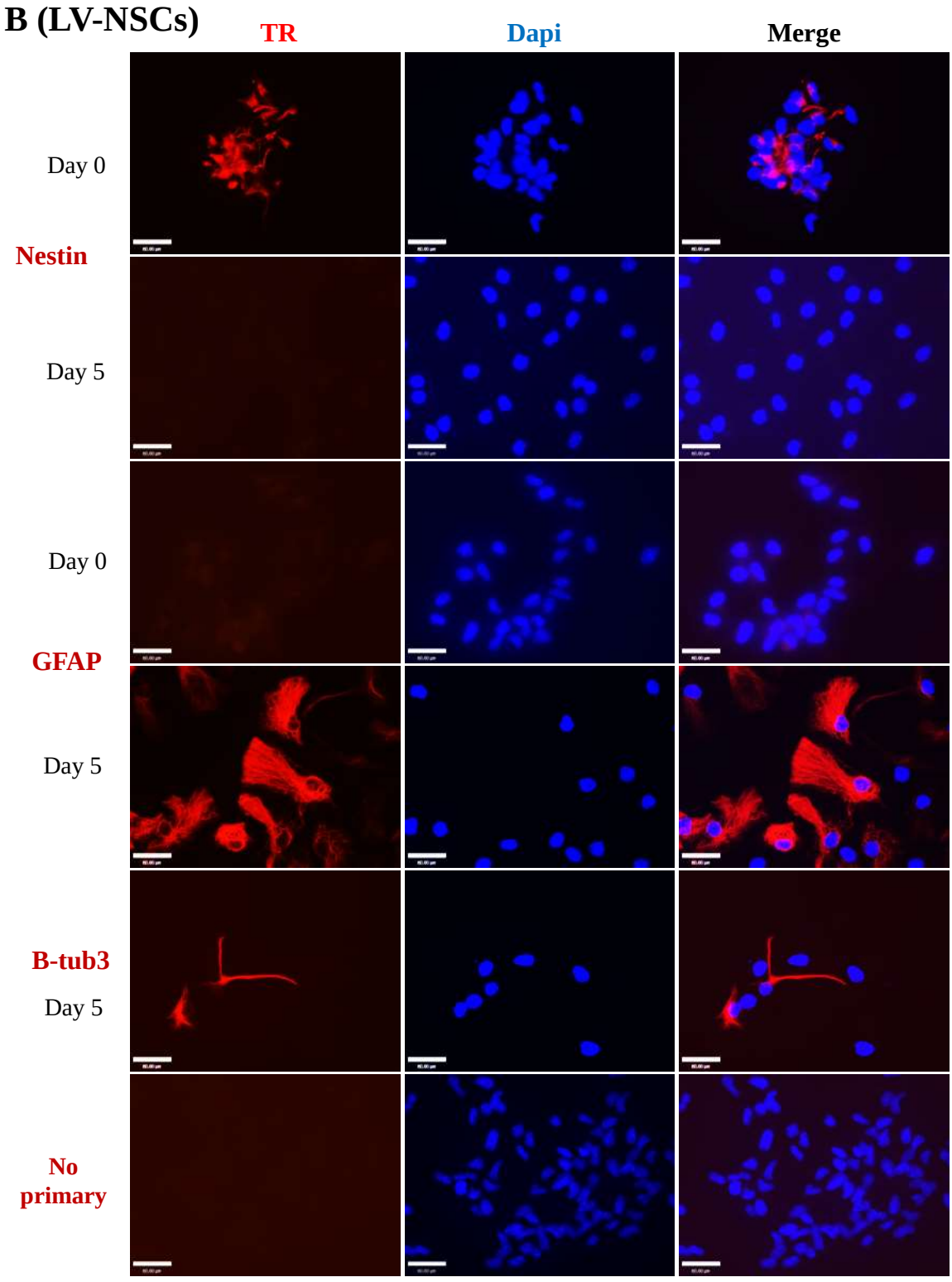

Figure 4.20 Multi-lineage differentiation analysis of NSCs derived from CB (A) and LV (B) of adult mouse. Immunofluorescence images of CB and LV NSCs after 5 days of differentiation. CB and LV cells were cultured for 2 days in the presence of EGF and FGF-2 followed by 4 days of in vitro differentiation in the presence of BDNF, EC23 and serum. After fixation, cells at D0 (control) and D5 were immunostained for Nestin (neural stem cell marker), B-tub3 (neuronal marker), and GFAP (astrocyte marker) counterstained with dapi (blue). The bottom panel showing the negative control stained with secondary antibody only. In both cell types, Nestin expression was detected only at D0. GFAP and B-tub3 expression was observed at D5 and the staining pattern was similar between CB and LV cells. Scale bar =60µm

4.2.6 Effect of EC23 treatment on CB-NSCs differentiation

EC23 is a synthetic retinoid analogue which has been developed by (Christie et al., 2008) and found to induce neuronal differentiation via the activation of all retinoic acid receptor pathways (Maltman et al., 2009). Christie et al., (2011) have shown that human pluripotent stem cell treated with 1µM of EC23 for 3 weeks induced neuronal differentiation similar to all-trans retinoic acid (ATRA). To analyse the effect of EC23 on the neuronal differentiation, CB and LV NSCs were differentiated with and without EC23 for 16 days followed by immunstaining with specific markers (listed in table 4.1) for neuronal and glial linages to identify the phenotype present in these cultures (Fig. 4.21). Furthermore, the number of B-tub3, MAP2, and DCX, Calbindin (selectively labels Purkinje cells) and Nestin positive cells were counted in 5 random fields of view in order to determine the percentage of the positive cells for each of these markers. Immunofluorescent staining revealed the existence of neurons, astrocytes, and oligodendrocytes in the CB and LV NSCs culture after 16 days in the presence and absence of EC23 (Fig. 4.21A and B and 4.22A and B respectively). Nestin staining was observed at D0 but lost in the differentiated cells, indicating that CB and LV NSCs were differentiated after treatment. $GFAP^+$ cells were the most abundant among all differentiated cultures, while the less abundant cell type were oligodendrocytes as observed by MBP immunostaining (Fig.4.21 and 4.22). Importantly, the presence of Calbindin-expressing cells was observed in CB-NSCs treated for 16 days in the presence and absence of EC23 (Fig. 4.21A and 4.22A respectively) but not in the LV culture (Fig. 4.21B and 4.22B respectively). Moreover, differentiation medium containing EC23 generated more Calbindin-positive cells than in the

absence of EC23, but this difference was proven to be non-significant (Fig.4.23A).

We noticed that when EC23 was omitted from the differentiation medium, the proportion of neurons was found to be increased in both CB and LV cells (Fig. 4.22 A and B respectively). However, statistically the difference in the percentage of B-tub3, MAP2, DCX, and Calbindin markers was not significant among CB or LV cells in the presence or absence of EC23 (Fig. 4.23 A and B respectively). Moreover, the highest percentage of neuronal marker detected in LV cells was DCX in +EC23 (16.61 ± 1.4% and –EC23 (15.62 ± 2.4%), and DCX in CB cells in +EC23 (42.89 ± 1.6%) and –EC23 (40.99 ± 5.8%) treatments respectively (Fig. 4.23). Statistical analysis revealed that the difference in neuronal number was highly significant between CB and LV cells for the selected neuronal markers used in this study (Fig.4.23 C) (Mean ±SEM is shown in table 4.2).

Table 4.2 Percentage of different neuronal markers after 16 days of differentiation in the presence of EC23. Values represent means ± SEM of cell counts obtained from 5 stained fields of view/marker

	B-tub3	**MAP-2**	**DXC**	**Calbindin**
CB-NSCs	34.8 ± 2.2	30.8 ± 2.5	42.8 ± 1.6	15.8 ± 4.9
LV-NSCs	16.6 ± 1.4	14.2 ± 1.5	19.3 ± 2.2	0

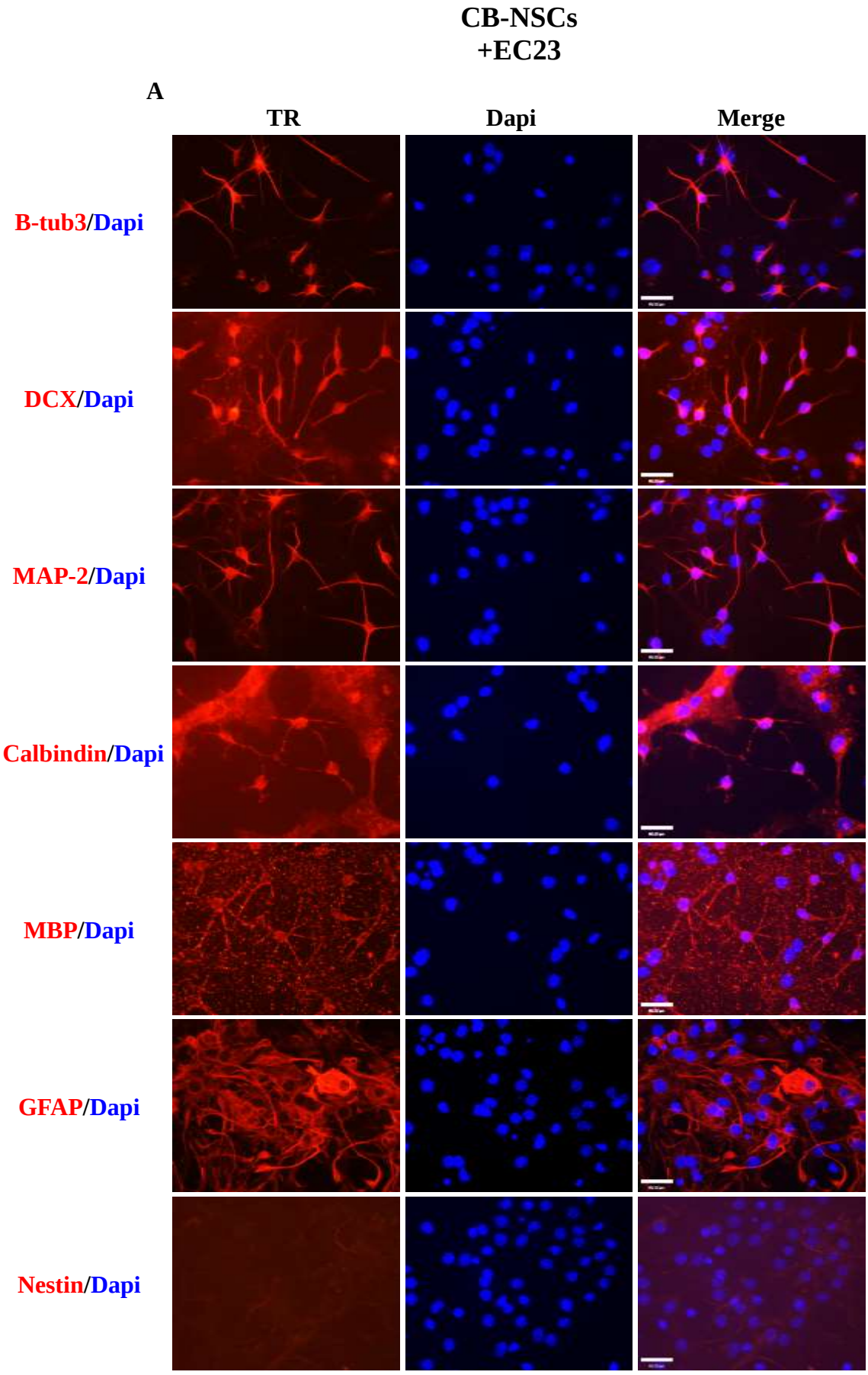
CB-NSCs
+EC23
A
TR
Dapi
Merge
B-tub3/Dapi
DCX/Dapi
MAP-2/Dapi
Calbindin/Dapi
MBP/Dapi
GFAP/Dapi
Nestin/Dapi

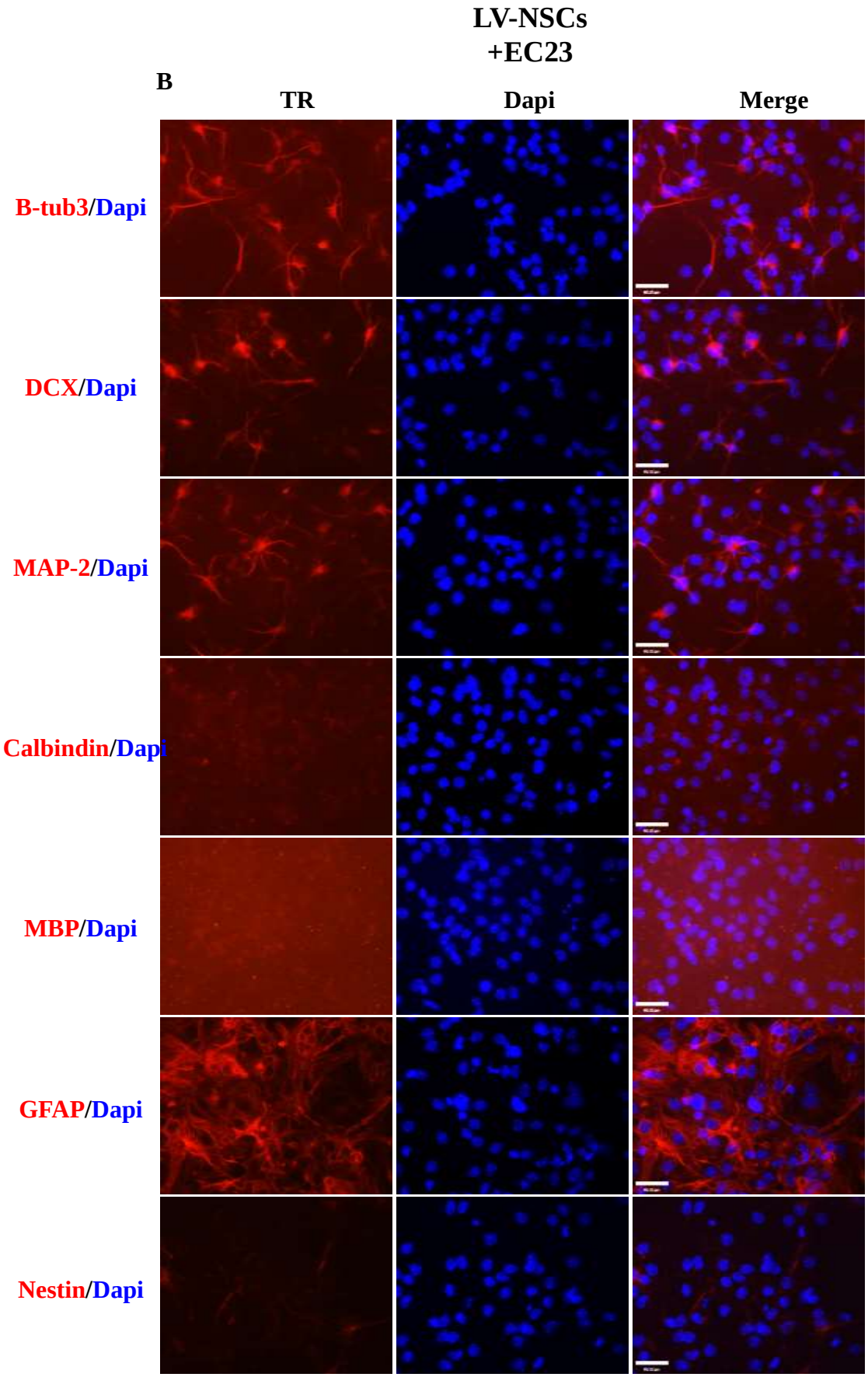
LV-NSCs
+EC23
B
TR
Dapi
Merge
B-tub3/Dapi
DCX/Dapi
MAP-2/Dapi
Calbindin/Dapi
MBP/Dapi
GFAP/Dapi
Nestin/Dapi

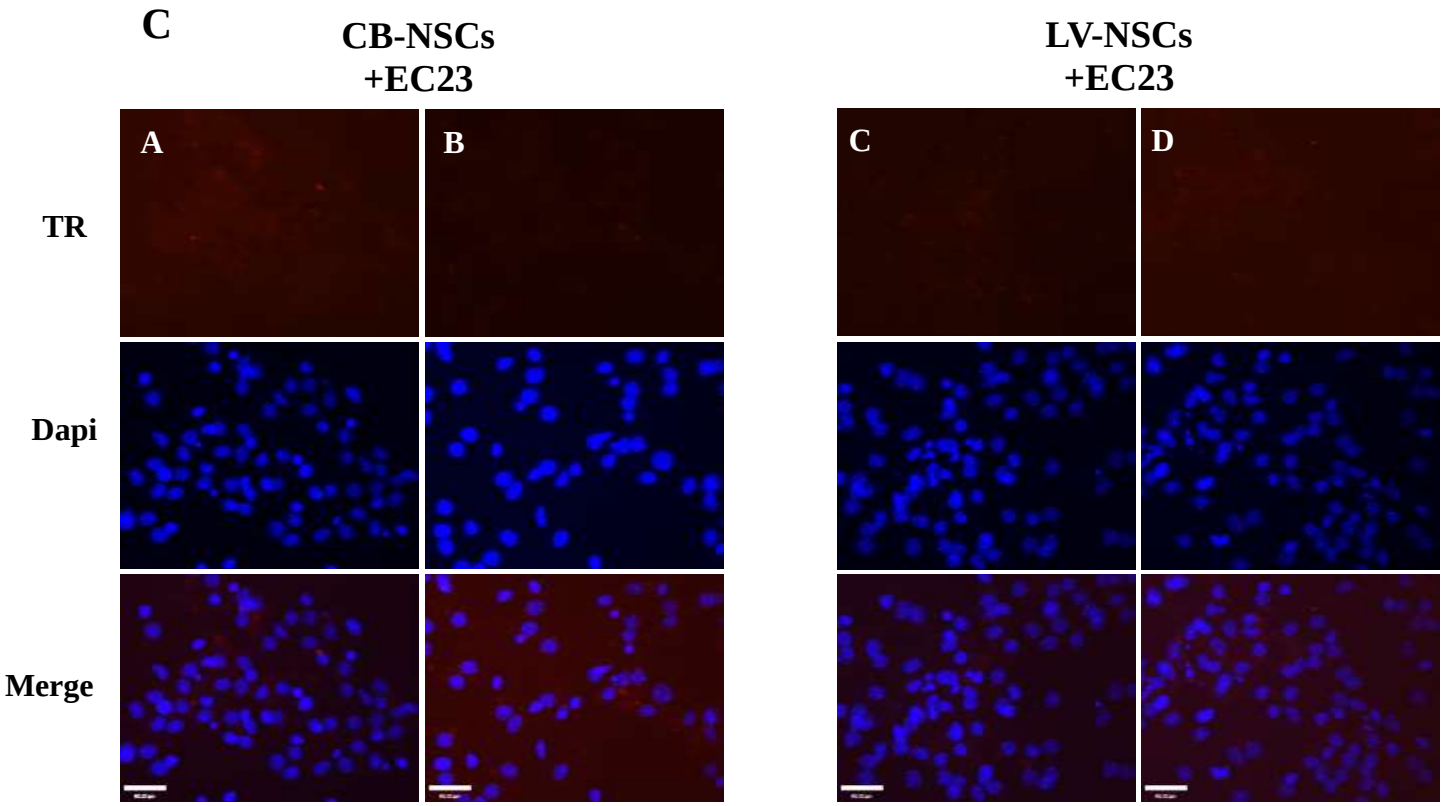

Figure 4.21 The effect of EC23 treatment on the in vitro differentiation response of CB and LV NSCs. Immunofluorescence images of CB **(A)** and LV **(B)** NSCs cultured for 2-3 days in the presence of EGF and FGF-2 followed by 16 days of differentiation in the presence of EC23 along with BDNF+serum. After fixation, cells were immunostained for Nestin (neural stem cell marker), GFAP (astrocyte marker), MBP (oligodendrocytes marker), and B-tub3, MAP2, DCX, Calbindin (neuronal markers), with dapi counterstained (blue). In both cell types, Nestin expression was absent at D16 indicating their differentiation.. All the neuronal markers used were detected at D16 in CB and LV cells. Interestingly, Calbindin^{+} cells were detected in the CB culture only suggesting that 16 days of differentiation promoted Purkinje cells (PCs) differentiation, a cerebellar neuron type. Surprisingly, MBP expression was detected in CB cells only and was absent from the LV culture. BDNF: brain derived neurotrophic factor; DCX: Doublecortin X; MBP: Myelin basic protein. (C) Negative controls for 16 days differentiation of CB and LV cells. In these images no primary antibodies were added for both D0 and D4. Cells were stained only with Texas red secondary antibody counter stained with dapi. (A) (C) represent control for TR anti rabbit in CB and LV cells respectively; (B) (D) represent control for TR anti mouse in CB and LV cells respectively. Scale bar =60µm

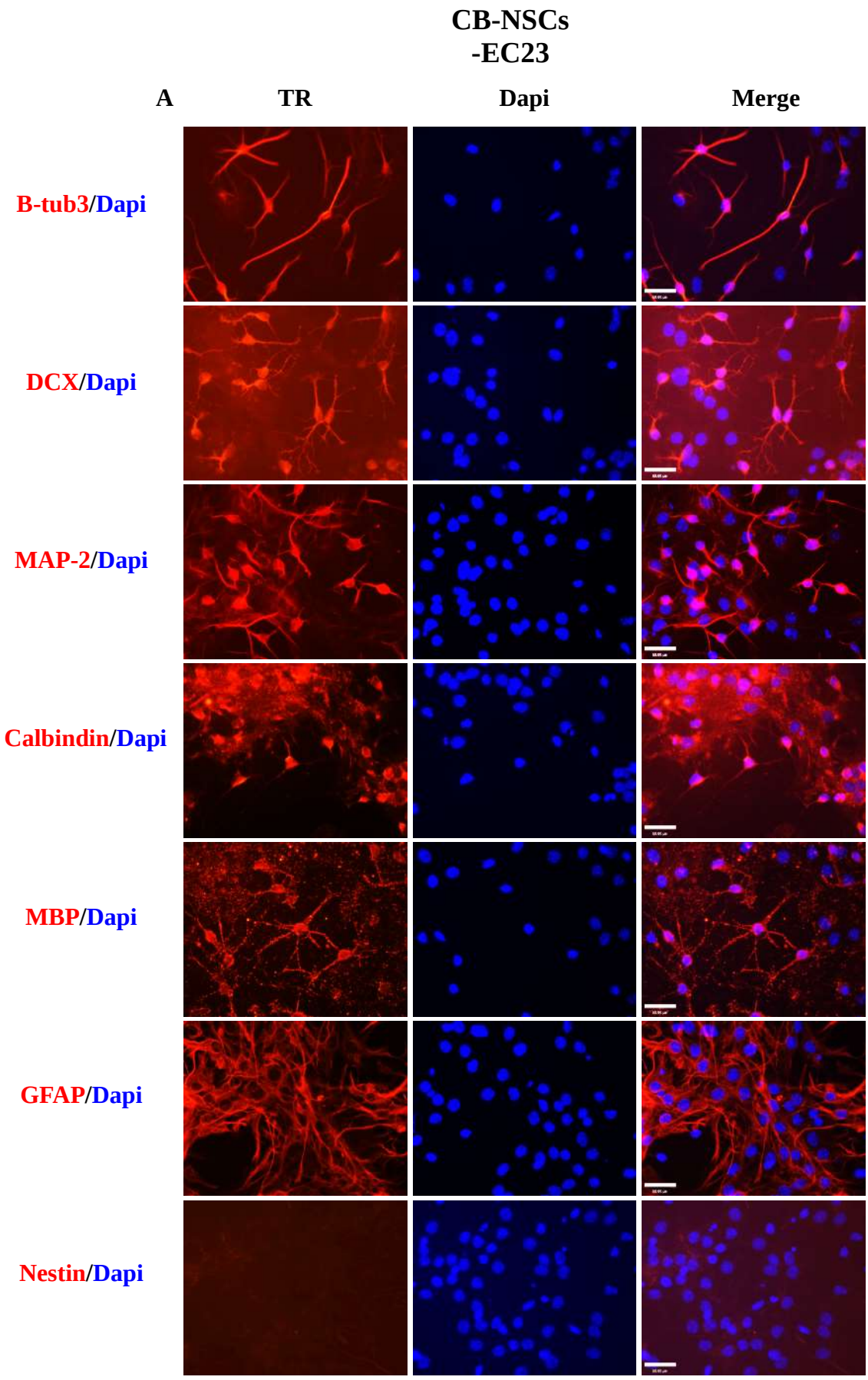
CB-NSCs
-EC23
A
TR
Dapi
Merge
B-tub3/Dapi
DCX/Dapi
MAP-2/Dapi
Calbindin/Dapi
MBP/Dapi
GFAP/Dapi
Nestin/Dapi

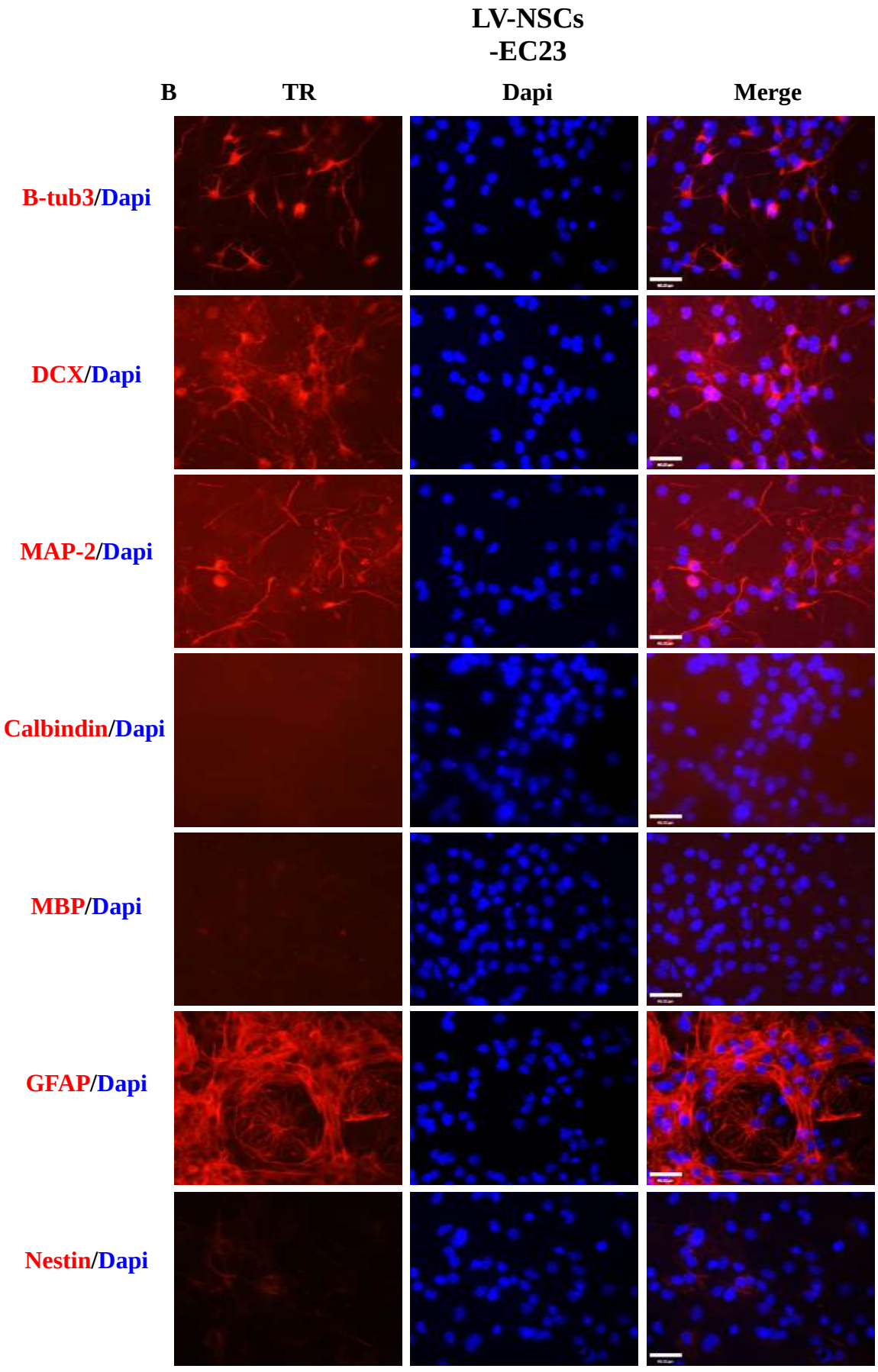
LV-NSCs
-EC23
B
TR
Dapi
Merge
B-tub3/Dapi
DCX/Dapi
MAP-2/Dapi
Calbindin/Dapi
MBP/Dapi
GFAP/Dapi
Nestin/Dapi

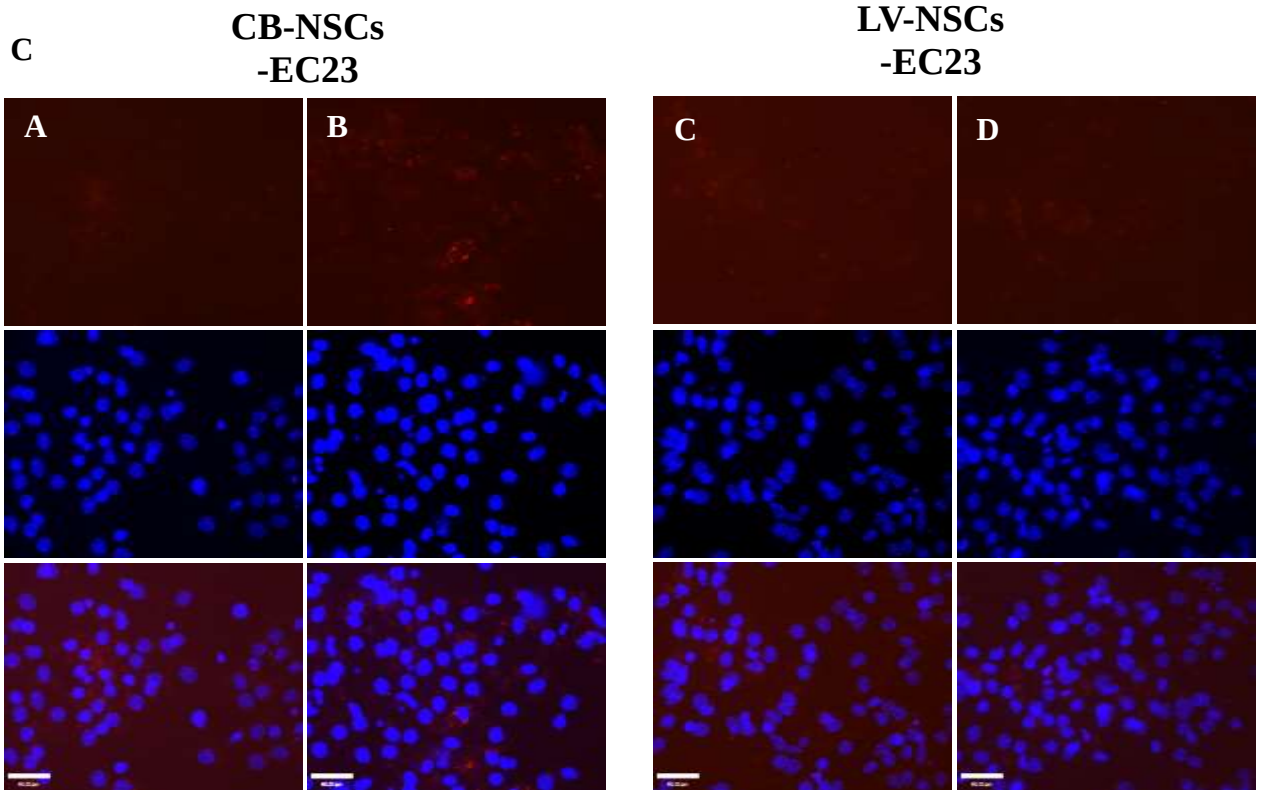

Figure 4.22 The effect of EC23 (retinoic acid analogue) withdrawal on the in vitro differentiation capacity of CB and LV NSCs (A) and (B) respectively. Immunofluorescence images of CB and LV NSCs after 16 days of differentiation in the absence of EC23. CB and LV cells were cultured for 2-3 days in the presence of EGF and FGF-2 followed by 16 days of in vitro differentiation in the absence of EC23 along with BDNF+serum. After fixation, cells were immunostained for Nestin (neural stem cell marker), GFAP (astrocyte marker), MBP (oligodendrocytes marker), and B-tub3, MAP2, DCX, Calbindin (neuronal markers) counterstained with dapi (blue). In both cell types, Nestin expression was absent at D16 indicating their differentiation. Removing EC23 treatment from the differentiation medium accounted for more neuronal generation. All the neuronal markers used were expressed at D16 in CB and LV cells. Calbindin+ cells were detected in the CB culture only indicating that 16 days of differentiation produced Purkinje cells (PCs). Surprisingly, oligodendrocytes were detected using MBP marker in CB cells only and was absent from the LV culture at this differentiation point. BDNF: brain derived neurotrophic factor; DCX: Doublecortin X; MBP: Myelin basic protein. (C) Negative controls for 16 days differentiation of CB and LV cells. In these images no primary antibodies were added for both D0 and D4. Cells were stained only with Texas red secondary antibody counter stained with dapi. (A) (C) represent control for TR anti rabbit in CB and LV cells respectively; (B) (D) represent control for TR anti mouse in CB and LV cells respectively. Scale bar =60µm

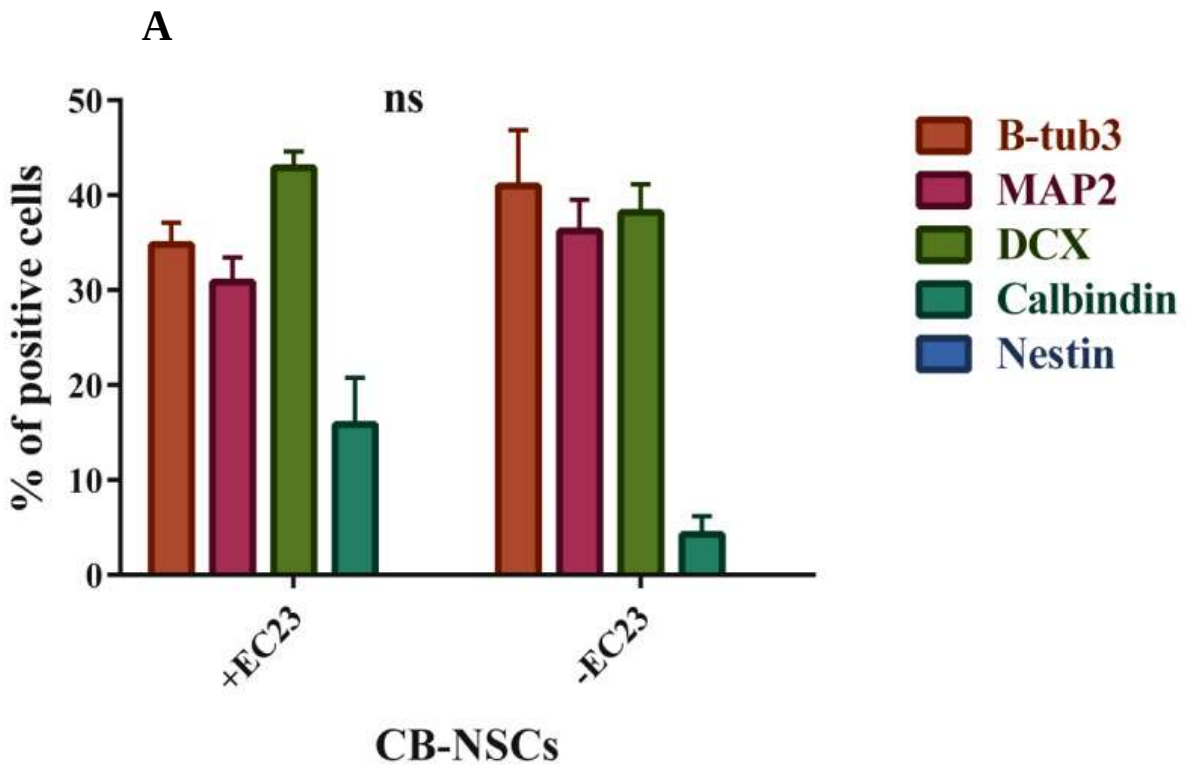
A
ns
% of positive cells
50
40
30
20
10
0
+EC23
-EC23
CB-NSCs
B-tub3
MAP2
DCX
Calbindin
Nestin

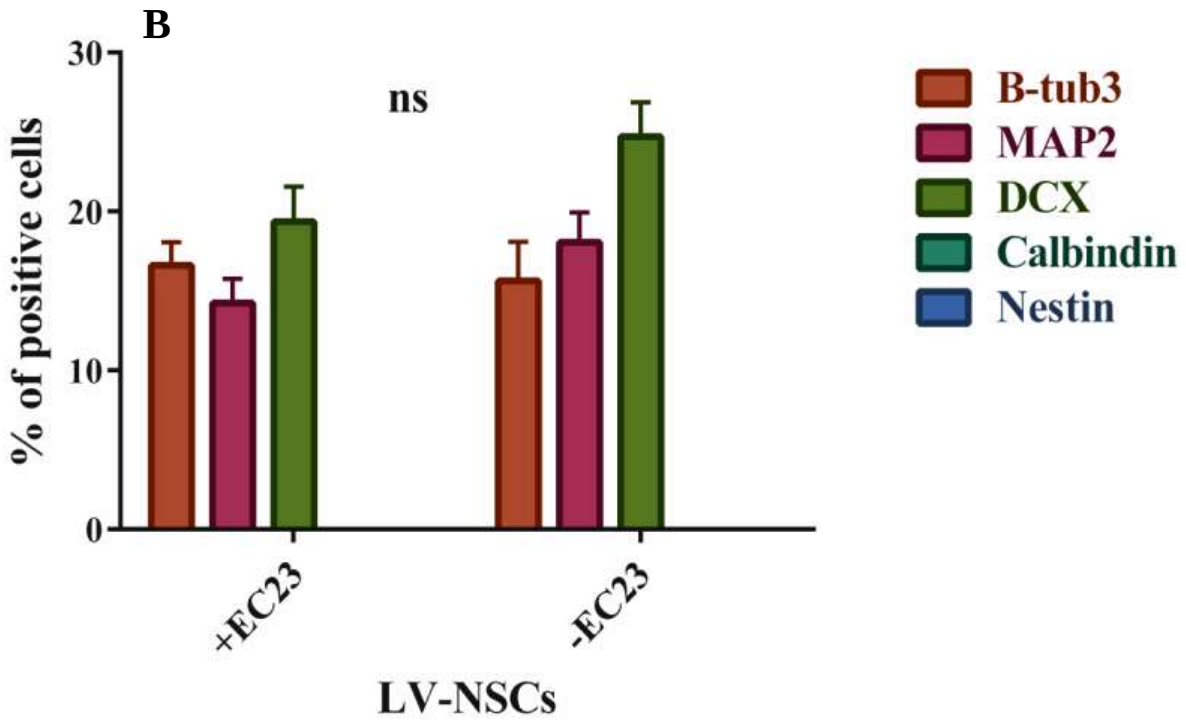
B
ns
% of positive cells
30
20
10
0
+EC23
-EC23
LV-NSCs
B-tub3
MAP2
DCX
Calbindin
Nestin

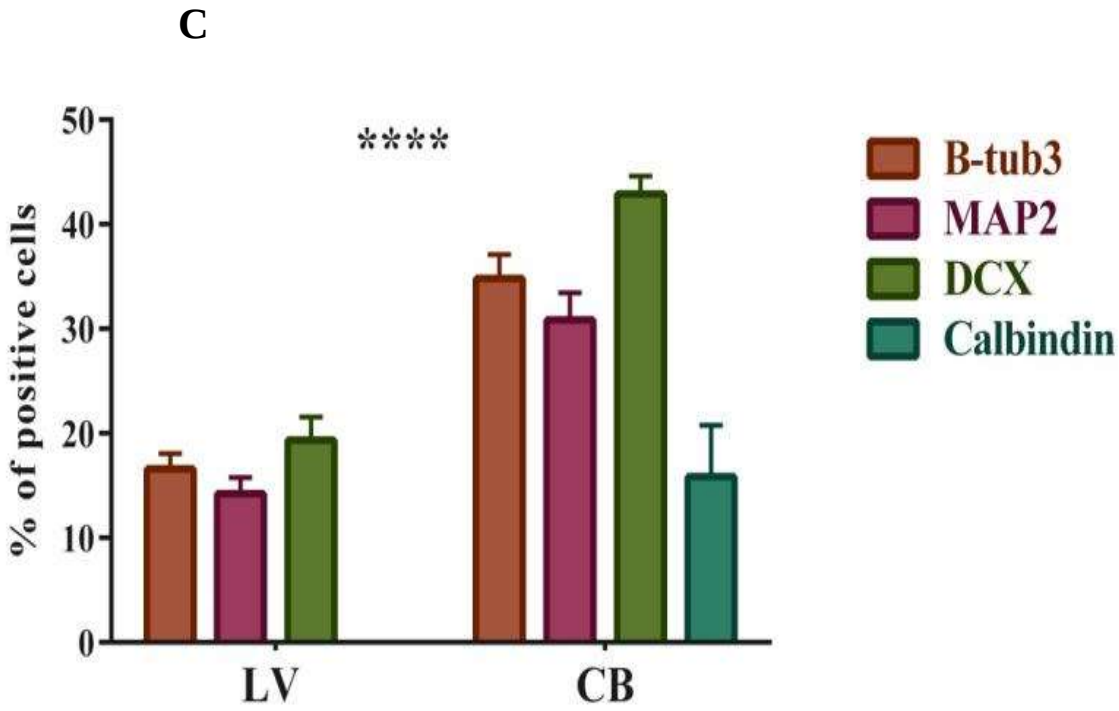

Figure 4.23 The effect of EC23 on lineage marker expression after 16 days of in vitro differentiation of CB and LV NSCs. CB **(A)** and LV **(B)** cells were differentiated for 16 days in the presence and absence of EC23, followed by immunostaining with Nestin (NSC marker) and neuronal markers (B-tub3, MAP2, DCX, and Calbindin). No significant effect was observed on the percentage of neurons generated in the presence and absence of EC23 for both cell types. **(C)** data from A and B were used for quantitative analysis of different neuronal markers after 16 days of in vitro differentiation of mouse CB and LV NSCs. CB and LV NSCs were differentiated for 16 days in the presence of BDNF, FCS, and EC23 followed by immunostaining with Nestin (NSC marker) and neuronal markers (B-tub3, MAP2, DCX, and Calbindin).The proportion of B-tub3, MAP2, DCX, and Calbindin were significantly higher in CB cells compared with LV cells. In both cell types, DCX^+ cells were significantly higher than the other neuronal markers. Calbindin (specific marker for PCs) was detected only in CB cells but not in LV cells. PCs: Purkinje cells. Data are presented as means ± SEM using Two-way ANOVA with Bonferroni method to compare the mean of each group (**** $P < 0.0001$), (n=5).

4.3 Discussion

In this study, in vitro characteristics of NSCs isolated from the cerebellum of adult mouse were assessed and compared to those isolated from the lateral ventricle, used as control. The main focus of this chapter was to determine the optimum culture conditions for the growth and expansion of cells in regard to growth factor requirements, and also to test their differentiation potential toward the generation of neurons, astrocytes, and oligodendrocytes.

4.4 Characterisation of NSCs derived from mature cerebellum

Cerebellum derived NSCs grown in cultures in the presence of EGF and FGF-2 were similar to the control NSCs derived from the LV. The optimum density determined in this study to produce the best culture for culture expansion was 7.5x 10^4 cells/ml in either T25 or 24 well plates. When the cells were seeded at very low density, they became compromised and couldn't survive after 2 days in culture with large distances between the cells being observed. This could be due to the fact that cell-to-cell paracrine signalling is greatly affected by the cell seeding density (Kim et al., 2009). When the cells were seeded at high densities, LV cells became over confluent next day, while the CB cells were not due to the differences in the growth rate of both cell types. Evidence from the literature suggests that seeding cells at high density leads to rapid depletion of the nutrients and alteration in pH of the medium due to high metabolic rate of the cells and this can finally affect their viability (Gritti et al., 2001). Cells isolated from the CB were able to form neurospheres similar to the control culture as previously reported by Alcock and Sottile, (2009). However, the formation of neurospheres

was not enough to confirm the stem cell nature of these cells as some transit-amplifying cells are also able to form neurospheres (Doetsch et al., 2002).

4.4.1 Effect of retinoic acid analogue (EC23) on the neuronal differentiation of CB NCS

It is well known that retinoic acid (RA), a metabolite of vitamin A, induces neuronal differentiation as well as other important functions such as axonal out growth, and neural patterning (Maden, 2007). EC23, an analogue of RA, has also more recently been found to induce neuronal differentiation via RA functional pathways (Maltman et al., 2009). In this study, it appeared that removing of EC23 from the differentiation medium had no obvious effect on the neuronal differentiation of both CB and LV cells. We have also shown that more neurons were generated in the absence of EC23 than in the presence of EC23 although the difference was not statistically significant. The concentration of EC23 used in this study was 1 μM, and this dose was shown to be toxic to embryonic stem cells (Christie, 2008) which might explain the lower proportion of neurons generated in the presence of EC23 than in the absence of EC23 observed in our study. Alternatively, it might be other factors used in the differentiation medium which enhanced the differentiation of CB and LV cells, such as serum and BDNF. The addition of serum-born factors along with BDNF are reported to be strong inducers of stem cell differentiation (Zhang et al., 2011). Furthermore, our results demonstrated that when CB and LV cells were differentiated for 16 days in the presence and absence of EC23, the proportion of neuronal population for CB cells was significantly higher than LV cells.

4.4.2 Effect of EGF and FGF-2 on CB-NSCs in culture proliferation and differentiation

Growth and cell proliferation for CB and LV NSCs were found to be significantly decreased when one of the growth factors was removed from the media compared to the control cells grown in normal media with both mitogens suggesting that these cells are EGF+FGF-2 dependent. Studies have shown that EGF and FGF-2 may act synergistically to promote NSCs growth and proliferation (Gritti et al., 1996, Weiss et al., 1996). However, compared with CB and LV cells expanded in EGF alone, FGF-2 culture revealed more heterogeneous morphology with smaller cell sizes. Cell proliferation assay also showed that CB-NSCs subjected to removal of one of the growth factors did not grow as well as the control culture. Addition of both growth factors to the culturing medium significantly increased the proliferation of CB and LV NSCs due to the synergistic effect compared with EGF or FGF-2 alone in line with previous observations (Weiss et al., 1996, Gritti et al., 1996).

These results suggest that although EGF and FGF-2 alone support the growth of both CB and LV derived NSCs, but the two mitogens need to be combined to approach maximum proliferation capacity. Previous studies have shown that FGF-2 responsive cells can be isolated from the neural plate in the developing mouse at E8.5 (Tropepe et al., 1999) or adult mouse striatum (Gritti et al., 1996). Other studies have reported that NSCs from adult striatum could be isolated in the presence of EGF alone (Reynolds and Weiss, 1992, Morshead et al., 1994), whereas stem cells derivation from the spinal cord for example require EGF+FGF-2 (Weiss et al., 1996).Thus, further studies would be important to test the possibility of using either EGF or FGF-2 for the isolation of NSCs from

embryonic and adult mouse CB compared to the previously mentioned regions of the brain.

4.4.3 Dose dependent effect of EGF and FGF-2 on the proliferation of CB-NSCs

Our results demonstrated that both mitogens acted on CB and LV derived NSCs in a low range at 2ng/ml. This observation suggests that they may be reacted with their receptors but not with a related receptor system. It might be that at very low doses both mitogens may act as survival factors and at higher doses as mitogens (Kalyani et al., 1998). In our study, FGF-2 showed more dose dependent effect on CB and LV NSCs than EGF consistent with previous observation for E10 cortical precursors previously reported (Qian et al., 1997a). Consistent with (Tropepe et al., 1999), the proliferation of both CB and LV cells were found to increase when both mitogens were combined in a dose dependent manner although the change was non-significant among 5, 10, and 20 (ng/ml) doses for both cells. This finding suggests that these mitogens can be used at lower than 20ng/ml for the expansion of adult NSCs without affecting much of their proliferative capacity.

Removing one growth factor and increasing the other in a dose dependent manner appeared to be additive only for FGF-2 when EGF was removed from the medium and the proliferation was saturated at 20ng/ml for both cells. Whereas omitting FGF-2 and increasing EGF in a dose dependent manner did not seem to have the same effect as FGF-2, and the effect of 5ng/ml of EGF was nearly as great as EGF+FGF-2 at 20ng/ml for both cells. Irrespective of the type of mitogen used, our data demonstrated that both EGF and FGF-2 are mitogens and can support the growth and expansion of CB and LV cells similar to stem cells in other regions of embryonic and adult brain (Reviewed in Gage et al. 1995). However, our data

suggested that FGF-2 might be more mitogenic for these cells than EGF as previously observed for embryonic hippocampal and adult subependymal layer stem cells (Kitchens et al., 1994, Johe et al., 1996).

4.5 Prolonged withdrawal of EGF and FGF-2 on CB derived NSCs proliferation and differentiation

4.5.1 Effect of withdrawal of EGF and FGF-2 on CB derived NSCs proliferation

After demonstrating the short term effect of EGF and FGF-2 on the metabolic activity of both CB and LV NSCs, we then sought to determine the effect of prolonged withdrawal of the two mitogens on the proliferation and the differentiation capacity of CB and LV cells. It was obvious from our results that CB and LV cells were morphologically similar regarding their response to each media condition (EGF, FGF-2, or EGF+FGF-2). However, the cell metabolic assay after 5 passages in each condition showed that the proliferation of LV cells were nearly similar in either EGF or FGF-2 culture condition whereas CB cells showed significant difference in the proliferation between the two groups. The result for LV cells conflicts our previous observation when cells grown in EGF alone showed a significantly higher rate of proliferation compared to FGF alone. This may be because after 3 weeks of expansion in EGF, the cells tended to form large neurospheres at the last passage that might have prevented the penetration of the reagent into the core of the neurospheres and thus lead to misleading result. Nevertheless, NSCs survived for 3 weeks after the removal of either EGF or FGF-2 from the culturing medium while retaining their proliferative capacity and the ability to differentiate into neurons and astrocytes in line with a study on NSCs

isolated from the striatum of postnatal mice (Einstein et al., 2006). Many in vitro studies support our result that both EGF and FGF-2 are able to maintain progenitor cells in mitotic cell division and thus keep them in an undifferentiated state (Reviewed in Kuhn et al., 1997). However, the present study showed that the proliferation capability was decreased significantly after EGF or FGF-2 removal. This finding was also observed in embryonic mouse neural precursor cells maintained in suspension (SCHWINDT et al., 2009). It might be the fact that mitogen withdrawal may cause down regulation of EGF and FGF-2 receptors after differentiation and as a result glial and neuronal markers show upregulation (Kalyani et al., 1998). We also noticed that CB-NSCs in FGF-2 alone did not grow as much as in EGF alone. We also noticed that short term removal of FGF-2 appeared to promote neurite extension observed by B-tub3 marker immunodetection (Schwindt et al., 2009). One of the most defining characters of stem cells is their ability to divide asymmetrically to produce one stem and one differentiated daughter cell or symmetrically in which a stem cell generates two stem or two differentiated cells (Morrison and Kimble, 2006). These two models of divisions can occur in any given population (Loeffler and Potten, 1997). Subcloning experiments by Gritti et al., (1999) have shown that culturing in EGF produces greater rate of progeny with stem cell characteristics than does FGF-2. The same study revealed that SVZ stem cells show significantly faster rate of expansion when cultured in the presence of EGF than in FGF-2, perhaps because symmetric division occurs more frequently in EGF culture than FGF-2. Similar mechanisms may have occurred in the present study, as both CB and LV NSCs showed similar results regarding their response to EGF and FGF-2.

4.5.2 Effect of short term withdrawal of EGF and FGF-2 on CB derived NSCs differentiation

CB and LV derived NSCs grown in EGF, FGF, and EGF+FGF-2 for 5 passages did not appear to drastically differ in their differentiation potential toward the generation of neuronal and glial lineages. Surprisingly, culturing CB NSCs in EGF for 3 weeks generated more neurons than FGF-2 or EGF+FGF-2 although the difference with EGF+FGF-2 was not significant. Our result regarding CB cells does not appear to support the existing studies which demonstrated that culturing neural progenitors isolate from the SVZ and striatum of embryonic and adult rodent or developing human cortex in EGF and FGF-2 biased the differentiation toward glial and neuronal lineages respectively (Burrows et al., 1997, Kuhn et al., 1997, Ostenfeld and Svendsen, 2004). A study by (Garcez et al., 2009) has shown that EGF and FGF-2 stimulate neuronal and glial differentiation respectively. However, results obtained for LV cells were in line with these studies in that FGF-2 exposure could generate more neurons than EGF culture. Moreover, these studies showed the effect of these mitogens on neurospheres and observations suggest that FGF-2 may not efficiently penetrate into the core of the neurosphere which might lead to some neuronal differentiation prior of plating (Ostenfeld and Svendsen, 2004). Combination of the two mitogens did not account for more neuronal or glial generation compared to EGF or FGF-2 cultures for CB and LV derived NSCs. Furthermore, studies have reported that FGF-2 has an important role in promoting gliogenesis, skeletogenesis, and chondrogenesis (Reviewed in (Garcez et al. 2009)). It remains to mention that the effects exerted by these mitogens on NSCs proliferation and differentiation have been shown to differ among neural

progenitor cells in long term expanded culture and fresh one (Ostenfeld and Svendsen, 2004). These effects depend largely on the developmental age of these progenitors, ligand concentration, and the level of EGFR (number/density) (Burrows et al., 2000).

Further characterization of CB derived NSCs in regard to the effect of EGF and FGF-2 withdrawal on their self-renewal, multipotentiality, and fate restriction is important to develop novel therapies for cell regeneration in some incurable cerebellar disorders.

4.6 In vitro differentiation of CB derived NSCs

One of the most important features of NSCs is their differentiation capacity to generate the 3 major cell types in the brain. In these experiments, immunohistochemical analysis revealed that CB-derived NSCs were able to differentiate into neurons, astrocytes, and oligodendrocytes. The absence of Nestin positive cells after differentiation was expected because NSC proliferation was reported to decline after GFs removal and the start of differentiation (SCHWINDT et al., 2009). In CB and LV NSCs cultures differentiated for 4 and 5 days, neurons and astrocytes were identified by B-tub3 and GFAP markers respectively. Oligodendrocytes were not assessed at these time points. However, when the differentiation was prolonged for 16 days, CB cells generated neurons, astrocytes, and oligodendrocytes characterised by B-tub3, MAP2, DCX, and Calbindin for neuronal lineages; GFAP for astrocytes, and MBP for oligodendrocytes. This observation is in line with a study from our lab showing the differentiation capacity of CB derived NSCs into the 3 major cell types of the brain (Alcock and Sottile, 2009). Surprisingly, in the LV culture only neurons and astrocytes were identified but no MBP^+ cells were detected after 16 days of

differentiation contrary to CB cells. This observation suggests that CB and LV cells may differ in the time points of oligodendrocytes generation as BMP^+ cells in LV culture were observed after 11 days of differentiation (see chapter 6 Fig. 6.13E) and seemed to be switched off after 16 days of differentiation. Interestingly, the time period of 16 days of differentiation was enough to detect the expression of Calbindin, a marker associated with one of the most important neuron types in the mature CB; the Purkinje cells (PCs). The few $Calbindin^+$ cells detected in CB-derived cultures in this study was in contrast with the absence of any $Calbindin^+$ cells in the LV-derived culture at D16 of differentiation. This observation suggests that the $Calbindin^+$ cells detected in CB culture might be PCs as no other cells are $Calbindin^+$ in the adult mouse CB (Verdes et al., 2010). There is a study by Tao et al., (2010) which described the efficient generation of PCs from mouse embryonic stem cells, using several factors such as (BDNF, NT3, and T3) to induce the differentiation and survival of PCs. In the present study, the only factor added that was also used by Tao et al., (2010) was BDNF, and it was reported that neurotrophins such as BDNF can increase PC survival and dendrite development in vitro (Morrison and Masson, 1998). In addition, BDNF is required for dendritic formation of PCs and the secretion of BDNF from the granule cell promote the differentiation of PCs dendrites (Ohashi et al., 2014). Thus, our results indicate that 16 days of exogenous BDNF treatment may be sufficient to induce the differentiation of PCs.

4.7 Conclusions

In this study, we showed that NSCs derived from adult CB and LV were able to respond to both EGF and FGF-2 as previously reported for NSCs from the adult mouse SVZ (Gritti et al., 1999). Each of these growth factors alone was observed to support the growth and the proliferation of these cells independently. The results presented in this study showed that CB and LV cells grew at a faster rate in EGF than FGF-2, and the proliferation was increased significantly and cells displayed typical NSCs morphology when EGF and FGF-2 were combined (Gritti et al., 1999, SCHWINDT et al., 2009). This indicated that EGF and FGF-2 may have different effects on CB-derived NSCs of adult mouse as they act through a completely different signalling pathway (Bayatti and Engele, 2002). This conclusion is supported by an in vivo study showing that infusion of exogenous EGF and FGF-2 revealed different effects on neural progenitor cells in the SVZ and hippocampus of adult rat brain (Kuhn et al., 1997).

When cultured in EGF or FGF-2 alone, CB and LV derived NSCs could be expanded over 5 passages, maintaining the capacity to differentiate although both cultures showed high incidence of cell death and morphological alterations compared to the control culture containing both growth factors. One limitation of our study is that glial cells were not quantified so it was not easy to conclude whether more glial cells were generated than neurons in either EGF or FGF-2. Thus it was difficult to predict any bias in the differentiation of CB and LV cells toward glial and neuronal fates after 3 weeks culturing in EGF, FGF-2, and EGF+FGF-2. Thus, further studies are needed to see the effect of longer expansion of CB and LV cells in these mitogenic conditions and determine their effect on neuronal or glial fate specification. In summary, this is the first study

investigated the effect of EGF and FGF-2 on CB-NSCs and their differentiation potential following mitogen withdrawal. Our approach of investigating the exact role of EGF and FGF-2 on the proliferation and differentiation potential of CB derived NSCs may be useful for characterising this population and provide additional means for their regenerative potential in CB neurodegenerative disorders. Based on my observation here, I hope that other researchers in this field will be able to answer some of the questions that I was not able to answer.

5 Quantitative, morphological and immunohistochemical study of Bergmann glia and Purkinje cells in Purkinje Cell Degeneration (*pcd*) 5J mutant mice

5.1 Introduction

Purkinje cell degeneration (*pcd*) is one of the common spontaneous mouse cerebellar mutant models, which are homozygous for Agtpbppcd/J mutations (Fernandez-Gonzalez et al., 2002). PCD mice carry a mutation in Nna1 gene which leads to the degeneration of all PCs, to gait ataxia, and to slow degeneration of mitral cells and photoreceptor retinal cells (Fernandez-Gonzalez et al., 2002, Cendelin, 2014). Thus, these *pcd* mice provide a useful model to understand the pathological mechanisms of PCs loss as it is closely resembles PCs loss in ataxic human. Because of the structural and close proximity of BG to Purkinje cells, these mutant mice may also provide information regarding the potential proliferative capacity of the BG after PCs loss.

The cerebellum (CB) is regarded as a static organ in which neurogenesis is limited only to the early postnatal life and lack with the disappearance of the external granular layer (EGL) (Ponti et al., 2008). Infusion of growth factors such as EGF, FGF-2, and brain derived neurotrophic factors (BDNF) into different regions of intact forebrain in adult rodents resulted in stimulating neuronal generation found to be ineffective in the adult rat cerebellum (Kuhn et al., 1997). Moreover, transplantation studies have indicated that the environment within the cerebellum is unpermissive to direct the donor cells both in normal conditions and after cerebellar damage (Suhonen et al., 1996a, Carletti and Rossi, 2005). The Purkinje cell degeneration phenotype activates astrocytes and glial cell, a process

called reactive gliosis (Baltanas et al., 2013). It has been postulated that injury to the CB induces BG proliferation and hypertrophy, and cause reactive gliosis (Wilhelmsson et al., 2004, Sofroniew and Vinters, 2010, Gelpi et al., 2014). Moreover, BG have shown to proliferate, undergo morphological changes, and upregulate some molecular markers such as Nestin, prominin 1, and PSA-NCAM following PCs loss in Purkinje cell degeneration mice (Sotelo et al., 1994, Grimaldi and Rossi, 2006).

The effect of glial activation are debated, as it might have beneficial effect conferring neuroprotection to injured brain, or detrimental effects and cause brain damage (Wilhelmsson et al., 2004, Baltanas et al., 2013). The most important hallmark characterising reactive gliosis is the upregulation of GFAP and vimentin, and hypertrophy of the astrocytic processes (Wilhelmsson et al., 2004). Glial activation is also characterized by increase in cell proliferation, cell body hypertrophy, secretion of inflammatory substances, phagocytosis, and migration to the site of injury (Sofroniew and Vinters, 2010). Few reports have so far described the molecular pathways that cause PC death and Bergmann gliosis in *pcd* disease, Studies have described these pathways as DNA damage, endoplasmic reticulum stress, apoptosis, mitochondrial dysfunction and autophagy (Reviewed in (Baltanas et al., 2013)). However, none of these studies quantified the number of Bergmann cells in pcd^{5J}. Our data presented in chapter 3 suggested BG as neural stem-like cells in adult mouse cerebellum. This led us to hypothesize that BG might be quiescent in the normal cerebellum and might be activated after injury.

Thus, we aimed in this chapter to:

1. Examine the response of BG cells to the CB damage caused by the degeneration of PCs by GFAP marker immunostaing.
2. Given the lack of quantitative analysis on BG in *pcd*^{5J} mice, we analysed the number of BG in cerebellar sagittal sections at different postnatal ages of both *pcd* mutant and wild type mice using Sox1, 2, and 9 to label BG.
3. Test whether NSCs could be isolated from the cerebellum of P21 aged *pcd*^{5J} and wild type mice.

5.2 Results

This study was designed to examine the time course of PC degeneration and concomitant BG response in sagittal sections of cerebellum of *pcd*^{5J} mice, compared to their wild type counterparts.

5.3 Phenotype of the *pcd*^{5J} mutant mice

The phenotypic characteristics for *pcd*^{5J} are an early degeneration of PCs and gait ataxia, as previously reported (Baltanas et al., 2011, Wang and Morgan, 2007). At birth, *pcd*^{5J} mice were indistinguishable from their wild type littermates (Chakrabarti et al, 2006). By p17 however, homozygous mice were smaller in size than their age matched littermates, and by P21 they exhibited an overt ataxic phenotype (Chakrabarti et al., 2009). Gross anatomy revealed that the hm *pcd*^{5J} mice have smaller brain size (Fig. 5.1) compared to the age matched controls in line with early report on *pcd* anatomy (Mullen et al., 1976).

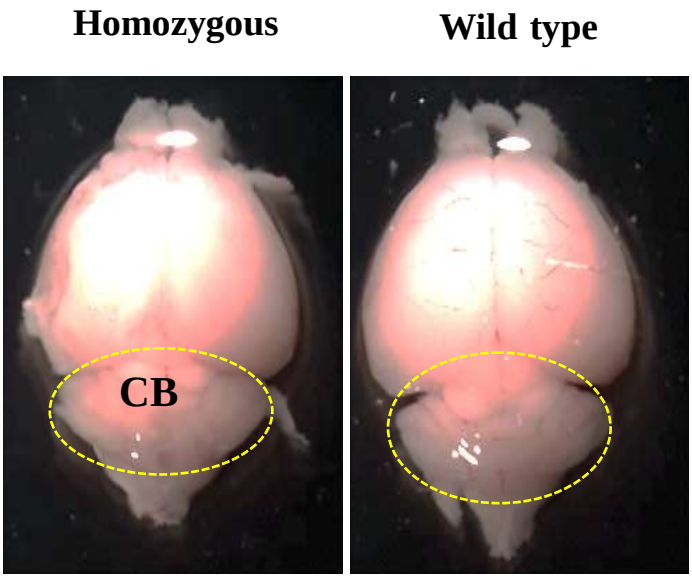

Figure 5.1 Gross apperance of homzygous *pcd* and wild type brain at P21. Dotted circles represent the cerebellum (CB) which appears smaller in homozygous mouse compared to smilar age wild type.

5.4 PCs degeneration in the *pcd*^{5J} mutant mice

We examined PC degeneration in *pcd*^{5J} mutant mice at P17, P21, P26, and P100 and compared with their wild type counterparts, using immunohistochemical staining with an anti-Calbindin antibody which selectively labels PCs in normal and degenerated PCs (Verdes et al., 2010). GFAP staining was used to label the BG population (Koirala and Corfas, 2010).

At P17, there was no visible difference in the staining pattern or distribution of PCs and BG when comparing mutant and control mice (Fig. 5.2A), although PCs looked less arborized in the mutant mice. After few days, at P21, the onset of PC death was clearly visible in the mutant mice (Fig. 5.2B), and it progressed rapidly to massive PCs loss (~70-80%) by P26 (Fig. 5.2C) compared to the control. At P100, PCs were virtually absent in the *pcd* mice, which showed marked shrinkage of the cerebellar cortex compared to control animals (Fig. 5.2D).

Figure 5.2 (overleaf) Purkinje cells degeneration in *pcd*^{5J} cerebellar sections. Cerebellar sagittal sections of both homozygous *pcd* and wild type mice stained for Calbindin (green) and counter stained with dapi (blue) at different ages reveal a normal number of PCs at P17 (A). PCs started to degenerate at P21 (arrows) (B) and drastically decreased at P26 (C), before no PCs were visible at P100 (D).

IGL, internal granular layer; **ML**, molecular layer; **PCL**, Purkinje cell layer; **WM**, white matter

Scale bar =130μm.

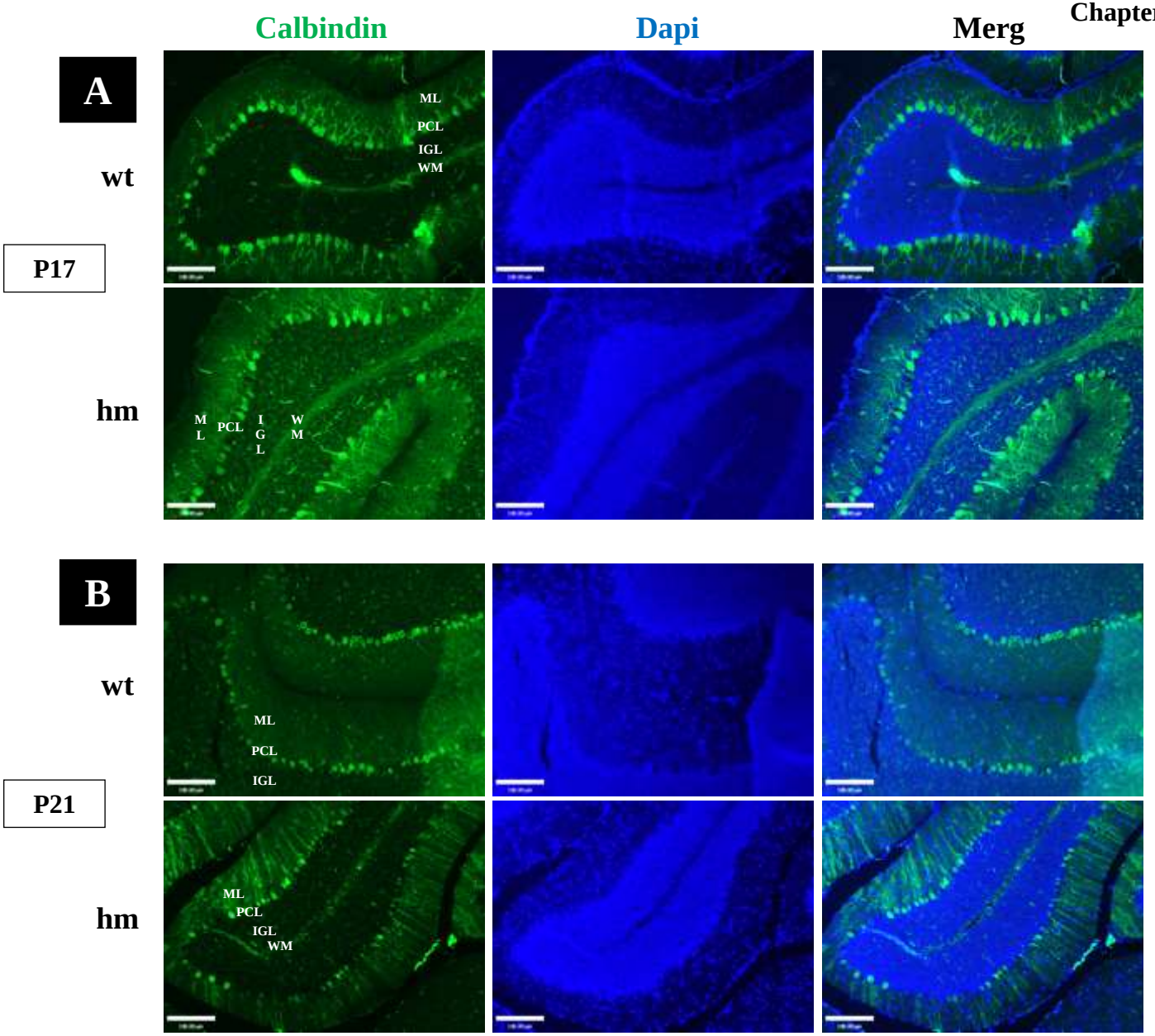
Calbindin
Dapi
Merg
A
wt
P17
hm
ML
PCL
IGL
WM
B
wt
P21
hm
ML
PCL
IGL
WM

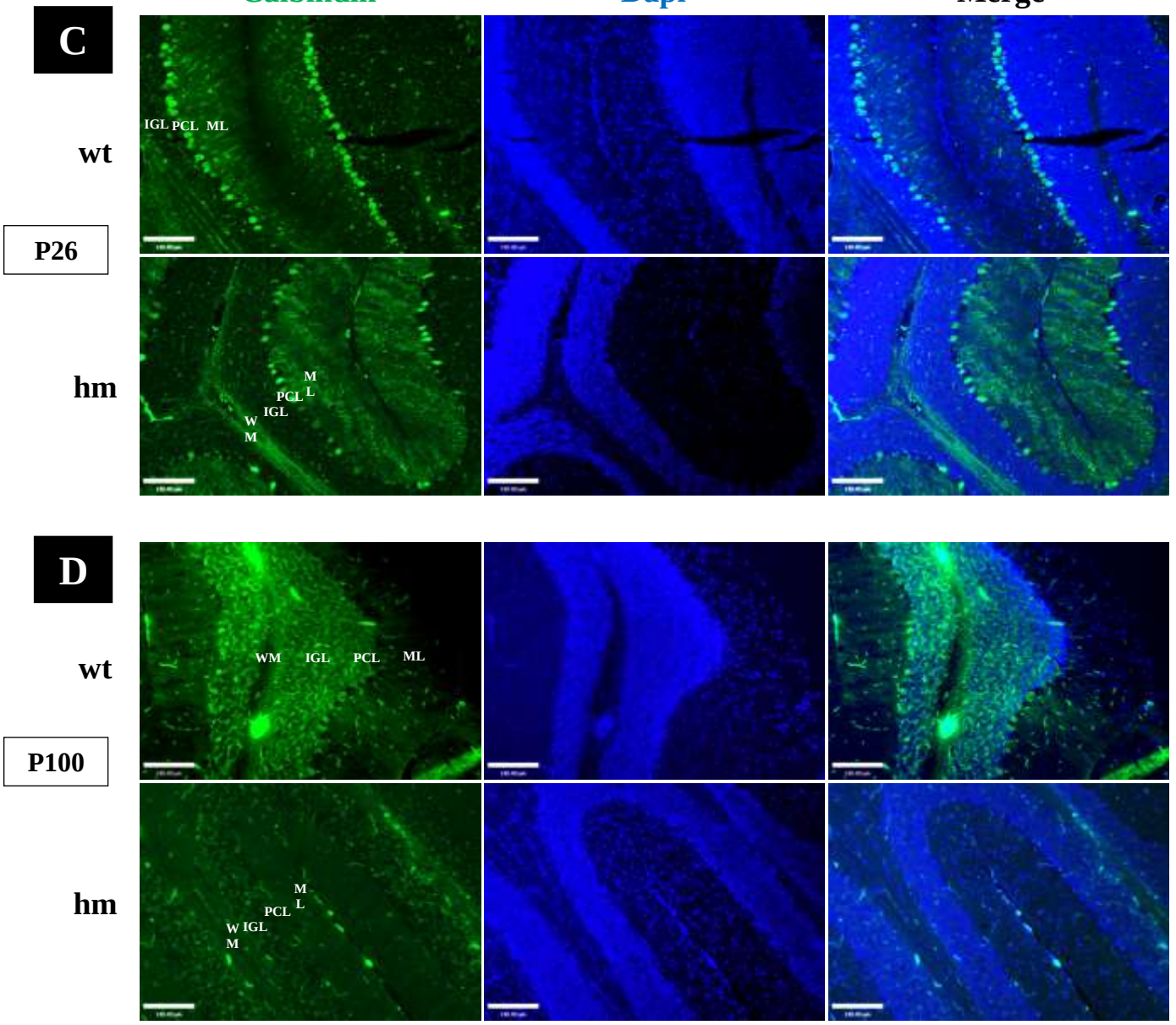
Calbindin
Dapi
Merge
C
wt
P26
hm
IGL PCL ML
M
L
PCL
IGL
W
M
D
wt
P100
hm
WM IGL PCL ML
M
L
PCL
W IGL
M

5.5 Sox gene expression in *pcd*^{5J} mice at different time points

The expression of Sox1, 2, and 9 genes in Sox1+/-GFP mice have been described earlier in this study (see chapter 3 for detail). Here, I performed similar double immunostaining of Sox1, 2, and 9 with Calbindin for PCs in *pcd* mutant and wild type mice at P17, P21, P26, and P100 to examine the changes in these Sox genes expression at different time course of PCs degeneration. at all time points examined here, it was demonstrated that Sox1 expression was found mainly in BG cells in the PCL (Fig. 5.3) and the staining pattern was similar in the *pcd* and WT mice. Similar to Sox1, Sox2 and Sox9 were also expressed in the BG of the mutant and WT mouse at P17, 21, 26, and 100 with very close staining pattern (Fig. 5.4 and 5.5 respectively). However, some glial cells in the molecular layer of both pcd and WT mice showed some immuunoreactivity for Sox2 and Sox9 (Fig. 5.4 and 5.5 respectively). No PCs were found at P100 in *the* pcd mice compared to their age matched controls (Fig. 5.3, 5.4 and 5.5) consistent with our previous observation in (Fig. 5.2).

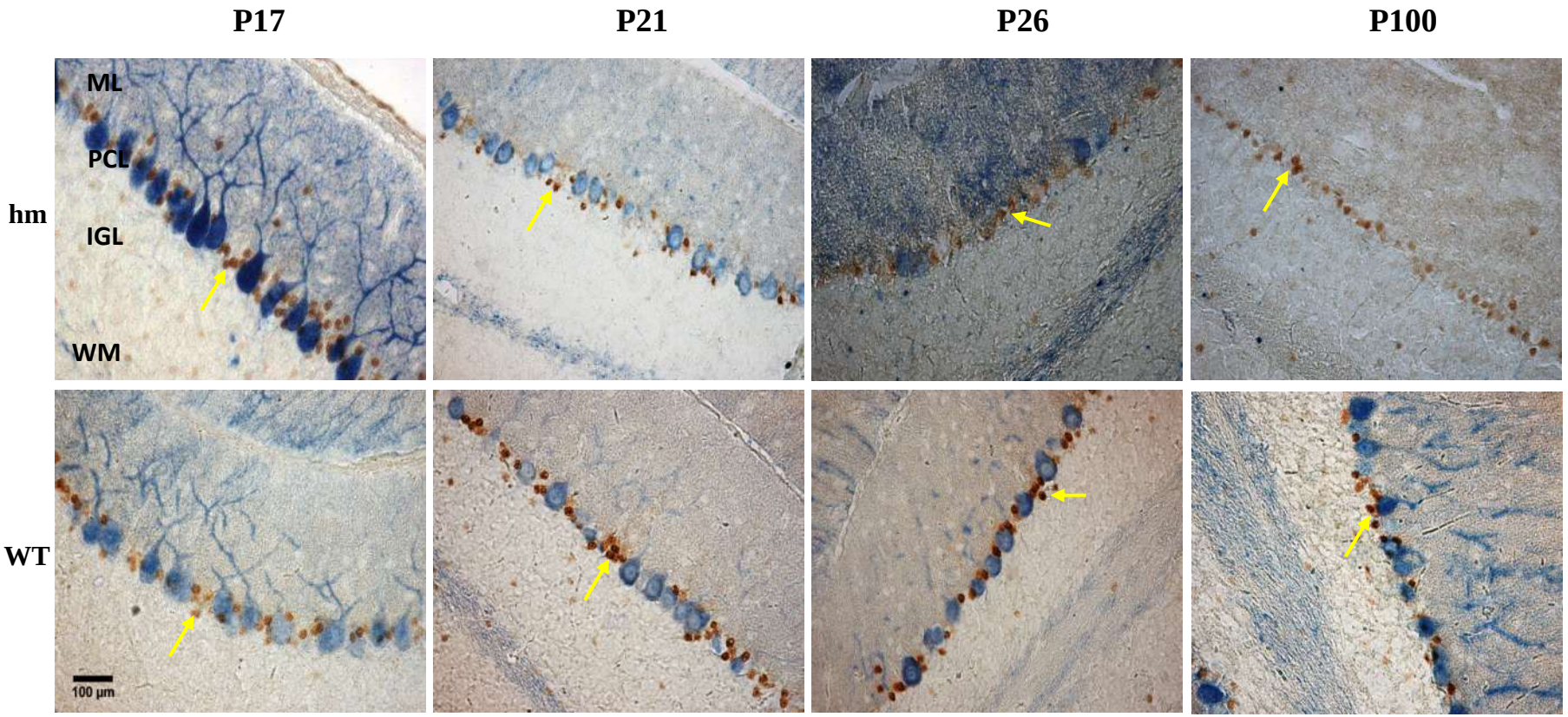

Figure 5.3 Immunohistochemical images of cerebellar sagittal sections of P17, P21, P26, and P100 *pcd*^{5J} mutant and wild type mice double stained for Sox1 (brown) and Calbindin (blue). Sox1 expression is restricted to BG (yellow arrows) in the PCL between the PC bodies (blue). At P17, both mutant and control tissue are similar. At P21, PCs started to degenerate with decreased numbers in the mutant mice compared to their control. Severe PCs loss was observed in the P26 mutant mice and by P100, no PCs are found in the mutant tissue with increased number of BG.

IGL, internal granular layer; ML, molecular layer; PCL, Purkinje cell layer; WM, white matter. Scale bar =100 µm

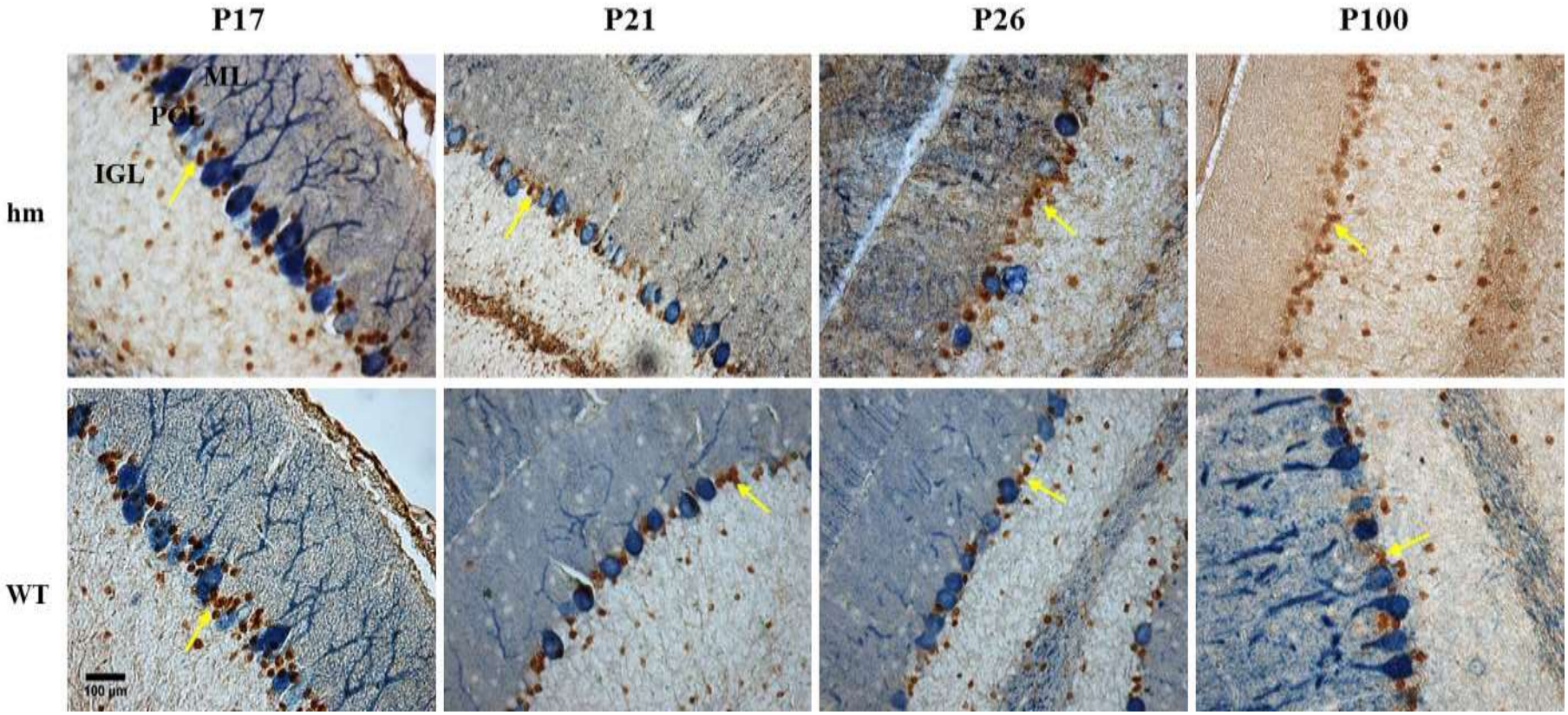

Figure 5.4 Immunohistochemical images of cerebellar sagittal sections of P17, P21, P26, and P100 *pcd*^{5J} mutant and wild type mice double stained for Sox2 (brown) and Calbindin (blue). Sox2 expression is confined to BG (yellow arrows) in the PCL between the PC bodies (blue) in all time points. At P17, both mutant and control tissue are similar. At P21, PCs started to degenerate with decreased number of BG in the mutant mice compared to their control. Severe PCs loss was observed in the P26 mutant mice and by P100, no PCs are found in the mutant tissue while increased numbers of BG and ML glial cells were observed.

IGL, internal granular layer; ML, molecular layer; PCL, Purkinje cell layer; WM, white matter. Scale bar =100 µm

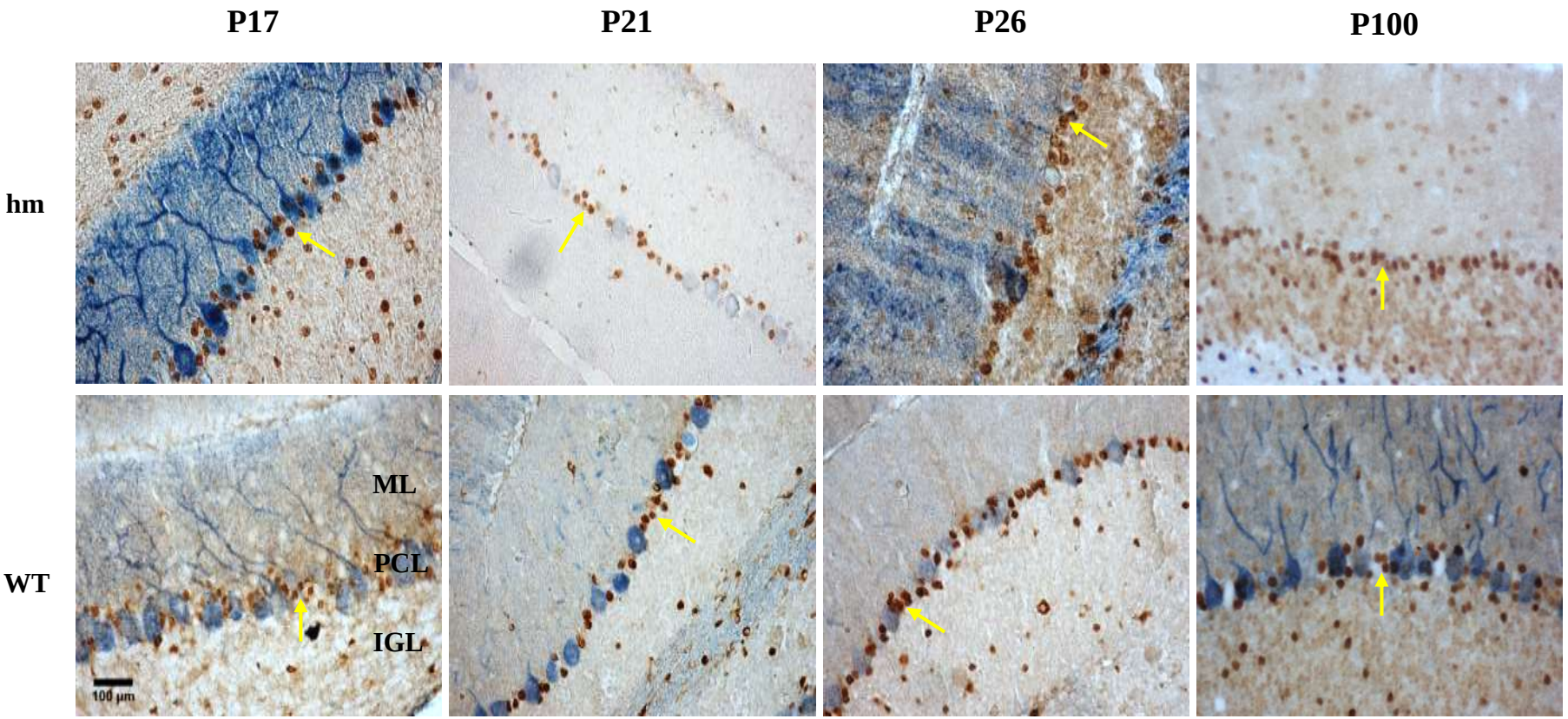

Figure 5.5 Immunohistochemical images of cerebellar sagittal sections of P17, P21, P26, and P100 *pcd*^{5J} mutant and wild type mice double stained for Sox9 (brown) and Calbindin (blue). (A) In the cortex, Sox9 expression is detected in the BG (yellow arrows) in the PCL between the PC bodies (blue) in all time points. At P17, both mutant and control tissue are similar and no PC loss was observed. At P21, PCs begin to degenerate with decreased number of BG in the mutant mice compared to their control. Massive PCs loss was observed in the P26 mutant mice and by P100, no PCs are found in the mutant tissue with increased number of BG and ML glial cells indicating reactive gliosis.

IGL, internal granular layer; ML, molecular layer; PCL, Purkinje cell layer; WM, white matter. Scale bar =100 µm

5.6 Quantitative analysis of Bergmann glia and Purkinje cells in *pcd*^{5J} mice

Next, changes in the BG cell population was analysed alongside PC degeneration at these increasing cerebellar stages, in order to determine whether BG vary in number in response to CB degeneration, as previously suggested (Perry and Brat, 2010, Gelpi et al, 2014, Buffo et al., 2008). For this purpose, BG and PCs numbers were monitored in the *pcd* and age-matched wild type mice at different postnatal ages (P17, P21, P26, and P100) using double immunolabeling for Calbindin (to mark PCs) and Sox1, 2, and 9, markers previously shown to be expressed in the adult BG (Brazel et al., 2005; Sottile et al, 2006).

Sox1 antibody was used alongside Sox2 and Sox9 as the Sox1 expression is restricted to BG in the adult cerebellum (Alcock and Sottile, 2009). BG cell bodies are located between the PC bodies in the PCL, and they can be easily identified based on the size of their nuclei (Fig. 5.3). Although the numbers of Calbindin positive PCs were significantly reduced at P26 and P100 in the mutant mice compared to their controls (Fig. 5.6B, 5.7B, 5.8B), Sox1 immunodetection showed no significant difference in the number of Sox1^{+} BG between the *pcd* group compared to their age matched controls at P17, P21, and P26 (Fig. 5.6A). Interestingly, there was significant increase in Sox1^{+} BG numbers in the mutant mice at P100 compared to the control (Fig. 5.6A).

Similar to Sox1, quantification of Sox2 and Sox9 positive BG cells showed that no significant differences were observed among the *pcd* mice at P17, P21, and P26 compared to their WT counterparts (Fig. 5.7A, 5.8A respectively). However, at P100 the number of BG cells positive for Sox2 and Sox9 were increased significantly (Fig. 5.7A, 5.8A respectively) compared to the age matched controls. The number of BG was significantly higher at P100 in the *pcd* mice compared to the control for Sox1, 2, and 9 stained with Calbindin, suggesting

that changes in Bergmann glia occurred at late stage of the disease. Surprisingly, the number of $Sox2^{+}$ glial cells in the IGL of P100 *pcd* mice showed no significant differences with their controls (Fig. 5.7C), suggesting that the degeneration-induced changes might confined only to BG cells. When the numbers of Calbindin positive PCs were compared between the *pcd* mutant groups at the examined time points, we observed a significant decrease in PCs number started by P21 down to zero at P100 (5.6B, 5.7B, 5.8B) in line with earlier results (Fig. 5.2D).

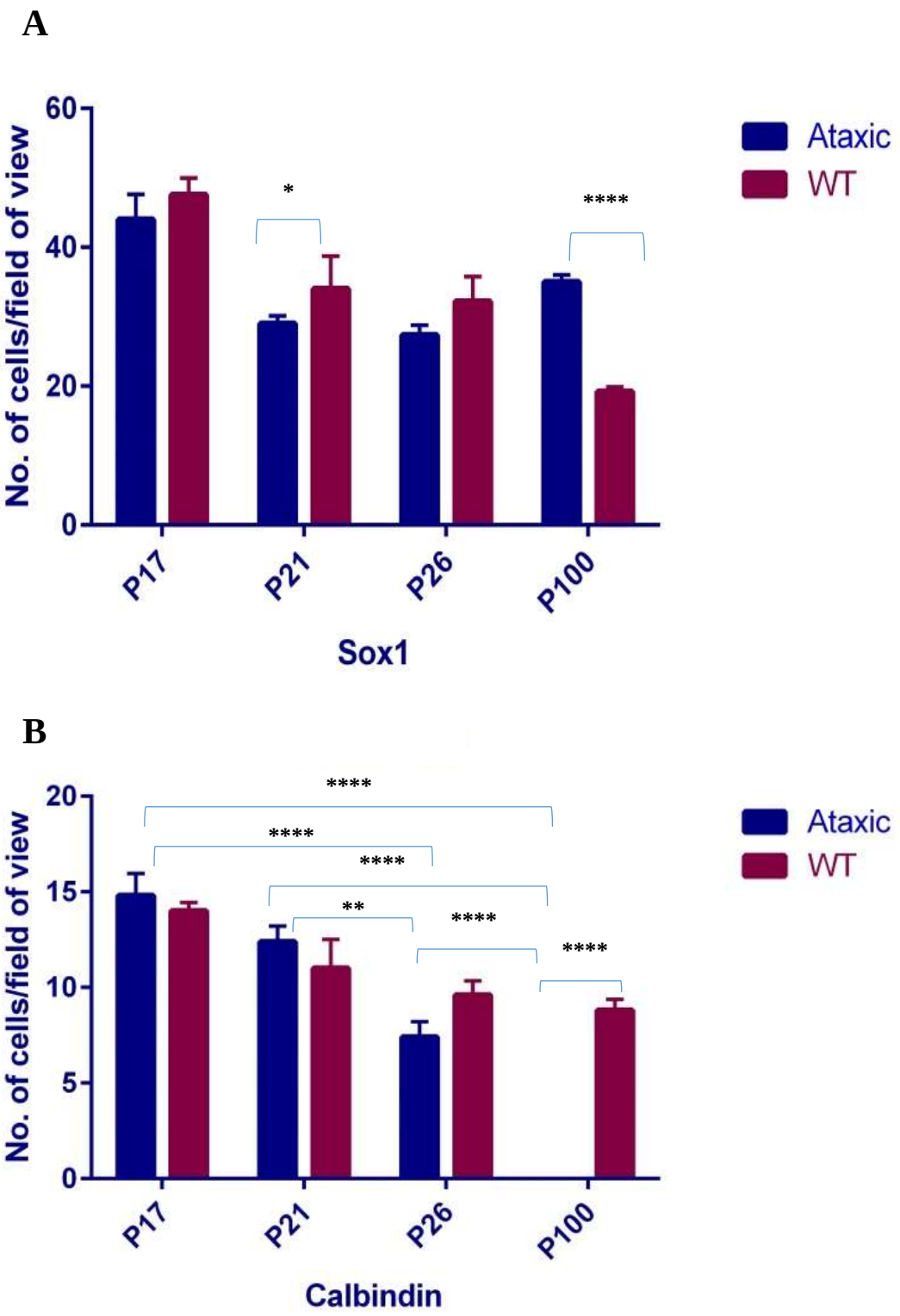

Figure 5.6 Quantification of Bergmann glia and Purkinje cell numbers in homozygous *pcd*^{5J} and wild type mice at different ages by immunostaining with Sox1 and Calbindin. (A) BG stained for Sox1 showed no significant difference at P17, P21, and P26 between the mutant and control, while by P100, BG number increased significantly in the *pcd* mice compared to the WT control. (B) Significant decrease of PCs was observed at P100 in the *pcd* mice compared to their control, and among the *pcd* group at postnatal ages P21, P26, and P100. Results are presented as mean (n=5 per each age) ± SEM using Two-way ANOVA with Tukey's method to compare the mean of each group (**** P < 0.0001, ***P< 0.0005, **P< 0.0041, *P< 0.0155).

A

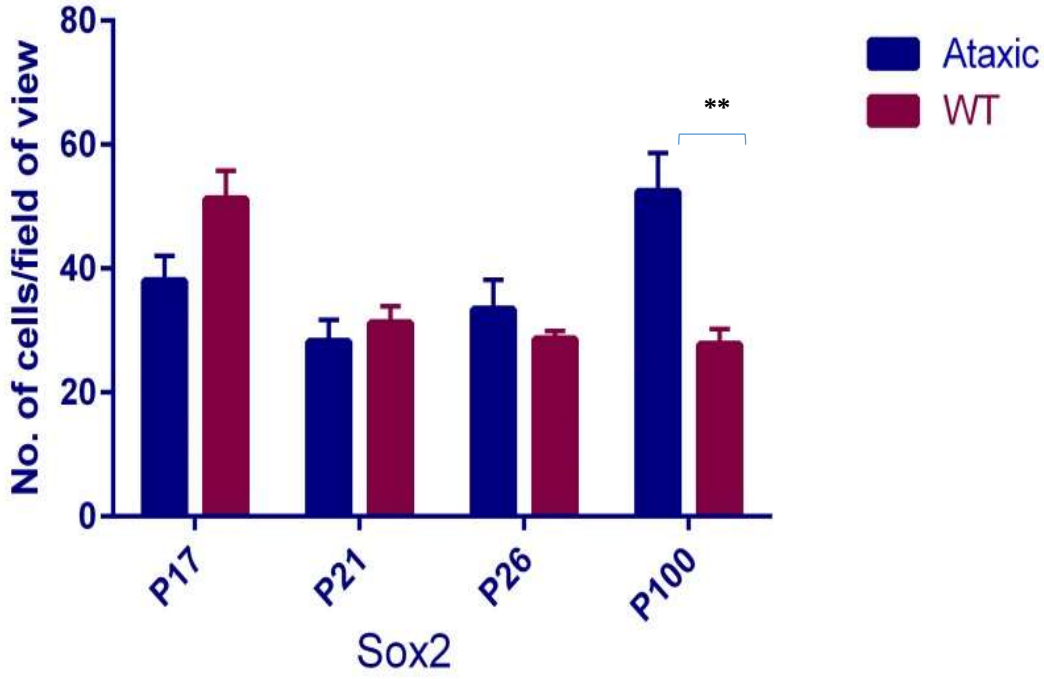
80
60
40
20
0
No. of cells/field of view
**
Ataxic
WT
P17
P21
P26
P100
Sox2

B

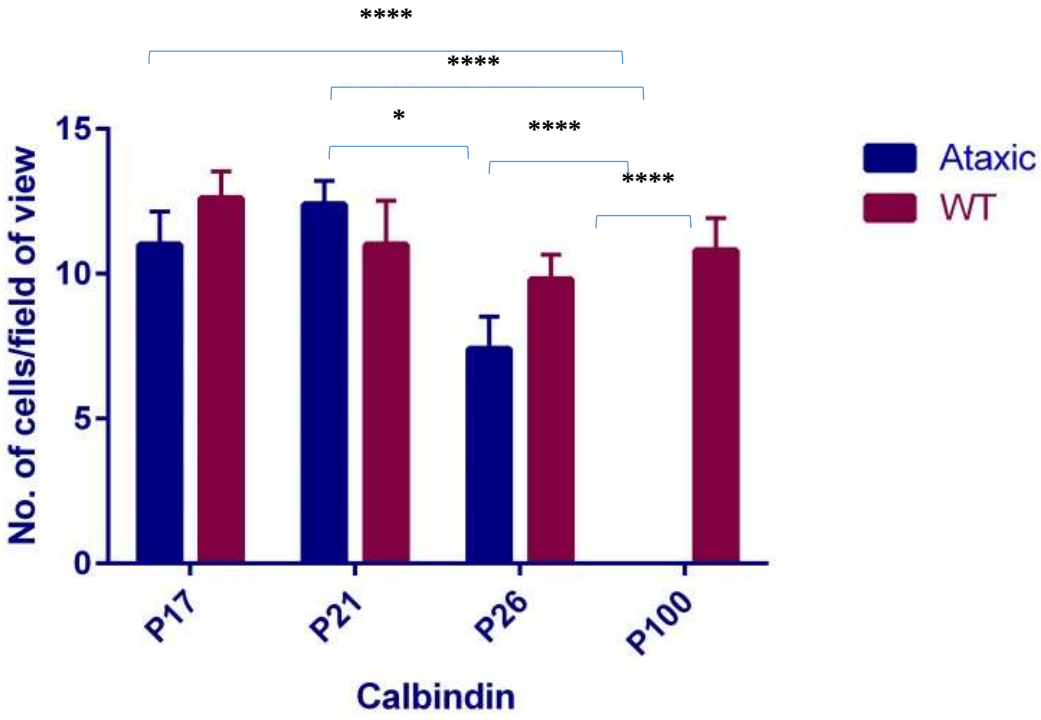
****
****
*
****
****
15
10
5
0
No. of cells/field of view
Ataxic
WT
P17
P21
P26
P100
Calbindin

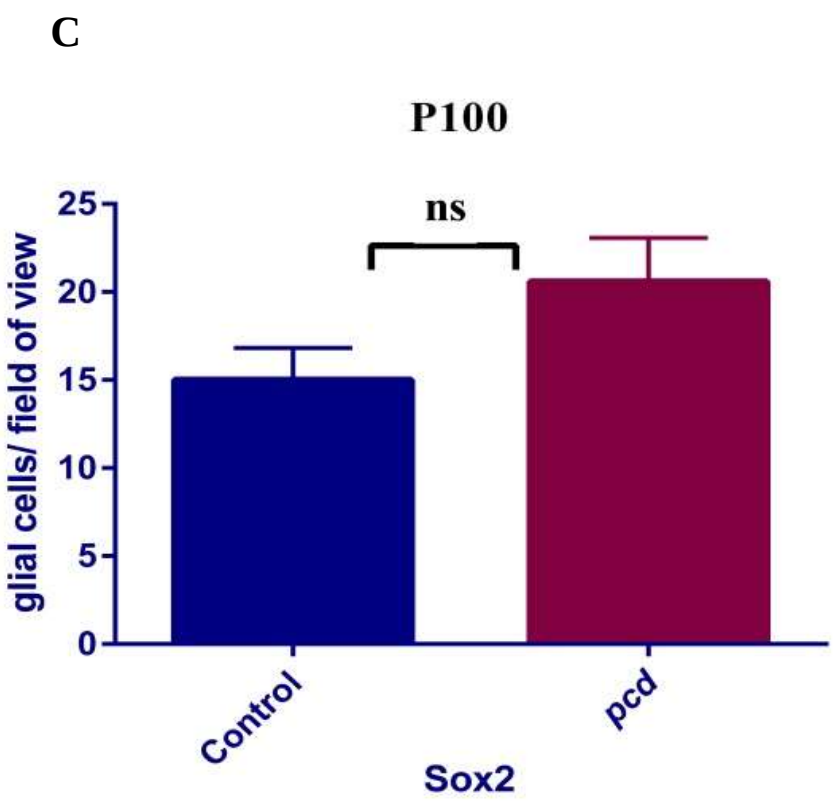

Figure 5.7 Quantification of Bergmann glia and Purkinje cell numbers in homozygous *pcd*^{5J} and wild type mice at different postnatal ages by immunostaining with Sox2 and Calbindin. (A) A significant increase of BG number was observed only at P100 in the *pcd* mice compared to the control. (B) Significant decrease of PCs was observed at P100 in the *pcd* mice compared to their control and among the *pcd* group at postnatal ages (P21, P26, and P100). (C) Quantification of IGL Sox2+ cells number showed no significant difference between the *pcd* and control animals at P100. Results are presented as mean (n=5 per each age) ± SEM using two-way anova with Tukey's method to compare between means (P**** < 0.0001, **P< 0.0027, *P< 0.0171).

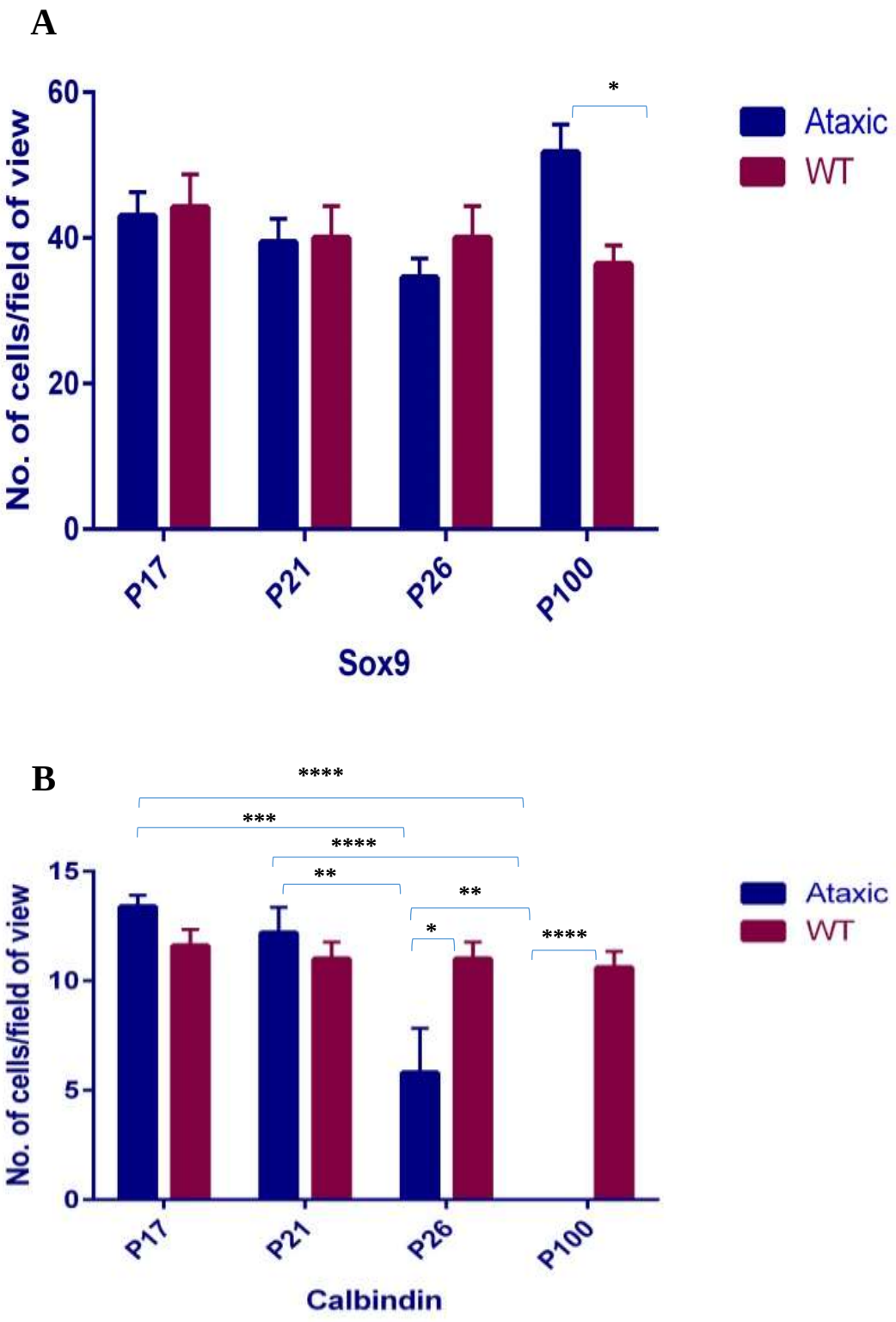

Figure 5.8 Quantification of Bergmann glia and Purkinje cell numbers in homozygous *pcd*^{5J} and wild type mice at different postnatal ages by immunostaining with Sox9 and Calbindin. (A) A significant increase of BG number was observed only at P100 in the *pcd* mice compared to the control. (B) Significant decrease of PCs was observed at P26 and P100 in the *pcd* mice compared to their control and among the *pcd* group between (P21, P26, and P100). Results are presented as mean (n=5 per each age) ± SEM using two way anova with tukey's method to compare between means (P**** < 0.0001, ***P< 0.0002, **P< 0.0019, *P< 0.0412 in A and 0.0178 in B).

5.7 Bergmann Glia radial fibers changes in the *pcd*^{5J} mice

In order to characterise the changes observed in the BG fibers of the *pcd* mutant mice, cerebellar tissue samples were analysed using immunostaining with Calbindin for PCs and GFAP for BG. GFAP is astrocytic marker previously shown to be upregulated after brain injury (Sofroniew and Vinters, 2012), and in the CB, GFAP is found to be expressed in all BG cells in a radial-like pattern (Sun and Jakobs, 2012). The location of BG and the distribution of their radial fibers in the ML and PCs dendrites are illustrated in (Fig. 5.9) of P17 *pcd* mutant mice and their age matched wild types. In the control and mutant mice, GFAP immunoreactivity was observed in the astrocyte of the IGL, BG cell bodies in the PCL and their long radially oriented processes in the ML (Fig. 5.10A). In P17 *pcd* mice, the morphology of BG and their fiber distribution and arrangement in the ML were similar to the control animals (Fig. 5.10A), although staining was slightly increased in the astrocytes of the IGL, and no PC loss was observed at this age. At P21, increased GFAP expression was more noticeable in the BG fibers which appeared disorganised in the mutant mice compared to their control, suggesting changes in the BG population (Fig. 5.10A), while the PC bodies appeared smaller in size compared to the wild type and started to degenerate (blue cells in Fig. 5.10A). At P26, PC loss was severe and the ML layer decreased in thickness, with less organised Bergmann glial fibers compared to P21 (Fig. 5.10A). In the P100 *pcd*^{5J} mice, pronounced upregulation of GFAP was observed together with thick, disorganised BG fibers in the ML. A dramatic decrease in the thickness of both ML and IGL (Fig. 5.10A and B) was observed, with small vacuoles found in the ML and complete loss of PCs (Fig. 5.10A and B). None of these abnormal changes was observed in the control wild type mice at P100 (Fig. 10). Moreover, no nestin expression was detected in the BG at P100 of both *pcd* mutant and control mice (Fig. 5.11).The above findings indicated that BG was also affected in the pathology of the Purkinje cell degeneration.

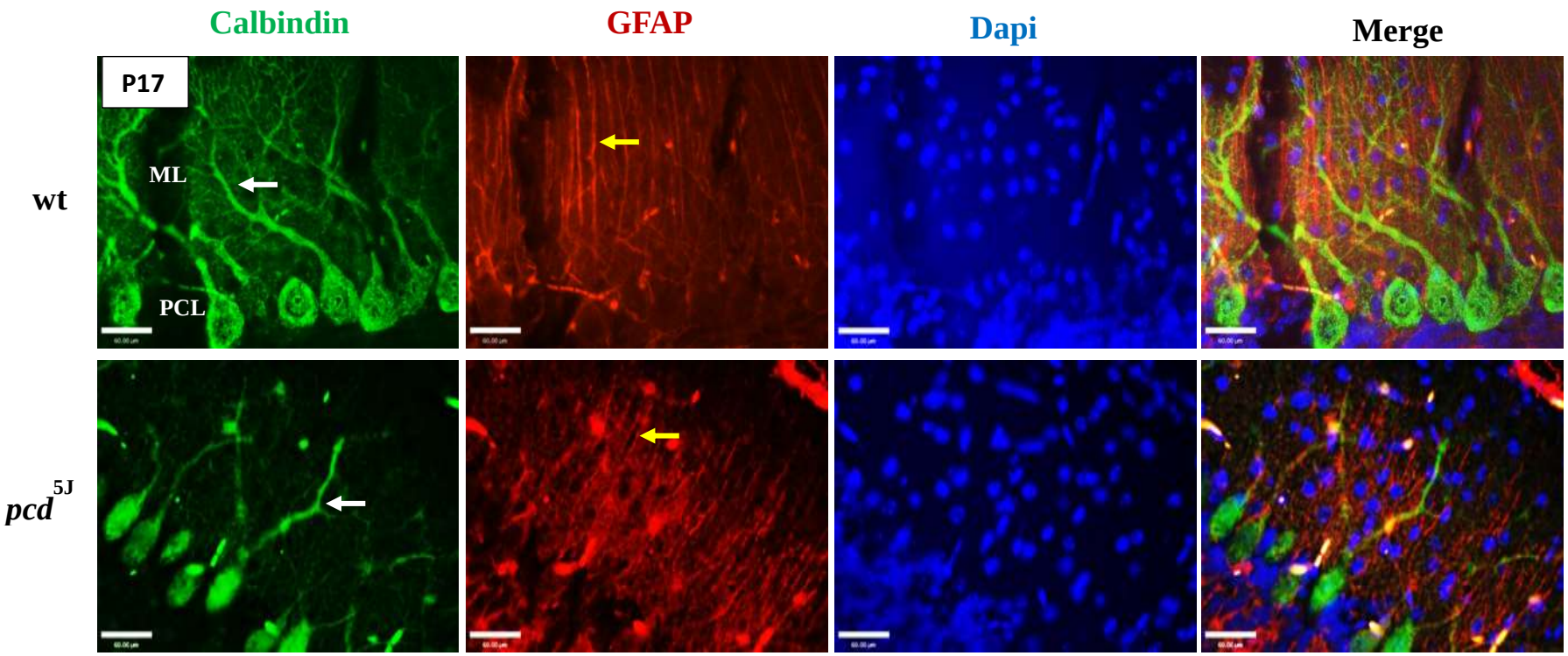

Figure 5.9 Double immunolabeling of Cabindin and GFAP in sagittal cerebellar sections of *pcd*^{5J} and wild type mice at P17 showing the distribution of BG fibers and PCs dendrities. Normal morphology of Bergmann glial fibers and their distribution in the ML are revealed by GFAP staining (yellow arrow) at this P17. PCs dendrites (white arrows) appear more arborized in the WT as shown by Calbindin immunostaing (Green). Dapi was used as nuclear counterstain (blue). PCL= Purkinje cell layer; ML= molecular layer; Scale bar=60µm

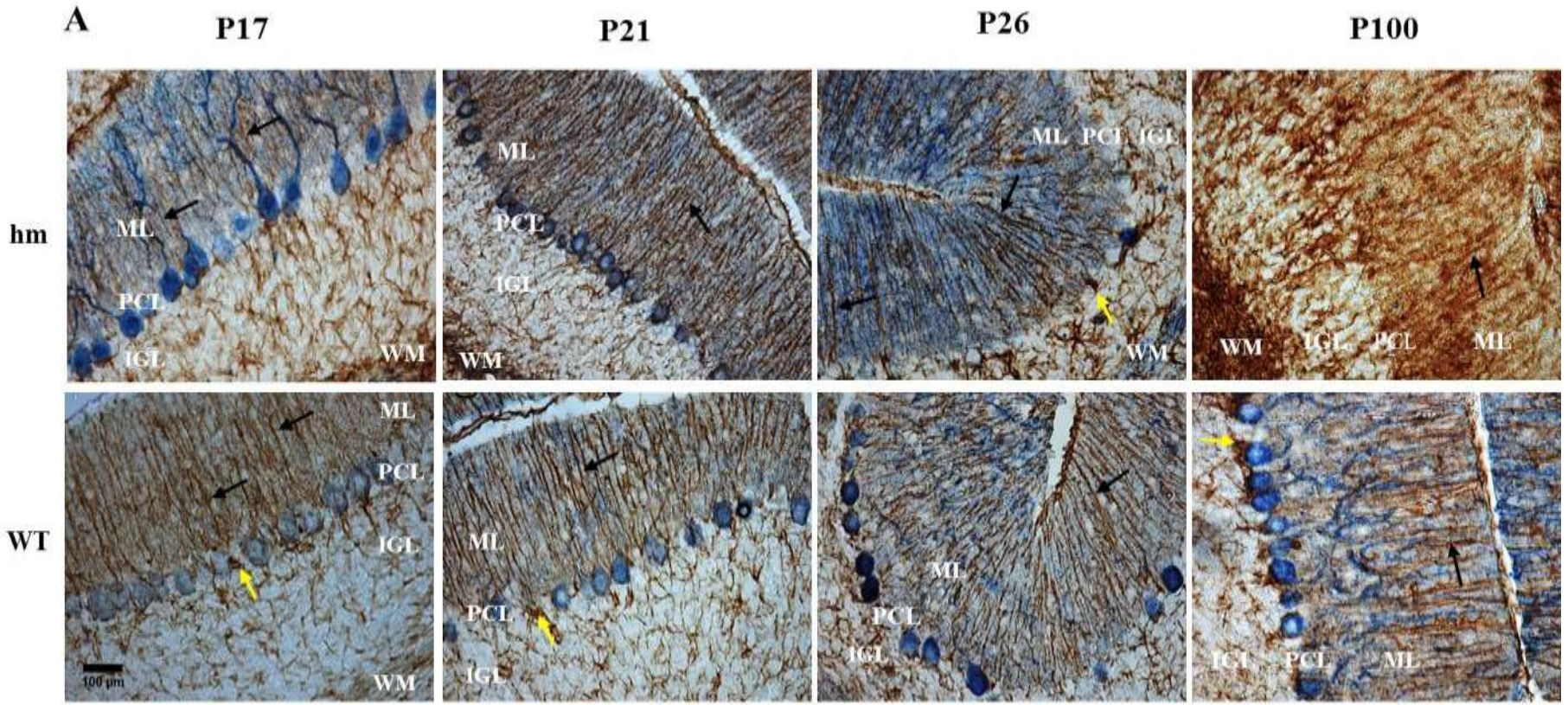
A
P17
P21
P26
P100
hm
WT
ML
PCL
IGL
WM
100 µm

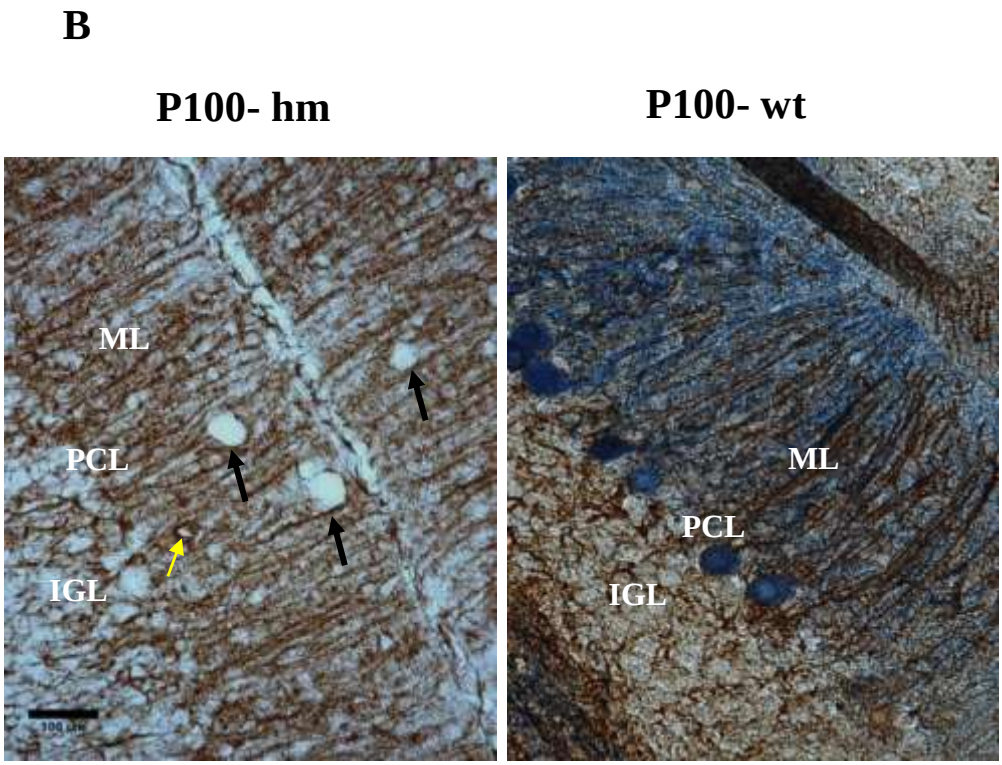

Figure 5.10 PC loss induce Bergmann gliosis in homozygous pcd^{5J} mice. GFAP (brown) co-labelled with Calbindin (blue) in cerebellar sagittal sections of homozygous pcd^{5J} (hm) and wild type (WT) mice at different ages. At P17, BG fibers (black arrows) distributed evenly in the ML and no PC loss (blue) was observed compared to the WT control. At P21, GFAP upregulation in the BG fibers was noticeable with smaller PC bodies compared to the control. In P26 mutant mice, large PC loss was observed with reactive astrocytes in the ML. At P100, BG fibers appeared hypertrophied, revealed marked upregulation of GFAP marker and lost their uniform appearance as long parallel fibres (black arrows) across the ML in the hm mutant mice but not in their controls. (B) Sagittal sections showing GFAP and Calbindin co-localisation in the cerebellar cortex of homozygous *pcd* and wt mice at P100. GFAP upregulation in the BG cells is clearly shown in the mutant mice indicating gliosis with large vacuoles (black arrows) in the ML and some BG cells are dislocated in the ML (yellow arrow) with total loss of calbindin positive PCs (blue). No tissue abnormality is detected in the wild type control.

IGL, internal granular layer; ML, molecular layer; PCL, Purkinje cell layer; WM, white matter. Scale bar= 100 µm

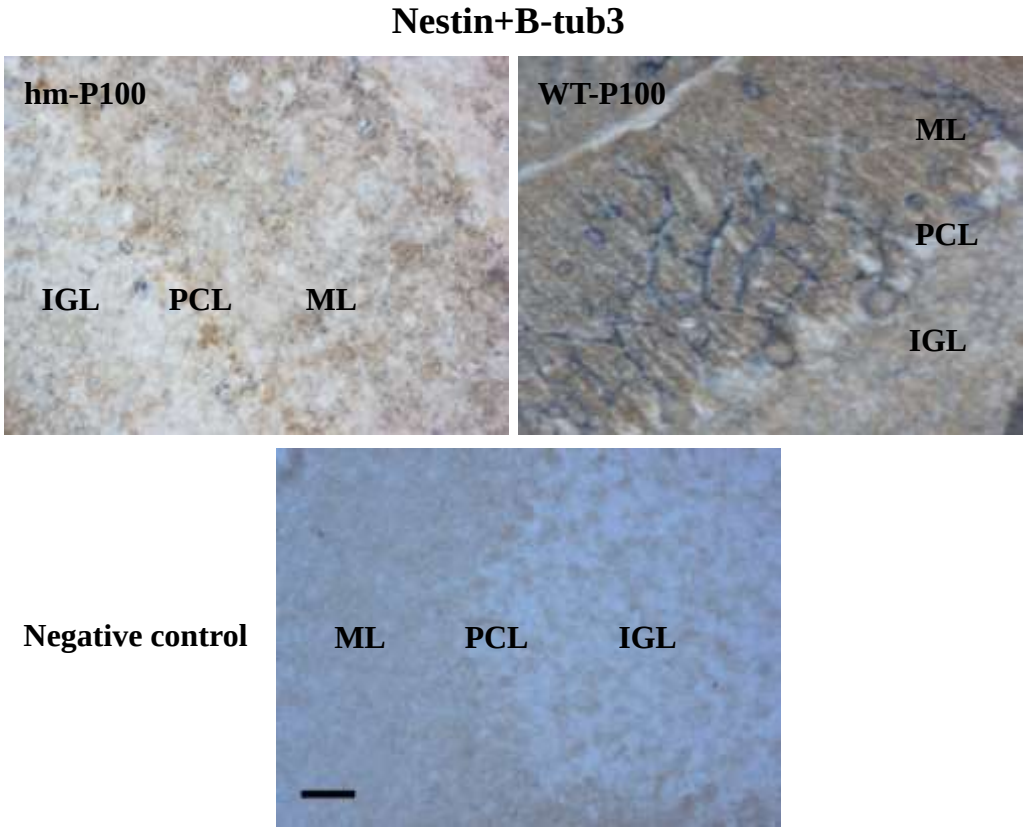

Figure 5.11 Double immunostaining images showing the expression of nestin (for BG cells) and B-tubulin 3 (for PCs) in sagittal sections of *pcd* mutant mice. No nestin expression (brown) was detected in the Bergmann glia of P100 homozygous (hm) mutant mice and their age matched WT control.

IGL, internal granular layer; ML, molecular layer; PCL, Purkinje cell layer; WM, white matter. Scale bar= 100 µm

5.8 NSCs derived from the *pcd*^{5J} ataxic cerebellum

To further analyse the changes occurring in the *pcd* CB, the isolation of NSCs from the CB of *pcd* mutant mice was attempted at P21, a time point where the disease phenotype was starting to be detected. Using an established protocol, a monolayer culture of NSCs was successfully isolated from the CB of homozygous *pcd* mice, alongside cultures from P21 wild type CB and LV tissue as controls. CB-NSCs derived from *pcd* and control mice were able to form neurospheres from the 1st passage (p.1) (Fig. 5.12), but the numbers of neurospheres in the mutant mice at the 2nd passage were significantly lower than both CB and LV wild type littermates (Fig.5.13A and B). However, after 2 passages, the number of neurospheres in the *pcd* culture increased markedly (Fig. 5.12, P4). The neurospheres were maintained in a culture medium supplemented with B27, N2, EGF and FGF-2, but they were unable to attach until passage 6 although they were enzymatically dissociated at each passaging (Fig. 5.12, p.6). They started to attach and grow as a monolayer culture at passage 6 (Fig. 5.12). Immunohistochemical analysis on undifferentiated monolayer culture of both *pcd* and WT cultures indicated the expression of nestin and Sox2 (Fig. 5.14), two established markers for NSCs (Lendahl et al., 1990; Brazel et al., 2005).

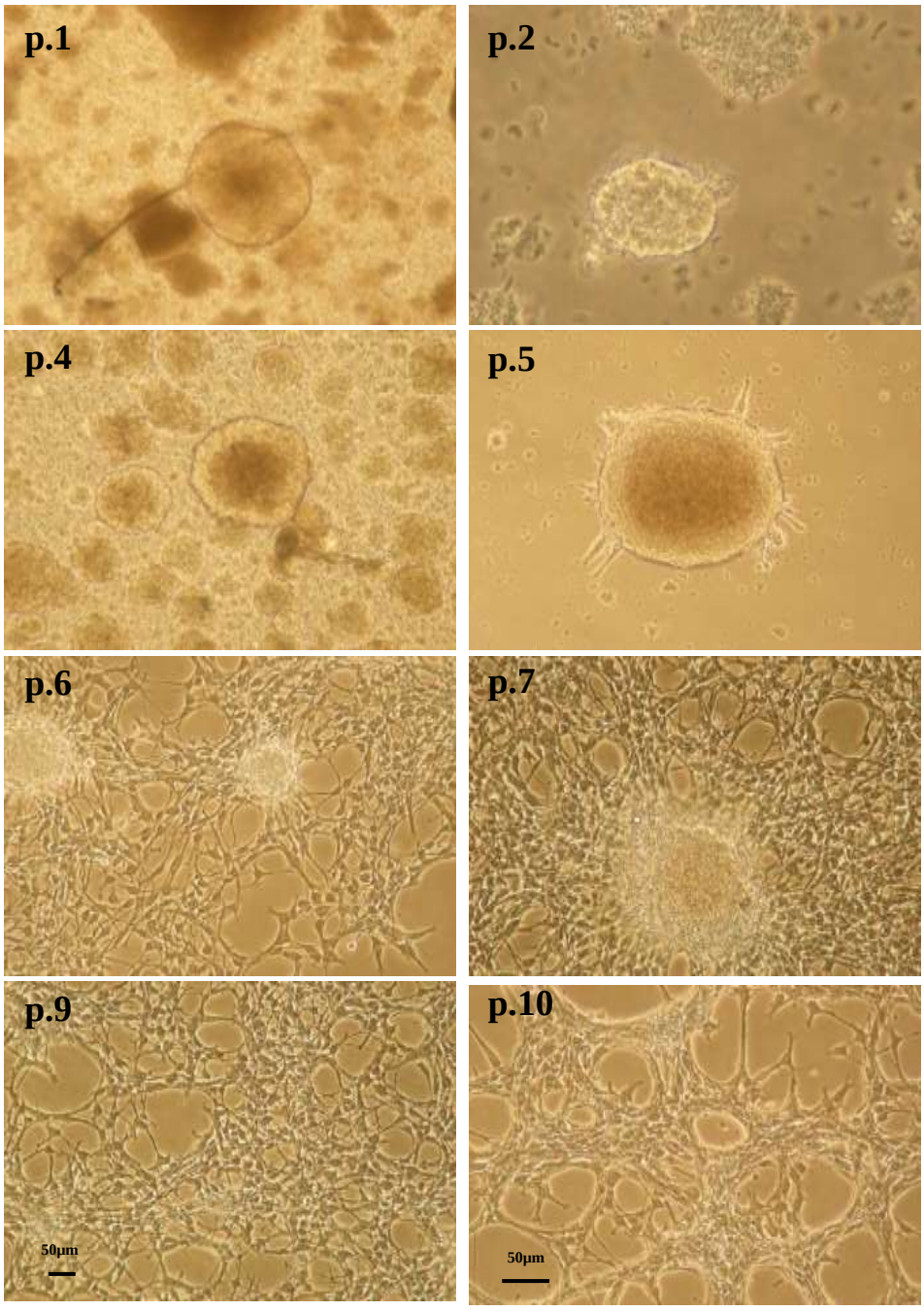

Figure 5.12 Brightfield image of *pcd*^{5J} mutant derived NSCs at different passages. Cells started to form neurospheres from passage 1 (p.1). At passage 5 (p.5), neurospheres seeded and cells started to extend processes from the neurospheres.The cells were grown as an adherent monolayer culture after passage 6.

Scale bar= 50µm

A

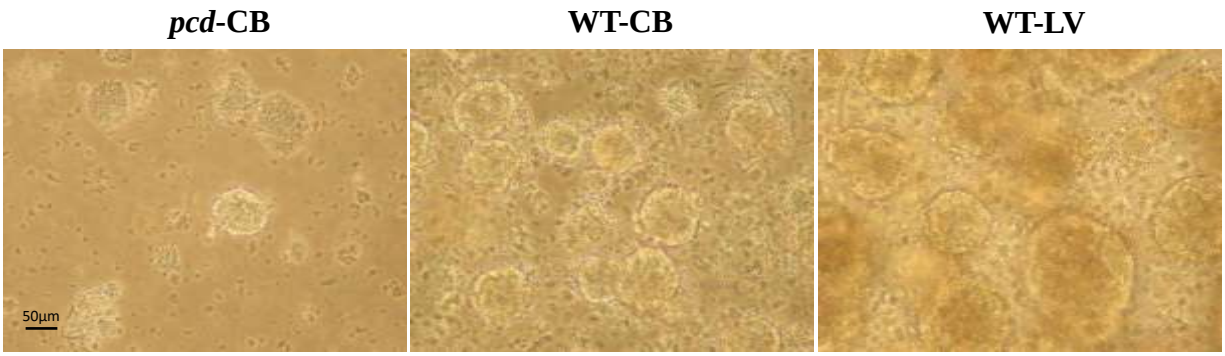

B

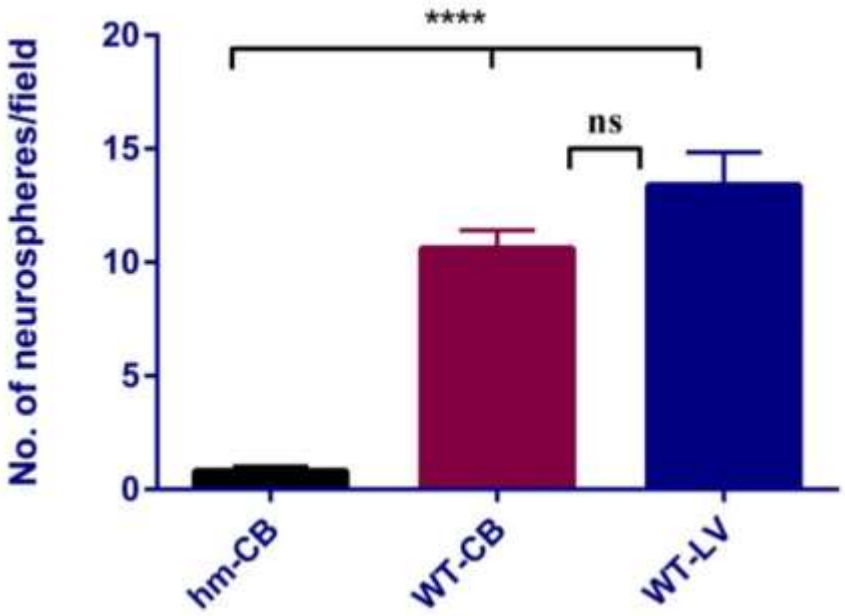

Figure 5.13 Generation of neurospheres in cultures isolated from homozygous *pcd* and wild type CB and LV. (A) Brightfield images showing neurospheres generated at passage 2 in the homozygous *pcd*^{5J} CB, and WT CB and LV controls. The *pcd* neurospheres were smaller and fewer in number compared to the control cultures (both CB and LV WTs). (B) The number of neurospheres in the pcd culture was significantly lower than for the WT animal. Results are presented as mean (n=5) ± SEM; P**** < 0.0001 calculated by ANOVA with Tukey's multiple comparisons test. Scale bar= 50µm

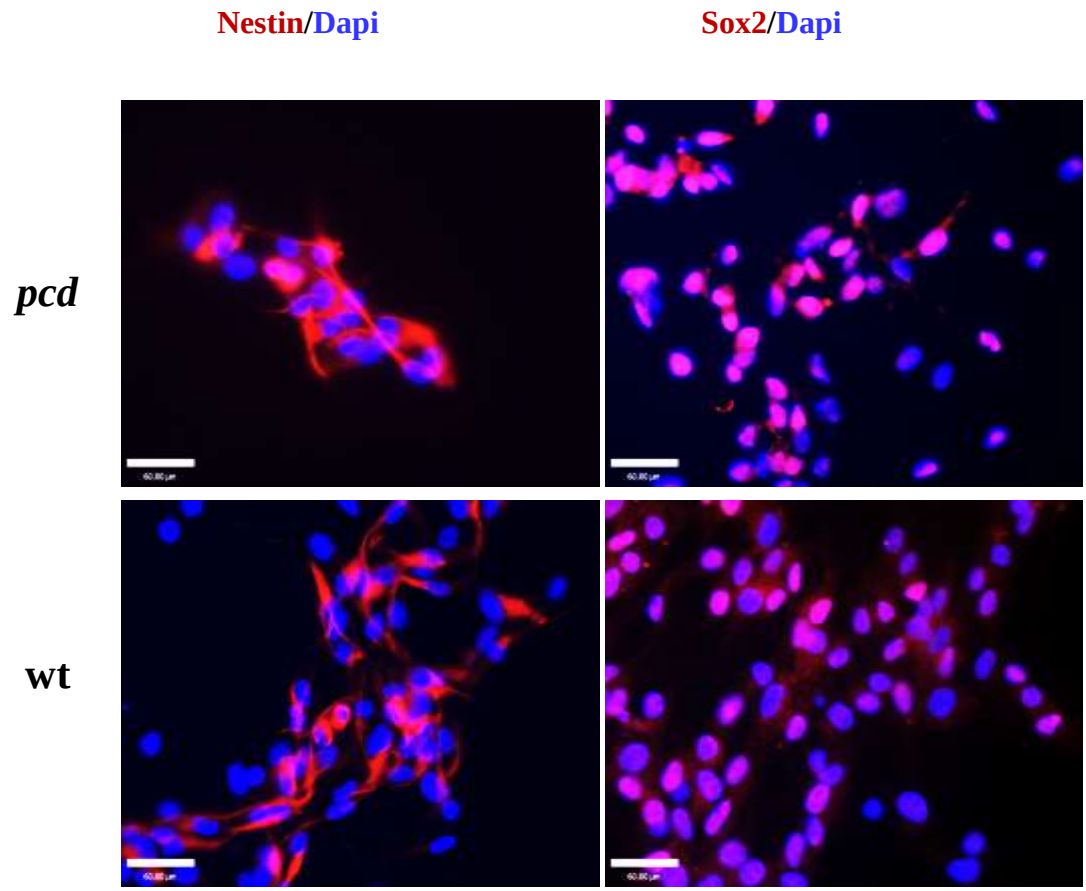

Figure 5.14 Fluroscent immunostaining showing Nestin and Sox2 expression in cerebellum-derived NSC cultures from *pcd* and wt mice at P21, with dapi counterstain (blue). Scale bar = 60µm.

5.8.1 Effect of growth factors withdrawal on the culture of pcd^{5J} derived CB-NSCs

To determine the growth factor responsiveness of pcd^{5J} CB-NSCs, *pcd* derived NSCs was analysed , were seeded in parallel at a known density and maintained in medium containing either EGF (20ng/ml), FGF-2 (20ng/ml), EGF+FGF-2 (20ng/ml), or no growth factors (negative control), followed by metabolic cell assay after 3 days in culture.

NSCs derived from *pcd* mutant and control mouse cerebellum showed significant difference in cell growth when maintained in different media conditions (EGF,

FGF-2, and EGF+FGF-2) (Fig. 5.15). Although cells were able to grow in all conditions except in the media without GFs, the highest metabolic response was observed in the medium supplemented with EGF and FGF-2 (Fig. 5.15A and B.). Both *pcd* and control CB-NSCs exhibited a similar response to these mitogens, suggesting that the onset of PCs loss at P21 didn't affect the surviving ability of these CB-derived cells.

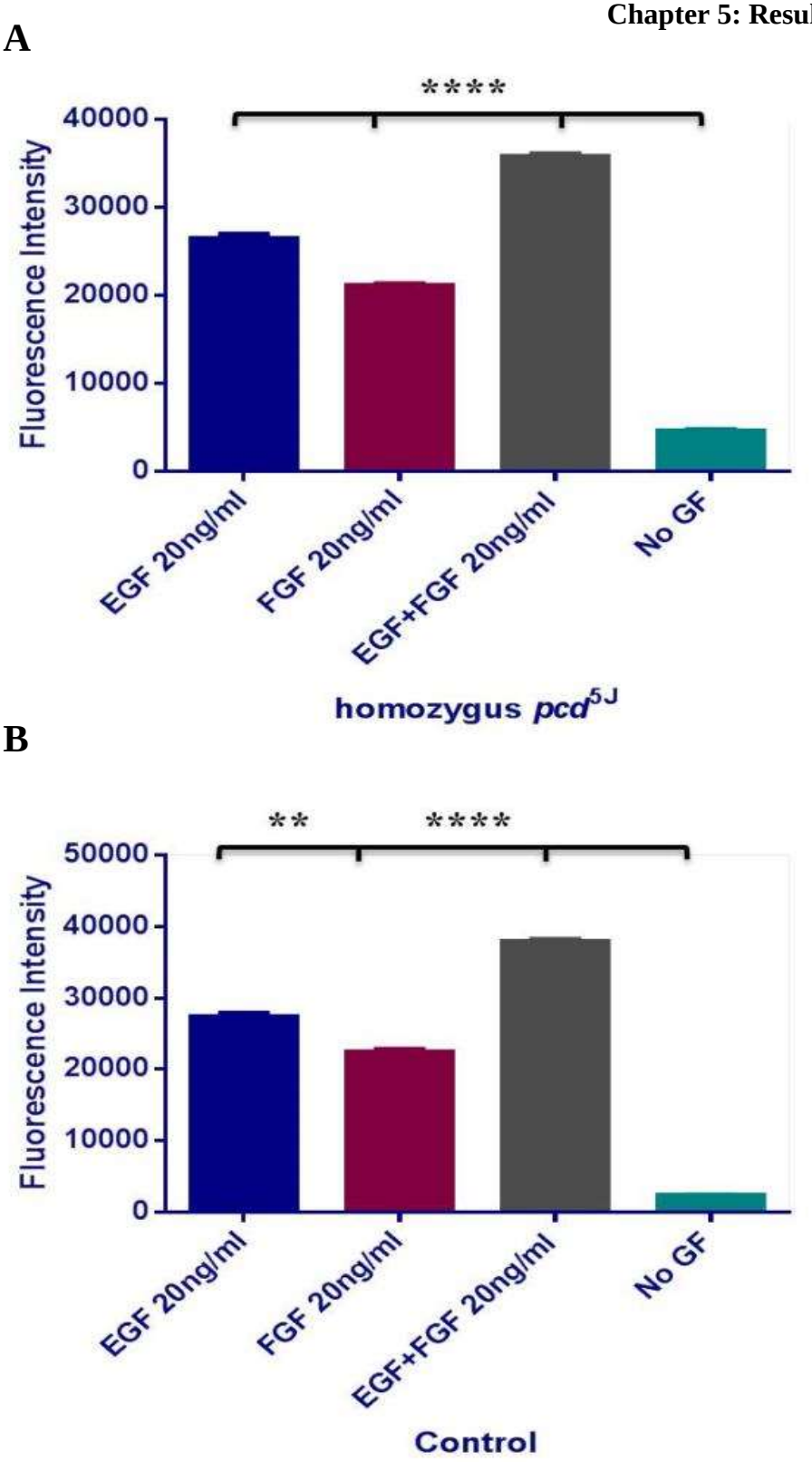

Figure 5.15 Effects of EGF and FGF-2 on NSCs derived from the cerebellum of *pcd*^{5J} mutant mice after 3 days in culture. Cell metabolic assay for both *pcd* (A) and wild type (B) cultures revealed that the maximum growth was achieved when both EGF and FGF-2 were combined. The metabolic cell activity was reported as mean ± SEM using one way ANOVA. Values were compared using tukey's multiple comparisons. ****P < 0.0001, **P< 0.0013. EGF= epidermal growth factor; FGF-2= fibroblast growth factor.

5.9 Discussion

5.9.1 Reactive Bergmann gliosis in *pcd*^{5J} mice

Mouse models of cerebellar neurodegenerative diseases of either spontaneous mutants or transgenic mice have been used to study cerebellar development, pathogenesis and cerebellar cell death mechanisms (Cendelin, 2014). PCD is an autosomal recessive mutation in mouse cerebellum that was first discovered by (Mullen et al., 1976). The mutation is caused by Nna1 gene, which leads to a noticeable phenotype by P20 resulting in gait ataxia, Purkinje cell degeneration, and retinal and Mitral cell loss (Cendelin, 2014). The degeneration of neurons such as Purkinje cells (PCs) releases many factors such as interleukins, prostaglandin E2 (PGE2), and tumour-necrosis factor-α (TNF α), that can activate astrocytes in a process called astrocyte gliosis, and as a result the immune system activates and triggers an inflammatory response (Reviewed in (Baltanas et al., 2013)). Here, we have studied the response of BG in the context of CB pathology, and investigated the response of Bergmann glia (BG) in response to PCs loss in *pcd*^{5J} mutant mice. A number of markers that specifically label BG in the cerebellar cortex such as Sox1, 2, and 9 were used for the quantification of Bergmann glial cells, while Calbindin was used for PCs quantification, and GFAP was used to detect reactive Bergmann gliosis.

Our data in *pcd*^{5J} mice illustrated that the degeneration of Purkinje cells (PCs) onset was observed at P21 and progressed rapidly as observed at P26 with no visible PCs by P100. The loss of PCs stimulated significant BG activation when compared to wt mice. We also reported that PCs loss triggered a number of morphological and pathological changes in the CB of *pcd*^{5J} mutant mouse.

Upregulation of GFAP and reactive gliosis was detected in the Bergmann glial cells at P21, and became more severe at P100. BG increased in number while PCs death proceeded. This was accompanied by drastic pathological changes observed at P100, such as shrinkage of the cerebellar cortex, complete loss of PCs, and disorganisation of Bergmann glial fibers in the molecular layer with increased GFAP expression. These observations strongly suggest that BG is affected in the Purkinje cell degeneration scenario in *pcd*^{5J} mice and the main glial cells in the cerebellar cortex that are activated following PCs degeneration.

The resultant Bergmann gliosis and proliferation caused by PCs loss was also observed in *pcd*^{1J} in which the proliferation rate of microglia was observed at P15 and became severe at P25 (Baltanas et al., 2013), suggesting that both *pcd* mutants exhibited the same phenotypes. Our results are in line with the fact that reactive gliosis is a reaction triggered by radial or astrocytes following brain injury (Buffo et al., 2008, Sofroniew and Vinters, 2010), and can be characterised by increased expression of intermediate filaments such as GFAP, as seen in our study (Robel et al., 2011). GFAP is widely used as a marker for mature astrocytes and BG (Eng et al., 2000, Koirala and Corfas, 2010), and GFAP upregulation following brain injury is a characteristic feature defining reactive gliosis (Sofroniew and Vinters, 2010, Baltanas et al., 2013). It is well known that glial cells provide support and protection for both healthy and diseased neurons (Gelpi et al., 2014). In the cerebellum, BG provide structural support for PCs via their radially oriented glial fibers in the ML, thereby maintaining the integrity of the CB (Sudarov and Joyner, 2007, Buffo and Rossi, 2013). This could explain that changing the interaction between BG and PCs as a result of PCs degeneration would contribute to the upregulation of GFAP and BG gliosis. Moreover, no

Nestin expression was detected in this study in the *pcd* mice at P100 or in the controls in contrast to the existing literature regarding re-expression of Nestin in the brain following injury (Sotelo et al., 1994). The fact that BG re-express the intermediate filament Nestin in the study by Sotelo et al., (1994) was to guide the embryonic PCs grafted into the CB of pcd mouse. This observation might explain the absence of Nestin in our study as BG did not seem to require Nestin because of PCs loss, suggesting that BG is only plastic in the presence of embryonic neurons (Sotelo et al., 1994, Sotelo et al., 2004).

The degree of gliosis depends on the severity and extent of the brain damage (Sofroniew and Vinters, 2010, Graeber and Streit, 2010). Reactive gliosis has been reported to be either beneficial or detrimental in different brain injury models (Wilhelmsson et al., 2004, Li et al., 2008). Baltanas et al (2013) showed that glial cells respond differentially to the same mutation that causes the death of PC and mitral cells of the olfactory bulb and they speculated that either beneficial or detrimental role of gliosis underlie these variations.

Our results in *pcd* mice demonstrated that the number of BG was comparable to the controls at P17, P21, and P26 but significantly increased by P100, the stage when no PCs were observed in the CB. Our findings are in opposition to a previous report that BG numbers were reduced in the spinocerebellar ataxia 1 (SCA1) human brains, an autosomal-dominant neurodegenerative disease of the CB (Shiwaku et al., 2013). In SCA1, mutant ataxin1 prevents the proliferation of BG and there is a loss of Bergmann glial function caused PCs degeneration, suggesting that reduced BG numbers might be detrimental in SCA1 (Shiwaku et al., 2013). The authors assumed that BG gliosis might be beneficial in case of SCA1, as mutation in ataxin-1 prevented BG proliferation and lead to ataxia

(Shiwaku et al., 2013). BG are thought to have similar functions to that of astrocytes in the mature cerebellum in maintaining neuronal survival (Grosche et al., 2002). Genomic analysis on reactive gliosis has shown that the phenotype of reactive astrocytes is greatly depending on the type of injury induced in stroke and neuroinflmmation (Zamanian et al., 2012). Changes in gene expression in reactive astrocytes induced by ischemic stroke appeared to have protective effect, whereas reactive gliosis induced by endotoxin LPS suggested to be detrimental (Zamanian et al., 2012). Thus, it may be that BG respond differentially to *pcd* and SCA1 and that increased numbers of BG in *pcd* mice indicate that Bergmann gliosis is a consequence of PCs loss, rather than BG loss of function contributing to PCs loss as seen in SCA1 (Shiwaku et al., 2013). The differential response of BG to PCS loss in pcd^{5J} and SCA1 may be because different genes are underpining both disorders. These data indicate that different scenarios may underlie BG response in different neurodegenerative and further investigations are needed to determine whether Bergmann gliosis is beneficial or detrimental in pcd^{5J} mice.

Evidence from the literature has shown that radial glial cells in the adult mouse cortex represent multipotent progenitors and can change from quiescent state into reactive gliosis in injured brain (Doetsch et al., 1999; Malatesta et al., 2000; buffo et al., 2008). These activated glial cells start to proliferate and form multipotent neurospheres and show self-renewing capacity in vitro (Buffo et al., 2008). Furthermore, an early study by Sotelo et al., (1994) has shown that embryonic PCs grafted into adult *pcd* mice replace the lost PCs and can integrate into the defective CB. The re-expression of Nestin in the recipient BG cells helps the migration of these grafted PCs in the host CB. Moreover, studies have also shown

that mature astrocytes can act as neural stem cells after brain injury, suggesting that they may contribute to the neuronal regeneration (Buffo et al., 2008, Doetsch et al., 1999). These findings, together with our observations support the hypothesis that BG cells are quiescent radial glial cells at the steady state in the mature cerebellum, and can be activated following CB injury resulting in Bergmann gliosis. At early postnatal ages, BG reach maximum proliferation between P6-P9 but ceases at P21 (Shiga et al., 1983, Oomman et al., 2005), although some Sox^+ BG are dividing in the CB of adult rabbit (Ponti et al., 2008). In light of this finding with our current observation that no Ki67 at P26 and Nestin at P26 and P100 were detected in BG in either *pcd* or wt mice, suggesting that BG at least in the adult mice are not proliferating even after PCs degenerations. The possible expansion for the difference in neurogenic potential would appear to be related to the difference in the growth, maturation, and differentiation between rodents and rabbit (Gould, 2007, Gage, 2000). Thus, the protracted ability of BG for proliferation in the rabbit appears to be restricted in rodents due to the unpermissive environment (Ponti et al., 2008, Komuro et al., 2001).

5.9.2 NSCs derived from the cerebellum of *pcd*^{5J} mutant mice

To isolate NSCs from *pcd* mice, P21 was selected as it is the time point by which PCs start to degenerate as studies have reported that injury induce the activation of endogenous stem cells (Ahmed et al., 2012). At P21 which is the time of weaning, the homozygous *pcd* mice display gait ataxia. In this study, P21 was the time point in which PCs loss was started as revealed by Calbindin immunostaining. To assess the role of P21 the stem cell activity in *pcd*^{5J} mice, we tested whether NSCs could be isolated from P21CB of homozygous *pcd* and wild

type mice, and whether they displayed similar characteristics to those isolated from wt cerebellum and the lateral ventricle with regard to expansion, growth factor requirements.

In standard culture condition, we were able to isolate NSCs from the CB and LV of mutant and wild type mice at P21. The adherent monolayer culture generated from *pcd* mice exhibited morphological characteristics similar to those isolated from P21 wild type CB and LV, used as controls in this study. Although the cells showed the ability to form neurospheres but the numbers of neurospheres at passage 2 were significantly lower in *pcd* mice compared to their control CB and LV, and by passage 4 numbers had increased to reach the level seen in the control culture. The reason for the subsequent increase seems to be unclear, but one possible explanation is that FGF receptor is expressed robustly in the astrocytes the hippocampus, olfactory bulb, and cerebellum (Chadashvili and Peterson, 2006) and that these after reaching a sufficient density, FGF-2 responsive cells can proliferate and generate more neurospheres which might allowed them to catch up with the LV control culture. There is published evidence that FGF-2 and FGFR are upregulated in reactive astrocytes following brain injury (Reviewed in (Iseki et al., 2002)) resulting in increasing in GFAP expression, which would support our earlier observation of Bergmann gliosis and GFAP upregulation after PC loss. Moreover, these isolated CB derived NSCs were found to express Nestin and Sox2 in culture, two markers commonly used for NSCs, supporting their NSC potential (Lendahl et al., 1990, Reynolds and Weiss, 1992, Brazel et al., 2005). Quantitative assessments carried out in this study showed that *pcd* derived CB-NSCs could be expanded in the presence of EGF or FGF-2, and exhibited maximum proliferative capacity when both factors were present as previously

reported for NSCs from other brain regions (Reynolds et al., 1992, Gritti et al., 1996, Gage, 2000). This provides the first evidence for the persistence of a population with NSC characteristics in the mature cerebellum of *pcd*^{5J} mice. Future studies are required to test the multipotent ability of these cells to generate neuronal and glial lineages, and compare them to wt to determine if the onset of pcd may be linked to changes in differentiation potential. This study provided evidence for the involvement of Bergmann glia in the pathology of Purkinje degeneration. Understanding the neuron-glial relationship in *pcd* disease is an important target for future therapeutic applications and for further understating the mechanisms underlying neuronal damage in other cerebellar ataxias.

It would be interesting to investigate the proliferative rate of BG cells in *pcd* mice at the time points examined in this study by BrdU administration as Ki67 analysis did not show any proliferation in the CB of *pcd* mice. Microarray analysis is also important to check for changes in gene expression involved in glial cells activation in *pcd* mice vs wild type at different time course of PCs degeneration which might disclose the role of these activated glial cells.

5.10 Conclusions

Our results presented here showed that the severe and progressive PCs degeneration in *pcd*^{5J} mice at different time points as revealed by Calbindin immunostaining was also accompanied by Bergmann gliosis detected through the upregulation of GFAP marker (Sofroniew and Vinters, 2010). As PCs loss proceeded, BG exhibited thick disorganised fibers revealed by GFAP expression, while no changes were seen in their control littermates. However, our data couldn't provide the exact time point at which the number of BG increased significantly in the *pcd* mice, which may be determined by a more comprehensive time-point analysis between P20 and P100. Future investigation is necessary to determine the consequences of Bergmann gliosis, and whether this cellular response may be beneficial or detrimental to CB function in *pcd*^{5J} mutant mice. Moreover, further studies using techniques such as real time PCR are also required to determine whether its nna1 gene deficiency or other reasons like PCs loss that trigger changes in BG and cause reactive gliosis. For the first time, this study presented evidence for the existence of NSCs in the CB of these mutant mice at P21. Studies investigating the differentiation potential of these *pcd* derived NSCs toward PCs generation will provide evidences for future clinical implications of neurodegenerative diseases affecting the CB.

6 Exploring the existence of neural stem cells in the third ventricle of adult GFP+/- Sox1 mouse

6.1 Introduction

Radial glial cells are a heterogeneous population of cells with long cell processes and having diverse functional roles across different brain regions. However, they are not heterogeneous in terms of their potential capacity to generate neurons and glial cells in the brain. Radial glial cells have been the subject of intense interest as neural stem/progenitor cells in some regions of adult brain such as SVZ and SGZ (Anthony et al., 2004, Malatesta et al., 2008). Tanycytes are special radial glial cells lining the 3V wall that recently shown to be neurogenic and gliogenic (Lee et al., 2012, hann et al., 2013, Robins et al., 2013). Thus, in this chapter I performed similar study conducted in chapter 3 on 3V tanycytes to determine their NSCs gene expression profile compared to Bergmann glia and NSCs in well-known neurogenic regions of adult brain.

Anatomically, tanycytes can be divided into 4 subtypes (for extensive detail see chapter 1 section 1.8), each with its own unique properties (Rodriguez et al., 2005). α1 tanycytes are located near the dorsomedial and ventromedial nuclei of the hypothalamus (see chapter 1 Fig. 1.9 for info.); α2 tanycytes are found near the arcuate nucleus (Rodriguez et al., 2005, Bolborea and Dale, 2013). β1 tanycytes line the area between the arcuate nucleus and the median eminence, and β2 tanycytes line the infundibulum and the median eminence (Rodriguez et al., 2005).

Adult neurogenesis has traditionally been described in two regions in the brain, the lateral ventricle (LV) and the hippocampus (Alvarez-Buylla and Garcia-Verdugo, 2002, Doetsch, 2003). More recently, the hypothalamus has emerged as a new site supporting neurogenesis, showing new neurons and astrocytes generation in rodents (Xu et al., 2005, Kokoeva et al., 2005, Migaud et al., 2010, Lee et al., 2012). Located on both sides of the 3V, the hypothalamus is involved in the regulation of neuroendocrine functions such as temperature regulation, sexual activity, water balance, and feeding behaviour (Yuan and Arias-Carrion, 2011). The 3V, part of the cerebrospinal fluid (CSF) filled ventricular system, where low proliferative activity was reported (Yuan and Arias-Carrion, 2011). In 2004, Markakis et al., have reported that cells isolated from the 3V of 7 weeks old rats can give rise to $Tuj1^+$ hypothalamic neurons in vitro. One year later, Xu et al (2005) were able to isolate neural progenitor cells from 8 weeks rat ependymal layer of the 3V using floating neurosphere assay and various labelling techniques such as Dil, GFP, and BrdU to show the presence of cells with mitotic activity in this brain region. However, there is no clear evidence for the identity of the neural stem cell population existing in the hypothalamus. Several studies recently identified different candidate cell populations in the hypothalamus that could be potential adult stem/progenitor candidate cells such as tanycytes of the 3V, subventricular astrocytes, ependymocytes and parenchymal glial cells (Reviewed in (Robins et al., 2013)). Moreover, another study have shown that cells located in the ventral zone corresponding to β2 tanycytes in the median eminence have higher proliferative activity than the mid-ventral zone corresponding to α1 tanycytes unless stimulated by IGF-I (Perez-Martin et al., 2010, Lee et al., 2012).

Two types of cells are lining the ependymal layer of the 3V, ciliated cuboidal ependymocytes with very short processes located in the dorsal zone, and non-ciliated tanycytes in the ventral zone with long processes penetrating the hypothalamic parenchyma (Flament-Durand and Brion, 1985, Xu et al., 2005, Bolborea and Dale, 2013). Tanycytes are involved in glucose metabolism, and express genes involved in food and energy balance (Reviewed in (Bolborea and Dale, 2013)).

Strong evidence has emerged suggesting that radial glia functions as neural progenitors in the neurogenic areas of the brain (Malatesta et al., 2000, Alvarez-Buylla et al., 2001, Anthony et al., 2004). NSCs in the adult lateral ventricle are of radial glial origin (Merkle et al., 2004). During brain development, all radial glia are transformed into astrocytes except for BG in the cerebellar cortex, Muller cells in the retina, and tanycytes in the 3V (Reviewed in (Rodriguez et al., 2005, Rodriguez et al., 2010)). However, only retinal Muller cells have been shown to be neurogenic upon induction (Fischer and Reh, 2001). Tanycytes have cell bodies lining the 3V, with long basal processes penetrating the stroma of the hypothalamus (Rodriguez et al., 2005). This morphology, closely resembling that of astrocytes and radial glia including BG, made some authors regard tanycytes as radial glia that persist throughout the adult life span in the hypothalamus (Bruni, 1998, Chauvet et al., 1996).

Tanycytes share properties with both astrocytes and radial glia as they have small cell bodies lining the ventricle and possess long processes that penetrate the surrounding hypothalamic parenchyma (Rodriguez et al., 2010). Tanacytes also differ from radial glia in that their neurogenic activity does not disappear in the adult brain (Rodriguez et al., 2005). Two studies have demonstrated that β2-

tanycytes residing the median eminence are neurogenic and can contribute to new neurons generation that are diet-responsive (Lee et al., 2012, Haan et al., 2013). In contrast, another study by Robins et al., (2013) has revealed that α-tanycytes rather than β2-tanycytes can proliferate in response to FGF, implicating them as one of the component of the hypothalamic stem cell niche. It has been shown that the isolation of stem cell from the spinal cord, fourth and third ventricle requires the presence of both EGF and bFGF (Weiss et al., 1996), as had been described for neural stem cells from the lateral ventricle (Gritti et al., 1999).

In the main neurogenic regions of the adult brain, the lateral ventricle and the hippocampus, stem cell populations have been identified using the expression of NSC markers such as Sox1, Sox2 and Nestin. Sox1 has shown to mark NSCs more specifically than Nestin as all $Sox1^+$ NSCs isolated from E10.5 rat neural tube were $Nestin^+$ whereas most $Nestin^+$ progenitors were not all $Sox1^+$ (Cai et al., 2004). Having previously shown that neural stem/progenitor cells exist in the 3V (Robins et al., 2013), and because of the close morphological similarity between tanycytes and BG as two radial glial cells in the adult brain, we hypothesized that NSCs markers previously being identified in other neurogenic regions of adult brain including cerebellum in this thesis (Chapter 3) may also be expressed in the hypothalamic 3V. Thus, I aimed in this chapter to:

1. Investigate whether a $Sox1^+$ population identified in the adult CB could also be detected in the hypothalamic 3V.
2. Determine the location of the $Sox1^+$ population lining the 3V wall and examine whether Sox1 is overlap with Sox2 and Sox9.

3. Determine whether the 3V could yield a culture of NSC-like cells in vitro similar to CB and whether this population is multipotent and can generate neurons, astrocytes, and oligodendrocytes.

6.2 Results

Marker analysis was carried out to investigate the presence and distribution of NSCs in the lining of the 3V. Tissues were collected from wild type and heterozygous Sox1-GFP +/- adult mice, which carry a GFP reporter inserted into Sox1 locus, Serial coronal sections (10 μm) of the forebrain were taken and processed for immunohistochemistry.

6.3 Neural stem cell marker expression in the 3V

6.3.1 SoxB analysis

Using Sox1-GFP+/- mice, we were able to further investigate Sox1 expression in the 3V and hypothalamus through expression of the GFP reporter.

Strong GFP signal was detected in the lining of the 3V from the dorsal axis, where ependymocytes are found, to the most ventral part in the median eminence where β tanycytes are present (Fig. 6.1 A-D). At the level of median eminence, dense GFP expression was detected in β2 tanycytes and their processes (Fig. 6.1D). Although positive cells for GFP were also observed in the surrounding hypothalamus (Fig. 6.1E), the number of these GFP^+ cells was much lower than that observed for Sox1 and not biased towards certain nuclei. Immunohistochemical analysis for Sox1 protein in the 3V indicated that Sox1 was expressed along the 3V lining (Fig 6.2). The expression of Sox1 was demonstrated in ependymocytes and α1 tanycytes populations in the dorsal part of the 3V (Fig. 6.2B). Toward the ventral region of the 3V, intense signal for Sox1 was found in α2 tanycytes (Fig. 6.2C), and also at the level of the median eminence in both β1 and β2 tanycytes (Fig. 6.2D). Similar to Sox1, Sox2

immunoreactivity was also demonstrated along the length of the 3V wall (Fig. 6.3). The expression of Sox2 was observed in ependymocytes (Fig. 6.3A, B) and all tanycytes population in a pattern very similar to Sox1 (Fig. 6.3C and D). Furthermore, a population of Sox1 and Sox2 positive cells were also detected in the hypothalamus (Fig. 6.2E, 6.3E respectively) and in the dentate gyrus of the hippocampus used as control (Fig.6.2F, 6.3 F respectively). These results showed that both Sox1 and Sox2 were expressed in the cells lining the hypothalamic ventricle, suggesting that tanycytes might exhibit NSCs features in the adult 3V.

Following the detection of Sox1 and Sox2 in the lining of the 3V, analysis of the expression of Sox9 was also carried out in the hypothalamic ventricle. Similar to Sox1 and Sox2, Sox9 showed strong immunoreactivity in the 3V (Fig. 6.4A). Intense Sox9 staining was seen in both ependymocytes and α1 tanycytes (Fig. 6.4B), and more ventrally in α2 tanycytes (Fig. 6.4C), in a pattern matching that observed for Sox1 and Sox2 in these regions. At the level of the median eminence, Sox9 also labelled the population of β1 and β2 tanycytes (Fig. 6.4D) similar to the staining pattern obtained for Sox1 and Sox2. Immunoreactivity for Sox9 was also demonstrated in the hypothalamus, where positive cells were not confined to a certain nucleus but appeared scattered throughout the hypothalamic nuclei (Fig. 6.4E).

Taking together, these results for Sox1, Sox2 and Sox9 analysis in the 3V confirmed that these markers were specifically detected across all tanycyte subsets. Moreover, robust numbers of Sox 1, 2, and 9 positive cells were also detected in the hypothalamic parenchyma surrounding the 3V (Fig. 6.2E, 6.3E, and 6.4E respectively).

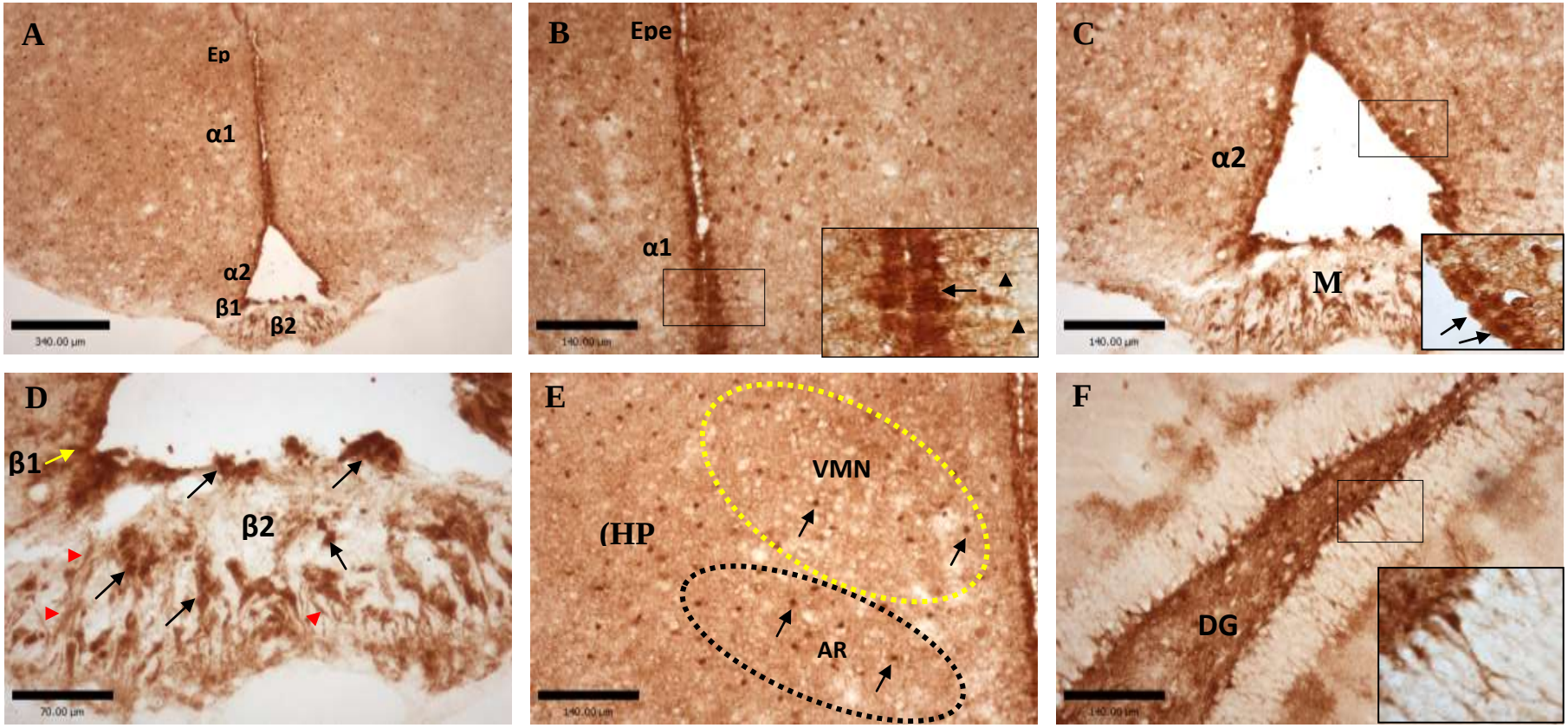

Figure 6.1 GFP expression in coronal sections of adult Sox1-GFP+/− mouse third Ventricle (3V), hypothalamus, and hippocampal dentate gyrus. (A) Overview image showing types of cells lining the 3V and the hypothalamus (HP). (B) GFP signal marks Sox1 positive cells in the ventral part of the 3V. Black arrows in the magnified boxed area point to α1tanycytes cell bodies and their processes (arrow heads). (C) GFP labeling in the dorsal part of the 3V showing high expression of GFP in α2 tanycytes (black arrows in the magnified boxed area). (D) Magnified image showing GFP detection in the 3V at the level of median eminence (ME), black arrows indicate GFP positive β2 tanycytes, yellow arrows indicate GFP positive β1 tanycytes. The expression of GFP is also seen in the processes of β tanycytes (red arrows head). (E) GFP labelling cells throughout the hypothalamic parenchyma (HP). (F) Positive control for GFP expression in the hippocampal dentate gyrus (DG). Scale bar =140 µm (in B,C,E,F), 340 µm (A), and 70 µm (D). **ME,** Median Eminence**; HP,** Hypothalamus**; Epe,** Ependymocytes**; VMN,** ventromedial nucleus**; ARC,** arcuate nucleus**; DG,** dentate gyrus**.**

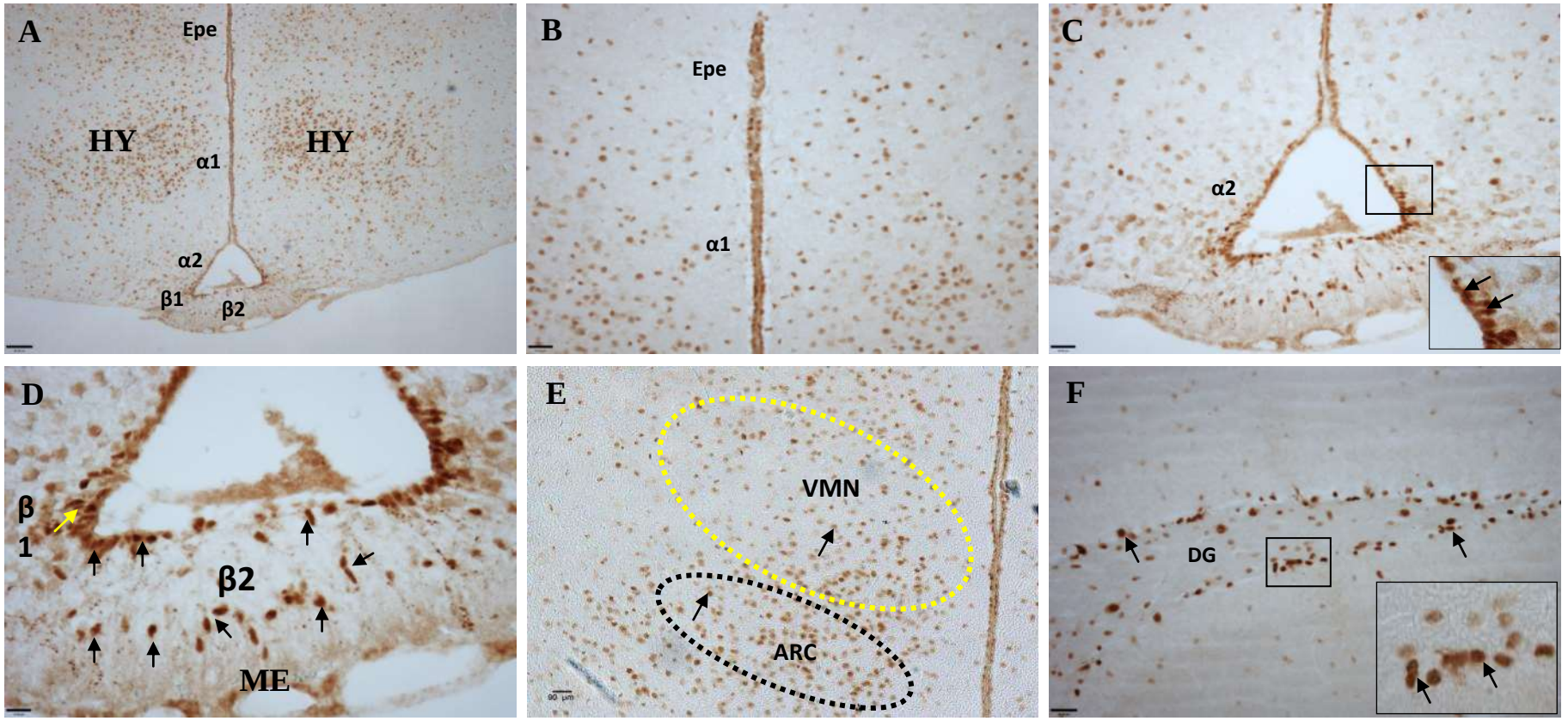

Figure 6.2 Sox1 expression in coronal sections of adult mouse third Ventricle (3V), hypothalamus, and hippocampal dentate gyrus. (A) Overview image showing types of cells lining the 3V and the hypothalamus (HP). (B) Signal for Sox1 is observed in the ventral part of the 3V, ependymocytes (Epe) and α1 tanycytes. (C) Dorsal part of the 3V showing strong expression of Sox1 in α2 tanycytes (black arrows in the magnified boxed area). (D) Magnified images of the 3V showing Sox1 detection in median eminence (ME), black arrows indicate positive β2 tanycytes, yellow arrows indicate β1 tanycytes. (E) Sox1 expression cells are distributed in the hypothalamus with highest level of expression shown in ventromedial nuclei (VMN) and few cells are found in the arcuate nucleus (ARC). (F) Positive control for Sox1 expression in the hippocampal dentate gyrus (DG). Scale bar ₌34 μm in (B, C, F); 90 μm in (A, E), 17 μm in (D).

ME, Median Eminence; **HP**, Hypothalamus; **Epe**, Ependymocytes; **VMN**, ventromedial nucleus; **ARC**, arcuate nucleus; **DG**, dentate gyrus.

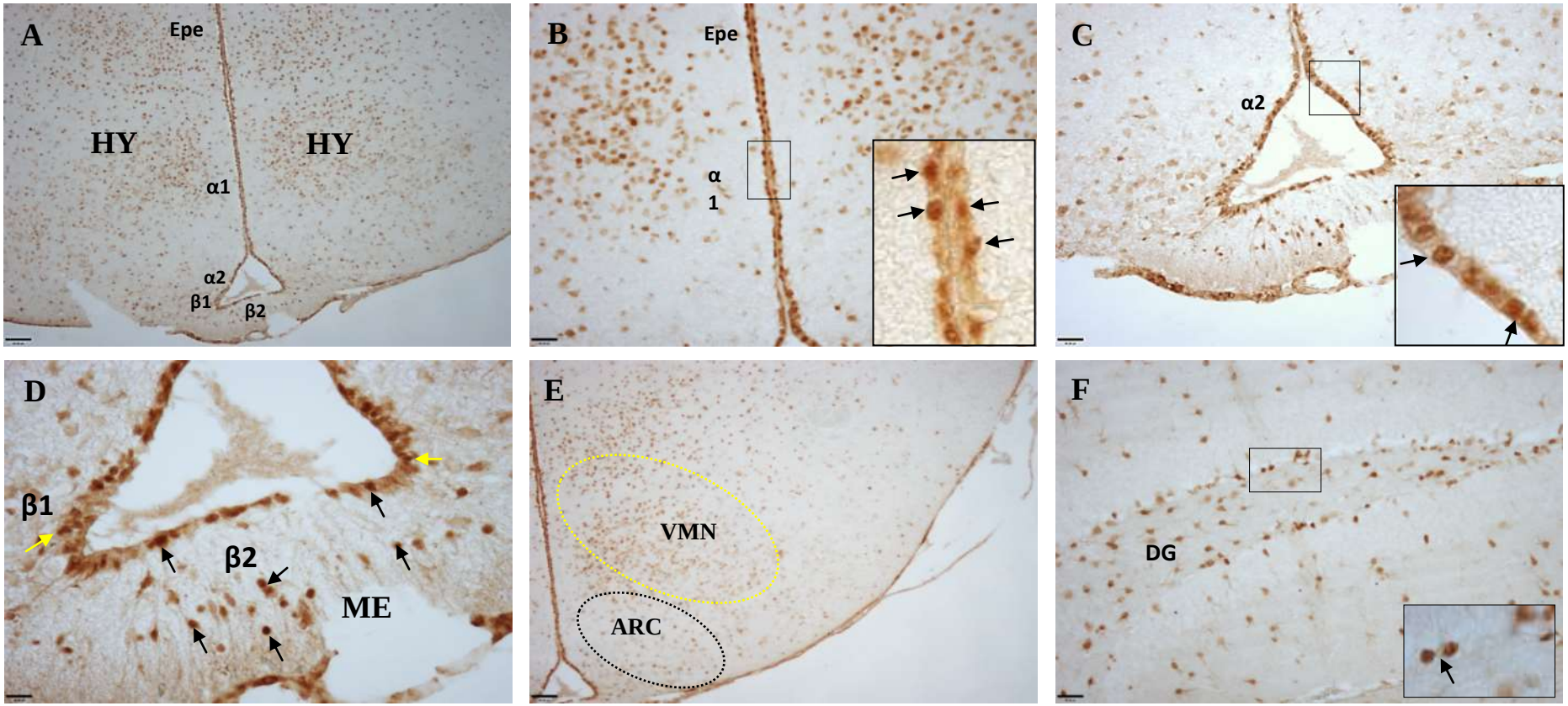

Figure 6.3 Sox2 expression in coronal sections of adult mouse third Ventricle (3V), hypothalamus, and hippocampal dentate gyrus. (A) Overview image showing types of cells lining the 3V and the hypothalamus (HY). (B) Sox2 expression strongly resembles that of Sox1 in the lining of the 3V. α1 tanycytes show strong immunoreactivity for Sox2 (black arrows in the high-power boxed area). (C) Sox2 marks α2 tanycytes nuclei (black arrows in the magnified boxed area). (D) Magnified images of the 3V showing Sox2 immunolabelling in the median eminence (ME), black arrows indicate positive β2 tanycytes, yellow arrows indicate Sox2 positive β1 tanycytes. (E) The hypothalamus nuclei also show intense staining for Sox2 with highest level of expression shown in ventromedial nuclei (VMN) and few cells are found in the arcuate nucleus (ARC). (F) Positive control for Sox2 expression in the hippocampal dentate gyrus (DG). Scale bar = 90 μm in (A, F); 34 μm in (B, C, G); 17 μm in (D). **ME**, Median Eminence; **HP**, Hypothalamus; **Epe**, Ependymocytes; **VMN**, ventromedial nucleus; **ARC**, arcuate nucleus; **DG**, dentate gyrus.

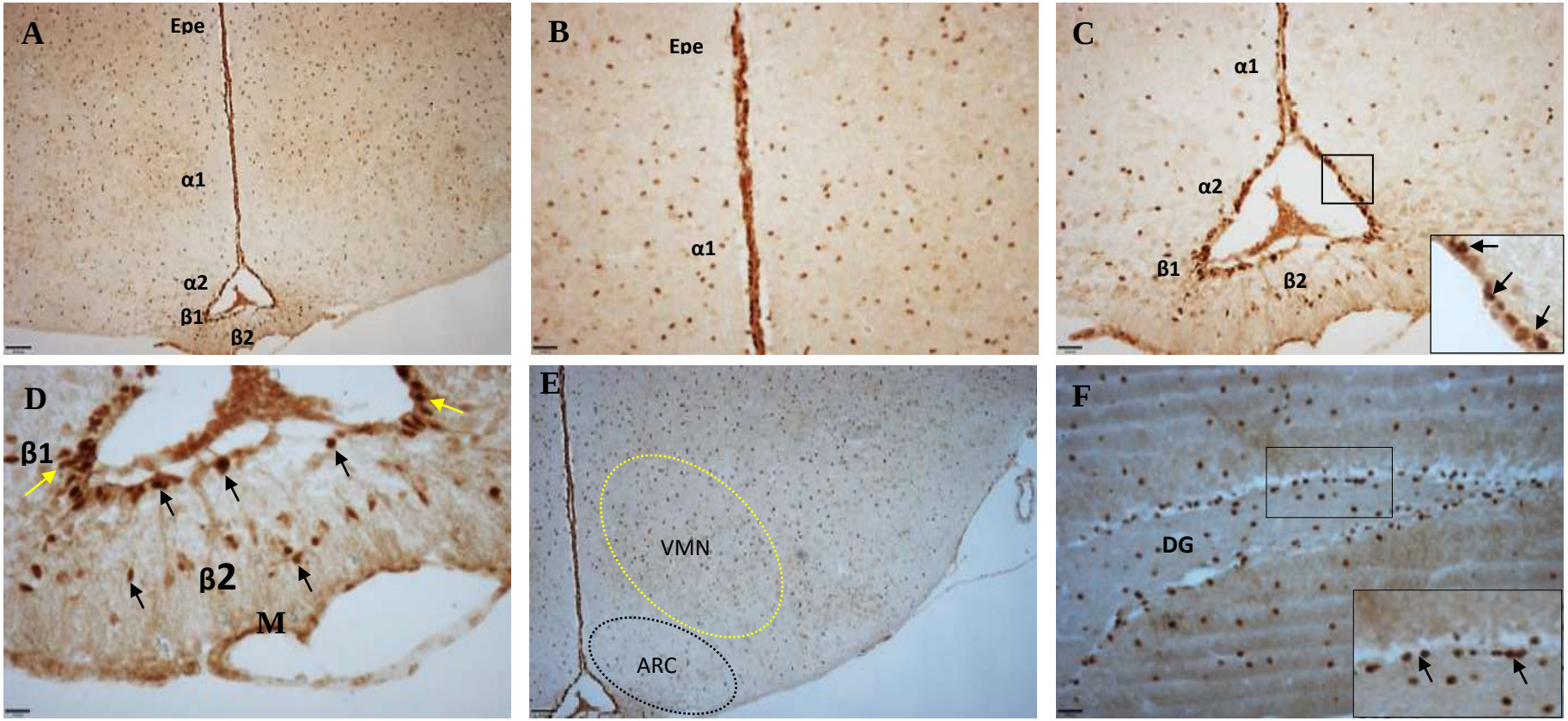

Figure 6.4 Sox9 expression in coronal sections of adult mouse third Ventricle (3V), hypothalamus, and hippocampal dentate gyrus. (A) Overview image showing types of cells lining the 3V and the hypothalamus (HP). (B) Signal for Sox9 is observed in the ventral part of the 3V, ependymocytes (Epe) and α1tanycytes. The staining pattern is similar to that of Sox1 and Sox2. (C) Dorsal part of the 3V showing strong expression of Sox9 in α2 tanycyte nuclei (black arrows in the magnified boxed area). (D) Magnified images of the 3V showing Sox9 detection in median eminence (ME), black arrows indicate positive β2 tanycytes, yellow arrows indicate β1 tanycytes. (E) Unlike Sox1 and Sox2, Sox9 expression in the hypothalamus is shown to be scattered evenly both in ventromedial nuclei (VMN) and in the arcuate nucleus (ARC). (F) Positive control for Sox9 expression in the hippocampal dentate gyrus (DG). Scale bar = 90 µm in (A, F); 34 µm in (B, C, G); 17 µm in (D).

ME, Median Eminence; **HP**, Hypothalamus; **Epe**, Ependymocytes; **VMN**, ventromedial nucleus; ARC, arcuate nucleus; DG, dentate gyrus.

6.3.2 Co-localization of Sox1 with Sox2 and Sox9 in the 3V

Based on the results gathered for single marker analysis in the 3V wall indicating strong immunoreactivity in the tanycytes for Sox1, Sox2, and Sox9, we investigated whether Sox1 expression (as reported by GFP) showed overlap with Sox2 and Sox9, in order to explore the co-expression of these transcription factors in the cells lining the 3V. Serial coronal sections analysed by double immunostaining against GFP and Sox2 or Sox9 markers showed clear co-localization of GFP with Sox2 and Sox9 (Fig. 6.5 and 6.6 respectively). Next, I tried to co-localise GFP in the fluorescent channel with Sox1, 2, and 9 using visible DAB substrate reaction. I observed that immunoreactivity for Sox1, 2, and 9 was detectable in the brightfield channel but no signal was observed for GFP in the 3V. This was in contradiction with the earlier single immuno-analysis for GFP carried out using DAB reaction when strong staining for GFP was observed in both ependymocytes and tanycytes (see Fig. 6.1 for details). This might be due to the fact that some of the fluorescent GFP signal could be masked by the precipitate generated by the DAB substrate reaction (brown) used in our protocol for both Sox2 and Sox9 detection in the visible range. To resolve this problem, the experiment was repeated with single GFP images being taken before initiating the final DAB reaction step for either Sox2 or Sox9 staining. In this case, the signal for GFP was strong in the ventral most portion of the 3V, starting from the region harbouring dorsal α1 and ventral α2 tanycytes toward the median eminence where β tanycytes are found (Fig. 6.5B, 6.6B respectively). At the level of the median eminence, β1 and β2 tanycytes were seen to coexpress GFP with Sox2 and Sox9 (Fig. 6.5B, 6.6B respectively). In all tanycyte populations, Sox2 and Sox9 showed intense staining in the nucleus, whereas GFP signal was detected in

the cytoplasm and long tanycytic processes, with more intense signal in the cells located in the ME region (Fig. 6.5B, 6.5C, 6.6B, 6.6C respectively). Our result suggests that in the adult mouse brain, Sox1/2/9 genes are co-expressed in cells lining the 3V.

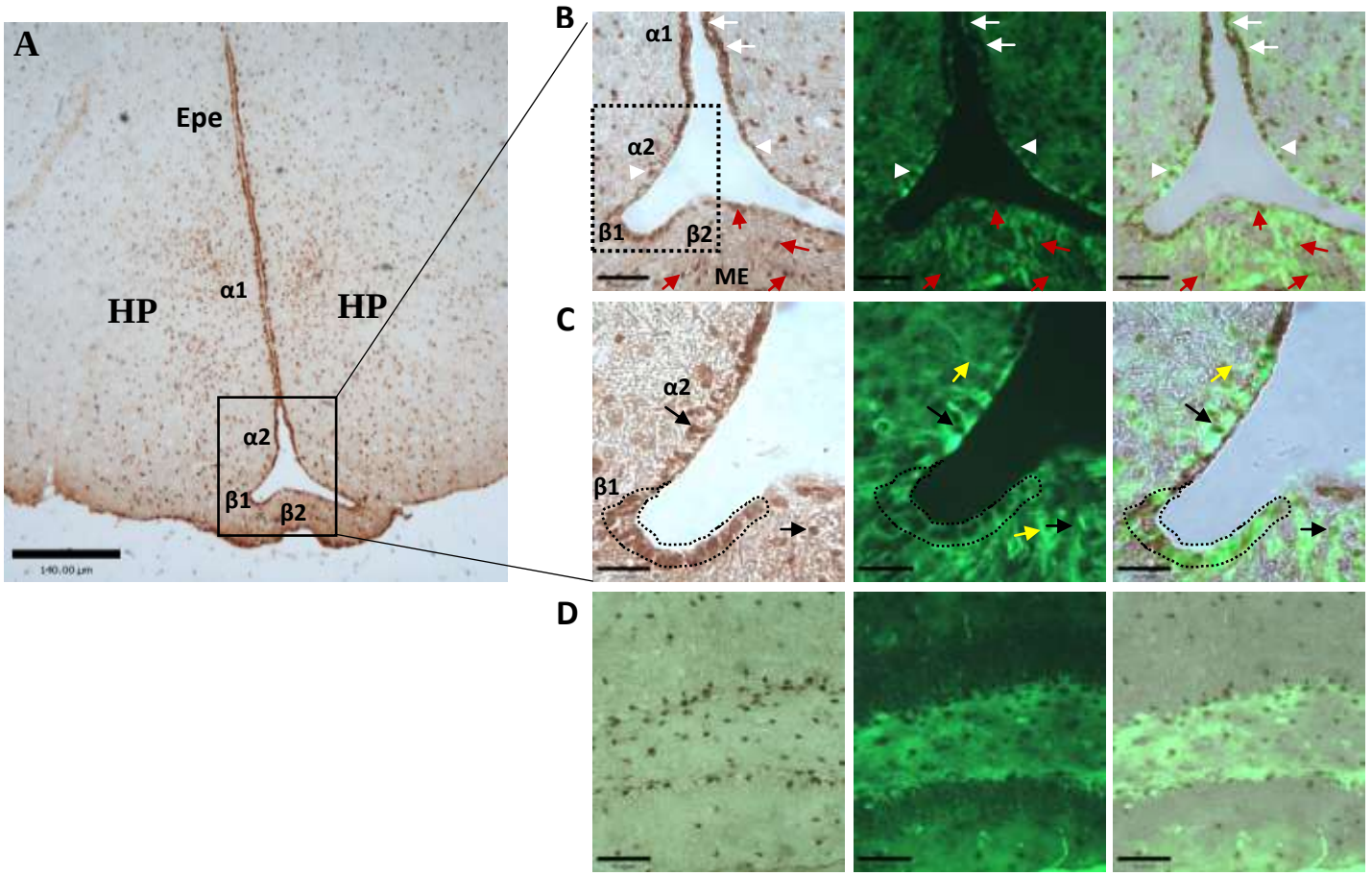

Figure 6.5 Compared expression of Sox2 and GFP in coronal sections of adult mouse third Ventricle (3V) and hippocampal dentate gyrus. (A) Overview image showing Sox2 staining in cells lining the 3V and the hypothalamus (HP). (B) and (C) Magnified image of the boxed area in (A) showing Sox2 (brightfield) and GFP (green) expression in the tanycytes. In (B), both α1 (white arrows) and α2 (arrow heads) tanycytes show strong immunoreactivity for Sox2 and for GFP . In the region of median eminence (ME), β2 tanycytes show clear stained nuclei corresponding to Sox2 (brown) and cytoplasmic GFP staining (green, red arrows). (C) A magnified image of the boxed area in (B) showing Sox2 and GFP expression in α2 (black arrows) and β1 tanycytes (black dotted area), yellow arrows point to the processes of the tanycytes. (D) Positive control for Sox2 and GFP detection in the hippocampal dentate gyrus (DG). Scale bar = 140 µm in (A); 340 µm in (B); 140 µm in the brightfield images and 70 µm in the fluorescent image s (C); 70 µm in (D)
ME, Median Eminence; **HP**, Hypothalamus; **Epe**, Ependymocytes.

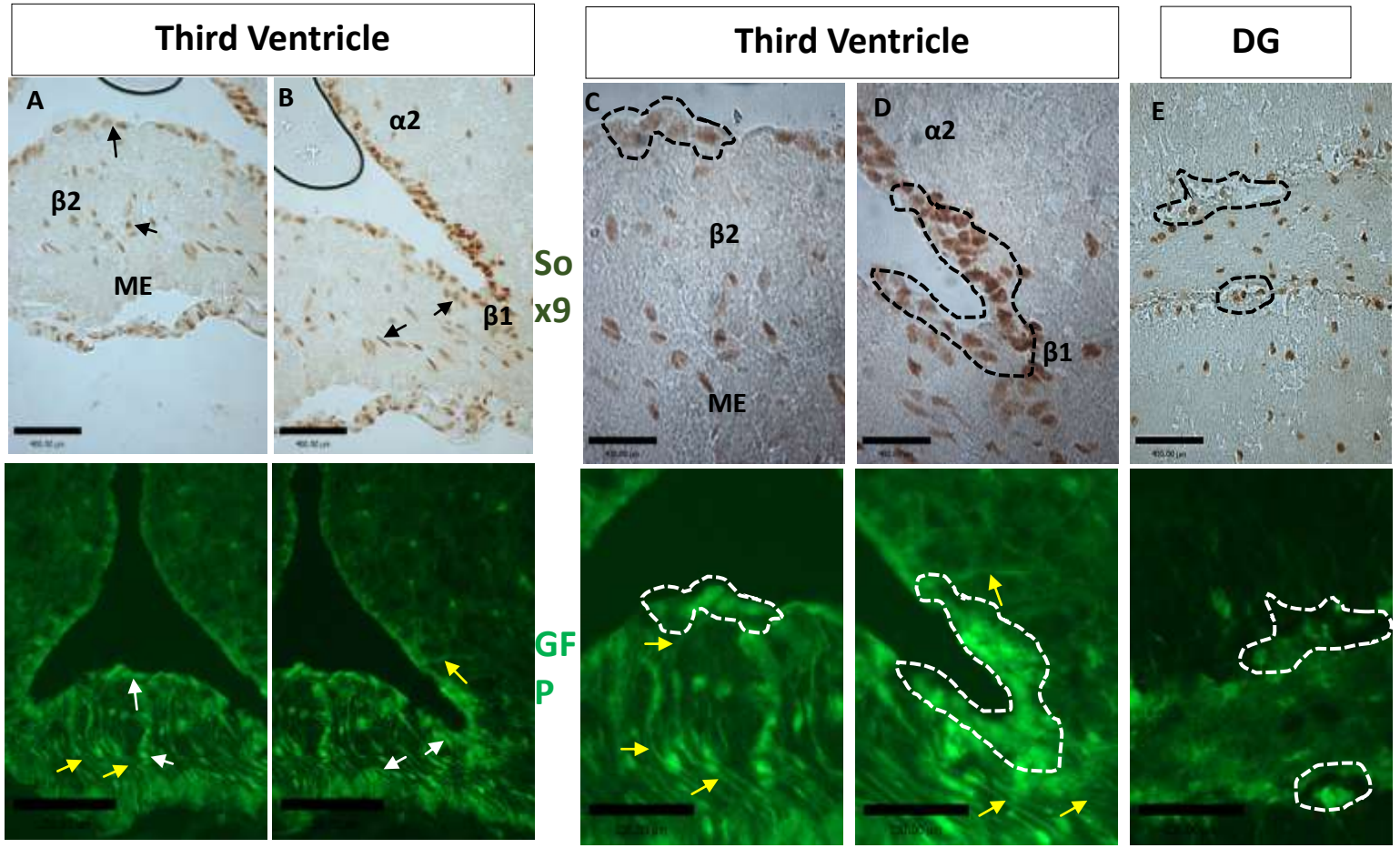

Figure 6.6 Co-detection of Sox9 and GFP in coronal sections of adult mouse third Ventricle (and hippocampal dentate gyrus (DG). (A) and (B) show the expression of Sox9 (brightfield) and GFP (green) in β2 tanycytes (black arrows), the staining pattern of Sox9 in the tanycytic nuclei (brown) resembles that of Sox2; GFP signal marks the tanycytic cytoplasm and their long processes (yellow arrows) similar to that seen for cells positive for Sox2 and GFP. (C) A magnified image of (A) showing Sox9 and GFP expression in in the ME region where β2 tanycytes reside (black dotted area); yellow arrows point to the processes of β2 tanycytes. (D) A magnified image of (B), β1 tanycytes show clear brown nuclei staining corresponding to Sox9 and green cytoplasmic GFP staining (black dotted area). (E) Positive control for Sox9 and GFP (black dotted area) detection in the hippocampal dentate gyrus (DG). Scale bar = 400 μm in the brightfield images; 130 μm in the fluorescent images. **ME**, Median Eminence

6.3.3 Co-localization of Sox1 with GFAP in the 3V

GFAP expression in the 3V

Although GFAP is a common astrocytic marker, recent studies have shown that it could be expressed by radial glia and NSCs (Imura et al., 2003). Numerous studies have identified a multipotent population of astrocytic stem cells expressing GFAP in the SVZ of immature and adult brain (Reviewed in Codega et al., 2014). In order to further characterise the nature and morphology of the Sox-positive tanycyte population, single and double marker analysis were performed to determine the presence of GFAP+ cells in the 3V and investigate their relative distribution.

Signal for GFAP single immunostaining was demonstrated along the anterior/posterior axis of the 3V (Fig. 6.7A), with expression in the cell bodies of ependymocytes (Fig. 6.7B), and more intense labelling in the cell bodies and the long processes of both α1 and α2 tanycytes (Fig. 6.7B-F). The unique expression of GFAP in the long processes of α1 and α2 tanycytes made it possible to distinguish them from ependymocytes (Robins et al., 2013) (Fig. 6.7B and C). In more ventral part of the 3V, GFAP immunoreactivity was also detected in the cell bodies and processes of β1 and β2 tanycytes (Fig. 6.7F).

Co-detection of GFP and GFAP was performed to analyse the relative localisation of $Sox1^{+}$ with $GFAP^{+}$ cells in the 3V (Fig. 6.8 and 6.9). Signal for GFAP and Sox1 expression were detected along the anterior/posterior axis of the 3V (Fig. 6.8 B and C), with more intense labelling in the cell bodies and the long processes of α1 tanycytes (Fig. 6.8 B). Few cells were also positive for GFAP+Sox1 in α2 tanycytes (Fig. 6.8C). However, no GFAP and Sox1 staining was observed in the ependymocytes (Fig. 6.8A) contrary to what was observed when GFAP marker

stained alone (Fig. 6.7B). Specific expression of GFAP in the long processes of α1 tanycytes differentiated them from ependymocytes and α2 tanycytes (Fig. 6.8A, B, C). In the ME region of the 3V, GFAP immunoreactivity was absent in β1 tanycytes, whereas β2 tanycytes coexpressed GFAP and Sox1 (Fig. 6.9A, B, C). In the hypothalamus, many astrocytes in the arcuate nucleus were GFAP immunopositive and larger numbers of $GFAP^{+}$ astrocytes were found in the ventromedial nucleus area (Fig.6.7C and E).

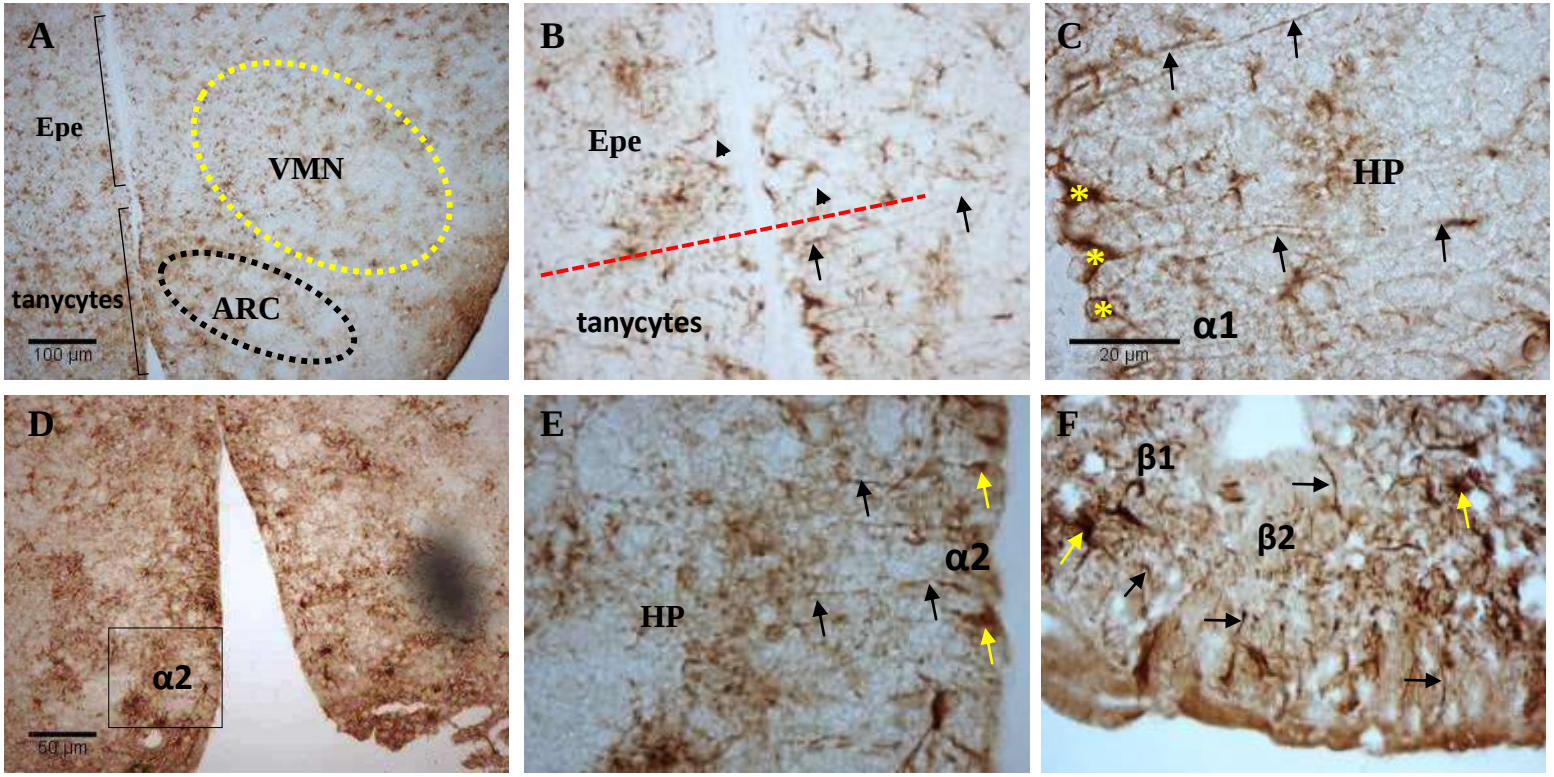

Figure 6.7 Coronal sections through the third ventricle (3V) showing GFAP expression. (A) Two types of cells lining the third ventricle, ependymocytes and tanycytes. (B) GFAP reactivity in the long processes of tanycytes (black arrows) clearly differentiates them from ependymocytes with very short processes (arrow heads). The red dashed line marks the border between ependymocytes and tanycytes, black arrows point to the long processes of α1 tanycytes, (C) magnified view of GFAP immunoreactivity in the α1 tanycytes cell bodies (yellow asterisk), the long processes (black arrows) of α1 tanycytes extend into the surrounding parenchyma of the hypothalamus (HP). (D) GFAP detection in α2 tanycytes. (E) High-power image of the boxed area in D showing the cell bodies of α2 tanycytes (yellow arrows), it is clear from the image that α2 tanycytes also possess long processes (black arrows) that penetrate the hypothalamus parenchyma (HP). (F) Immunoreactivity of GFAP in the more ventral part of the 3V, both β1 and β2 tanycytes show reactivity to GFAP. Scale bar = 100 µm in (A) ; 50µm in (B, D, F) ; 20 µm in (C, E).

ME, Median Eminence; **HP**, Hypothalamus; **Epe**, Ependymocytes, **VMN**, ventromedial nucleus; **ARC**, arcuate nucleus; DG, dentate gyrus.

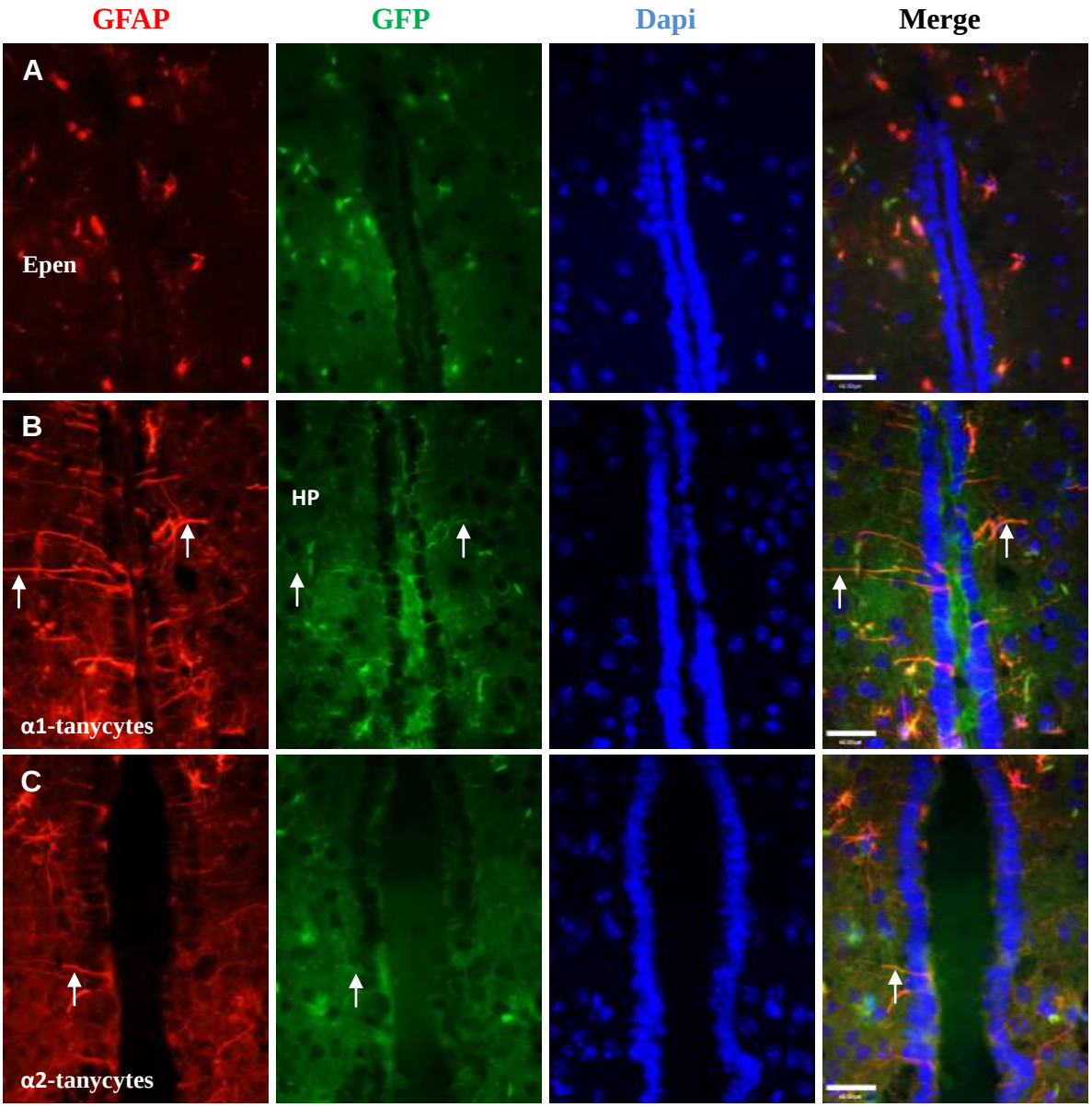

Figure 6.8 Coronal sections through the dorsal part of the third ventricle (3V) showing co-localization of GFP and GFAP. (A) Double labelling of GFP (green) and GFAP (red) counterstained with Dapi (blue) showing reactivity in the astrocytes located close to the area of the 3V wall where ependymocytes are found, but no signal could be observed in the short processes of the ependymocytes, distinguishing them from the α1tanycytes located below. (B) Clear overlap of GFAP signal with GFP in the α1 tanycytes cell bodies and long processes (white arrows) which extend into the surrounding parenchyma of the hypothalamus (HP); but the coexpression of GFAP and GFP is weaker in α2 tanycytes with fewer processes (white arrows) compared to those of α1 tanycytes (C). Scale bar = 60 μm.

Epe, Ependymocytes; HP, Hypothalamus

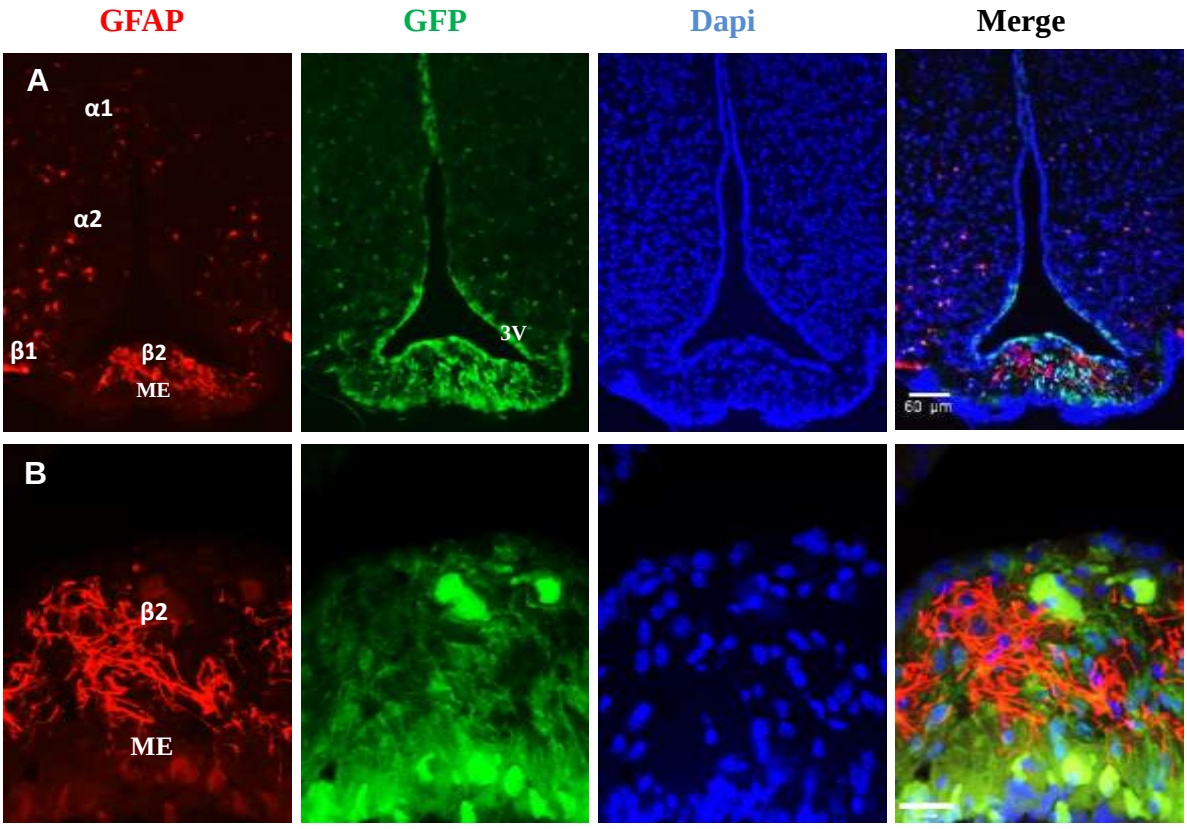

Figure 6.9 Coronal sections of the ventral part of 3V showing co-localization of GFP and GFAP. (A) Fluorescent images showing double labelling of GFP (green) and GFAP (red) counterstained with Dapi (blue) in the lining of the 3V wall. GFAP colabeled with GFP in β1 tanycytes (A) and more intense staining was detected in the β2 tanycytes processes in the ME region (C). Scale bar = 60 µm

ME, Median Eminence; **HP**, Hypothalamus; **Epe**, Ependymocytes.

6.4 Characterisation of NSCs derived from the 3V

6.4.1 In vitro isolation and culture

In the mouse brain, NSCs can be maintained and expanded in vitro in the presence of EGF and FGF as clusters of cells called neurospheres (Reynolds and Weiss, 1992, 1996, Morshead et al., 1994, Tropepe et al., 1999). To test whether cells isolated from the 3V wall display NSC characteristics in vitro, cells derived from 3V of adult GFP+/-Sox1 mouse were cultured in DMEM-F12 supplemented with B27, N2, as well as EGF and FGF-2 (both at 20ng/ml). Single cells plated this medium generated large neurospheres (Fig. 6.10A and B). In the presence of EGF and FGF, expandable NSC–like cells could be maintained and passaged in culture for up to 30 passages. 3V derived NSCs started to form neurospheres of varying sizes after 10 days in vitro (DIV) (Fig 6.10), and reached a size of about 273 μm after one week in vitro (Fig. 6.10B). Upon neurosphere dissociation, cells finally attached and could be maintained as adherent monolayer culture (Fig. 6.10C).

6.4.2 Expression of NSC markers

Immunostaining carried out on these 3V derived NSC-like cells found them to express intermediate filament Nestin, a NSC marker in undifferentiated culture conditions (Fig. 6.12B). Furthermore, Sox2 another NSCs marker was also found to be expressed in undifferentiated 3V-NSCs (Fig. 6.12B). This observation together with the previous findings indicates the presence of neural stem-like population in the 3V wall.

6.4.3 Effect of EGF and FGF-2 withdrawal on the proliferation of NSCs derived from the third ventricle (3V)

The two mitogens, namely, EGF and FGF-2 are required for promoting NSC proliferation (Reynolds et al., 1992). bFGF is required to maintain the NSC population in the neurogenic regions of adult brain, the SVZ and the SGZ (Mudo et al., 2009). Weiss et al., (1996) have shown that NSCs derived from spinal cord and 3V of adult mice depend on both mitogens for their survival and proliferation in vitro. To examine the requirement of 3V derived NSCs for EGF and FGF-2, the effect of EGF or FGF withdrawal on NSC proliferation was investigated NSCs from 3V and LV for control were seeded in parallel at a known density, and maintained in medium containing either EGF (20ng/ml) alone, FGF-2 (20ng/ml) alone, EGF+FGF-2 (20ng/ml), or no growth factors (negative control), followed by metabolic cell activity assay after 3 days.

Cell metabolic assay showed that 3V cells grown in EGF+FGF showed significantly higher rate of proliferation than cells grown in EGF or FGF alone, which performed similarly (Fig. 6.11C). For NSCs-LV too, the highest proliferative activity was achieved when both growth factors were combined, however a significantly higher rate of proliferation was observed when cells were grown in FGF-2 alone than in EGF alone (Fig. 6.11C). In all of the four medium conditions, the NSCs-3V and LV grew as neurospheres at day1 (Fig. 6.11A, B respectively). Cells observed at day2 revealed a clear morphological difference between cells grown in each medium condition, with cells expanded in EGF only mostly maintaining as neurospheres, while cells in the presence of FGF appeared smaller with long extended neurites (Fig. 6.12A). However, cells grown in EGF+FGF retained their homogenous morphology, and only few differentiated

cells were observed in the medium with neither growth factor. Observations showed very similar morphological results for cells derived from 3V and from LV (Fig. 6.12B).

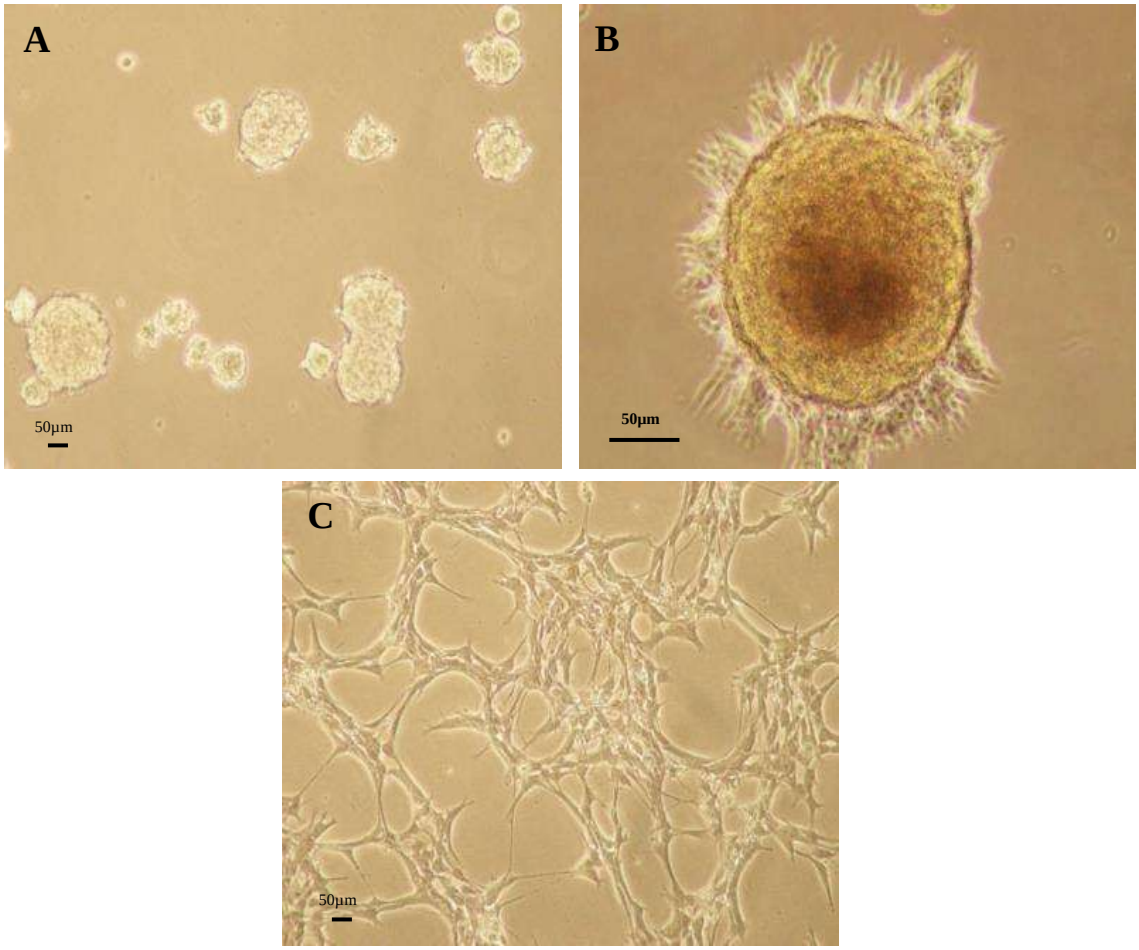

Figure 6.10 Brightfield image showing the morphology of 3V derived neuroshpheres. (A) Neurospheres formed in the presence of EGF and FGF-2 (20ng/ml) at varying sizes after 10 DIV. (B) Magnified image showing migrating cells on the outer surface of the neurosphere after seeding at the bottom of the plate, which is an indicator of viable healthy neurosphere. (C) Monolayer culture of 3V derived NSCs after neurosphere dissociation and single cell attachment. Scale bar= 50 µm.

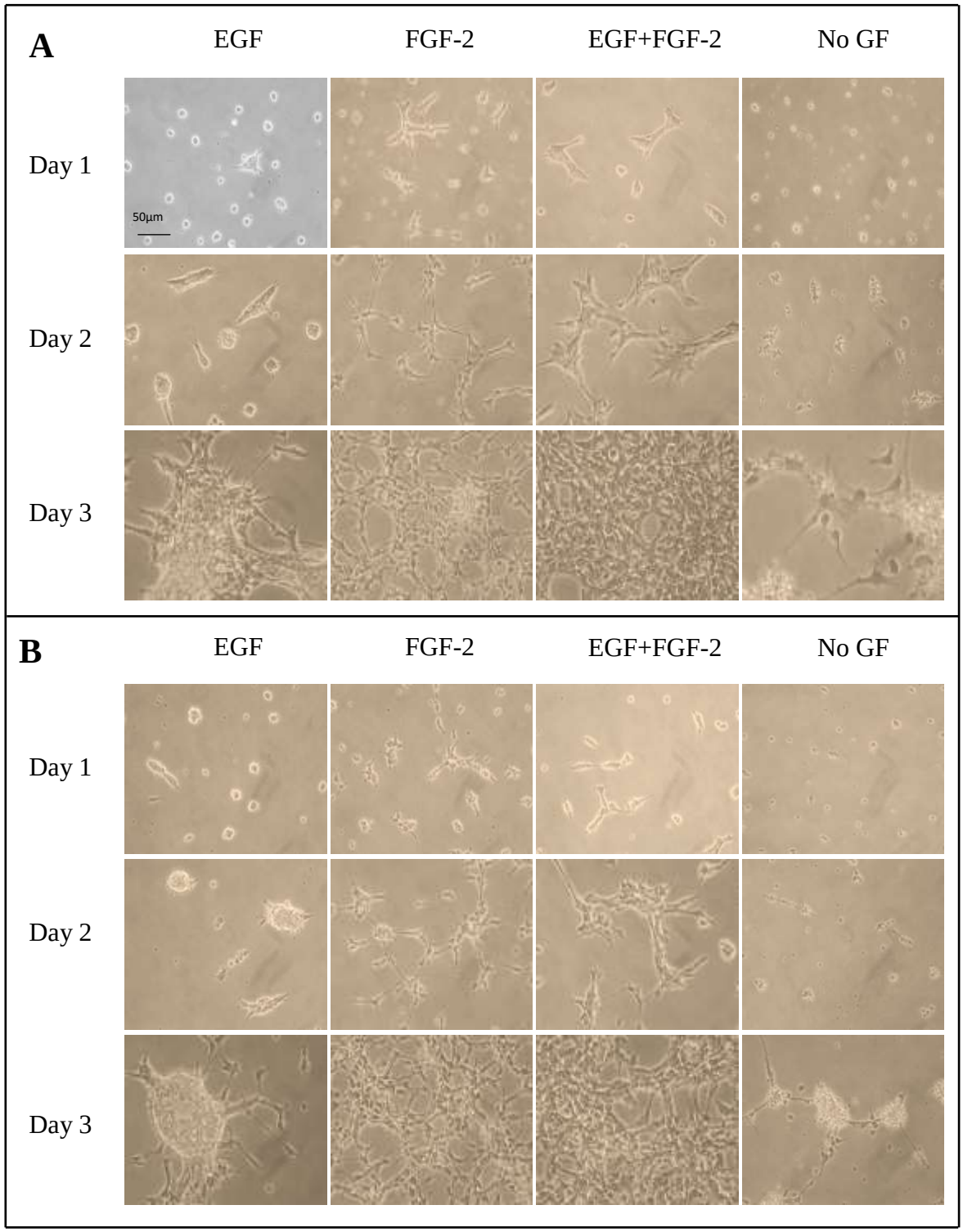
A
EGF
FGF-2
EGF+FGF-2
No GF
Day 1
Day 2
Day 3
50µm
B
EGF
FGF-2
EGF+FGF-2
No GF
Day 1
Day 2
Day 3

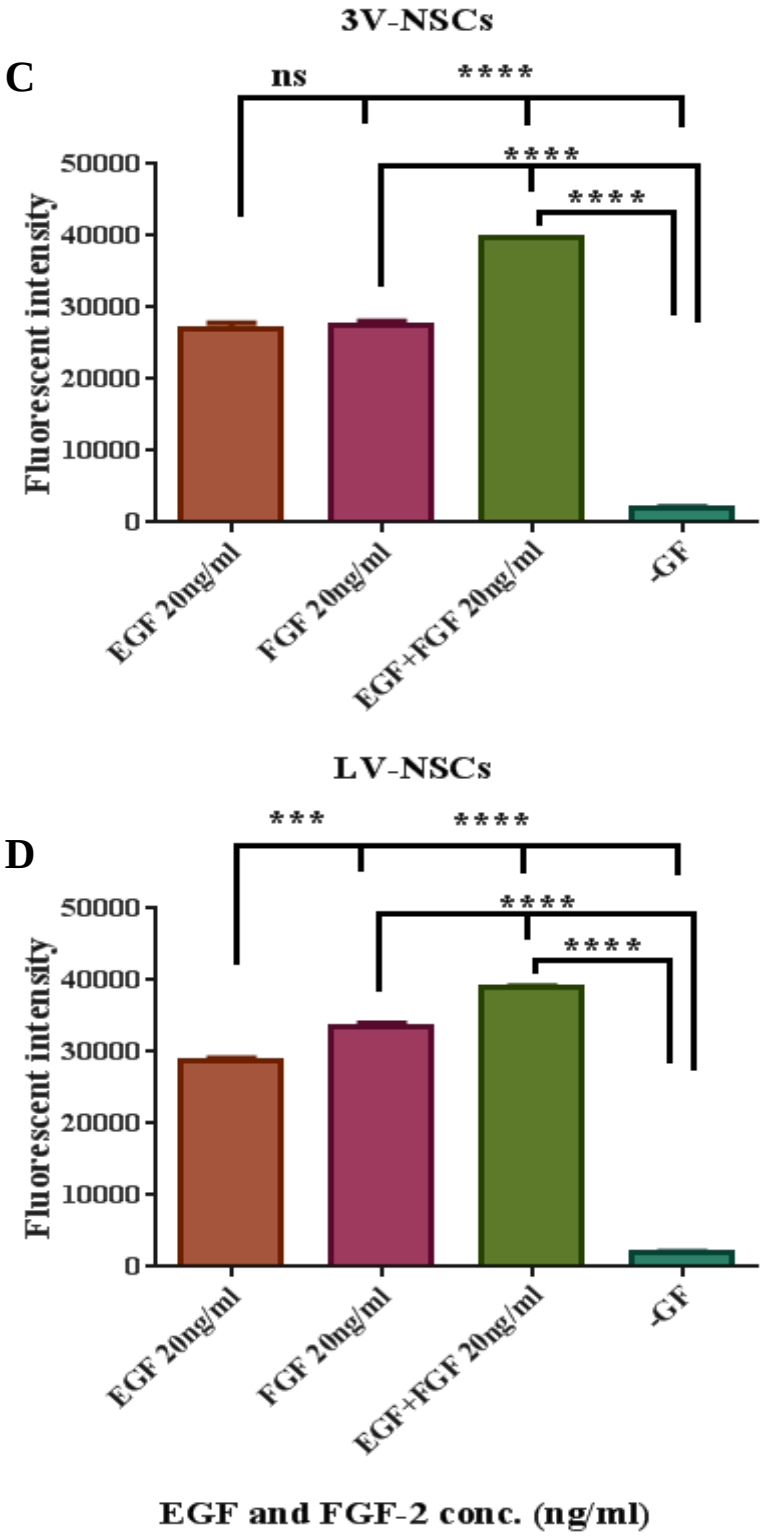

Figure 6.11 Effects of different growth factor conditions on mouse 3V and LV NSCs after 3 days in culture. (A), (B) Morphology of mNSCs-3V and LV respectively expanded in EGF (20ng/ml), FGF-2 (20ng/ml), EGF+FGF-2 (20ng/ml each), and without growth factor. At day 1, cells in each medium condition form neurospheres and start to attach at day 2 while at day 3, cells in EGF only remained as neurospheres with single cells extended from them. NSCs in FGF-2 alone have more heterogeneous appearance. (C) and (D) Cell metabolic assay of mNSCs-3V and LV respectively after 3 days in culture. For both cell types, the maximum proliferative rate was achieved when both growth factors were combined. The values are mean ± SEM. (***), (****) $P < 0.0001$ were considered significant using Tukey's multiple comparisons test with one way ANOVA.
EGF= epidermal growth factor; FGF-2= fibroblast growth factor. Scale bar =50µm.

6.4.4 Neural stem cells derived from the 3V have the ability to differentiate into neurons, astrocytes, and oligodendrocytes

To evaluate the differentiation potential of NSCs derived from the 3V, cells were exposed to differentiation medium for either 5 or 11 days before being fixed and processed for immunostaining, alongside LV-NSCs used as control. The expression of differentiation markers was analysed using GFAP (astrocytic marker); B-tub3 and DCX (neuronal markers); MBP (oligodendrocyte marker); while Nestin and Sox2 specific antibodies were used to detect undifferentiated cells (Fig. 6.12B). Glial and neuronal markers were detected in the treated cells (Fig. 12B, C) but not in D0 cultures indicating that NSCs derived from the 3V wall were able to generate glial and neuronal derivatives. Conversely, Nestin expression was only found at D0 (Fig. 12B) while absent at D5 or 11 suggesting that NSCs-derived from the 3V were successfully differentiated.

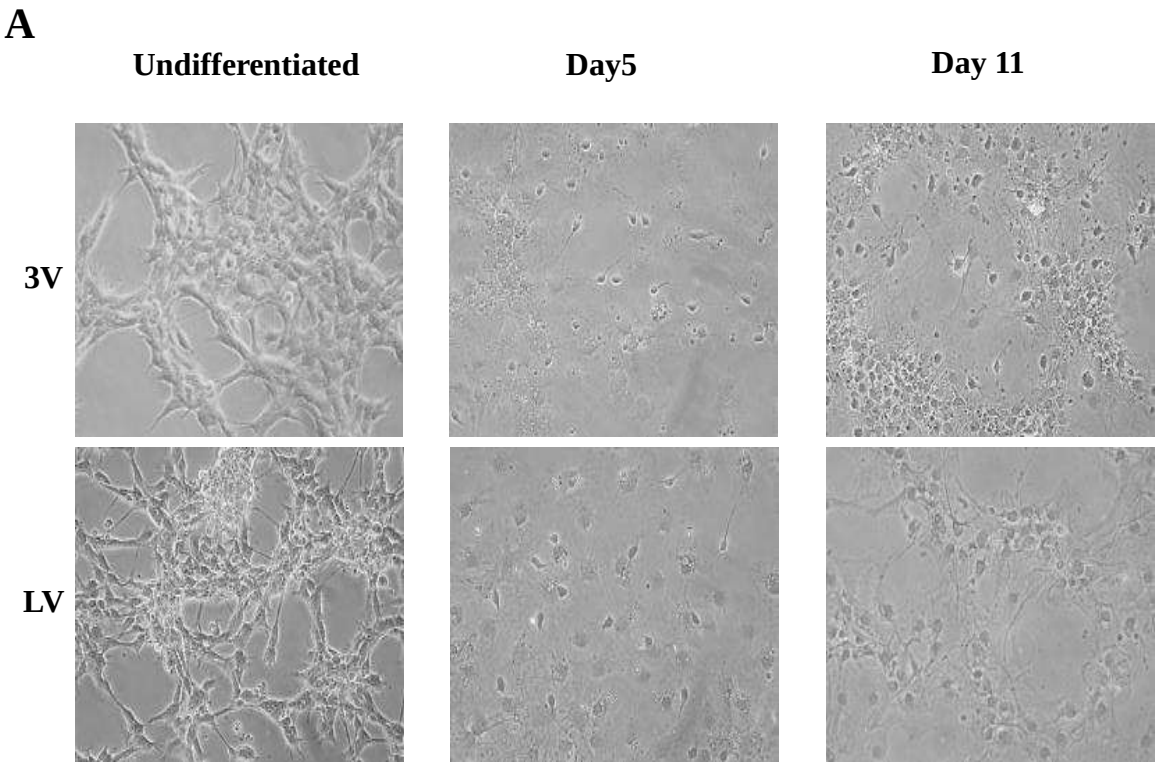

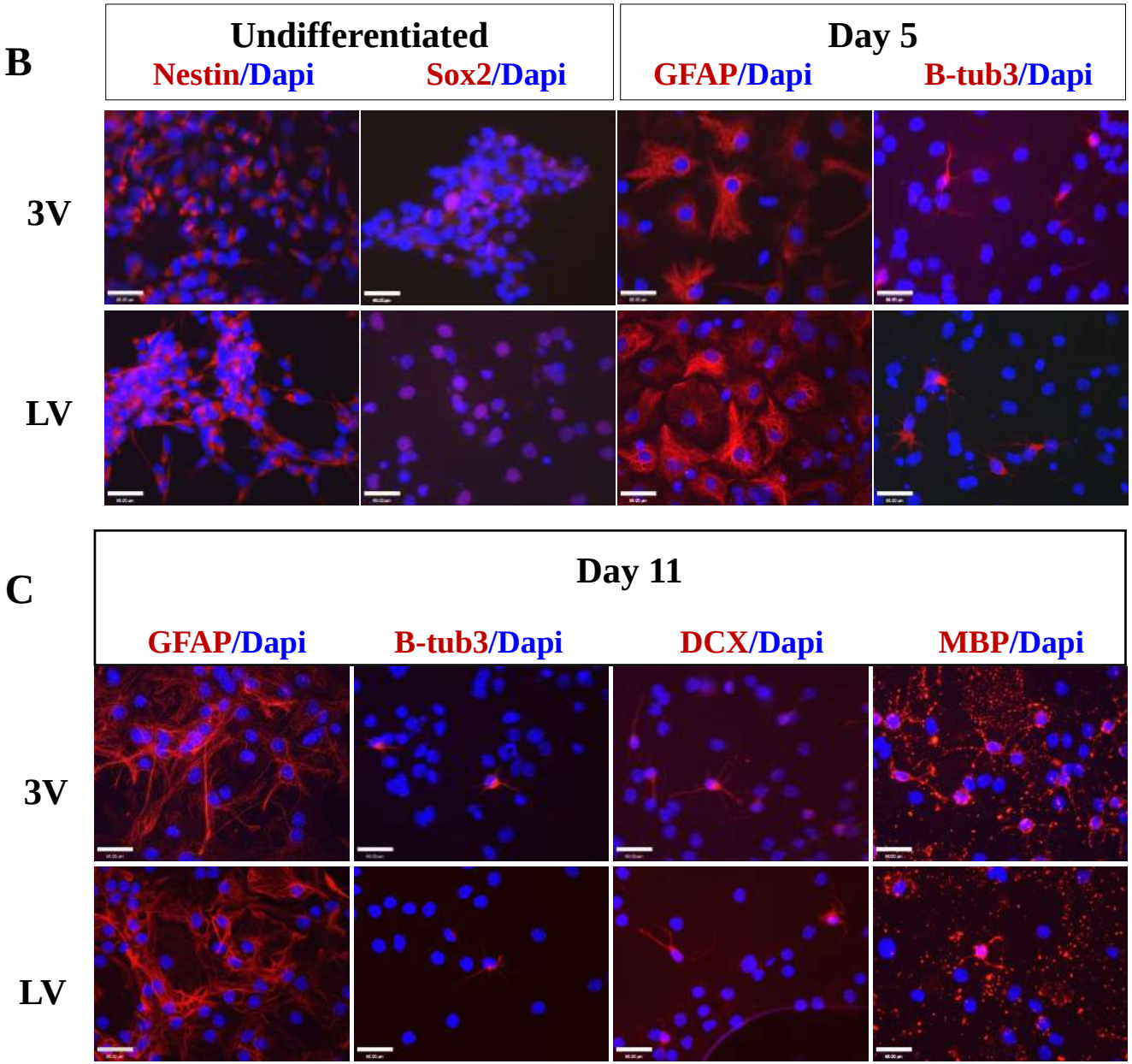

Figure 6.12 Differentiation analysis of NSCs derived from the third ventricle (3V) and lateral ventricle (LV). Brightfield images of mNSCs-3V and LV before differentiation (A), at day 5 of differentiation (B), and at day 11 of differentiation (C). Immunofluorescence images of mNSCs-3V and LV at day 5 (B) or 11 (C) of differentiation in medium without growth factors (EGF and FGF-2) and in the presence of BDNF, EC23 and serum. After 5 or 11 days, cells were fixed and immunostained for Nestin (neural stem cell marker), GFAP (astrocyte marker), B-tub3 (neuronal marker), DCX (immature neuronal marker), and MBP (oligodendrocyte marker) with Dapi counterstain (blue). Scale bar =60 µm.

6.5 Discussion

In this study, direct and indirect Sox1 analysis through the use of the GFP reporter were used to provide first evidence that Sox1 is strongly expressed in the lining of the 3V. The expression was demonstrated in all tanycyte subpopulations, and in the surrounding hypothalamus. I also analysed the expression of neural stem cells (NSCs) and radial glial markers in the population of tanycytes in the ependymal lining of adult mouse 3V, and provided first evidence of co-expression of Sox1 with Sox2 and Sox9, known markers for NSCs, in this population. Furthermore, co-staining experiments showed that all tanycyte subpopulations expressed proteins associated with NSCs in other brain regions such as Sox1, 2, and 9, while they show subtype-specific expression of other proteins such as GFAP. Furthermore, in vitro experiments carried out here showed that derivation of NSC-like cells from the 3V was possible in the presence of both EGF and FGF-2 (Weiss et al., 1996).

To evaluate the degree of overlap between Sox1 and Sox2 expression in populations of the 3V, double immunolabeling was used and confirmed co-expression across the different tanycyte populations, while sporadic expression was also observed in the surrounding hypothalamus in which neurogenesis has been described (Xu et al., 2005, Kokoeva et al., 2005, Migaud et al., 2010). Positive Sox1 and Sox2 detection was confirmed in the hippocampus, a region in the adult brain in which neurogenesis is an ongoing process (Venere et al., 2012, Brazel et al., 2005).

The transcription factor Sox1 is expressed in neural progenitor cells both in vitro and in vivo (Li et al., 2001, Barraud et al., 2005). In the

developing CNS, Sox1 is an early marker for neuroprogenitors, and its expression is also observed in vivo in adult neural progenitor cells (Kan et al., 2007). In vitro, Sox1 expression has been used for the isolation of neuroprogenitors obtained from ES cultures (Li et al., 1998). Sox2, another member of SoxB family, is a transcription factor maintaining pluripotency in embryonic stem cells which is also expressed by the neuroepithelial cells in the developing brain (Ferri et al., 2004, Chambers and Tomlinson, 2009) and plays an important role in maintaining NSCs identity (Pevny and Placzek, 2005, Koirala and Corfas, 2010). Both Sox1 and Sox2 are expressed in embryonic neuroprogenitors and in the neurogenic niches of adult brain such as the subventricular area of the lateral ventricles and the dentate gyrus of the hippocampus (Ferri et al., 2004, Ellis et al., 2004, Brazel et al., 2005), and Sox2-positive populations in these regions have demonstrated NSCs characteristics and behaviour in vitro (Brazel et al., 2005) and in vivo (Suh et al., 2007). Li et al., (2012) observed that tanycytes strongly coexpressed Nestin and Sox2 in the upper portion of the 3V wall, while the expression of Sox2 was weak or absent in the ME region despite the strong signal for Nestin. Another report by Lee et al., (2012) however revealed strong coexpression of Nestin and Sox2 in the ME portion of the 3V. My result partly agree with Li et al., (2012) concerning Sox2 expression in the upper portion of the 3V wall, however our study showed intense Sox2 signal in the ME region in line with Lee et al., (2012) and Haan et al., (2013). Altogether, data presented here show that Sox1 and Sox2 are expressed in all tanycytes of the 3V in a closely similar pattern. Additionaly, double immunostaining was

performed to establish the co-localization of Sox1 with Sox2, Sox9, and GFAP expression within the same tanacyte population in the mature 3V. Using the GFP reporter to visualise Sox1 co-expression with Sox2 and Sox9, we observed significant numbers of GFP^+ cells co-localized with Sox2 and Sox9 signal in both α and β tanycytes. In the median eminence, both β1 and β2 tanycytes co-expressed GFP with Sox2 and Sox9 more intensely than α tanycytes. Sox9 also demonstrated strong immunoreactivity in the lining of the 3V, and confirmed that the $Sox9^+$ population represented tanycytes, as previously suggested in the literature (Lee et al., 2012). The demonstrated co-expression of Sox1with Sox2 and Sox9 point to a known NSC signature as observed in other brain regions, suggesting that tanycytes might represent another source of Sox1/Sox2/Sox9 positive adult NSCs (Sottile et al., 2006, Alcock et al., 2007). The present study provides the first evidence that the tanycytes co-express Sox1 with Sox2 and Sox9, while other studies have shown the coexpression of Sox2/BrdU with Nestin (Lee et al., 2012), Nestin and GFAP (Bennett et al., 2009, Lee et al., 2012), Vimentin and Nestin or Viementin and GFAP (Robins et al., 2013) in tanycytes. The co-expression Sox1 with both Sox2 and Sox9 support the hypothesis that tanycytes may constitute a neurogenic niche in the adult hypothalamic 3V. However, although my study did not provide the evidence regarding which population of tanycytes described here may be the one generated NSCs in vitro, but at least enough evidence was provided in this study that both α and β tancytes are an important component of the NSC population in the 3V.

6.5.1 Tanycytes are radial glial cells

Tanycytes constitute a heterogenous cell population of four subtypes, α1,2 and β1,2 (Reviewed in (Rodriguez et al., 2005)). These subtypes differ in their location, morphology, spatial relationship, cytochemistry, and the functional molecules they express (Rodriguez et al., 2005, Rodriguez et al., 2010). Our findings further highlighted differences in tanycyte subtypes. In my study, GFAP expression was detected in ependymocytes and in α tanycytes but not β1 tanycytes. GFAP signal observed in the cell bodies and long α1 tanycytic processes clearly distinguished them from ependymocytes, α2, and β tanycytes as previously described (Robins et al., 2013). However, my observation for GFAP expression in tanycytes contradicts another report which showed GFAP expression in the β1 tanycytes of rat brain (Cortés-Campos et al., 2011). This could be due to species differences and the fact that rat and mouse astrocytes express different levels of GFAP under normal conditions (Gudino-Cabrera and Nieto-Sampedro, 2000, Puschmann et al., 2010) and after a scratch insult (Puschmann et al., 2010). Furthermore, adult NSCs described in the LV and the hippocampus have radial glial morphology (Ming and Song, 2011, Bonaguidi et al., 2012), and tanycytes lining the 3V wall express radial glial and neural progenitor markers such as Nestin, vimentin, Sox2, and GFAP (Rodriguez et al., 2005, Xu et al., 2005, Kokoeva et al., 2007, Lee et al., 2012, Robins et al., 2013) but lack the expression of neuronal markers (Saaltink et al., 2012). Moreover, previous studies have shown that radial glial cells guide neuron migration during brain development, and more recent studies have shown that radial

glia act as neuronal progenitors in the adult brain such as the astrocytes of subventrcular (SVZ) and sugraular (SGZ) zones of the lateral ventricle and the dentate gyrus respecively (Malatesta et al., 2000; Alvarez-buylla et al., 2000; Anthony et al., 2004). The radial glial features of the tanycytes shown by markers localized to the long tanycytic processes may position these cells as modified radial glial cells in the adult brain (Levitt and Rakic, 1980). Based on these observtions and and my observation of GFAP immunoreactivity, these radial glial-like cells in the adult mouse 3V correspond to tanycytes (Robins et al., 2013).

6.5.2 3V NSCs derivation and characterisation

Previous studies in adult mouse have shown that neural progenitor cells exist in the ependymal lining of the third ventricle (Xu et al., 2005, Lee et al., 2012). These progenitors have radial glial properties are capable of generating new functional neurons, and they require local FGF signalling for their proliferation (Xu et al., 2005, Perez-Martin et al., 2010, Lee et al., 2012; Robins et al., 2013).

Haan et al., (2013) have shown that ventral FGF-10 expressing tanycytes are neurogenic in the mouse hypothalamus, while Robins et al., (2013) suggested that dorsal Glast expressing tanycytes are highly neurogenic. Also in vitro study on adult rat brain revealed that Dil labeled ependymal cells in the 3V have neural stem/progenitor properties, they were able to generate neurospheres, proliferate, self-renew and differentiate into neurons, astrocytes and oligodendrocytes (Xu et al., 2005).

Cells isolated from the 3V wall were cultured and exhibited morphological characteristics similar to those generated from adult LV, used as a control in our study. The capacity to generate neurospheres in the presence of EGF and FGF-2 has been used as an indicator for the presence of NSCs, (Morshead et al., 1994), allowing cells that are unresponsive to these mitogens to be lost over culture and passaging. In my study, cells isolated from the 3V started to form spherical clusters of cells after 10 days in culture similar to the neurospheres reported by Reynolds and Weiss (1992), suggesting that EGF and FGF-2 can maintain and support the expansion of 3V derived cells as previously reported for SVZ neural progenitor cells (Morshead et al., 1994; Gage et al., 1995; Gritti et al., 1995, 1996). The 3V cells isolated in vitro were found to express Nestin and Sox2, two commonly used neural progenitor markers (Lee et al., 2012; Robins et al., 2013). Our results also confirmed a more recent report that Sox2 positive cells from the 3V and the hypothalamus formed neurospheres in culture which could be passaged for over 15 generations (Li et al., 2012). However, a serial neurosphere assay was not performed in this study and all the expreiments were done on adherent monolayer culture of the 3V NSCs. Several studies have reported that culturing NSCs in floating neuropshere culture does not maintain homogenous NSC population (Conti and Cattaneo, 2010). In contrast, monolayer adherent culture showed a high degree of homogeneity (Conti et al., 2005, Pollard et al., 2006, Conti and Cattaneo, 2010). We were able to expand the monolayer culture of 3V-NSCs for over 30 passages using this method,

and the results obtained were comparable to that of LV derived NSCs used in this study as a control.

Upon growth factors withdrawal, these 3V derived $Sox2^+$ cells were able to differentiate into neurons, astrocytes, and oligodendrocytes as previously reported in the hypothalamus of amphibians (Chetverukhin and Polenov, 1993), rats (Xu et al., 2005), mice (Lee et al., 2012; Robins et al., 2013). We observed that differentiated 3V-NSCs contained large number of $GFAP^+$ astrocytes with fewer numbers of B-$tub3^+$ neurons and oligodendrocytes. We also observed that Sox2 expression was found in undifferentiated and differentiated cells consistent with Ferri et al., (2004) who demonstrated the expression of Sox2 in some differentiated neurons of the striatum and thalamus in adult mouse brain. These findings indicate that NSCs present in the ependymal linging of the 3V may be similar to the NSCs isolated from other parts of the embryonic and adult brain (Conti et al., 2005, Pollard et al., 2006, Murrell et al., 2013).

Although combined EGF and FGF-2 treatment has been widely reported as supporting the proliferation of NSCs in different brain regions (Santa-Olalla and Covarrubias, 1999)(Santa- Olalla and Covarrubias, 1999), some studies have shown that stem cells from the forebrain can be isolated and expanded in the presence of EGF alone (Reynolds and Weiss, 1992; Morshead et al., 1994). I found that maintenance and expansion of NSCs from the 3V required the presence of EGF and FGF-2 to achieve maximum proliferation activity. This observation is supported by Weiss et al., (1996) who showed that multipotent stem cells from the 3V and spinal cord require the presence of EGF and FGF-2 for their isolation and

proliferation. The results observed by Weiss et al., 1996 contrasts with previously reported data concerning the isolation of cells from adult subependymal/forebrain region, for which EGF (Reynolds and Weiss, 1992) and FGF-2 (Gritti et al., 1996) were able to act individually as mitogens for the cultures. Although the cells were able to survive in either EGF or FGF-2 for 2 or 3 days but achieved their highest rate of proliferation when both mitogens were combined. Upon the removal of both growth factors and addition of differentiation factors such as BDNF and serum, cells promptly stopped proliferation and underwent differentiation. This behaviour has previously been observed in NSC cultures from adult mouse SVZ (Gritti et al., 1999). FGF-2 was shown to induce the expression of EGF receptors in the cultures of NSCs (Ciccolini et al., 2005), and a study has shown that FGF exposure could make neural precursor cells (NPCs) responsive to EGF. This suggests that EGF and FGF may not act separately but rather in a sequential way (Santa- Olalla and Covarrubias, 1999). This could explain the highest rate of survival and growth when the two mitogens are combined to exert a synergistic effect on NSCs (Ciccolini and Svendsen, 1998).

6.6 Conclusions

Although the identity of these NSCs is not clear as they were found both in the hypothalamus and the 3V wall, both α and β tanycytes are strong candidate as components of this neurogenic niche (Xu et al., 2005; Lee et al., 2012; Robbins et al., 2013). Evidence of co-expression of Sox1, 2, and 9 in all tanycyte populations from the dorsal to the ventral portion suggests that the 3V ependymal layer might be an interesting region since these genes are typically co-expressed other NSC populations in the adult brain.

Taken together, observations in this study and those of others (Xu et al., 2005, Kokoeva et al., 2005, Lee et al., 2012, Robins et al., 2013) suggest tanycytes as strong stem cell candidates in the 3V, that might be maintained in a quiescent state and could be modulated by inductive stimuli such as high fat diet (Lee et al., 2012, Li et al., 2012), hormones (Ahmed et al., 2008), and growth factors (Robins et al., 2013) or after ischemic stroke injury (Lin et al., 2015).Whether all types of tanycytes or only a subset can be induced to generate neurons is still a matter for debate and further investigation is required.

7 Concluding Discussion

7.1 Major thesis findings

The work contained in this thesis has attempted to explore for the presence of neural stem cells (NSCs) in the adult mouse cerebellum (CB) and third ventricle (3V). In chapter 3 (Investigating the presence and distribution of neural stem cells in the mature cerebellum of mouse, primate, and chick adult CB of mouse, chick, and primates), we analysed the adult CB of these species for NSC markers expression such as Sox1, 2, 9 and other NSC associated markers such as GFAP and BLBP using double immunohistochemical technique. Our results proved that the CB contains a population of radial glial cells, namely Bergmann glia (BG) that express NSC markers that are highly conserved between the 3 species examined.

In chapter 4 (Isolation and characterisation of cerebellar derived neural stem cells of adult GFP+/- Sox1 mouse), NSCs from adult CB were isolated and characterised in terms of neurospheres formation, growth factor requirement, and multipotency compared to the existing NSC population in the adult brain, the lateral ventricle (LV). Our results proved that CB derived NSCs have the ability to form neurospheres and differentiate into neurons, astrocytes, and oligodendrocytes. More importantly, these cells showed the ability to differentiate into calbindin positive cells, suggesting that the generation of PCs is possible under the culture condition used in this study. In chapter 5 (Quantitative, morphological and immunohistochemical study of Bergmann glia and Purkinje cells in Purkinje Cell Degeneration (pcd) 5J mutant mice), BG response to CB

damage caused by rapid loss of PCs were analysed in Purkinje cell degeneration (*pcd*^{5J}) mutant mice. It was hypothesized that astrocytes undergo gliosis after injury which is characterised by GFAP upregulation (Wilhelmsson et al., 2004). BG showed clear signs of gliosis revealed by GFAP staining and increased in number at the very advance stages of PCs degeneration. The work in chapter 6 (Exploring the existence of neural stem cells in the third ventricle of adult GFP+/-Sox1 mouse), examined whether tanycytes lining the 3V could also express NSCs markers as BG such as Sox1, 2, and 9 and whether NSCs could be extracted from the 3V. Based on the results obtained for BG concerning NSCs markers expression, we hypothesized that tanycytes might also express these markers as both cells are the only cells in the adult brain maintained as radial glial cells. Results showed that tanycytes lining the 3V co-express Sox1, 2, 9, and GFAP in a closely resemble staining pattern. Moreover, NSCs were successfully isolated from the 3V with the characteristics of neurospheres formation and multipotency.

7.2 Is there NSCs population in the mature cerebellum and third ventricle

My own data has provided enough evidence that the CB and the 3V of adult mouse harbour populations of stem-like cells identified by expression of NSCs markers such as Sox1, 2, 9, and GFAP. These labelled populations displayed the positional characterisations of BG and tanycytes, two radial glial cells in the CB and 3V of adult mouse respectively. Furthermore, the expression of these markers in the BG observed in other species such as chick and primate CB suggests that Sox genes expression in these cells is conserved. This would lead us to conclude that neurogenesis might also be conserved between rodents and other mammals (Oikari et al., 2014).

The fact that no neurons are added in the adult brain has been proved incorrect (Reviewed in (Oyarce et al., 2014)). Recent reports have provided enough evidences that neurogenesis and proliferation also occur in other areas of the adult brain other than SVZ and SGZ. Researchers started to address the question whether NSCs are present in other regions of the mature brain such as CB and the lining of the 3V. However, lower BrdU incorporation has been demonstrated in these regions, suggesting that neurogenesis in these regions is in sufficient to produce physiologically functional neurons. Identification of new population of NSCs in other regions of adult mouse brain such as CB and 3V might help to discover new neurogenic regions in the human brain that could be exploit for stem cell therapy. Thus, the study of neurogenesis in rodent would help for better understanding of NSCs and neurogenesis in primates that can also be applied in human. However, there is a very little published data describing neurogenesis in adult rodents CB compared to the robust material published on hypothalamus and 3V neurogenesis.

Studies have shown similarities between NSCs in the SVZ and radial glial cells both morphologically and by the expression of some markers such as BLBP, RC2, and GLAST (Doetsch et al., 1999, Laywell et al., 2000, Imura et al., 2003, Götz, 2003, Rakic, 2003) . Other studies have demonstrated that cells with radial glia or astrocytic characteristics are able to act as neuronal precursors or NSCs in the adult brain (Doetsch et al., 1999, Alvarez-Buylla et al., 1990, Anthony et al., 2004). Similarly, BG and the tanycytes population shared some morphological, functional, and molecular features with astrocytes and radial glia by the expression of GFAP, BLBP, GLAST, and S100. Authors have suggested that

tanycytes could also serve as neuronal progenitors (Rodriguez et al., 2005). Moreover, I demonstrated that NSCs markers such as Sox1, Sox2, and Sox9 were expressed in BG and 3V of adult mouse. These observations raise the possibility that BG and tanycytes might be potential stem cell populations in the CB and the 3V respectively. Further studies are required to examine whether the same conclusion might be extended to other unexplored areas of the adult brain.

Although it is risky to rely on NSCs marker expression to demonstrate the existence of NSCs in the mature CB or 3V, both CB and 3V derived NSCs showed the ability to form neurospheres and to expand as adherent culture in the presence of mitogens such as EGF and FGF-2, in a way similar to the control LV cells. After mitogens removal, CB and 3V cells exhibited the ability to differentiate into neurons, astrocytes, and oligodendrocytes, suggesting that these cells were multipotent. Our results are consistent with previous observations on the differentiation potential of neurospheres isolated from CB of adult mouse (Alcock and Sottile, 2009) and 3V of adult mouse (Robins et al., 2013) and rats (Xu et al., 2005). It is important for future work to approve that single stem cells from CB and 3V are capable of generating neurons, astrocytes, and oligodendrocytes. Although his study didn't provide the evidence that the isolated NSCs from the adult CB and 3V corresponded to BG and tanycytes respectively. However, the radial glial phenotype of both BG and tanycytes described in our study support our conclusion that both cells might represent two NSCs populations in the CB and 3V respectively. This observation suggests that BG and tanycytes may possess similar properties of astrocytes of the SVZ in the adult rodent brain (Doetsch et al., 1999). Evidence from this thesis and elsewhere

(Sottile et al., 2006, Alcock and Sottile, 2009, Xu et al., 2005, Lee et al., 2012, Robins et al., 2013) suggest that BG in the cerebellar cortex and tanycytes lining the 3V are strong NSCs candidates in the adult brain and that the CB and 3V might be two new neurogenic areas in the adult brain yet to be clarified.

Two types of cells lining the 3V, the tanycytes located at the ventral two thirds of the 3V and ependymocytes occupy the dorsal third (Rodriguez et al., 2005). This raises an important question concerning which cell type in the 3V wall represent the NSCs population. Numerous studies in the literature have suggested that tanycytes are the NSCs of the 3V (Xu et al., 2005, Lee et al., 2012, Robins et al., 2013). The fact that tanycytes might be descendants of the embryonic radial glia that persist as specialised radial glial cells in the adult 3V strengths the hypothesis that tanycytes might be NSCs in the adult brain (Rodriguez et al., 2005). The coexpression of Sox1 with GFAP in the tanycytes population demonstrated in my study (Chapter 6) and the lack of coexpression in the ependymocytes appear to support the idea of tanycytes being strong candidate as NSCs in the hypothalamic 3V. Observation from the literature also support the concept of tanycytes as NSCs of the hypothalamus revealed by the formation of neurospheres and the response of α-tanycytes in adult mice to proliferate following FGF-2 infusion in vivo (Robins et al., 2013). Other lineage tracing studies have shown that β-tanycytes proliferate and generate neurons in response to high fat diet (Lee et al., 2012). These observations suggest that α-tanycytes and β-tanycytes differ in respect to their response to mitogens and other hormonal stimuli (Lee et al., 2012, Robins et al., 2013).

7.3 EGF and FGF-2 as mitogens for CB derived NSCs

This is the first study that looked at the effect of EGF and FGF-2 withdrawal on CB-derived NSCs. Thus, our attempt was to analyse the influence of EGF and FGF-2 on the proliferation and differentiation capacity of CB and 3V derived NSCs. Our results demonstrated that EGF and FGF-2 supported the growth and survival of CB and 3V derived NSCs as described for LV cells, suggesting that EGF and FGF-2 were mitogenic for both cell types. This observation is consistent with a number of in vitro studies showing that the addition of EGF and FGF-2 support the isolation and long-term in vitro survival and expansion of NSCs (Reviewed in (Kuhn et al., 1997)). My data showed that EGF and FGF-2 have mitogenic action and can maintain and support the growth and proliferation of CB and 3V NSCs as previously described for NSCs from other regions of the brain (Tropepe et al., 1999, Zhu et al., 1999). It was also noticed that the growth and proliferation of CB and 3V cells were significantly affected when one of the growth factors was removed from the culturing medium, suggesting that combination of EGF and FGF-2 increased the proliferation of these cells in line with reports in the literature (Weiss et al., 1996, Gritti et al., 1996). I also noticed that LV cells in FGF-2 alone generated more neurons than EGF in LV culture, whereas CB cells cultured in EGF produced more neurons than FGF-2. This would suggest that although EGF and FGF-2 acted as mitogens for the growth and proliferation of CB and LV cells, but their effect on fate determination differs between the two populations. This might reflect the diversity of NSCs population in different regions of adult brain although both CB and LV NSCs populations shared common features such as multipotency and the ability to form neurospheres.

My finding suggest that CB-NSCs maintain multipotentiality when EGF or FGF were used and that withdrawal of either EGF or FGF-2 for long period did not alter the capacity of CB derived NSCs to commit neuronal or glial fates. Taken together, these results indicate that EGF and FGF-2 may expand distinct NSC populations in the brain and may have differential effect on their lineage restriction with FGF-2 tend to increase neuronal number while EGF induce glial differentiation (Gritti et al., 1996, Whittemore et al., 1999, Johe et al., 1996).

7.4 Bergmann glia in the PCD^{5J} mutant mice

The Purkinje cell degeneration (pcd) is regarded as a classic ataxia mutant that has been used as an animal model to provide insights into the process of neuron degeneration in the cerebellum (Hatten et al., 1997).

Our quantitative analysis showed that the numbers of Sox1, Sox2, and Sox9 positive BG were increased in the mutant *pcd* mice. However, our data indicated that the number of BG was not affected in the mutant mice at early time points (P17, 21, and 26) but increased significantly by P100. Abnormalities of BG in the number, morphology, and distribution of Bergmann fibers became very apparent after 3 months in the *pcd* mice. In our study, PC loss caused severe gliosis characterised by upregulation of GFAP, morphological changes and BG proliferation as reported by Baltanas et al (2013). We also noticed cerebellar cortical atrophy at P100 characterised by the shrinkage of the ML and IGL as a result of PCs loss.

During cerebellar development, BG cells help in guiding the migration of granule cells and also provide a scaffold for the PCs dendrites (Sudarov and Joyner,

2007). Injury to the CB induces the reactive Bergmann gliosis which is characterised by increased expression of GFAP as observed in this study and in other studies (Sofroniew and Vinters, 2010, Gelpi et al., 2014). Reactive gliosis can also induce the proliferation of astrocytes in case of severe brain injury as observed in our study (Sofroniew, 2005). Thus, the increased expression of GFAP and the reactive Bergmann gliosis observed in this study might be induced by the change of interactions between BG and PCs as a result of PCs loss. In normal adult CB, BG are shown to be quiescent and negative for Nestin marker (Dahlstrand et al., 1995, Mignone et al., 2004), however, BG have been observed to re-express Nestin following CB injury in *pcd* mice (Sotelo et al., 1994, Sotelo, 2004). We did not observe any Nestin re-expression in the *pcd* mice at late time points of the disease. The loss of PCs in the *pcd* mice may explain the difference between our results and that of Sotelo et al., (1994), and that in his study the re-expression of Nestin by BG of the host tissue was needed to guide the migration of the grafted embryonic PCs. This observation suggests that BG may only plastic and re-express Nestin in the presence of embryonic neurons and then disappear after the migratory process is finished (Sotelo et al., 1994, Sotelo, 2004). Alternatively it might be that the grafted embryonic PCs induced the host BG to transiently re-express molecules that is important for their migration, or may be the age of embryonic astrocytes (E12) allowed the expression of signal factors required for their migration and acquisition of BG phenotype and thus supported the migration of the grafted PCs (Sotelo et al., 1994). Additionally, the age of the *pcd* animals used in our study (P17, P21, P26, and P100) differed from the *pcd* mice (3 and 4 months) used as host in Sotelo et al., (1994) study. We conclude that BG cells are activated following cerebellar degeneration but they are unable

to regenerate the lost PCs in *pcd*^{5J} mutant mice under normal disease progression and may lack the appropriate molecular signals needed for cellular repair. Future in vivo studies in CB affected disorders such as *pcd* mice are needed to examine the regenerative capacity of BG to replace the lost PCs.

7.5 Conclusion and future directions

The results from this study indicated that populations of neural like-stem cells are present in the mature CB and 3V, based on the expression of NSCs markers and in vitro ability to form neurospheres and generating neurons, astrocytes, and oligodendrocytes. It worth mentioning that my thesis has presented enough evidence that the adult CB and 3V contain NSCs. The limitation was that we couldn't precisely identify their identity. However, our NSCs marker analysis indicated that these populations might be BG and tanycytes of the CB and 3V respectively. Further evidence support our conclusion is that the BG was the only radial glial cells that underwent gliosis following CB injury (Chapter 5) and increased in number. Thus, it would be interesting to perform lineage tracing experiments for BG and tanycytes subpopulations to characterise the neural stem/progenitor cells in the lining of the CB and the 3V.

Characterisation of CB and 3V derived NSCs will provide crucial insight into the aetiology of brain disorders and allow the possibility to study the contribution of endogenous NSC populations to CNS repair. Furthermore, studies have shown that quiescent astrocytes in the cerebral cortex of adult mouse start to proliferative and undergo reactive gliosis after inducing brain injury. The fact that BG may under specific circumstances be able to re-express Nestin after injury in vivo (Sotelo et al., 1994), together with the ability to expand NSCs derived from the CB suggest that this radial glial population may represent a quiescent stem-like that could be stimulated under certain circumstances which could be of therapeutic value for CB repair.

I believe that my thesis produced enough evidences that the mature CB and the 3V harbour a population of cells that show stem cell characteristic features similar to well-known NSCs in the adult brain. Moreover, NSCs can be isolated from both regions of adult mouse and can be propagated in the presence of EGF an FGF-2. Thus, future studies will be important to test whether EGF or FGF-2 alone is sufficient to generate NSCs from the mature CB expansion in either EGF or FGF-2 promote the differentiation of NSCs toward neuronal or glial fates. I have also presented evidence that BG undergo morphological and molecular changes after the degeneration of PCs in *pcd*^{5J} mutant mouse that lead to Bergmann gliosis. It is important to evaluate the potential regenerative ability of BG within the *pcd* CB. One way to achieve approach is by in vitro organotypic slice culture model using CB of *pcd* mutant and wild type mice. One advantage of tissue slice culture over other in vitro systems is that it maintains the morphological architecture and physiological state and preserves neuronal activities with intact functional local synaptic circuitry. This approach is needed to:

1. Determine whether BG can be activated in response to the degeneration of PCs and investigate their specification, migration and differentiation capacity toward the damaged areas.
2. Determine whether the CB of *pcd* mice show appropriate environment to allow grafted CB derived NSCs to integrate and replace the lost PCs.

References

AHMED, A. I., SHTAYA, A. B., ZABEN, M. J., OWENS, E. V., KIECKER, C. & GRAY, W. P. 2012. Endogenous GFAP-positive neural stem/progenitor cells in the postnatal mouse cortex are activated following traumatic brain injury. *J Neurotrauma,* 29**,** 828-42.

AHMED, E. I., ZEHR, J. L., SCHULZ, K. M., LORENZ, B. H., DONCARLOS, L. L. & SISK, C. L. 2008. Pubertal hormones modulate the addition of new cells to sexually dimorphic brain regions. *Nature neuroscience,* 11**,** 995-997.

AHMED, S., REYNOLDS, B. A. & WEISS, S. 1995. BDNF enhances the differentiation but not the survival of CNS stem cell-derived neuronal precursors. *J Neurosci,* 15**,** 5765-78.

AKITA, K. & ARAI, S. 2009. The ataxic Syrian hamster: an animal model homologous to the pcd mutant mouse? *Cerebellum,* 8**,** 202-10.

ALCOCK, J., LOWE, J., ENGLAND, T., BATH, P. & SOTTILE, V. 2009. Expression of Sox1, Sox2 and Sox9 is maintained in adult human cerebellar cortex. *Neurosci Lett,* 450**,** 114-6.

ALCOCK, J., SCOTTING, P. & SOTTILE, V. 2007. Bergmann glia as putative stem cells of the mature cerebellum. *Med Hypotheses,* 69**,** 341-5.

ALCOCK, J. & SOTTILE, V. 2009. Dynamic distribution and stem cell characteristics of Sox1-expressing cells in the cerebellar cortex. *Cell Res,* 19**,** 1324-33.

ALTMAN, J. & DAS, G. 1965. Autoradiographic and histological evidence of postnatal hippocampal neurogenesis in rats. *J Comp Neurol,* 124**,** 319 - 335.

ALVAREZ-BUYLLA, A. & GARCIA-VERDUGO, J. 2002. Neurogenesis in adult subventricular zone. *J Neurosci,* 22**,** 629 - 634.

ALVAREZ-BUYLLA, A., GARCIA-VERDUGO, J. & TRAMONTIN, A. 2001. A unified hypothesis on the lineage of neural stem cells. *Nat Rev Neurosci,* 2**,** 287 - 293.

ALVAREZ-BUYLLA, A. & TEMPLE, S. 1998. Stem cells in the developing and adult nervous system. *J Neurobiol,* 36**,** 105-10.

ALVAREZ-BUYLLA, A., THEELEN, M. & NOTTEBOHM, F. 1990. Proliferation "hot spots" in adult avian ventricular zone reveal radial cell division. *Neuron,* 5**,** 101-9.

ANDERSON, D. J., GAGE, F. H. & WEISSMAN, I. L. 2001. Can stem cells cross lineage boundaries? *Nat Med,* 7**,** 393-5.

ANTHONY, T. E., KLEIN, C., FISHELL, G. & HEINTZ, N. 2004. Radial glia serve as neuronal progenitors in all regions of the central nervous system. *Neuron,* 41**,** 881-90.

ANTHONY, T. E., MASON, H. A., GRIDLEY, T., FISHELL, G. & HEINTZ, N. 2005. Brain lipid-binding protein is a direct target of Notch signaling in radial glial cells. *Genes & Development,* 19**,** 1028-1033.

APPS, R. & GARWICZ, M. 2005. Anatomical and physiological foundations of cerebellar information processing. *Nat Rev Neurosci,* 6**,** 297-311.

ARGENTE-ARIZÓN, P., FREIRE-REGATILLO, A., ARGENTE, J. & CHOWEN, J. A. 2015. Role of non-neuronal cells in body weight and appetite control. *Frontiers in Endocrinology,* 6.

ASTORI, S., LUJAN, R. & KOHR, G. 2009. GABA release from cerebellar stellate cells is developmentally regulated by presynaptic GABA(B) receptors in a target-cell-specific manner. *Eur J Neurosci.*

AUBERT, J., STAVRIDIS, M. P., TWEEDIE, S., O'REILLY, M., VIERLINGER, K., LI, M., GHAZAL, P., PRATT, T., MASON, J. O., ROY, D. & SMITH, A. 2003. Screening for mammalian neural genes via fluorescence-activated cell sorter purification of neural precursors from Sox1-gfp knock-in mice. *Proc Natl Acad Sci U S A,* 100 Suppl 1**,** 11836-41.

BALTANAS, F. C., BERCIANO, M. T., VALERO, J., GOMEZ, C., DIAZ, D., ALONSO, J. R., LAFARGA, M. & WERUAGA, E. 2013. Differential glial activation during the degeneration of Purkinje cells and mitral cells in the PCD mutant mice. *Glia,* 61**,** 254-72.

BALTANAS, F. C., CASAFONT, I., LAFARGA, V., WERUAGA, E., ALONSO, J. R., BERCIANO, M. T. & LAFARGA, M. 2011. Purkinje cell degeneration in pcd mice reveals large scale chromatin reorganization and gene silencing linked to defective DNA repair. *J Biol Chem,* 286**,** 28287-302.

BARRAUD, P., THOMPSON, L., KIRIK, D., BJORKLUND, A. & PARMAR, M. 2005. Isolation and characterization of neural precursor cells from the Sox1-GFP reporter mouse. *Eur J Neurosci,* 22**,** 1555-69.

BAUMANN, N. & PHAM-DINH, D. 2001. Biology of oligodendrocyte and myelin in the mammalian central nervous system. *Physiol Rev,* 81**,** 871-927.

BAUMEL, Y., JACOBSON, G. A. & COHEN, D. 2009. Implications of functional anatomy on information processing in the deep cerebellar nuclei. *Front Cell Neurosci,* 3**,** 14.

BAYATTI, N. & ENGELE, J. 2002. Cyclic AMP differentially regulates the expression of fibroblast growth factor and epidermal growth factor receptors in cultured cortical astroglia. *Neuroscience,* 114**,** 81-9.

BAZAN, E., ALONSO, F. J., REDONDO, C., LOPEZ-TOLEDANO, M. A., ALFARO, J. M., REIMERS, D., HERRANZ, A. S., PAINO, C. L., SERRANO, A. B., COBACHO, N., CASO, E. & LOBO, M. V. 2004. In vitro and in vivo characterization of neural stem cells. *Histol Histopathol,* 19**,** 1261-75.

BELLAMY, T. C. 2006. Interactions between Purkinje neurones and Bergmann glia. *Cerebellum,* 5**,** 116-26.

BENNETT, L., YANG, M., ENIKOLOPOV, G. & IACOVITTI, L. 2009. Circumventricular organs: a novel site of neural stem cells in the adult brain. *Mol Cell Neurosci,* 41**,** 337-47.

BHARTIYA, D., BOHELER, K. R. & RAMESHWAR, P. 2013. Multipotent to Pluripotent Properties of Adult Stem Cells. *Stem Cells International,* 2013**,** 2.

BLAZQUEZ, J. L., GUERRA, M., PASTOR, F., PERUZZO, B., AMAT, P. & RODRIGUEZ, E. M. 2002. Antibodies obtained by xenotransplantation of organ-cultured median eminence specifically recognize hypothalamic tanycytes. *Cell Tissue Res,* 308**,** 241-53.

BOLBOREA, M. & DALE, N. 2013. Hypothalamic tanycytes: potential roles in the control of feeding and energy balance. *Trends Neurosci,* 36**,** 91-100.

BONAGUIDI, M. A., SONG, J., MING, G.-L. & SONG, H. 2012. A unifying hypothesis on mammalian neural stem cell properties in the adult hippocampus. *Current opinion in neurobiology,* 22**,** 754-761.

BONFANTI, L. & PERETTO, P. 2011. Adult neurogenesis in mammals--a theme with many variations. *Eur J Neurosci,* 34**,** 930-50.

BOWLES, J., SCHEPERS, G. & KOOPMAN, P. 2000. Phylogeny of the SOX family of developmental transcription factors based on sequence and structural indicators. *Dev Biol,* 227**,** 239-55.

BRAMANTI, V., TOMASSONI, D., AVITABILE, M., AMENTA, F. & AVOLA, R. 2010. Biomarkers of glial cell proliferation and differentiation in culture. *Front Biosci (Schol Ed),* 2**,** 558-70.

BRAZEL, C. Y., LIMKE, T. L., OSBORNE, J. K., MIURA, T., CAI, J., PEVNY, L. & RAO, M. S. 2005. Sox2 expression defines a heterogeneous population

of neurosphere-forming cells in the adult murine brain. *Aging Cell,* 4**,** 197-207.
BRUNI, J. E. 1998. Ependymal development, proliferation, and functions: a review. *Microsc Res Tech,* 41**,** 2-13.
BRUNNE, B., ZHAO, S., DEROUICHE, A., HERZ, J., MAY, P., FROTSCHER, M. & BOCK, H. H. 2010. Origin, maturation, and astroglial transformation of secondary radial glial cells in the developing dentate gyrus. *Glia,* 58**,** 1553-69.
BUFFO, A., RITE, I., TRIPATHI, P., LEPIER, A., COLAK, D., HORN, A. P., MORI, T. & GOTZ, M. 2008. Origin and progeny of reactive gliosis: A source of multipotent cells in the injured brain. *Proc Natl Acad Sci U S A,* 105**,** 3581-6.
BUFFO, A. & ROSSI, F. 2013. Origin, lineage and function of cerebellar glia. *Prog Neurobiol,* 109**,** 42-63.
BURROWS, R. C., WANCIO, D., LEVITT, P. & LILLIEN, L. 1997. Response diversity and the timing of progenitor cell maturation are regulated by developmental changes in EGFR expression in the cortex. *Neuron,* 19**,** 251-67.
CAI, J., CHENG, A., LUO, Y., LU, C., MATTSON, M. P., RAO, M. S. & FURUKAWA, K. 2004. Membrane properties of rat embryonic multipotent neural stem cells. *Journal of Neurochemistry,* 88**,** 212-226.
CALDWELL, M. A., GARCION, E., TERBORG, M. G., HE, X. & SVENDSEN, C. N. 2004. Heparin stabilizes FGF-2 and modulates striatal precursor cell behavior in response to EGF. *Exp Neurol,* 188**,** 408-20.
CARLETTI, B. & ROSSI, F. 2005. Selective rather than inductive mechanisms favour specific replacement of Purkinje cells by embryonic cerebellar cells transplanted to the cerebellum of adult Purkinje cell degeneration (pcd) mutant mice. *Eur J Neurosci,* 22**,** 1001-12.
CARSON, F. L. 1997. Histotechnology: A Self-Instructional Text. Chicago: ASCP Press.
CASSIMERIS, L. & SPITTLE, C. 2001. Regulation of microtubule-associated proteins. *International Review of Cytology - a Survey of Cell Biology, Vol 210,* 210**,** 163-226.
CENDELIN, J. 2014. From mice to men: lessons from mutant ataxic mice. *Cerebellum Ataxias,* 1:4.
CHADASHVILI, T. & PETERSON, D. A. 2006. Cytoarchitecture of fibroblast growth factor receptor 2 (FGFR-2) immunoreactivity in astrocytes of neurogenic and non-neurogenic regions of the young adult and aged rat brain. *J Comp Neurol,* 498**,** 1-15.
CHAKRABARTI, L., ENG, J., IVANOV, N., GARDEN, G. A. & LA SPADA, A. R. 2009. Autophagy activation and enhanced mitophagy characterize the Purkinje cells of pcd mice prior to neuronal death. *Mol Brain,* 2**,** 24.
CHAKRABARTI, L., ENG, J., MARTINEZ, R. A., JACKSON, S., HUANG, J., POSSIN, D. E., SOPHER, B. L. & LA SPADA, A. R. 2008. The zinc-binding domain of Nna1 is required to prevent retinal photoreceptor loss and cerebellar ataxia in Purkinje cell degeneration (pcd) mice. *Vision Res,* 48**,** 1999-2005.
CHAKRABARTI, L., NEAL, J. T., MILES, M., MARTINEZ, R. A., SMITH, A. C., SOPHER, B. L. & LA SPADA, A. R. 2006. The Purkinje cell degeneration 5J mutation is a single amino acid insertion that destabilizes Nna1 protein. *Mamm Genome,* 17**,** 103-10.
CHAKRABARTI, L., ZAHRA, R., JACKSON, S. M., KAZEMI-ESFARJANI, P., SOPHER, B. L., MASON, A. G., TONEFF, T., RYU, S., SHAFFER, S., KANSY, J. W., ENG, J., MERRIHEW, G., MACCOSS, M. J., MURPHY, A., GOODLETT, D. R., HOOK, V., BENNETT, C. L., PALLANCK, L. J. & LA SPADA, A. R. 2010. Mitochondrial dysfunction in NnaD mutant flies and

Purkinje cell degeneration mice reveals a role for Nna proteins in neuronal bioenergetics. *Neuron,* 66**,** 835-47.
CHAMBERS, I. & TOMLINSON, S. R. 2009. The transcriptional foundation of pluripotency. *Development,* 136**,** 2311-22.
CHAUVET, N., PRIVAT, A. & ALONSO, G. 1996. Aged median eminence glial cell cultures promote survival and neurite outgrowth of cocultured neurons. *Glia,* 18**,** 211-23.
CHETVERUKHIN, V. & POLENOV, A. 1993. Ultrastructural radioautographic analysis of neurogenesis in the hypothalamus of the adult frog, Rana temporaria, with special reference to physiological regeneration of the preoptic nucleus. *Cell and Tissue Research,* 271**,** 341-350.
CHIZHIKOV, V. & MILLEN, K. J. 2003. Development and malformations of the cerebellum in mice. *Molecular Genetics and Metabolism,* 80**,** 54-65.
CHRISTIE, V. B. 2008. Evaluation and Comparison of Natural and Synthetic Retinoids on Models of Neural Development.

CHRISTIE, V. B., BARNARD, J. H., BATSANOV, A. S., BRIDGENS, C. E., CARTMELL, E. B., COLLINGS, J. C., MALTMAN, D. J., REDFERN, C. P., MARDER, T. B., PRZYBORSKI, S. & WHITING, A. 2008. Synthesis and evaluation of synthetic retinoid derivatives as inducers of stem cell differentiation. *Org Biomol Chem,* 6**,** 3497-507.
CICCOLINI, F. 2001. Identification of two distinct types of multipotent neural precursors that appear sequentially during CNS development. *Mol Cell Neurosci,* 17**,** 895-907.
CICCOLINI, F., MANDL, C., HÖLZL-WENIG, G., KEHLENBACH, A. & HELLWIG, A. 2005. Prospective isolation of late development multipotent precursors whose migration is promoted by EGFR. *Developmental Biology,* 284**,** 112-125.
CICCOLINI, F. & SVENDSEN, C. N. 1998. Fibroblast growth factor 2 (FGF-2) promotes acquisition of epidermal growth factor (EGF) responsiveness in mouse striatal precursor cells: identification of neural precursors responding to both EGF and FGF-2. *J Neurosci,* 18**,** 7869-80.
CLARKE, D. L. 2003. Neural stem cells. *Bone Marrow Transplant,* 32 Suppl 1**,** S13-7.
COLLIGNON, J., SOCKANATHAN, S., HACKER, A., COHEN-TANNOUDJI, M., NORRIS, D., RASTAN, S., STEVANOVIC, M., GOODFELLOW, P. N. & LOVELL-BADGE, R. 1996. A comparison of the properties of Sox-3 with Sry and two related genes, Sox-1 and Sox-2. *Development,* 122**,** 509-20.
CONTI, L. & CATTANEO, E. 2010. Neural stem cell systems: physiological players or in vitro entities? *Nat Rev Neurosci,* 11**,** 176-87.
CONTI, L., POLLARD, S. M., GORBA, T., REITANO, E., TOSELLI, M., BIELLA, G., SUN, Y., SANZONE, S., YING, Q.-L., CATTANEO, E. & SMITH, A. 2005. Niche-Independent Symmetrical Self-Renewal of a Mammalian Tissue Stem Cell. *PLoS Biology,* 3**,** e283.
CORTÉS-CAMPOS, C., ELIZONDO, R., LLANOS, P., URANGA, R. M., NUALART, F. & GARCÍA, M. A. 2011. MCT Expression and Lactate Influx/Efflux in Tanycytes Involved in Glia-Neuron Metabolic Interaction. *PLoS ONE,* 6**,** e16411.
COUTU, D. L. & GALIPEAU, J. 2011. Roles of FGF signaling in stem cell self-renewal, senescence and aging. *Aging (Albany NY),* 3**,** 920-933.
CRAIG, VINCE TROPEPE, CINDI M. MORSHEAD, BRENT A. REYNOLDS, SAMUEL WEISS & KOOY, A. D. V. D. 1996. In Viva Growth Factor Expansion of Endogenous Subependymal Neural Precursor Cell Populations in the Adult Mouse Brain. *The Journal of Neuroscience,,* 16(8):**,** 2649-2658.

CRESPEL, A., RIGAU, V., COUBES, P., ROUSSET, M. C., DE BOCK, F., OKANO, H., BALDY-MOULINIER, M., BOCKAERT, J. & LERNER-NATOLI, M. 2005. Increased number of neural progenitors in human temporal lobe epilepsy. *Neurobiol Dis,* 19**,** 436-50.

DAHLSTRAND, J., LARDELLI, M. & LENDAHL, U. 1995. Nestin mRNA expression correlates with the central nervous system progenitor cell state in many, but not all, regions of developing central nervous system. *Brain Res Dev Brain Res,* 84**,** 109-29.

DALE, N. 2011. Purinergic signaling in hypothalamic tanycytes: potential roles in chemosensing. *Semin Cell Dev Biol,* 22**,** 237-44.

DANIEL, P. M. 1976. Anatomy of the hypothalamus and pituitary gland. *Journal of Clinical Pathology. Supplement (Ass. Clin. Path.),* 7**,** 1-7.

DAVIS, S. F., HOOD, J., THOMAS, A. & BUNNELL, B. A. 2006. Isolation of adult rhesus neural stem and progenitor cells and differentiation into immature oligodendrocytes. *Stem Cells and Development,* 15**,** 191-199.

DE ROBERTIS, E. M. & KURODA, H. 2004. Dorsal-ventral patterning and neural induction in Xenopus embryos. *Annu Rev Cell Dev Biol,* 20**,** 285-308.

DIETRICH, J. & KESARI, S. 2009. Effect of cancer treatment on neural stem and progenitor cells. *Cancer Treat Res,* 150**,** 81-95.

DOETSCH, LEOPOLDO PETREANU, ISABELLE CAILLE, JOSE-MANUEL GARCIA-VERDUGO & ALVAREZ-BUYLLA, A. 2002. EGF Converts Transit-Amplifying Neurogenic Precursors in the Adult Brain into Multipotent Stem Cells.

DOETSCH, F. 2003. A niche for adult neural stem cells. *Curr Opin Genet Dev,* 13**,** 543-50.

DOETSCH, F., CAILLE, I., LIM, D. A., GARCIA-VERDUGO, J. M. & ALVAREZ-BUYLLA, A. 1999. Subventricular zone astrocytes are neural stem cells in the adult mammalian brain. *Cell,* 97**,** 703-16.

DOETSCH, F., GARCIA-VERDUGO, J. M. & ALVAREZ-BUYLLA, A. 1997. Cellular composition and three-dimensional organization of the subventricular germinal zone in the adult mammalian brain. *J Neurosci,* 17**,** 5046-61.

DOETSCH, F. & HEN, R. 2005. Young and excitable: the function of new neurons in the adult mammalian brain. *Curr Opin Neurobiol,* 15**,** 121-8.

DONO, R. 2003. Fibroblast growth factors as regulators of central nervous system development and function. *Am J Physiol Regul Integr Comp Physiol,* 284**,** R867-81.

DOREY, K. & AMAYA, E. 2010. FGF signalling: diverse roles during early vertebrate embryogenesis. *Development,* 137**,** 3731-42.

DREUX, A. C., LAMB, D. J., MODJTAHEDI, H. & FERNS, G. A. 2006. The epidermal growth factor receptors and their family of ligands: their putative role in atherogenesis. *Atherosclerosis,* 186**,** 38-53.

DURR, A. 2010. Autosomal dominant cerebellar ataxias: polyglutamine expansions and beyond. *Lancet Neurol,* 9**,** 885-94.

DYER, C. A., PHILLBOTTE, T., WOLF, M. K. & BILLINGS-GAGLIARDI, S. 1997. Regulation of cytoskeleton by myelin components: studies on shiverer oligodendrocytes carrying an Mbp transgene. *Dev Neurosci,* 19**,** 395-409.

EINSTEIN, O., BEN-MENACHEM-TZIDON, O., MIZRACHI-KOL, R., REINHARTZ, E., GRIGORIADIS, N. & BEN-HUR, T. 2006. Survival of neural precursor cells in growth factor-poor environment: implications for transplantation in chronic disease. *Glia,* 53**,** 449-55.

ELIAS, L. A. B., WANG, D. D. & KRIEGSTEIN, A. R. 2007. Gap junction adhesion is necessary for radial migration in the neocortex. *Nature,* 448**,** 901-907.

ELLIS, P., FAGAN, B. M., MAGNESS, S. T., HUTTON, S., TARANOVA, O., HAYASHI, S., MCMAHON, A., RAO, M. & PEVNY, L. 2004. SOX2, a persistent marker for multipotential neural stem cells derived from embryonic stem cells, the embryo or the adult. *Dev Neurosci,* 26**,** 148-65.

ENG, L. F., GHIRNIKAR, R. S. & LEE, Y. L. 2000. Glial fibrillary acidic protein: GFAP-thirty-one years (1969-2000). *Neurochemical Research,* 25**,** 1439-1451.

EVANS, M. J. & KAUFMAN, M. H. 1981. Establishment in culture of pluripotential cells from mouse embryos. *Nature,* 292**,** 154-6.

FENG, L., HATTEN, M. E. & HEINTZ, N. 1994. Brain Lipid-Binding Protein (Blbp) - a Novel Signaling System in the Developing Mammalian Cns. *Neuron,* 12**,** 895-908.

FERNANDEZ-GONZALEZ, A., LA SPADA, A. R., TREADAWAY, J., HIGDON, J. C., HARRIS, B. S., SIDMAN, R. L., MORGAN, J. I. & ZUO, J. 2002. Purkinje cell degeneration (pcd) phenotypes caused by mutations in the axotomy-induced gene, Nna1. *Science,* 295**,** 1904-6.

FERRI, A. L. M., CAVALLARO, M., BRAIDA, D., DI CRISTOFANO, A., CANTA, A., VEZZANI, A., OTTOLENGHI, S., PANDOLFI, P. P., SALA, M., DEBIASI, S. & NICOLIS, S. K. 2004. Sox2 deficiency causes neurodegeneration and impaired neurogenesis in the adult mouse brain. *Development,* 131**,** 3805-3819.

FISCHER, A. J. & REH, T. A. 2001. Muller glia are a potential source of neural regeneration in the postnatal chicken retina. *Nat Neurosci,* 4**,** 247-252.

FLAMENT-DURAND, J. & BRION, J. P. 1985. Tanycytes: morphology and functions: a review. *Int Rev Cytol,* 96**,** 121-55.

FORD-PERRISS, M., ABUD, H. & MURPHY, M. 2001. Fibroblast growth factors in the developing central nervous system. *Clin Exp Pharmacol Physiol,* 28**,** 493-503.

FRANCIS, F., KOULAKOFF, A., BOUCHER, D., CHAFEY, P., SCHAAR, B., VINET, M. C., FRIOCOURT, G., MCDONNELL, N., REINER, O., KAHN, A., MCCONNELL, S. K., BERWALD-NETTER, Y., DENOULET, P. & CHELLY, J. 1999. Doublecortin is a developmentally regulated, microtubule-associated protein expressed in migrating and differentiating neurons. *Neuron,* 23**,** 247-56.

FRAYLING, C., BRITTON, R. & DALE, N. 2011. ATP-mediated glucosensing by hypothalamic tanycytes. *J Physiol,* 589**,** 2275-86.

GAGE, F. H. 2000. Mammalian neural stem cells. *Science,* 287**,** 1433-8.

GAGE, F. H., COATES, P. W., PALMER, T. D., KUHN, H. G., FISHER, L. J., SUHONEN, J. O., PETERSON, D. A., SUHR, S. T. & RAY, J. 1995. Survival and differentiation of adult neuronal progenitor cells transplanted to the adult brain. *Proc Natl Acad Sci U S A,* 92**,** 11879-83.

GARCEZ, R. C., TEIXEIRA, B. L., SCHMITT SDOS, S., ALVAREZ-SILVA, M. & TRENTIN, A. G. 2009. Epidermal growth factor (EGF) promotes the in vitro differentiation of neural crest cells to neurons and melanocytes. *Cell Mol Neurobiol,* 29**,** 1087-91.

GELPI, E., BOMBI, J. A., MARTINEZ-SAEZ, E., CARAL, L. & RIBALTA, T. 2014. Prominent EMA 'dots' in tumour-induced Bergmann gliosis. *Histopathology,* 64**,** 445-52.

GIMENEZ, Y. R. M., LANGA, F., MENET, V. & PRIVAT, A. 2000. Comparative anatomy of the cerebellar cortex in mice lacking vimentin, GFAP, and both vimentin and GFAP. *Glia,* 31**,** 69-83.

GOETZ, R. & MOHAMMADI, M. 2013. Exploring mechanisms of FGF signalling through the lens of structural biology. *Nature reviews. Molecular cell biology,* 14**,** 166-180.
GOLDOWITZ, D. & HAMRE, K. 1998. The cells and molecules that make a cerebellum. *Trends Neurosci,* 21**,** 375-82.
GÖTZ, M. 2003. Glial Cells Generate Neurons—Master Control within CNS Regions: Developmental Perspectives on Neural Stem Cells. *The Neuroscientist,* 9**,** 379-397.
GOULD, E. 2007. How widespread is adult neurogenesis in mammals? *Nat Rev Neurosci,* 8**,** 481-488.
GOULD, E., BEYLIN, A., TANAPAT, P., REEVES, A. & SHORS, T. J. 1999. Learning enhances adult neurogenesis in the hippocampal formation. *Nat Neurosci,* 2**,** 260-5.
GRAEBER, M. B. & STREIT, W. J. 2010. Microglia: biology and pathology. *Acta Neuropathol,* 119**,** 89-105.
GRAHAM, V., KHUDYAKOV, J., ELLIS, P. & PEVNY, L. 2003. SOX2 Functions to Maintain Neural Progenitor Identity. *Neuron,* 39**,** 749-765.
GRANDEL, H. & BRAND, M. 2013. Comparative aspects of adult neural stem cell activity in vertebrates. *Dev Genes Evol,* 223**,** 131-47.
GRANDEL, H., KASLIN, J., GANZ, J., WENZEL, I. & BRAND, M. 2006. Neural stem cells and neurogenesis in the adult zebrafish brain: Origin, proliferation dynamics, migration and cell fate. *Developmental Biology,* 295**,** 263-277.
GRAY, G. E. & SANES, J. R. 1992. Lineage of radial glia in the chicken optic tectum. *Development,* 114**,** 271-83.
GRITTI, E. A. PARATI, L. COVA, P. FROLICHSTHAL, GALL, R., E. WANKE, Z. L., FARAVELLI, D. J. MORASSUTTI, F. ROISEN, D. D. NICKEL & VESCOVI', A. A. L. 1996. Mul tipotential Stem Cells from the Adult Mouse Brain Proliferate and Self-Renew in Response to Basic Fibroblast Growth Factor

GRITTI, PAOLA FRO¨ LICHSTHAL-SCHOELLER, ROSSELLA GALLI, EUGENIO A. PARATI, LIDIA COVA, STEFANO F. PAGANO, CHRISTOPHER R. BJORNSON & VESCOVI, A. L. 1999. Epidermal and Fibroblast Growth Factors Behave as Mitogenic Regulators for a Single Multipotent Stem Cell-Like Population from the Subventricular Region of the Adult Mouse Forebrain.

GRITTI, A., BONFANTI, L., DOETSCH, F., CAILLE, I., ALVAREZ-BUYLLA, A., LIM, D. A., GALLI, R., VERDUGO, J. M., HERRERA, D. G. & VESCOVI, A. L. 2002. Multipotent neural stem cells reside into the rostral extension and olfactory bulb of adult rodents. *J Neurosci,* 22**,** 437-45.
GRITTI ET AL. 2001. Cultures of Stem Cells of the Central Nervous System.

GROSCHE, J., KETTENMANN, H. & REICHENBACH, A. 2002. Bergmann glial cells form distinct morphological structures to interact with cerebellar neurons. *J Neurosci Res,* 68**,** 138-49.
GUDINO-CABRERA, G. & NIETO-SAMPEDRO, M. 2000. Schwann-like macroglia in adult rat brain. *Glia,* 30**,** 49-63.
HAAN, N., GOODMAN, T., NAJDI-SAMIEI, A., STRATFORD, C. M., RICE, R., EL AGHA, E., BELLUSCI, S. & HAJIHOSSEINI, M. K. 2013. Fgf10-expressing tanycytes add new neurons to the appetite/energy-balance regulating centers of the postnatal and adult hypothalamus. *J Neurosci,* 33**,** 6170-80.
HACHEM, S., LAURENSON, A. S., HUGNOT, J. P. & LEGRAVEREND, C. 2007. Expression of S100B during embryonic development of the mouse cerebellum. *BMC Dev Biol,* 7**,** 17.

HALTERMAN, M. W. 2005. Neuroscience, 3rd Edition. *Neurology,* 64**,** 769-769-a.
HARADA, A., TENG, J., TAKEI, Y., OGUCHI, K. & HIROKAWA, N. 2002. MAP2 is required for dendrite elongation, PKA anchoring in dendrites, and proper PKA signal transduction. *J Cell Biol,* 158**,** 541-9.
HARRIS, A., MORGAN, J. I., PECOT, M., SOUMARE, A., OSBORNE, A. & SOARES, H. D. 2000. Regenerating motor neurons express Nna1, a novel ATP/GTP-binding protein related to zinc carboxypeptidases. *Mol Cell Neurosci,* 16**,** 578-96.
HARRIS, R. C., CHUNG, E. & COFFEY, R. J. 2003. EGF receptor ligands. *Exp Cell Res,* 284**,** 2-13.
HARTFUSS, E., GALLI, R., HEINS, N. & GOTZ, M. 2001. Characterization of CNS precursor subtypes and radial glia. *Dev Biol,* 229**,** 15-30.
HATTEN, M. E., ALDER, J., ZIMMERMAN, K. & HEINTZ, N. 1997. Genes involved in cerebellar cell specification and differentiation. *Curr Opin Neurobiol,* 7**,** 40-7.
HAUNERLAND, N. H. & SPENER, F. 2004. Fatty acid-binding proteins--insights from genetic manipulations. *Prog Lipid Res,* 43**,** 328-49.
HAWKES, R. B. 2001. Cerebellum: Anatomy and Organization. *eLS.* John Wiley & Sons, Ltd.
HERBST, R. S. 2004. Review of epidermal growth factor receptor biology. *Int J Radiat Oncol Biol Phys,* 59**,** 21-6.
HERRUP, K. & KUEMERLE, B. 1997. The compartmentalization of the cerebellum. *Annu Rev Neurosci,* 20**,** 61-90.
HOCKFIELD, S. & MCKAY, R. D. 1985. Identification of major cell classes in the developing mammalian nervous system. *J Neurosci,* 5**,** 3310-28.
HORSTMANN, E. 1954. Die Faserglia des Selachiergehirns. *Zeitschrift für Zellforschung und Mikroskopische Anatomie,* 39**,** 588-617.
HOSHINO, M., NAKAMURA, S., MORI, K., KAWAUCHI, T., TERAO, M., NISHIMURA, Y. V., FUKUDA, A., FUSE, T., MATSUO, N., SONE, M., WATANABE, M., BITO, H., TERASHIMA, T., WRIGHT, C. V., KAWAGUCHI, Y., NAKAO, K. & NABESHIMA, Y. 2005. Ptf1a, a bHLH transcriptional gene, defines GABAergic neuronal fates in cerebellum. *Neuron,* 47**,** 201-13.
IHRIE, R. A. & ALVAREZ-BUYLLA, A. 2008. Cells in the astroglial lineage are neural stem cells. *Cell Tissue Res,* 331**,** 179-91.
IMURA, T., KORNBLUM, H. I. & SOFRONIEW, M. V. 2003. The predominant neural stem cell isolated from postnatal and adult forebrain but not early embryonic forebrain expresses GFAP. *J Neurosci,* 23**,** 2824-32.
IP, N. Y., LI, Y., YANCOPOULOS, G. D. & LINDSAY, R. M. 1993. Cultured hippocampal neurons show responses to BDNF, NT-3, and NT-4, but not NGF. *J Neurosci,* 13**,** 3394-405.
ISEKI, K., HAGINO, S., MORI, T., ZHANG, Y., YOKOYA, S., TAKAKI, H., TASE, C., MURAKAWA, M. & WANAKA, A. 2002. Increased syndecan expression by pleiotrophin and FGF receptor-expressing astrocytes in injured brain tissue. *Glia,* 39**,** 1-9.
JAYADEV, S. & BIRD, T. D. 2013. Hereditary ataxias: overview. *Genet Med,* 15**,** 673-83.
JIN, K. & GALVAN, V. 2007. Endogenous neural stem cells in the adult brain. *J Neuroimmune Pharmacol,* 2**,** 236-42.
JOHE, K. K., HAZEL, T. G., MULLER, T., DUGICH-DJORDJEVIC, M. M. & MCKAY, R. D. 1996. Single factors direct the differentiation of stem cells from the fetal and adult central nervous system. *Genes Dev,* 10**,** 3129-40.
JOYNER, A. L. 2002. *Establishment of anterior-posterior and dorsal-ventral pattern in the early central nervous system,* San Diego, Academic Press, .

KALININA, E., BISWAS, R., BEREZNIUK, I., HERMOSO, A., AVILES, F. X. & FRICKER, L. D. 2007. A novel subfamily of mouse cytosolic carboxypeptidases. *FASEB J,* 21**,** 836-50.

KALYANI, TAHMINA MUJTABA & RAO, M. S. 1998. Expression of EGF Receptor and FGF Receptor Isoforms during Neuroepithelial Stem Cell Differentiation.

KAN, L., JALALI, A., ZHAO, L. R., ZHOU, X., MCGUIRE, T., KAZANIS, I., EPISKOPOU, V., BASSUK, A. G. & KESSLER, J. A. 2007. Dual function of Sox1 in telencephalic progenitor cells. *Dev Biol,* 310**,** 85-98.

KANDEL, E., SCHWARTZ, J., AND JESSELL T. 2000. Principles of Neural Science. New York: McGraw-Hill.

KASLIN, J., GANZ, J. & BRAND, M. 2008. Proliferation, neurogenesis and regeneration in the non-mammalian vertebrate brain. *Philosophical Transactions of the Royal Society B: Biological Sciences,* 363**,** 101-122.

KEEFE, L. J., SONDEK, J., SHORTLE, D. & LATTMAN, E. E. 1993. The alpha aneurism: a structural motif revealed in an insertion mutant of staphylococcal nuclease. *Proceedings of the National Academy of Sciences,* 90**,** 3275-3279.

KENT, J., WHEATLEY, S. C., ANDREWS, J. E., SINCLAIR, A. H. & KOOPMAN, P. 1996. A male-specific role for SOX9 in vertebrate sex determination. *Development,* 122**,** 2813-22.

KIEFER, J. C. 2007. Back to basics: Sox genes. *Dev Dyn,* 236**,** 2356-66.

KIM, K., DEAN, D., MIKOS, A. G. & FISHER, J. P. 2009. Effect of initial cell seeding density on early osteogenic signal expression of rat bone marrow stromal cells cultured on cross-linked poly(propylene fumarate) disks. *Biomacromolecules,* 10**,** 1810-7.

KITCHENS, D. L., SNYDER, E. Y. & GOTTLIEB, D. I. 1994. FGF and EGF are mitogens for immortalized neural progenitors. *J Neurobiol,* 25**,** 797-807.

KLEIN, C., BUTT, S. J., MACHOLD, R. P., JOHNSON, J. E. & FISHELL, G. 2005. Cerebellum- and forebrain-derived stem cells possess intrinsic regional character. *Development,* 132**,** 4497-508.

KOBIELAK, A. & FUCHS, E. 2004. Alpha-catenin: at the junction of intercellular adhesion and actin dynamics. *Nat Rev Mol Cell Biol,* 5**,** 614-25.

KOIRALA, S. & CORFAS, G. 2010. Identification of novel glial genes by single-cell transcriptional profiling of Bergmann glial cells from mouse cerebellum. *PLoS One,* 5**,** e9198.

KOKOEVA, M. V., YIN, H. & FLIER, J. S. 2005. Neurogenesis in the hypothalamus of adult mice: potential role in energy balance. *Science,* 310**,** 679-83.

KOKOEVA, M. V., YIN, H. & FLIER, J. S. 2007. Evidence for constitutive neural cell proliferation in the adult murine hypothalamus. *J Comp Neurol,* 505**,** 209-20.

KOMITOVA, M. & ERIKSSON, P. S. 2004. Sox-2 is expressed by neural progenitors and astroglia in the adult rat brain. *Neuroscience Letters,* 369**,** 24-27.

KOMURO, H., YACUBOVA, E., YACUBOVA, E. & RAKIC, P. 2001. Mode and tempo of tangential cell migration in the cerebellar external granular layer. *J Neurosci,* 21**,** 527-40.

KORDES, U., CHENG, Y. C. & SCOTTING, P. J. 2005. Sox group E gene expression distinguishes different types and maturational stages of glial cells in developing chick and mouse. *Brain Res Dev Brain Res,* 157**,** 209-13.

KOTAI, I., HAJOS, F. & SERESS, L. 1989. Comparative study of glial fibrillary acidic protein (GFAP)--immunoreactivity in the rat and monkey cerebellum. *Acta Morphol Hung,* 37**,** 85-92.

KRIEGSTEIN, A. R. & GOTZ, M. 2003. Radial glia diversity: a matter of cell fate. *Glia,* 43**,** 37-43.

KRISHNAN, K., MITRA, N. K., YEE, L. S. & YANG, H. M. 2012. A comparison of neurotoxicity in cerebellum produced by dermal application of chlorpyrifos in young and adult mice. *J Neural Transm,* 119**,** 345-52.

KUHN, H. G., WINKLER, J., KEMPERMANN, G., THAL, L. J. & GAGE, F. H. 1997. Epidermal growth factor and fibroblast growth factor-2 have different effects on neural progenitors in the adult rat brain. *J Neurosci,* 17**,** 5820-9.

LAFARGA, M., ANDRES, M. A., CALLE, E. & BERCIANO, M. T. 1998. Reactive gliosis of immature Bergmann glia and microglial cell activation in response to cell death of granule cell precursors induced by methylazoxymethanol treatment in developing rat cerebellum. *Anat Embryol (Berl),* 198**,** 111-22.

LALONDE, R. & STRAZIELLE, C. 2007. Spontaneous and induced mouse mutations with cerebellar dysfunctions: behavior and neurochemistry. *Brain Res,* 1140**,** 51-74.

LANDRY, C. F., IVY, G. O., DUNN, R. J., MARKS, A. & BROWN, I. R. 1989. Expression of the gene encoding the beta-subunit of S-100 protein in the developing rat brain analyzed by in situ hybridization. *Brain Res Mol Brain Res,* 6**,** 251-62.

LAYWELL, E. D., RAKIC, P., KUKEKOV, V. G., HOLLAND, E. C. & STEINDLER, D. A. 2000. Identification of a multipotent astrocytic stem cell in the immature and adult mouse brain. *Proc Natl Acad Sci U S A,* 97**,** 13883-8.

LEE, A., KESSLER, J. D., READ, T. A., KAISER, C., CORBEIL, D., HUTTNER, W. B., JOHNSON, J. E. & WECHSLER-REYA, R. J. 2005. Isolation of neural stem cells from the postnatal cerebellum. *Nat Neurosci,* 8**,** 723-9.

LEE, D. A., BEDONT, J. L., PAK, T., WANG, H., SONG, J., MIRANDA-ANGULO, A., TAKIAR, V., CHARUBHUMI, V., BALORDI, F., TAKEBAYASHI, H., AJA, S., FORD, E., FISHELL, G. & BLACKSHAW, S. 2012. Tanycytes of the hypothalamic median eminence form a diet-responsive neurogenic niche. *Nat Neurosci,* 15**,** 700-2.

LEFEBVRE, V., DUMITRIU, B., PENZO-MENDEZ, A., HAN, Y. & PALLAVI, B. 2007. Control of cell fate and differentiation by Sry-related high-mobility-group box (Sox) transcription factors. *Int J Biochem Cell Biol,* 39**,** 2195-214.

LENDAHL, U., ZIMMERMAN, L. B. & MCKAY, R. D. 1990. CNS stem cells express a new class of intermediate filament protein. *Cell,* 60**,** 585-95.

LETO, K., CARLETTI, B., WILLIAMS, I. M., MAGRASSI, L. & ROSSI, F. 2006. Different types of cerebellar GABAergic interneurons originate from a common pool of multipotent progenitor cells. *J Neurosci,* 26**,** 11682-94.

LI, H., BABIARZ, J., WOODBURY, J., KANE-GOLDSMITH, N. & GRUMET, M. 2004. Spatiotemporal heterogeneity of CNS radial glial cells and their transition to restricted precursors. *Dev Biol,* 271**,** 225-38.

LI, J., TANG, Y. & CAI, D. 2012. IKKbeta/NF-kappaB disrupts adult hypothalamic neural stem cells to mediate a neurodegenerative mechanism of dietary obesity and pre-diabetes. *Nat Cell Biol,* 14**,** 999-1012.

LI, L., LUNDKVIST, A., ANDERSSON, D., WILHELMSSON, U., NAGAI, N., PARDO, A. C., NODIN, C., STAHLBERG, A., APRICO, K., LARSSON, K., YABE, T., MOONS, L., FOTHERINGHAM, A., DAVIES, I., CARMELIET, P., SCHWARTZ, J. P., PEKNA, M., KUBISTA, M., BLOMSTRAND, F.,

MARAGAKIS, N., NILSSON, M. & PEKNY, M. 2008. Protective role of reactive astrocytes in brain ischemia. *J Cereb Blood Flow Metab,* 28**,** 468-81.
LI, M., PEVNY, L., LOVELL-BADGE, R. & SMITH, A. 1998. Generation of purified neural precursors from embryonic stem cells by lineage selection. *Current Biology,* 8**,** 971-974.
LI, M., PRICE, D. & SMITH, A. 2001. Lineage selection and isolation of neural precursors from embryonic stem cells. *Symp Soc Exp Biol***,** 29-42.
LILLIEN & RAPHAEL, A. 2000. BMP and FGF regulate the development of EGF-responsive neural progenitor cells.

LIN, R., CAI, J., NATHAN, C., WEI, X., SCHLEIDT, S., ROSENWASSER, R. & IACOVITTI, L. 2015. Neurogenesis is enhanced by stroke in multiple new stem cell niches along the ventricular system at sites of high BBB permeability. *Neurobiol Dis,* 74**,** 229-39.
LIU, Y., LIU, R. R., WANG, L., ZENG, L., LONG, Z. Y. & WU, Y. M. 2012. The effects of different phenotype astrocytes on neural stem cells differentiation in co-culture. *Neurosci Lett,* 508**,** 61-6.
LIU, Y. P., LANG, B. T., BASKAYA, M. K., DEMPSEY, R. J. & VEMUGANTI, R. 2009. The potential of neural stem cells to repair stroke-induced brain damage. *Acta Neuropathol,* 117**,** 469-80.
LOEFFLER & POTTEN 1997. Stem-like cells and cellular pedigrees—conceptual introduction. *Stem-like cells (Potten CS, ed), San Diego: Academic.,* pp 1–27.

LOPEZ-BAYGHEN, E. & ORTEGA, A. 2011. Glial glutamate transporters: new actors in brain signaling. *IUBMB Life,* 63**,** 816-23.
LUSKIN, M. B., ZIGOVA, T., SOTERES, B. J. & STEWART, R. R. 1997. Neuronal progenitor cells derived from the anterior subventricular zone of the neonatal rat forebrain continue to proliferate in vitro and express a neuronal phenotype. *Mol Cell Neurosci,* 8**,** 351-66.
MADEN, M. 2007. Retinoic acid in the development, regeneration and maintenance of the nervous system. *Nat Rev Neurosci,* 8**,** 755-65.
MALATESTA, P., HARTFUSS, E. & GOTZ, M. 2000. Isolation of radial glial cells by fluorescent-activated cell sorting reveals a neuronal lineage. *Development,* 127**,** 5253-5263.
MALTMAN, D. J., CHRISTIE, V. B., COLLINGS, J. C., BARNARD, J. H., FENYK, S., MARDER, T. B., WHITING, A. & PRZYBORSKI, S. A. 2009. Proteomic profiling of the stem cell response to retinoic acid and synthetic retinoid analogues: identification of major retinoid-inducible proteins. *Mol Biosyst,* 5**,** 458-71.
MARKAKIS, E. A., PALMER, T. D., RANDOLPH-MOORE, L., RAKIC, P. & GAGE, F. H. 2004. Novel neuronal phenotypes from neural progenitor cells. *J Neurosci,* 24**,** 2886-97.
MARTIN-IBANEZ, R., URBAN, N., SERGENT-TANGUY, S., PINEDA, J. R., GARRIDO-CLUA, N., ALBERCH, J. & CANALS, J. M. 2007. Interplay of leukemia inhibitory factor and retinoic acid on neural differentiation of mouse embryonic stem cells. *J Neurosci Res,* 85**,** 2686-701.
MASUI, S., NAKATAKE, Y., TOYOOKA, Y., SHIMOSATO, D., YAGI, R., TAKAHASHI, K., OKOCHI, H., OKUDA, A., MATOBA, R., SHAROV, A. A., KO, M. S. & NIWA, H. 2007. Pluripotency governed by Sox2 via regulation of Oct3/4 expression in mouse embryonic stem cells. *Nat Cell Biol,* 9**,** 625-35.
MAUK, M. D., MEDINA, J. F., NORES, W. L. & OHYAMA, T. 2000. Cerebellar function: coordination, learning or timing? *Curr Biol,* 10**,** R522-5.
MCKAY, R. 1997. Stem cells in the central nervous system. *Science,* 276**,** 66-71.

MCLENDON, R. E. & BIGNER, D. D. 1994. Immunohistochemistry of the glial fibrillary acidic protein: basic and applied considerations. *Brain Pathol,* 4**,** 221-8.
MENEZES, J. R. & LUSKIN, M. B. 1994. Expression of neuron-specific tubulin defines a novel population in the proliferative layers of the developing telencephalon. *J Neurosci,* 14**,** 5399-416.
MERKLE, F. T., TRAMONTIN, A. D., GARCIA-VERDUGO, J. M. & ALVAREZ-BUYLLA, A. 2004. Radial glia give rise to adult neural stem cells in the subventricular zone. *Proc Natl Acad Sci U S A,* 101**,** 17528-32.
MIGAUD, M., BATAILLER, M., SEGURA, S., DUITTOZ, A., FRANCESCHINI, I. & PILLON, D. 2010. Emerging new sites for adult neurogenesis in the mammalian brain: a comparative study between the hypothalamus and the classical neurogenic zones. *Eur J Neurosci,* 32**,** 2042-52.
MIGNONE, J. L., KUKEKOV, V., CHIANG, A. S., STEINDLER, D. & ENIKOLOPOV, G. 2004. Neural stem and progenitor cells in nestin-GFP transgenic mice. *J Comp Neurol,* 469**,** 311-24.
MING, G.-L. & SONG, H. 2011. Adult Neurogenesis in the Mammalian Brain: Significant Answers and Significant Questions. *Neuron,* 70**,** 687-702.
MORISHIMA, N., NAKANISHI, K., TAKENOUCHI, H., SHIBATA, T. & YASUHIKO, Y. 2002. An endoplasmic reticulum stress-specific caspase cascade in apoptosis. Cytochrome c-independent activation of caspase-9 by caspase-12. *J Biol Chem,* 277**,** 34287-94.
MORRISON, S. J. & KIMBLE, J. 2006. Asymmetric and symmetric stem-cell divisions in development and cancer. *Nature,* 441**,** 1068-74.
MORSHEAD, C. M., REYNOLDS, B. A., CRAIG, C. G., MCBURNEY, M. W., STAINES, W. A., MORASSUTTI, D., WEISS, S. & VAN DER KOOY, D. 1994. Neural stem cells in the adult mammalian forebrain: a relatively quiescent subpopulation of subependymal cells. *Neuron,* 13**,** 1071-82.
MUDO, G., BONOMO, A., DI LIBERTO, V., FRINCHI, M., FUXE, K. & BELLUARDO, N. 2009. The FGF-2/FGFRs neurotrophic system promotes neurogenesis in the adult brain. *J Neural Transm,* 116**,** 995-1005.
MUGURUMA, K., NISHIYAMA, A., KAWAKAMI, H., HASHIMOTO, K. & SASAI, Y. 2015. Self-organization of polarized cerebellar tissue in 3D culture of human pluripotent stem cells. *Cell Rep,* 10**,** 537-50.
MULLEN, R. J., BUCK, C. R. & SMITH, A. M. 1992. NeuN, a neuronal specific nuclear protein in vertebrates. *Development,* 116**,** 201-11.
MULLEN, R. J., EICHER, E. M. & SIDMAN, R. L. 1976. Purkinje cell degeneration, a new neurological mutation in the mouse. *Proc Natl Acad Sci U S A,* 73**,** 208-12.
MURRELL, W., PALMERO, E., BIANCO, J., STANGELAND, B., JOEL, M., PAULSON, L., THIEDE, B., GRIEG, Z., RAMSNES, I., SKJELLEGRIND, H. K., NYGÅRD, S., BRANDAL, P., SANDBERG, C., VIK-MO, E., PALMERO, S. & LANGMOEN, I. A. 2013. Expansion of Multipotent Stem Cells from the Adult Human Brain. *PLoS ONE,* 8**,** e71334.
NAKANO, I. & KORNBLUM, H. 2003. Stage-Specific and Cell Fate Markers. *In:* BOTTENSTEIN, J. (ed.) *Neural Stem Cells.* Springer US.
NAMIMATSU, S., GHAZIZADEH, M. & SUGISAKI, Y. 2005. Reversing the effects of formalin fixation with citraconic anhydride and heat: a universal antigen retrieval method. *J Histochem Cytochem,* 53**,** 3-11.
NISHIMOTO, Y. & OKANO, H. 2010. New insight into cancer therapeutics: Induction of differentiation by regulating the Musashi/Numb/Notch pathway. *Cell Research,* 20**,** 1083-1085.
NOCTOR, S. C., FLINT, A. C., WEISSMAN, T. A., DAMMERMAN, R. S. & KRIEGSTEIN, A. R. 2001. Neurons derived from radial glial cells establish radial units in neocortex. *Nature,* 409**,** 714-20.

NOCTOR, S. C., FLINT, A. C., WEISSMAN, T. A., WONG, W. S., CLINTON, B. K. & KRIEGSTEIN, A. R. 2002. Dividing precursor cells of the embryonic cortical ventricular zone have morphological and molecular characteristics of radial glia. *Journal of Neuroscience,* 22**,** 3161-3173.

OHASHI, R., SAKATA, S., NAITO, A., HIRASHIMA, N. & TANAKA, M. 2014. Dendritic differentiation of cerebellar Purkinje cells is promoted by ryanodine receptors expressed by Purkinje and granule cells. *Dev Neurobiol,* 74**,** 467-80.

Oikari LE, Griffiths LR, Haupt LM. The current state of play in human neural stem cell models: what we have learnt from the rodent. OA Stem Cells 2014 Apr 08;2(1):7.

OKANO, H., KAWAHARA, H., TORIYA, M., NAKAO, K., SHIBATA, S. & IMAI, T. 2005. Function of RNA-binding protein Musashi-1 in stem cells. *Exp Cell Res,* 306**,** 349-56.

OOMMAN, S., STRAHLENDORF, H., FINCKBONE, V. & STRAHLENDORF, J. 2005. Non-lethal active caspase-3 expression in Bergmann glia of postnatal rat cerebellum. *Brain Res Dev Brain Res,* 160**,** 130-45.

OSTENFELD, T. & SVENDSEN, C. N. 2004. Requirement for neurogenesis to proceed through the division of neuronal progenitors following differentiation of epidermal growth factor and fibroblast growth factor-2-responsive human neural stem cells. *Stem Cells,* 22**,** 798-811.

OYARCE, K., BONGARZONE, E. R. & NUALART, F. 2014. Unconventional Neurogenic Niches and Neurogenesis Modulation by Vitamins. *J Stem Cell Res Ther,* 4**,** 184.

PALMER, T. D., TAKAHASHI, J. & GAGE, F. H. 1997. The adult rat hippocampus contains primordial neural stem cells. *Mol Cell Neurosci,* 8**,** 389-404.

PARENT, J. M. 2002. The role of seizure-induced neurogenesis in epileptogenesis and brain repair. *Epilepsy Res,* 50**,** 179-89.

PARNAVELAS, J. G. & NADARAJAH, B. 2001. Radial glial cells. are they really glia? *Neuron,* 31**,** 881-4.

PATRO, N., NAIK, A. & PATRO, I. K. 2015. Differential temporal expression of S100beta in developing rat brain. *Front Cell Neurosci,* 9**,** 87.

PEREZ-MARTIN, M., CIFUENTES, M., GRONDONA, J. M., LOPEZ-AVALOS, M. D., GOMEZ-PINEDO, U., GARCIA-VERDUGO, J. M. & FERNANDEZ-LLEBREZ, P. 2010. IGF-I stimulates neurogenesis in the hypothalamus of adult rats. *Eur J Neurosci,* 31**,** 1533-48.

PEVNY, L. & PLACZEK, M. 2005. SOX genes and neural progenitor identity. *Curr Opin Neurobiol,* 15**,** 7-13.

PEVNY, L. & RAO, M. S. 2003. The stem-cell menagerie. *Trends Neurosci,* 26**,** 351-9.

PEVNY, L. H. & LOVELLBADGE, R. 1997. Sox genes find their feet. *Current Opinion in Genetics & Development,* 7**,** 338-344.

PEVNY, L. H., SOCKANATHAN, S., PLACZEK, M. & LOVELL-BADGE, R. 1998. A role for SOX1 in neural determination. *Development,* 125**,** 1967-78.

PEYRE, E. & MORIN, X. 2012. An oblique view on the role of spindle orientation in vertebrate neurogenesis. *Dev Growth Differ,* 54**,** 287-305.

PIERCE, A. A. & XU, A. W. 2010. De novo neurogenesis in adult hypothalamus as a compensatory mechanism to regulate energy balance. *J Neurosci,* 30**,** 723-30.

PIXLEY, S. K. R. & DE VELLIS, J. 1984. Transition between immature radial glia and mature astrocytes studied with a monoclonal antibody to vimentin. *Developmental Brain Research,* 15**,** 201-209.

POLLARD, S. M., CONTI, L., SUN, Y., GOFFREDO, D. & SMITH, A. 2006. Adherent neural stem (NS) cells from fetal and adult forebrain. *Cereb Cortex,* 16 Suppl 1**,** i112-20.

POMPOLO, S. & HARLEY, V. R. 2001. Localisation of the SRY-related HMG box protein, SOX9, in rodent brain. *Brain Res,* 906**,** 143-8.

PONTI, G., PERETTO, P. & BONFANTI, L. 2008. Genesis of neuronal and glial progenitors in the cerebellar cortex of peripuberal and adult rabbits. *PLoS One,* 3**,** e2366.

PREVOT, V., HANCHATE, N. K., BELLEFONTAINE, N., SHARIF, A., PARKASH, J., ESTRELLA, C., ALLET, C., DE SERANNO, S., CAMPAGNE, C., DE TASSIGNY, X. & BARONCINI, M. 2010. Function-related structural plasticity of the GnRH system: a role for neuronal-glial-endothelial interactions. *Front Neuroendocrinol,* 31**,** 241-58.

PUSCHMANN, T. B., DIXON, K. J. & TURNLEY, A. M. 2010. Species differences in reactivity of mouse and rat astrocytes in vitro. *Neurosignals,* 18**,** 152-63.

QIAN, ANDREW A. DAVIS & SUSAN K. GODERIE 1997a. FGF2 Concentration Regulates the Generation of Neurons and Glia from Multipotent Cortical Stem Cells.

QIAN, X., DAVIS, A. A., GODERIE, S. K. & TEMPLE, S. 1997b. FGF2 Concentration Regulates the Generation of Neurons and Glia from Multipotent Cortical Stem Cells. *Neuron,* 18**,** 81-93.

RAKIC, P. 2003. Elusive radial glial cells: historical and evolutionary perspective. *Glia,* 43**,** 19-32.

RALAY, CRAFT, J. M., HU, W., GUO, L., WING, L. K., VAN ELDIK, L. J. & WATTERSON, D. M. 2006. Glia as a therapeutic target: selective suppression of human amyloid-beta-induced upregulation of brain proinflammatory cytokine production attenuates neurodegeneration. *J Neurosci,* 26**,** 662-70.

RAMÓN Y CAJAL, S. 1914. *Estudios sobre la degeneración y regeneración del sistema nervioso,* Madrid,, Impr. de hijos de N. Moya.

REEBER, S. L., ARANCILLO, M. & SILLITOE, R. V. 2014. Bergmann Glia are Patterned into Topographic Molecular Zones in the Developing and Adult Mouse Cerebellum. *Cerebellum*.

REUSS, B. & VON BOHLEN UND HALBACH, O. 2003. Fibroblast growth factors and their receptors in the central nervous system. *Cell Tissue Res,* 313**,** 139-57.

REX, M., ORME, A., UWANOGHO, D., TOINTON, K., WIGMORE, P. M., SHARPE, P. T. & SCOTTING, P. J. 1997. Dynamic expression of chicken Sox2 and Sox3 genes in ectoderm induced to form neural tissue. *Dev Dyn,* 209**,** 323-32.

REYNOLDS, B. A., TETZLAFF, W. & WEISS, S. 1992. A multipotent EGF-responsive striatal embryonic progenitor cell produces neurons and astrocytes. *J Neurosci,* 12**,** 4565-74.

REYNOLDS, B. A. & WEISS, S. 1992. Generation of neurons and astrocytes from isolated cells of the adult mammalian central nervous system. *Science,* 255**,** 1707-10.

ROBEL, S., BERNINGER, B. & GOTZ, M. 2011. The stem cell potential of glia: lessons from reactive gliosis. *Nat Rev Neurosci,* 12**,** 88-104.

ROBINS, S. C., STEWART, I., MCNAY, D. E., TAYLOR, V., GIACHINO, C., GOETZ, M., NINKOVIC, J., BRIANCON, N., MARATOS-FLIER, E., FLIER, J. S., KOKOEVA, M. V. & PLACZEK, M. 2013. alpha-Tanycytes of the adult hypothalamic third ventricle include distinct populations of FGF-responsive neural progenitors. *Nat Commun,* 4**,** 2049.

RODRIGUEZ, E., BLAZQUEZ, J., PASTOR, F., PELAEZ, B., PENA, P., PERUZZO, B. & AMAT, P. 2005. Hypothalamic Tanycytes: A Key Component of

Brain–Endocrine Interaction. *International Review of Cytology,* 247**,** 89-164.

RODRIGUEZ, E. M., BLAZQUEZ, J. L. & GUERRA, M. 2010. The design of barriers in the hypothalamus allows the median eminence and the arcuate nucleus to enjoy private milieus: the former opens to the portal blood and the latter to the cerebrospinal fluid. *Peptides,* 31**,** 757-76.

ROGERS, N., CHEAH, P. S., SZAREK, E., BANERJEE, K., SCHWARTZ, J. & THOMAS, P. 2013. Expression of the murine transcription factor SOX3 during embryonic and adult neurogenesis. *Gene Expr Patterns,* 13**,** 240-8.

SAALTINK, D. J., HAVIK, B., VERISSIMO, C. S., LUCASSEN, P. J. & VREUGDENHIL, E. 2012. Doublecortin and doublecortin-like are expressed in overlapping and non-overlapping neuronal cell population: implications for neurogenesis. *J Comp Neurol,* 520**,** 2805-23.

SANTA-OLALLA, J. & COVARRUBIAS, L. 1999. Basic fibroblast growth factor promotes epidermal growth factor responsiveness and survival of mesencephalic neural precursor cells. *J Neurobiol,* 40**,** 14-27.

SARKAR, A. & HOCHEDLINGER, K. 2013. The Sox Family of Transcription Factors: Versatile Regulators of Stem and Progenitor Cell Fate. *Cell stem cell,* 12**,** 15-30.

SCHMIDT, R., STRAHLE, U. & SCHOLPP, S. 2013. Neurogenesis in zebrafish - from embryo to adult. *Neural Development,* 8**,** 3.

SCHWINDT, FABIANA L. MOTTA, GABRIELA F. BARNABÉ1, CRISTINA G. MASSANT, ALESSANDER O. GUIMARÃES, MARIA ELISA CALCAGNOTTO, PESQUERO, J. B. & MELLO, L. E. 2009. Effects of FGF-2 and EGF removal on the differentiation of mouse neural precursor cells.

SCOTT, C. E., WYNN, S. L., SESAY, A., CRUZ, C., CHEUNG, M., GOMEZ GAVIRO, M. V., BOOTH, S., GAO, B., CHEAH, K. S., LOVELL-BADGE, R. & BRISCOE, J. 2010. SOX9 induces and maintains neural stem cells. *Nat Neurosci,* 13**,** 1181-9.

SEITA, J. & WEISSMAN, I. L. 2010. Hematopoietic Stem Cell: Self-renewal versus Differentiation. *Wiley interdisciplinary reviews. Systems biology and medicine,* 2**,** 640-653.

SEQUIER, J. M., HUNZIKER, W. & RICHARDS, G. 1988. Localization of calbindin D28 mRNA in rat tissues by in situ hybridization. *Neurosci Lett,* 86**,** 155-60.

SGAIER, S. K., MILLET, S., VILLANUEVA, M. P., BERENSHTEYN, F., SONG, C. & JOYNER, A. L. 2005. Morphogenetic and cellular movements that shape the mouse cerebellum; insights from genetic fate mapping. *Neuron,* 45**,** 27-40.

SHANTHLY, N., ARUVA, M. R., ZHANG, K., MATHEW, B. & THAKUR, M. L. 2006. Stem cells: a regenerative pharmaceutical. *Q J Nucl Med Mol Imaging,* 50**,** 205-16.

SHI, S. R., CHAIWUN, B., YOUNG, L., COTE, R. J. & TAYLOR, C. R. 1993. Antigen retrieval technique utilizing citrate buffer or urea solution for immunohistochemical demonstration of androgen receptor in formalin-fixed paraffin sections. *J Histochem Cytochem,* 41**,** 1599-604.

SHIBATA, T., YAMADA, K., WATANABE, M., IKENAKA, K., WADA, K., TANAKA, K. & INOUE, Y. 1997. Glutamate transporter GLAST is expressed in the radial glia-astrocyte lineage of developing mouse spinal cord. *J Neurosci,* 17**,** 9212-9.

SHIGA, T., ICHIKAWA, M. & HIRATA, Y. 1983. Spatial and temporal pattern of postnatal proliferation of Bergmann glial cells in rat cerebellum: an autoradiographic study. *Anat Embryol (Berl),* 167**,** 203-11.

SHIWAKU, H., YAGISHITA, S., EISHI, Y. & OKAZAWA, H. 2013. Bergmann glia are reduced in spinocerebellar ataxia type 1. *Neuroreport,* 24**,** 620-5.

SHORS, T. J., MIESEGAES, G., BEYLIN, A., ZHAO, M., RYDEL, T. & GOULD, E. 2001. Neurogenesis in the adult is involved in the formation of trace memories. *Nature,* 410**,** 372-6.

SIEGEL, A., REICHENBACH, A., HANKE, S., SENITZ, D., BRAUER, K. & SMITH, T. G., JR. 1991. Comparative morphometry of Bergmann glial (Golgi epithelial) cells. A Golgi study. *Anat Embryol (Berl),* 183**,** 605-12.

SILD, M. & RUTHAZER, E. S. 2011. Radial glia: progenitor, pathway, and partner. *Neuroscientist,* 17**,** 288-302.

SILLITOE, R. V. & JOYNER, A. L. 2007. Morphology, molecular codes, and circuitry produce the three-dimensional complexity of the cerebellum. *Annu Rev Cell Dev Biol,* 23**,** 549-77.

SKARDELLY, M., HEMPEL, E., HIRRLINGER, J., WEGNER, F., MEIXENSBERGER, J. & MILOSEVIC, J. 2014. Fluorescent Protein-Expressing Neural Progenitor Cells as a Tool for Transplantation Studies. *PLoS ONE,* 9**,** e99819.

SNAIDERO, N. & SIMONS, M. 2014. Myelination at a glance. *J Cell Sci,* 127**,** 2999-3004.

SOFRONIEW, M. V. 2005. Reactive astrocytes in neural repair and protection. *Neuroscientist,* 11**,** 400-7.

SOFRONIEW, M. V. & VINTERS, H. V. 2010. Astrocytes: biology and pathology. *Acta Neuropathol,* 119**,** 7-35.

SOLTANI, M. H., PICHARDO, R., SONG, Z., SANGHA, N., CAMACHO, F., SATYAMOORTHY, K., SANGUEZA, O. P. & SETALURI, V. 2005. Microtubule-associated protein 2, a marker of neuronal differentiation, induces mitotic defects, inhibits growth of melanoma cells, and predicts metastatic potential of cutaneous melanoma. *Am J Pathol,* 166**,** 1841-50.

SORG, B. A., SMITH, M. M. & CAMPAGNONI, A. T. 1987. Developmental expression of the myelin proteolipid protein and basic protein mRNAs in normal and dysmyelinating mutant mice. *J Neurochem,* 49**,** 1146-54.

SOTELO, C. 2004. Cellular and genetic regulation of the development of the cerebellar system. *Prog Neurobiol,* 72**,** 295-339.

SOTELO, C., ALVARADO-MALLART, R. M., FRAIN, M. & VERNET, M. 1994. Molecular plasticity of adult Bergmann fibers is associated with radial migration of grafted Purkinje cells. *J Neurosci,* 14**,** 124-33.

SOTTILE, V., LI, M. & SCOTTING, P. J. 2006. Stem cell marker expression in the Bergmann glia population of the adult mouse brain. *Brain Res,* 1099**,** 8-17.

STERNBERGER, N. H., ITOYAMA, Y., KIES, M. W. & WEBSTER, H. D. 1978. Myelin Basic-Protein Demonstrated Immunocytochemically in Oligodendroglia Prior to Myelin Sheath Formation. *Proceedings of the National Academy of Sciences of the United States of America,* 75**,** 2521-2524.

STOLP, H. B. & MOLNAR, Z. 2015. Neurogenic niches in the brain: help and hindrance of the barrier systems. *Frontiers in Neuroscience,* 9.

STOLT, C. C., LOMMES, P., SOCK, E., CHABOISSIER, M. C., SCHEDL, A. & WEGNER, M. 2003. The Sox9 transcription factor determines glial fate choice in the developing spinal cord. *Genes Dev,* 17**,** 1677-89.

SU, H. L., MUGURUMA, K., MATSUO-TAKASAKI, M., KENGAKU, M., WATANABE, K. & SASAI, Y. 2006. Generation of cerebellar neuron precursors from embryonic stem cells. *Dev Biol,* 290**,** 287-96.

SU, X., GUAN, W., YU, Y. C. & FU, Y. 2014. Cerebellar stem cells do not produce neurons and astrocytes in adult mouse. *Biochem Biophys Res Commun,* 450**,** 378-83.

SUDAROV, A. & JOYNER, A. L. 2007. Cerebellum morphogenesis: the foliation pattern is orchestrated by multi-cellular anchoring centers. *Neural Dev,* 2**,** 26.

SUGIHARA, I. 2011. Compartmentalization of the deep cerebellar nuclei based on afferent projections and aldolase C expression. *Cerebellum,* 10**,** 449-63.

SUH, H., CONSIGLIO, A., RAY, J., SAWAI, T., D'AMOUR, K. A. & GAGE, F. H. 2007. In vivo fate analysis reveals the multipotent and self-renewal capacities of Sox2+ neural stem cells in the adult hippocampus. *Cell Stem Cell,* 1**,** 515-28.

SUHONEN, J. O., PETERSON, D. A., RAY, J. & GAGE, F. H. 1996a. Differentiation of adult hippocampus-derived progenitors into olfactory neurons in vivo. *Nature,* 383**,** 624-7.

SUHONEN, J. O., PETERSON, D. A., RAY, J. & GAGE, F. H. 1996b. Differentiation of adult hippocampus-derived progenitors into olfactory neurons in vivo. *Nature,* 383**,** 624-627.

SUN, M. ROSS BULLOCK, NABIL ALTEMEMI, ZHENGWEN ZHOU, SARAH HAGOOD, ANDREW ROLFE, MELISSA J. MCGINN, ROBERT HAMM & COLELLO, A. R. J. 2010. The Effect of Epidermal Growth Factor in the Injured Brain after Trauma in Rats. *JOURNAL OF NEUROTRAUMA* 27:**,** 923–938.

SUN, D. & JAKOBS, T. C. 2012. Structural remodeling of astrocytes in the injured CNS. *Neuroscientist,* 18**,** 567-88.

TANAKA, M., YAMAGUCHI, K., TATSUKAWA, T., THEIS, M., WILLECKE, K. & ITOHARA, S. 2008. Connexin43 and bergmann glial gap junctions in cerebellar function. *Front Neurosci,* 2**,** 225-33.

TAO, O., SHIMAZAKI, T., OKADA, Y., NAKA, H., KOHDA, K., YUZAKI, M., MIZUSAWA, H. & OKANO, H. 2010. Efficient generation of mature cerebellar Purkinje cells from mouse embryonic stem cells. *J Neurosci Res,* 88**,** 234-47.

TAUPIN, P. 2006. Neural progenitor and stem cells in the adult central nervous system. *Ann Acad Med Singapore,* 35**,** 814-20.

THOMSON, J. A., ITSKOVITZ-ELDOR, J., SHAPIRO, S. S., WAKNITZ, M. A., SWIERGIEL, J. J., MARSHALL, V. S. & JONES, J. M. 1998. Embryonic stem cell lines derived from human blastocysts. *Science,* 282**,** 1145-7.

TOMA, J. G., AKHAVAN, M., FERNANDES, K. J., BARNABE-HEIDER, F., SADIKOT, A., KAPLAN, D. R. & MILLER, F. D. 2001. Isolation of multipotent adult stem cells from the dermis of mammalian skin. *Nat Cell Biol,* 3**,** 778-84.

TONCHEV, A. B., YAMASHIMA, T., SAWAMOTO, K. & OKANO, H. 2006. Transcription factor protein expression patterns by neural or neuronal progenitor cells of adult monkey subventricular zone. *Neuroscience,* 139**,** 1355-67.

TRIARHOU, L. C., ZHANG, W. & LEE, W. H. 1996. Amelioration of the behavioral phenotype in genetically ataxic mice through bilateral intracerebellar grafting of fetal Purkinje cells. *Cell Transplant,* 5**,** 269-77.

TROPEPE, MARIA SIBILIA, BRIAN G. CIRUNA, JANET ROSSANT, ERWIN F. WAGNER & KOOY, D. V. D. 1999. Distinct Neural Stem Cells Proliferate in Response to EGF and FGF in the Developing Mouse Telencephalon. *Developmental Biology , ,* 208**,** 166–188.

UCHIDA, N., BUCK, D. W., HE, D. P., REITSMA, M. J., MASEK, M., PHAN, T. V., TSUKAMOTO, A. S., GAGE, F. H. & WEISSMAN, I. L. 2000. Direct isolation of human central nervous system stem cells. *Proceedings of the National Academy of Sciences of the United States of America,* 97**,** 14720-14725.

UWANOGHO, D., REX, M., CARTWRIGHT, E. J., PEARL, G., HEALY, C., SCOTTING, P. J. & SHARPE, P. T. 1995. Embryonic expression of the chicken Sox2, Sox3 and Sox11 genes suggests an interactive role in neuronal development. *Mechanisms of Development,* 49**,** 23-36.

VENERE, M., HAN, Y. G., BELL, R., SONG, J. S., ALVAREZ-BUYLLA, A. & BLELLOCH, R. 2012. Sox1 marks an activated neural stem/progenitor cell in the hippocampus. *Development,* 139**,** 3938-49.

VERDES, J. M., MORANA, J. A., BATTES, D., GUTIERREZ, F., GUERRERO, F., GOICOA, A., FIDALGO, L. E., BARBEITO, C. G., ZANUZZI, C. N., PORTIANSKY, E. L. & GIMENO, E. J. 2010. Calbindin D28k expression and the absence of apoptosis in the cerebellum of Solanum bonariense L-intoxicated bovines. *Vet Pathol,* 47**,** 569-72.

VON BOHLEN UND HALBACH, O. 2011. Immunohistological markers for proliferative events, gliogenesis, and neurogenesis within the adult hippocampus. *Cell Tissue Res,* 345**,** 1-19.

VOOGD, J. & GLICKSTEIN, M. 1998. The anatomy of the cerebellum. *Trends in Cognitive Sciences,* 2**,** 307-313.

WALKER, T. L., YASUDA, T., ADAMS, D. J. & BARTLETT, P. F. 2007. The doublecortin-expressing population in the developing and adult brain contains multipotential precursors in addition to neuronal-lineage cells. *J Neurosci,* 27**,** 3734-42.

WALTON, R. M. 2012. Postnatal neurogenesis: of mice, men, and macaques. *Vet Pathol,* 49**,** 155-65.

WALTON, R. M., PARMENTIER, T. & WOLFE, J. H. 2013. Postnatal neural precursor cell regions in the rostral subventricular zone, hippocampal subgranular zone and cerebellum of the dog (Canis lupus familiaris). *Histochem Cell Biol,* 139**,** 415-29.

WANG, S., WANG, B., PAN, N., FU, L., WANG, C., SONG, G., AN, J., LIU, Z., ZHU, W., GUAN, Y., XU, Z. Q., CHAN, P., CHEN, Z. & ZHANG, Y. A. 2015. Differentiation of human induced pluripotent stem cells to mature functional Purkinje neurons. *Sci Rep,* 5**,** 9232.

WANG, T. & MORGAN, J. I. 2007. The Purkinje cell degeneration (pcd) mouse: an unexpected molecular link between neuronal degeneration and regeneration. *Brain Res,* 1140**,** 26-40.

WEINER, L. P. 2008. Definitions and criteria for stem cells. *Methods Mol Biol,* 438**,** 3-8.

WEISS, CHRISTINE DUNNE, JENNIFER HEWSON, CHERYL WOHL, MATT WHEATLEY, ALAN C. PETERSON, AND & REYNOLDS, B. A. 1996. Multipotent CNS Stem Cells Are Present in the Adult Mammalian Spinal Cord and Ventricular Neuroaxis.

WHITTEMORE, S. R., MORASSUTTI, D. J., WALTERS, W. M., LIU, R. H. & MAGNUSON, D. S. 1999. Mitogen and substrate differentially affect the lineage restriction of adult rat subventricular zone neural precursor cell populations. *Exp Cell Res,* 252**,** 75-95.

WILHELMSSON, U., LI, L., PEKNA, M., BERTHOLD, C. H., BLOM, S., ELIASSON, C., RENNER, O., BUSHONG, E., ELLISMAN, M., MORGAN, T. E. & PEKNY, M. 2004. Absence of glial fibrillary acidic protein and vimentin prevents hypertrophy of astrocytic processes and improves post-traumatic regeneration. *J Neurosci,* 24**,** 5016-21.

WU, H. Y., WANG, T., LI, L., CORREIA, K. & MORGAN, J. I. 2012. A structural and functional analysis of Nna1 in Purkinje cell degeneration (pcd) mice. *FASEB J,* 26**,** 4468-80.

XU, H., YANG, Y., TANG, X., ZHAO, M., LIANG, F., XU, P., HOU, B., XING, Y., BAO, X. & FAN, X. 2013. Bergmann glia function in granule cell migration during cerebellum development. *Mol Neurobiol,* 47**,** 833-44.

XU, Y., TAMAMAKI, N., NODA, T., KIMURA, K., ITOKAZU, Y., MATSUMOTO, N., DEZAWA, M. & IDE, C. 2005. Neurogenesis in the ependymal layer of the adult rat 3rd ventricle. *Exp Neurol,* 192**,** 251-64.

YADIRGI, G. & MARINO, S. 2009. Adult neural stem cells and their role in brain pathology. *J Pathol,* 217**,** 242-53.

YAMADA, K., FUKAYA, M., SHIBATA, T., KURIHARA, H., TANAKA, K., INOUE, Y. & WATANABE, M. 2000. Dynamic transformation of Bergmann glial fibers proceeds in correlation with dendritic outgrowth and synapse formation of cerebellar Purkinje cells. *Journal of Comparative Neurology,* 418**,** 106-120.

YAMADA, K. & WATANABE, M. 2002. Cytodifferentiation of Bergmann glia and its relationship with Purkinje cells. *Anat Sci Int,* 77**,** 94-108.

YARDEN, Y. & SLIWKOWSKI, M. X. 2001. Untangling the ErbB signalling network. *Nat Rev Mol Cell Biol,* 2**,** 127-37.

YOUNG, J. K., BAKER, J. H. & MULLER, T. 1996. Immunoreactivity for brain-fatty acid binding protein in gomori-positive astrocytes. *Glia,* 16**,** 218-26.

YUAN, A., RAO, M. V., VEERANNA & NIXON, R. A. 2012. Neurofilaments at a glance. *J Cell Sci,* 125**,** 3257-63.

YUAN, T. F. & ARIAS-CARRION, O. 2011. Adult neurogenesis in the hypothalamus: evidence, functions, and implications. *CNS Neurol Disord Drug Targets,* 10**,** 433-9.

ZAMANIAN, J. L., XU, L., FOO, L. C., NOURI, N., ZHOU, L., GIFFARD, R. G. & BARRES, B. A. 2012. Genomic analysis of reactive astrogliosis. *J Neurosci,* 32**,** 6391-410.

ZHANG, Q., LIU, G., WU, Y., SHA, H., ZHANG, P. & JIA, J. 2011. BDNF promotes EGF-induced proliferation and migration of human fetal neural stem/progenitor cells via the PI3K/Akt pathway. *Molecules,* 16**,** 10146-56.

ZHAO, Q., EBERSPAECHER, H., LEFEBVRE, V. & DE CROMBRUGGHE, B. 1997. Parallel expression of Sox9 and Col2a1 in cells undergoing chondrogenesis. *Dev Dyn,* 209**,** 377-86.

ZHU, G., MEHLER, M. F., MABIE, P. C. & KESSLER, J. A. 1999. Developmental changes in progenitor cell responsiveness to cytokines. *J Neurosci Res,* 56**,** 131-45.

ZUPANC, G. K. 2006. Neurogenesis and neuronal regeneration in the adult fish brain. *J Comp Physiol A Neuroethol Sens Neural Behav Physiol,* 192**,** 649-70.

Appendix I-Chemicals, Medium, and Reagents

Chemical	Product	Provider	Cat. Number
PFA	paraformaldehyde	VWR/Merck	294474L
Parafilm	Parafilm	SLS	FL1022
Vectashield	Vectashield with Dapi	VectorLabs	H-1200
OCT	CellPath	KMA-0100-00A	0364017
slides	Superfrost plus slides	Thermo scientific	080513-9
Sucrose	Sucrose	Fisher	S/8600/53
Isopentane	Isopentane	Fisher	P/1030/17
Tween20	Tween-20	Sigma	P1379
DMEM/F-12	DMEM	Life technologies	21331-020
NB (-phenol)	Neurobasal medium	Life technologies	12348-017
FGF-2	Human Recombinant FGF-2	LifeTech	PHG0026/ABC8255
EGF	Human Recombinant EGF	Source Bioscience	ABC016
Heparin	Heparin Sodium Salt	Stem cell technologies	07980
BDNF	Brain derived neurotrophic factor	Source Bioscience	ABC011
P/S	Pen/Strep	Invitrogen (Fisher)	15140-122
N2	N2 supplement (100x)	Life technologies	17502-048
B27	B27 supplement (50x)	Life technologies	17504-044
Pen/Strep	Penicillin/ Streptomycin	Life technologies	15140-122
FBS	Fetal Bovine Serum	Invitrogen (Fisher)	10108-165
Vectashield with dapi	Vectashield mounting medium with dapi	Vector Laboratoreis	H-1200
Vector® Blue Substrate kit	Alkaline phosphatase substrate	Vector Laboratories	SK-5300
ImmPACT DAB Substrate	DAB peroxidase substrate	Vector Laboratories	SK-4105
Tri-sodium citrate	Sodium citrate buffer	Fisher chemicals	S/3320/53
Presto Blue kit	Prestoblue cell viability reagent	Invitrogen	A13262
H2O2	Hydrogen peroxide	Fisher chemicals	H/1750/15
HBSS	Hanked Balanced Salt Solution	Sigma	H8264
Hematoxylin	Hematoxylin	Vector Laboratories	H-3404
Phosphate buffer saline	PBS	Oxoid	BR0014
Accutase	Accutase	Sigma	A6964
Methanol	Methanol	Fisher chemicals	M/4056/17
Ethanol	Ethanol	Fisher chemicals	E/0650DF/17

Histolene	HISTOLENE CLEARING AGENT	Cell path	EGB-0500-00A
Sodium chloride	Sodium chloride	Fisher chemicals	C/3160/63
Magnesium chloride	Magnesium chloride	Sigma	M8266-100G
Gelatin	Gelatin	Sigma	G1393

Appendix II-Solutions, Buffers and Media Preparation

Phosphate buffer saline (PBS)

PBS was used regularly during the immunostaining protocol for washing the sections, it was prepared by the addition of 1 tablet of phosphate buffered saline to 100 ml of dH_2O, sterilized by autoclave and stored at room temperature.

PBS

2.7mM KCl

137mM NaCl

0.01M Phosphate buffer (Na2HPO4+KH2PO4) pH 7.4

PBT

PBS with 0.1% Tween20

Sodium citrate buffer

Prepared by mixing 2.94g of tris sodium citrate with 1000 ml dH_2O, after complete dissolving the PH was adjusted to 6.0 with 1N HCL, and finally 0.5ml of tween-20 (sigma) was added, the solution was stored at 4°C. This solution was used for the antigen retrieval treatment.

Wax embedding process

Cerebellum isolated from mouse, chick, and primates pre fixed in 4% paraformaldehyde (PFA) were placed in small cassettes and then processed using automatic tissue processor.

Medium

NB medium

For 50ml:

25ml Neurobasal A (Life Technologies, cat.no. 12348-017)

25ml DMEM F12 (-L-Glutamine) (Life Technologies, cat.no. 21331-020)

1ml B27 (Life Technologies, cat.no. 17504-044)

0.5ml N2 (Life Technologies, cat.no. 17502-048)

0.25ml Pen-Strep (Life Technologies, cat.no. 15140-122)

5µl Heparin (Life Technologies)

On the day of treatment add to medium:

- 20ng/ml bFGF (fibroblast growth factor)
- 20ng/ml EGF (epidermal growth factor)

Neural Differentiation medium

NB medium without EGF and bFGF

Add on the day of use

10ng/ml BDNF

1 µM Retinoic Acid (RA) or EC23 (Tocris)

0.5% FCS (Life Technologies, cat.no. 10695023)

Gelatine coating

Gelatine provides a matrix for mouse NSCs to aid attachment.

- Prepare 0.1% stock
- Add 2.5ml gelatine to 47.5ml PBS
- Sterile filter through
- Add enough 0.1% Gelatine solution to cover the surface (e.g. 3ml per T25 or 0.5ml per well of a 24-well-plate)
- Incubate for 10-30min at room temperature
- Aspirate the gelatine solution and add media or cell suspension (take care that the surface does not dry).